Thomson, Catriona E. (2008) *Investigation of phototropin blue light receptor function and signalling in arabidopsis.* PhD thesis.

http://theses.gla.ac.uk/170/

INVESTIGATION OF PHOTOTROPIN BLUE LIGHT RECEPTOR FUNCTION AND SIGNALLING IN *ARABIDOPSIS*

By

Catriona E Thomson

Thesis submitted for the degree of Doctor of Philosophy

Division of Biochemistry and Molecular Biology
Institute of Biomedical and Life Sciences
University of Glasgow

September, 2007

Abstract

The global success of plants depends largely on their ability to perceive and respond to light, mainly in two regions of the electromagnetic spectrum. Phytochromes are light sensors for the red and far-red wavelengths of light while cryptochromes, phototropins and members of the ZTL/ADO family respond to blue and UV-A wavelengths of light.

Phototropins are UV-A/blue-light receptor kinases found ubiquitously in plants from the unicellular green alga *Chalmydomonas reinhardtii* through bryophytes and pteridophytes up to angiosperms. The model plant *Arabidopsis* possesses two phototropins (phot1 and phot2) and is the subject of the work presented in this thesis.

The general structure of the phototropin protein comprises a photosensory region at the N-terminal that contains two LOV (light, oxygen and voltage sensing) domains and a C-terminal kinase domain belonging to the large AGC family of protein kinases. The LOV domains form a covalent adduct with the chromophore flavin mononucleotide (FMN) in response to illumination with blue light which in turn leads to structural changes throughout the protein resulting in autophosphorylation of the N-terminal region by the kinase domain.

Phototropins function redundantly to mediate a number of physiological responses *in planta* which serve to promote plant fitness and maximise photosynthetic potential. Phototropism, chloroplast accumulation, blue light-induced stomatal opening, leaf expansion and leaf movements can be induced through the activation of both phot1 and phot2 in response to different intensities of light, with phot1 being more light sensitive than phot2. In addition to the functionally redundant responses, phot1 alone is responsible for destabilisation of certain mRNA transcripts and the rapid inhibition of hypocotyl elongation when etiolated seedlings are transferred to blue light, while phot2 is solely responsible for the high light induced chloroplast avoidance response.

While much is known about the mechanisms of light perception by the phototropins at the molecular level, and the responses mediated by them have been well described, little is known about their methods of signalling to induce these physiological responses upon photoactivation by blue light. Therefore, the aims of this study were to identify novel phot-interacting proteins and to investigate the modes of phot1 signalling by structure/function analyses in order to better understand the way

phototropins elicit signal transduction to downstream components in order to bring about the responses described above.

Initially, a yeast two-hybrid screen was carried out to try to identify immediate interacting partners for phot1. The results of the yeast two-hybrid screen are described in Chapter 3. One hundred and thirty yeast colonies containing putative phot1-interacting proteins were identified from the screen and preliminary characterisation of six of these proteins are described in this chapter. Two of the proteins investigated are members of the ADP-ribosylation family which is involved in the regulation of membrane trafficking. The ARF proteins identified show a blue-light-sensitive interaction with phot1 and also interact with phot2. These proteins are of interest given the subcellular movement of phototropins from the plasma membrane after exposure to blue light.

The C-terminal kinase domain of phot1 was found to interact with p-glycoprotein 19 (PGP19), a protein involved in polar auxin transport. The interaction between these proteins is interesting because of the role auxin plays in phot1-mediated responses such as phototropism and leaf expansion, and preliminary characterisation of the interaction *in vitro* is shown in Chapter 3. The implications of a direct link between phototropins and the proteins involved in auxin transport are discussed.

A further two proteins identified from the screen are members of the NPH3/RPT2-Like (NRL) family. RPT2 has already been identified as a phot1-interacting protein and identification of this protein increased confidence in the efficacy of the screen to identify genuine interacting proteins. A novel member of the NRL family, designated NPH3-L, was also identified from the screen. Chapter 4 describes the tissue specific and subcellular localisation of NPH3-L and contains results of preliminary investigations into the function of NPH3-L *in planta*.

14-3-3λ was identified from the screen using full-length phot1 as bait. A 14-3-3 protein has been shown previously to bind to autophosphorylated phototropin in *Vicia faba* (Kinoshita *et al.,* 2003). Chapter 5 details the localisation of 14-3-3λ at tissue and subcellular levels and shows that 14-3-3λ binding to plant-derived phot1-GFP is both light dependent and induced by receptor autophosphorylation. Creation of GFP-14-3-3λ overexpressing lines in wild-type and *phot1-5phot2-1* backgrounds allowed investigation into the roles that light and phototropins play in regulating the subcellular localisation of 14-3-3λ. It is shown that light-induced movement of 14-3-3λ at the

plasma membrane is dependent on the presence of endogenous phototropins. Physiological implications of this interaction are discussed.

Finally, in order to determine the modes of phototropin signalling, structure/function studies were carried out by expressing different regions of phot1 in a variety of *Arabidopsis* backgrounds. The results of the structure/function studies are described in Chapter 6. Known phot1-mediated responses were investigated in the transgenic plants to determine the effects of individual domains of phot1. Particular attention was paid to the role of receptor autophosphorylation in phot1-mediated responses to light. A transgenic line overexpressing the LOV2-kinase region of phot1 demonstrates that phot1 autophosphorylation is not the primary signalling event involved in phot1-mediated responses to light and shows that the truncated version of phot1 is sufficient to complement most phot1-mediated responses. This also shows that the LOV1 domain is dispensable and suggests phot1 may signal through phosphorylation of substrates. Comparisons are drawn between phot1 kinase overexpressing lines and inactive phot1 kinase overexpressing lines. Preliminary observations of a transgenic line overexpressing phot1 in a wild-type background indicate that overexpression of phot1 may alter polar auxin transport. Together these studies provide new insights into possible mechanisms of phot1 signalling and the function of major domains of phot1.

Foreword

Part of the work presented in Chapter 6 of this thesis has been published as:

Thomson, C.E., Sullivan, S., Lamont, D. J., Jones, M. A. & Christie, J. M. (2008) *In Vivo* Phosphorylation Site Mapping and Functional Characterization of Arabidopsis Phototropin 1. *Mol. Plant*, **1(1)**: 178-194.

Contents of Thesis

Chapter 1: Introduction to photoreception and signalling in plants

Chapter 3: Isolation of phot1 interacting proteins

Chapter 4: Investigation of the phot1-interacting protein, NPH3-L

Chapter 5: Investigation of the phot1 interaction with 14-3-3λ

Chapter 6: Structure/function studies of phot1

Chapter 7: General Discussion

List of Figures and Tables

Abbreviations

ABC	ATP-binding cassette
AD	activation domain
ADO	Adagio
ADP	adenosine diphosphate
α-gal	5-bromo-4-chloro-3-indolyl-α-D-galactopyranoside
AP	alkaline phosphatase
ARF	ADP-ribosylation factor
ATP	adenosine triphosphate
BD	binding domain
BFA	Brefeldin A
bHLH	basic helix loop helix
bp	base pair
BTB/POZ	broad complex, tram track, bric a brac/pox virus and zinc finger
bZIP	basic leucine zipper
CBP	calmodulin binding peptide
CC	coiled coil
CCT	Cryptochrome C-terminal
CDF1	cycling Dof 1
cDNA	complimentary DNA
CNT	Cryptochrome N-Terminal
CO	Constans
CO2	carbon dioxide
Col	Columbia
COP	constitutively photomorphogenic
CPD	cyclobutane pyrimadine dimer
cry	Cryptochrome
Del.	deletion
dH$_2$O	distilled water
DMF	dimethyl formamide
DMSO	dimethyl sulphoxide
DNA	deoxyribonucleic acid

DNase	deoxyribonuclease
dNTP	deoxynucleotide triphosphate
EDTA	ethylene diamine tetra-acetic acid
EGTA	ethylene glycol tetra-acetic acid
ER	endoplasmic reticulum
EXP	expansin
FAD	flavin adenine dinucleotide
FHY1	far-red elongated hypocotyl
FKF1	flavin-binding, kelch repeat, F-box 1
FMN	Flavin mononucleotide
FRET	fluorescence resonance energy transfer
gDNA	genomic DNA
GDP	guanadine diphosphate
GFP	green fluorescent protein
grf	G-box regulating factor
GST	glutathione-S-transferase
GTP	guanadine triphosphate
GUS	β-glucuronidase
HRP	horse radish peroxidase
HY5	long hypocotyl 5
IAA	indole-3-acetic acid
IAN	indole-3-acetonitrile
IM	integral membrane
IPTG	isopropyl β-D-galactopyranoside
kDa	kilo Daltons
L2K	LOV2-kinase
LEI	leaf expansion index
Lhcb	light-harvesting complexes of photosystem II
LHY	long hypocotyl
LiOAc	lithium acetate
LKP2	LOV, Kelch protein 2
LOV	Light, Oxygen or Voltage
mRNA	messanger RNA

MSG	Massugu
MTHF	methenyltetrahydrofolate
NaOAc	sodium acetate
NASC	Nottingham Arabidopsis Stock Centre
NCBI	National Centre for Biotechnology Information
neo	neochrome
NIT1	nitrilase 1
NLS	nuclear localisation signal
nm	nanometres
NMR	nuclear magnetic resonance
NPA	naphthylphthalamic acid
NPH	non-phototropic hypocotyl
NPL	non-phototropic hypocotyl-like
NRL	NPH3/RPT2-Like
OD	optical density
PAS	Per, ARNT, Sim
PCR	polymerase chain reaction
PEG	polyethylene glycol
P_{FR}	far-red light absorbing form of phytochrome
PGP	p-glycoprotein
pH	$-\log_{10}$ (hydrogen ion concentration)
phot	Phototropin
PHR	photolyase-related
phy	Phytochrome
PID	pinoid
PIF3	phytochrome interacting factor 3
PIN	pin-formed
PKA	protein kinase A
PKS1	phytochrome kinase substrate 1
PMSF	phenylmethylsulphonyl fluoride
PNP	p-nitrophenyl
P_R	red light absorbing form of phytochrome
rbcL/S	Rubisco large/small subunit

RNA	ribonucleic acid
RNase	ribonuclease
RPT2	root phototropism 2
RT-PCR	reverse transcriptase PCR
Rubisco	Ribulose-1,5-bisphosphate carboxylase/oxygenase
RWC	relative water content
SCF	SKP1-Cullin1-F-box
SD	synthetic dropout
SDS	sodium dodecyl sulphate
SDS-PAGE	SDS polyacrylamide gel electrophoresis
SV	simian virus
TAIR	The Arabidopsis Information Resource
T-DNA	transfer DNA
TOC1	timing of Cab expression 1
U	units
UDP	uradine diphosphate
UGPase	UDP-glucose pyrophosphorylase
UPS	ubiquitin proteasome system
UV	ultra violet
UVR8	ultra violet resistance 8
v/v	volume/volume
w/v	weight/volume
WUE	water use efficiency
ZTL	Zeitlupe

Acknowledgements

Chapter 1: Introduction to photoreception and signalling in plants

1.1 The necessity of light for plant growth

As sessile organisms, it is essential that plants derive all that is necessary to complete their life cycle from the immediate environment. Of the environmental factors around plants, light is surely one of the most important. In addition to providing the energy required for photosynthesis, light also provides a range of cues and stimuli to regulate the growth and development of plants. From germination to flowering and seed setting, cues from the light environment allow plants to orientate themselves in the soil, forage for light, avoid competitors, and also to ensure reproduction is carried out at the most favourable time of year. The light-dependent responses are known collectively as photomorphogenesis. Considering the current energy and food production problems facing the Earth's population, understanding how plants perceive and utilise light effectively is surely of the utmost importance.

1.2 Plant photoreceptors

In order to act upon the environmental cues supplied by the light environment, plants have evolved a number of photoreceptors that function to sense the quality and quantity of ambient light, and to then transduce the signal. There are several classes of photoreceptors that absorb mainly in two regions of the spectrum. Red and far-red wavelengths of light (600-750 nm) are absorbed by the phytochromes. Ultra-violet-A (UV-A) and blue wavelengths of light (320-500 nm) are absorbed by two distinct classes of photoreceptor: cryptochromes and phototropins. Recently, a third class of UV-A and blue light receptors (the ZTL/ADO family) has been identified. These known photoreceptors are discussed below.

1.2.1 Introduction to phytochromes

Phytochrome was the first photoreceptor to be identified in plants (Butler *et al.,* 1959) and phytochromes (phy) have subsequently been identified in bacteria and algae (Montgomery & Lagarias, 2002). The physiological responses for which members of the phytochrome family are responsible in plants are wide reaching and diverse. These include germination, de-etiolation, shade avoidance, flowering, gene expression and regulation of the circadian clock (Schepens *et al.,* 2004). The phytochromes absorb in

the red (600-700 nm) and far-red (700-750 nm) regions of the electromagnetic spectrum and one of their most noticeable features is their unique ability to interconvert between the red-absorbing form (P_R, λ-max ~ 670nm) and far-red-absorbing form (P_{FR}, λ-max ~ 730nm) (Schmidt *et al.,* 1973). Light activation of the phytochromes results from conversion from the P_R form to the P_{FR} form which activates signalling pathways.

There are five phytochromes in *Arabidopsis*, phyA-phyE, which exhibit different, but sometimes overlapping functions (Whitelam & Devlin, 1997; Schepens *et al.,* 2004). The *Arabidopsis* phytochrome family arose through four primary duplication events with the initial event producing the phyA and phyB groups at around the time of seed plant appearance (Mathews & Sharrock, 1997). The most physiologically important phytochromes are phyA and phyB while phyC, phyD and phyE play more minor roles in plant photomorphogenesis. PhyD and phyE are partially redundant with phyB in seedling establishment and flowering and may serve to fine-tune responses to changes in the micro-environment (Franklin *et al.,* 2003b). PhyC is dependent on phyB to mediate red light-induced de-etiolation and also functions with phyA to mediate leaf development, de-etiolation and flowering time in response to blue light (Franklin *et al.,* 2003a). Essentially, the *Arabidopsis* phytochromes can be spilt into two classes: type I phytochromes such as phyA are light labile and mediate responses stimulated by far-red wavelengths of light, while the type II phytochromes (phyB-phyE) are light-stable and are generally responsible for the classical red/far-red reversible responses. PhyB undergoes dark reversion from the P_{FR} form to the P_R form, but phyA does not do this significantly and is instead targeted for degradation by the E3 ubiquition ligase, COP1 (constitutively photomorphogenic 1; Seo *et al.,* 2004). While the main biological function of phytochromes depends upon their ability to both sense and distinguish between red and far-red wavelengths of light they can also absorb in the blue and green regions of the spectrum.

1.2.2 Phytochrome structure and function

The generic phytochrome molecule is a soluble, homodimeric chromoprotein of around 120 kDa. Each monomer binds one molecule of the linear tetrapyrrolle chromophore, phytochromobilin (Fig. 1.1; Quail 1997). Phytochromobillin is synthesised in the chloroplast from heme, and *Arabidopsis* plants carrying mutations in

the heme oxygenase gene (*hy1*) cannot produce the chromophore necessary for functional phytochromes (Terry, 1997). The structure of phytochromes is comprised of an N-terminal photosensory region where the chromophore is bound and a C-terminal region that contains two PAS domains and a histidine-kinase related domain (Fig. 1.1; Montgomery & Lagarias, 2002). Phytochromes undergo dimerisation and this dimerisation requires the presence of the PAS2 (Per, ARNT, Sim) domain in phyA (Kim *et al.,* 2006). Phytochromes show specificity for different wavelengths of light and this is exemplified in seedling de-etiolation responses to red and far-red wavelengths of light. Etiolated seedlings exposed to monochromatic far-red light become de-etiolated solely by phyA-mediated responses, whereas seedlings exposed to monochromatic red light become de-etiolated mainly by the action of phyB (Quail *et al.,* 1995). To mediate this effect, the N-terminal photosensory region detects and determines the wavelength of light so the N-terminal of phyA senses far-red light, while the N-terminal of phyB senses red light. However, the C-terminal domains appear to be interconvertable for signalling the perception of light to common partners in order to bring about de-etiolation suggesting a common molecular function in signalling (Wagner *et al.,* 1996). While it has been shown the nuclear transportation of phyB is necessary for its function (Huq *et al.,* 2003) it also appears that nuclear localisation of phyB N-terminal dimers is sufficient to induce phyB responses suggesting that the C-terminus is not directly involved in signal transduction (Matsushita *et al.,* 2003). PhyA is also transported to the nucleus in response to far-red wavelengths of light. PhyA in the P_{FR} form has been shown to interact with the novel, plant-specific protein far-red elongated hypocotyl (FHY1) which, unlike phyA, has a nuclear localisation signal (NLS) and it is proposed that this may function to take activated phyA to the nucleus (Hiltbrunner *et al.,* 2005). However, phytochromes additionally function in cellular compartments other than the nucleus as interacting factors such as Phytochrome Kinase Substrate 1 (PKS1), which is phosphorylated by phyA and interacts with phototropin 1, are localised in the cytosol and at the plasma membrane (Fankhauser *et al.,* 1999; Lariguet *et al.,* 2006).

1.2.3 Phytochrome signalling

In order for photoreceptors to mediate physiological responses to light *in planta*, it is necessary for the activated photoreceptor to directly interact with one or more

signalling partners to transduce the light-sensing event to downstream signalling components. To date, over 20 proteins have been identified as having some degree of interaction with one or more phytochromes (Quail, 2007). Therefore, it is out with the scope of this chapter to discuss them all fully, so I will concentrate on some of those that are best described and understood, and that have a detailed physiological effect in response to light.

Phytochrome Interacting Factor 3 (PIF3) was isolated from a yeast two-hybrid screen using the non-chromophoric C-terminal of phyB as bait and was identified as a member of the 162-member basic helix-loop-helix (bHLH) transcription factor family (Ni *et al.,* 1998). Subsequent *in vitro* pull down experiments showed that the interaction of phyB with PIF3 is stronger if the full-length chromophoric phyB protein is used than with the non-chromophoric C-terminal, which was used as bait (Huq & Quail, 2002). In addition, it was demonstrated that the binding of PIF3 to phyB requires phyB to be in the P_{FR} form and that binding is reversible upon conversion of phyB to the P_R form (Ni *et al.,* 1999). PIF3 was also found to interact with phyA, but with lower affinity than for phyB (Zhu *et al.,* 2000). This suggests that the interaction between phyB and PIF3 *in planta* would be light dependent and possibly have an effect on gene transcription. Indeed, it was found that PIF3 is constitutively nuclear and that it binds to a G-box DNA core motif found in light-responsive genes such as ribulose-1,5-bisphosphate carboxylase/oxygenase small subunit 1A (RBCS-1A) and Long Hypocotyl (LHY) (Martínez-García *et al.,* 2000). As phyB is transported to the nucleus upon light-treatment (Mas *et al.,* 2000), this suggests that a physical interaction could occur between the two proteins. Microarray experiments using a PIF3-null mutant (*pif3*) showed that PIF3 induces the expression of a number of genes encoding proteins ultimately destined for the chloroplast (Monte *et al.,* 2004), indicating that PIF3 plays an early role in chloroplast biogenesis when etiolated plants are exposed to one hour of red light through the action of phytochromes.

In addition to PIF3, a number of other bHLH transcription factors have been identified at some level as having a role in photomorphogenesis and/or as phytochrome interacting partners (reviewed in Quail, 2007). This would provide a mechanism for phytochromes to light-regulate the transcription of many suites of genes through their interaction with the appropriate transcription factors.

A second phytochrome-interacting partner, PKS1, was also identified by yeast two-hybrid screening, this time using the 160 amino acids at the C-terminus of phyA as bait (Fankhauser *et al.,* 1999). Like PIF3, PKS1 can bind to both full-length phyA and phyB, but the presence or absence of chromophore has no effect on the interaction and PKS1 shows equal affinity for the P_R and P_{FR} forms of both phytochromes (Fankhauser *et al.,* 1999). However, *in vitro* studies using recombinant oat phyA showed that the N-terminal of PKS1 was phosphorylated on serine and threonine residues by phyA and the level of phosphorylation was over 2-fold higher when phyA was in the activated P_{FR} form (Fankhauser *et al.,* 1999). As PKS1 is found in the phosphorylated form in seedlings grown under continuous red light and un-phosphorylated in dark-grown seedlings, this suggests that phyA can act as a light-activated kinase (Fankhauser *et al.,* 1999). Therefore, there is evidence of two possible means for light to regulate the activity of phy-interacting proteins: either by promoting the interaction between phys and an interacting partner by spatial regulation of phy; or by causing phosphorylation of the interacting partner by phy in response to light although the interaction is light-independent, such as the light-mediated phosphorylation of PIF3.

In addition to phy-specific signalling pathways, there is evidence that phys play a role in modulating the physiological responses mediated by other photoreceptors. Yeast two-hybrid and *in vitro* pull-down studies have shown that the non-chromophoric C-terminal of phyB interacts with the putative blue-light receptor, Zeitlupe (ZTL; Jarillo *et al.,* 2001). However, further yeast two-hybrid studies show no interaction between full-length phyB and ZTL (Kevei *et al.,* 2006), and as yet, no functional significance has been identified for this interaction. Phytochromes also appear to interact with cryptochromes (cry). The C-termini of phyA and cry1 interact *in vitro* (Ahmad *et al.,* 1998c) and fluorescence energy resonance transfer (FRET) studies show that phyB and cry2 co-localise in the nucleus in response to light (Mas *et al.,* 2000). However, a biological function for the interaction between these two classes of photoreceptor remains to be elucidated, although both phys and crys are known to be involved in the photoperiodic control of flowering.

1.2.4 Introduction to Cryptochromes

Cryptochromes (cry) are photoreceptors for blue and UV-A light (320-500 nm) and can essentially be categorised into three basic groups: plant cryptochromes, animal cryptochromes and cry-DASH (the cry-DASH subfamily is named because of the similarity of its members to cryptochromes from _Drosophila_, _Arabidopsis,_ _Synechocystis_ and _Homo sapiens_). The first cryptochrome gene (_HY4_) identified was from _Arabidopsis_ and encodes the protein cry1 (Ahmad & Cashmore, 1993). Subsequently, the gene encoding cry2 (_FAH1_) was identified (Lin _et al.,_ 1996), and recently a third cryptochrome, cry3 (a member of the cry-DASH subfamily) has been identified in _Arabidopsis_ (Kleine _et al.,_ 2003). Cryptochromes share similar structures to their probable ancestors, prokaryotic DNA photolyases, at the N-terminal but do not show any photolyase activity which suggests that they perform a different role in plants (Lin _et al.,_ 1995; Malhotra _et al.,_ 1995). Indeed, cry1 and cry2 are involved in blue light-mediated responses including inhibition of hypocotyl elongation, leaf and cotyledon expansion, stomatal opening, changes in gene expression and entrainment of the circadian clock.

1.2.5 Cryptochrome structure and function

In _Arabidopsis,_ cry1, cry2 and cry3 have an N-terminal photolyase-related (PHR) domain which binds two chromophores: flavin adenine dinucleotide (FAD) and the pterin, methenyltetrahydrofolate (MTHF), which acts as the light-harvesting chromophore (Fig. 1.1; Sancar, 1994; Lin & Todo, 2005). The C-terminal region of cryptochromes is less conserved however, and is longer in plant than in animal cryptochromes and is lacking entirely from cry-DASH proteins (Fig. 1.1). Despite the overall lack of similarity between the C-termini of cryptochromes, plants show three identifiable amino acid sequence motifs in the C-terminal region, collectively known as the DAS domain because of the amino acids prevalent in the domain (Lin & Shalitin, 2003). Consequently, in _Arabidopsis,_ cry1 and cry2 contain a C-terminal domain, (cry C-terminal, CCT), and cry3 does not. Instead, cry3 has an N-terminal extension which contains the DAS domain (Batschauer _et al.,_ 2007).

The lack of a C-terminal domain is not the only difference between _Arabidopsis_ cry1, cry2 and cry3. Crystal structures have been resolved for the PHR domain of cry1 (Brautigam _et al.,_ 2004) and for cry3 (Huang _et al.,_ 2006). These

reveal that the FAD binding cavity of cry3 has a positively charged groove with the potential to bind single stranded DNA, similar to the ability of CPD (cyclobutane pyrimidine dimer) photolyases to bind the pyrimidine dimer of damaged DNA, and consistent with the observation that cry3 binds DNA in a sequence-independent fashion (Kleine *et al.,* 2003; Huang *et al.,* 2006). Recently is has been shown that cry3 can bind to single stranded DNA and repair CPD damage and the authors propose that cry3 should be re-classified as a photolyase (Selby & Sancar, 2006). The FAD binding pocket of the cry1 PHR does not have this DNA binding groove which suggests it may not bind DNA directly (Brautigam *et al.,* 2004; Lin & Todo, 2005) and although cry2 has been shown to associate with chromatin (Cutler *et al.,* 2000), only cry3 has been definitively shown to bind to DNA.

Most work has been carried out on cry1 and cry2 since they were discovered before cry3, so the remainder of this introduction to the cryptochrome family of blue light receptors will concentrate on cry1 and cry2. Cry1 and cry2 are predominantly nuclear localised where they regulate gene expression and entrain the circadian clock. A proportion of cry1 moves to the cytosol upon exposure to light, whereas cry2 is rapidly degraded in response to light and it has been proposed that this degradation is promoted by cry2 itself (Ahmad *et al.,*1998a; Lin *et al.,* 1998; Kleiner *et al.*, 1999; Yang *et al.,* 2000). The CCT of both cry1 and cry2 have been shown to mediate a constitutively morphogenic phenotype (COP) in darkness when expressed in *Arabidopsis* as a fusion protein with β-glucuronidase (GUS; Yang *et al.,* 2000), suggesting that the N-terminal, chromophore-binding region acts as a negative regulator of CCT activity in the dark. A subsequent study showed that the function of the CCT of cry1 and cry2 in mediating the COP phenotype is dependent on the formation of multimers by GUS (Sang *et al.,* 2005). In a manner analogous to GUS multimerisation, the N-terminal of cry1 (CNT1) mediates homodimerisation of cry1 in a light-independent manner which is then modified by exposure to light resulting in activation of the cry1 signalling pathway (Sang *et al.,* 2005).

1.2.6 Cryptochrome signalling
Perhaps the best understood method of cry signalling comes from the studies associated with over-expressing the C-terminal domains of cry1 and cry2 which resulted in a COP phenotype (Yang *et al.,* 2000). COP1 is an E3 ubiquitin ligase that

contains a ring finger domain, a coiled coil region and a WD-40 repeat (Yang *et al.,* 2000). COP1 functions to target the basic leucine zipper (bZIP) transcription factor Long Hypocotyl 5 (HY5) for degradation in the dark (Hardtke *et al.,* 2000). In the light, however, COP1 levels in the nucleus decrease which results in less degradation of HY5 and consequently, increased transcription of photomorphogenesis-associated genes by HY5 (von Armin & Deng, 1994; Osterlund & Deng, 1998). Both the C-teminal regions of cry1 and cry2 bind to the WD-40 repeat of COP1 in a light-independent manner (Yang *et al.,* 2001; Wang *et al.,* 2001). Therefore, it is likely that light activation of cry functions to inhibit the activity of COP1 and/or facilitate its removal from the nucleus in order to prevent degradation of HY5 and allow expression of photomorphogenic genes. It is possible that this is a result of blue light-dependent phosphorylation as CCT2 was found to be constitutively phosphorylated in transgenic plants expressing CCT2 (Shalitin *et al.,* 2000; Yang *et al.,* 2000), and cry1 has been found to have auto-kinase activity (Özgür & Sancar, 2006). When CCT1 and CCT2 are fused to GUS it appears that they are constitutively in the same signalling state as light-activated full-length cry proteins and therefore, the photosensory N-terminal of crys must negatively regulate the activity of the C-terminal region in the dark.

In the same *in vitro* studies that identified phyB as an interacting partner for ZTL (see Section 1.2.3), Jarillo *et al.* (2001) showed that the C-terminus of cry1 also interacts with ZTL. However, a biological function for this interaction has yet to be identified *in planta* (Jarillo *et al.,* 2001).

This is by no means a comprehensive list of cry signalling and is intended merely as an introductory description to some of the mechanisms employed by photoreceptors in plants to bring about physiological responses to light. Calcium has also been implicated in both cry and phyA mediated signalling to regulate hypocotyl development via an EF-hand-containing protein (Guo *et al.,* 2001) and a protein phosphatase has been shown to have a role in the regulation of hypocotyl elongation by crys (Møller *et al.,* 2001). As knowledge of the cry photocycle is still incomplete, many primary signal transduction steps remain to be determined, although progress is being made to elucidate the cry photocycle (Zeugner *et al.,* 2005; Bouly *et al.,* 2007; Banjeree *et al.,* 2007).

1.2.7 The ZTL/ADO family

As described in detail later, the LOV domain is a blue light-absorbing photsensory module that binds FMN or FAD as chromophore. Although phototropins are the only proteins in *Arabidopsis* that contain two consecutive LOV (light, oxygen or voltage-sensing) domains, there are several other single LOV domain-containing proteins encoded in the *Arabidopsis* genome (Christie, 2007). Three of these proteins form a family of putative blue-light receptors thought to be involved in entrainment of the circadian clock.

ZEITLUPE (ZTL) was the first member of the family to be identified in a screen for *Arabidopsis* mutants with an altered circadian clock (Somers *et al.,* 2000) and was also identified from separate screens at roughly the same time and is also known as ADAGIO (ADO; Kiyosue & Wada, 2000; Nelson *et al.,* 2000; Jarillo *et al.,* 2001). Both Zeitlupe and Adagio refer to the phenotype of plants with a mutation in the *ZTL* locus which show an elongated circadian period that is more prominent in low light intensities compared to high light intensities (Somers *et al.,* 2000). The light dependency of this phenotype lends weight to the idea that ZTL functions as a photoreceptor to entrain the clock, but it also appears to have a more central role in clock maintenance as plants grown in completely dark conditions also exhibit a long-period phenotype (Somers *et al.,* 2004). Moreover, it has been shown recently that ZTL is a photoreceptor for blue light (Kim *et al.,* 2007). Oscillation of ZTL protein levels requires a direct interaction between ZTL and GIGANTEA (GI), which is promoted by absorption of blue light by the LOV domain of ZTL (Kim *et al.,* 2007). Because GI protein levels are under control of the circadian clock, this confers a rhythmicity onto ZTL which in turn regulates degradation of the clock protein Timing of Cab Expression 1 (TOC1; Kim *et al.,* 2007).

The second member of the family to be identified was FKF1 (flavin-binding, kelch repeat, F-box1; Nelson *et al.,* 2000). FKF1 functions to regulate flowering time in response to day length by controlling the expression and activity of CONSTANS (CO) which is a key factor required for the photoperiodic control of flowering (Imaizumi *et al.,* 2003).

LKP2 (LOV, Kelch Protein 2) was the third member of the family to be isolated from a screen for novel proteins in *Arabidopsis* that contain a LOV domain (Schultz *et al.,* 2001). Over-expression of LKP2 results in arrhythmic phenotypes for

several circadian responses and alters the photoperiodic control of flowering (Schultz *et al.,* 2001).

ZTL, FKF1 and LKP2 all share three characteristic domains: an N-terminal LOV domain followed by and F-box motif and then six kelch repeats at the C-terminus (Fig. 1.1). The LOV domains of the members of this family contain the eleven conserved residues necessary for binding the flavin chromophore, flavin mononucletide (FMN), and undergo photochemistry to form a covalent adduct between FMN and a conserved cysteine residue within the LOV domain (Imaizumi *et al.,* 2003). In this respect they are similar to the LOV domains of phototropins which are described in detail below (see Section 1.4.2); however, unlike phototropins the LOV domains of the ZTL/ADO family fail to revert to inactive dark state over time (Imaizumi *et al.,* 2003). The F-box motif is typically found in E3 ubiquitin ligases which target proteins for degradation by the ubiquitin proteasome system (UPS; Smalle & Viestra, 2004). Recent results show that ZTL and LKP2 are part of SKP1-Cullin1-F-box (SCF) complexes *in vivo* (Han *et al.,* 2004). FKF1 interacts with and controls degradation of the transcription factor cycling Dof factor 1 (CDF1), which controls transcription of Constans (CO) (Imaizumi *et al.,* 2005) and ZTL controls degradation of Pseudo-Response Regulator 5 (PRR5), a component of the central oscillator (Kiba *et al.,* 2007). The kelch repeats found within this family of proteins form a β-propeller structure thought to confer specificity to the proteins they interact with (Smalle & Viestra, 2004). Indeed, the C-terminal domains of FKF1 and LKP2 are necessary for their interaction with CDF1 (Imaizumi *et al.,* 2005) and, as mentioned earlier, the C-terminal region of ZTL interacts with the C-termini of both phyB and cry1 (Jarillo *et al.,* 2001). These results are consistent with the notion that members of the ZTL/ADO family have a role in light input into the circadian clock and also direct other clock-associated proteins for proteolysis (Kim *et al.,* 2007; Kiba *et al.,* 2007).

As FKF1 and ZTL have now been confirmed as *bona fide* photoreceptors, it is likely that LKP2 will subsequently be proven to be a true photoreceptor with a role in circadian clock entrainment to regulate flowering time, given the similarity in structure and function between them.

1.2.8 Unidentified photoreceptors in *Arabidopsis*

There is a wealth of knowledge regarding photoperception by plants in the UV-A/blue and red/far-red regions of the spectrum but in reality this only covers a fraction of the light that plants are exposed to in natural conditions. Although red and blue light are the most photosynthetically and photomorphogenically important, it seems unlikely that plants would have failed to evolve photoreceptors that could intercept other wavelengths of light.

As green light is readily transmitted through plant tissues (Folta & Maruhnich, 2007), the ability to detect these wavelengths would alert plants to competition for light from neighbours, in much the same way as shade avoidance syndrome is mediated by the ability of phytochromes the determine the ratio of red to far-red wavelengths of light (Franklin & Whitelam, 2007). There has been limited recent work on the effects of green light on plant growth, but the studies available suggest that green light is antagonist to the effects of red and blue light. This may be due in part to the ability of green light to reverse the photocycle of crys (Banjeree *et al.,* 2007; Bouly *et al.,* 2007) but there is also evidence to suggest a cry-independent pathway for green light signalling. A study investigating the effects of different wavelengths of light on the rapid inhibition of hypocotyl elongation found that all wavelengths from UV to far-red rapidly suppressed hypocotyl elongation, with the exception of green light which caused a transient increase in growth rate to 150% of that in dark-grown seedlings (Folta, 2004). This was not due to cryptochromes or phototropins, and although phytochromes modulated the response they were not responsible for it. Another report showed that zeaxanthin is involved in green light reversal of blue-light induced stomatal opening but phototropins are not involved in this aspect of stomatal opening (Tabott *et al.,* 2006; see Section 1.5.2 for further discussion of the role played by phototropins in stomatal opening). Other studies are consistent with the idea that light enriched in green regions of the spectrum attenuates the promotion of growth caused by red and blue light. Phys and crys form species that can absorb in the green region of the spectrum, but these spectral species are generally extremely short lived and a specific photoreceptor for green light remains to be identified.

Around 7% of the electromagnetic radiation emitted from the sun is in the UV region of the spectrum, and while atmospheric gases absorb all the highest energy UV-C wavelengths, some UV-B (280-320nm) is transmitted through the ozone layer to

Earth (Frohnmeyer & Staiger, 2003). High levels of UV-B cause extensive photodamage, while at low levels, UV-B can act as a developmental signal to promote photomorphogenesis (Paul & Gwynn-Jones, 2003). Consequently, high levels of UV-B could be perceived by plants through general stress response pathways, but how plants perceive low levels of UV-B remains a mystery. It seems likely that there is a mechanism for sensing low intensity UV-B as low doses of UV-B can enhance phyB-mediated cotyledon expansion in a pathway that does not involve phys, cry or DNA in the perception (Boccalandro *et al.,* 2001). Additionally, photomorphogenic responses mediated by phys, crys and phototropins can all be induced by UV-B in the absence of these receptors (Kim *et al.,* 1998; Schinkle *et al.,* 1999; Suesslin & Frohnmeyer, 2003). Signalling components of UV-B perception have been identified. Mutations in the UVR8 locus block the flavanoid biosynthesis pathway responsible for producing plant "sunscreens" in response to UV-B, and *uvr8* mutants fail to induce up-regulation of *HY5* in response to UV-B resulting in plants that show increased sensitivity to UV-B (Kliebenstein *et al.,* 2002; Brown *et al.,* 2005). However, the photoreceptor for UV-B remains to be identified.

1.3 The phototropins

It has been well over one hundred years since the initial, detailed descriptions of blue light-induced bending in etiolated coleoptiles were made (Darwin, 1881), however, it is only relatively recently that the genes responsible for this response have been identified. Briggs and colleagues observed that a plasma-membrane associated protein of around 120kDa in size was phosphorylated in response to blue light and this corresponded to the phototropic response shown by etiolated pea hypocotyls suggesting that this protein could be involved in the phototropic response (Gallagher *et al.,* 1988; Reymond *et al.,* 1992; Palmer *et al.,* 1993).

1.3.1 Discovery of the phototropins

To try to identify the genes involved in the phototropic response, Liscum and Briggs (1995) screened populations of *Arabidopsis* seedlings mutagenised by fast neutron bombardment and T-DNA insertion, and by a classical genetic approach revealed four loci involved in phototropism: *non-phototropic hypocotyl 1 (NPH1), NPH2, NPH3 and NPH4*. Focussing on characterisation of the *NPH1* locus, it was found that mutations

in this locus resulted in abolishment of the phosphorylation of the membrane-associated protein and a total loss of phototropic curvature in the seedlings (Liscum & Briggs, 1995). Subsequent analysis showed that the NPH1 protein was indeed autophosphorylated in response to blue light, that it bound the flavin co-factor, flavin mononucleotide (FMN), and that the fluorescence excitation spectrum for insect cell-expressed NPH1 correlated closely with the action spectrum for phototropism in alfalfa (Christie *et al.,* 1998). And so, the first photoreceptor for phototropism was identified. A search of the *Arabidopsis* genome revealed a gene with 58% sequence identity to *NPH1,* which was designated *NPL1* (<u>*NPH1*-L</u>ike; Jarillo *et al.,* 1998).

Following identification of genes homologous to *NPH1* and *NPL1* from other plants species, it was decided to clarify the nomenclature of phototropin genes using the terminology already in place for phytochromes. Hence, the *NPH1* gene became *PHOT1* and *NPL1* was renamed *PHOT2; PHOT* being the shortened form of "phototropin", reminiscent of the phototropic response from which the gene was identified (Briggs *et al.,* 2001). From this point, wild-type genes are designated *PHOT1* and *PHOT2*; mutated genes are *phot1* and *phot2;* the holoproteins (which have the FMN bound to them) are phot1 and phot2 while the apoproteins are PHOT1 and PHOT2 (Briggs *et al.,* 2001).

1.3.2 Evolutionary context of phototropins

Phototropins have been identified from a number of higher plants species in addition to *Arabidopsis*, including oat (*Avena sativum*), maize (*Zea mays*), rice (*Oryza sativa*) and pea (*Pisum sativum*), indicating that phototropins are widely conserved throughout higher plants. However, the presence of phototropins is not restricted to higher plants as they have also been identified in the fern, *Adiantum capillus-veneris* which has two phototropins (Nozue *et al.,* 1998), and the moss *Physcomitrella patens* which has four phototropins (Kasahara *et al.,* 2004). In addition to this, the filamentous green algae *Mougeotia scalaris* has two phototropins (Kagawa & Suetsugu, 2007), and the unicellular green algae *Chlamydomonas reinhartii* has one phototropin (Huang & Beck, 2003).

Phylogenetic analysis of phototropin protein sequences indicate that the *Chlamydomonas* phot sequence is ancestral to true plant phot sequences and is probably most similar to the *PHOT* ancestral gene from which plant *PHOTS* evolved

(Lariguet & Dunand, 2005). Phot1 and phot2 clades seem to have been caused by a major duplication event after the occurrence of seed plants but before the divergence of monocotyledonous and dicotyledonous plants, resulting in *PHOT1* genes being more similar to other *PHOT1* genes from different species than to *PHOT2* genes from the same species. Phototropins appear to be restricted to green plants and the evolutionary conservation of at least two phototropin genes is apparent in all species investigated with the exception of *Chlamydomonas*. This suggests that the presence of two phots in green plants is necessary for the role of optimising photosynthesis and that the phot in *Chlamydomonas* is more ancestral, consistent with its differing role in the sexual cycle of the unicellular algae (Ermilova *et al.,* 2004).

An unusual chimeric light receptor has been identified in both ferns (*Adiantum;* Kawai *et al.,* 2003) and green algae (*Mougeotia;* Suetsugu *et al.,* 2005b). The *NEOCHROME* (*NEO*) genes encode proteins of approximately 1500 amino acids in size (Suetsugu & Wada, 2007) that comprise the photosensory domain of a phytochrome fused to the N-terminal of an entire phototropin photoreceptor (Fig. 1.1). The phot-like neo proteins formed an independent branch after the appearance of seed plants and show more similarity to phot2 proteins than to phot1 proteins (Lariguet & Dunand, 2005). Neo proteins sense and respond to both red and blue light, and the presence of both wavelengths results in a synergistic response (Kanegae *et al.,* 2006). This is thought to have been particularly important for the growth and development of ferns in the Cretacious period when angiosperms proliferated and created dense canopies of taller vegetation under which ferns had to grow (Kanegae *et al.,* 2006, Kagawa & Suetsugu, 2007). However, perhaps the most interesting observation is that *NEO* genes have apparently arisen twice during plant evolution, suggesting an extremely important role for neo photoreceptors in cryptogamic plants. *Adiantum* plants with a mutation in the *NEO1* gene can be rescued by transformation with *MsNEO1* or *MsNEO2* suggesting that regardless of the origin, the functional role of neo is conserved throughout ferns and algae (Suetsugu *et al.,* 2005b).

1.4 Light sensing by the phototropins

1.4.1 Protein structure

The structure of phototropins can essentially be divided into two parts. At the N-terminal region is a light-sensing domain and at the C-terminus of the protein is a serine/threonine kinase domain (Fig. 1.1).

The N-terminal photosensory region comprises two very similar domains of ~110 amino acids in length, designated LOV1 and LOV2. These domains are members of the large and diverse PAS (Per, ARNT, Sim) domain superfamily which are associated with co-factor binding and protein-protein interactions (Taylor & Zhulin, 1999). A subset of this family particularly sense l̲ight, o̲xygen and v̲oltage, hence the acronym, LOV. The LOV domains of phototropins each bind one molecule of the chromophore FMN and function as blue-light sensors (Christie *et al.,* 1999; Salomon *et al.,* 2000).

The kinase domain at the C-terminal region of phototropins is a member of the AGC family of serine/threonine kinases (cAMP-dependent protein kinase (PKA), cGMP-dependent protein kinase G (PKG) and phospholipid-dependent protein kinase C (PKC)) and falls into subfamily AGC-VIIIb (Hanks & Hunter, 1995; Bogre *et al.,* 2003). While the kinase domain of phototropins is closely related to the catalytic subunit of PKA (sub-family AGC-I), there are two noticeable differences between them. Firstly, an amino acid extension between the sub-domains VII and VIII of phototropin kinases is not present in PKA. The presence of this extension is consistent for other members of the AGC-VIII sub-family, although the length and sequence of the insert varies between kinases (Watson, 2000). As sub-domain VIII plays a role in substrate recognition (Hanks & Hunter, 1995), it possible that this extension may confer specificity to the proteins that are phosphorylated by a particular kinase from the sub-family. Secondly, other members of the AGC family usually contain the amino acid motif DFG which is located in sub-domain VII and is required for chelating the Mg^{2+} ion necessary for phosphate transfer (Knighton *et al.,* 1991), while sub-domain VII of the phototropins contains a DFD motif where the initial aspartate residue is necessary for Mg^{2+} binding (Hanks & Hunter, 1995, Watson, 2000).

1.4.2 LOV domain structure and function

Large quantities (milligrams) of purified LOV domains can be obtained by expressing them in bacteria, either separately or together with the linker region that joins them. Expressing LOV1 and LOV2 together with the intervening linker region (LOV1+LOV2) in bacteria results in a truncated protein with more similar photochemical characteristics to the full-length phototropin protein than if the LOV domains are expressed separately (Kasahara et al., 2002). Because of their ability to bind the chromophore FMN, LOV domains appear yellow in colour and emit a strong green fluorescence when illuminated with UV light. This property of the LOV domains has greatly facilitated studies of their photochemistry, as the photocycle can be monitored by absorbance or fluorescence microscopy (Christie, 2007).

Crystal structures have been determined for the LOV2 domain of *Adiantum* and the LOV1 domain of *Chlamydomonas* (Crosson & Moffat, 2001, Crosson & Moffat, 2002, Federov et al., 2003). The structures reveal that the five anti-parallel β-strands are flanked by three α-helices to form a structure with a central cavity where the flavin is located (Fig 1.2A; Crosson & Moffat, 2001). The general structure of the LOV domains are similar to the PAS domains from a diverse range of proteins, but the position of and the co-factor that is bound show considerable variation between members of the PAS domain superfamily. Although amino acid sequences may be divergent among members of the PAS domain-containing family, the structure of the co-factor binding fold is conserved suggesting these evolutionarily conserved domains form part of key signal-transduction pathways in a variety of organisms (Crosson & Moffat, 2001).

In the dark state, 11 conserved residues within the LOV domain hold the flavin moiety in place by hydrogen binding and van der Waals forces (Crosson & Moffat, 2001). This spectral species absorbs maximally in the blue region of the spectrum at approximately 447nm (LOV$_{447}$; Christie et al., 1999; Salomon et al., 2000). Irradiation by blue light results in formation of a cysteinyl-adduct between the C(4a) carbon of FMN and a conserved cysteine residue at amino acid position 39 within the LOV domain (Fig 1.2B; Salomon et al., 2000; Crosson & Moffat, 2001). The conserved cysteine residue is essential for formation of the adduct, as mutation of the cysteine to alanine or serine abolishes photochemical reactivity (Salomon et al., 2000). Initial absorption of blue light by the FMN chromophore results in formation of an excited

singlet state, which subsequently decays into a flavin triplet state which absorbs maximally in the red region of the spectrum (LOV$_{660}$; Swartz *et al.,* 2001; Kennis *et al.,* 2003; Kotte *et al.,* 2003). Decay of the triplet state then results in formation of the flavin-cysteinyl adduct. Formation of the flavin-cysteinyl adduct occurs in the order of microseconds and results in a spectral species (LOV$_{390}$) which absorbs maximally in the near-UV region of the spectrum at 390nm and slowly (tens to hundreds of seconds) decays back to the LOV$_{447}$ form in the dark (Salomon *et al.,* 2000; Swartz *et al.,* 2001; Kasahara *et al.,* 2002). Thus, the LOV domain undergoes a photocycle between the inactive LOV$_{447}$ state where the FMN chromophore is non-covalently bound and the active LOV$_{390}$ state when FMN is covalently bound by the cysteine adduct to the LOV domain. LOV$_{390}$ is proposed to be the active, signalling state.

1.4.3 Functional role of the LOV domains

While the crystal structures of LOV1 and LOV2 are very similar and each domain binds one molecule of the FMN chromophore, there are differences between the domains when quantum efficiencies and photochemical reaction kinetics are investigated (Christie *et al.,* 1999; Salomon *et al.,* 2000; Kasahara *et al.,* 2002). Expression of individual LOV domains in *Escherichia coli* has shown that LOV2 has a higher quantum efficiency for formation of the flavin-cysteinyl adduct than LOV1 for both phot1 and phot2 in a number of species (Salomon *et al.,* 2000; Kasahara *et al.,* 2002). These findings suggest that the LOV domains may have different physiological roles. Indeed, studies abolishing the function of either or both LOV domains by mutagenising the conserved cysteine at position 39 within the LOV domain to alanine have shown that LOV2 is the main light sensor for phot1 and phot2 and is sufficient to induce light-dependent autophosphorylation (Christie *et al*., 2002; Cho *et al*., 2007). Moreover, it was demonstrated that in transgenic *Arabidopsis phot1-5* single mutant plants expression of a mutated form of phot1 with a non-functional LOV1 domain and a functional LOV2 domain was sufficient to complement the phototropic response (Christie *et al.,* 2002). Conversely, functional LOV1 with non-functional LOV2 did not complement the phototropic response, nor could it induce autophosphorylation in response to light (Christie *et al.,* 2002). A separate study using phot2 from *Adiantum* supports the theory that LOV2 is the main functional light sensor in phototropin-mediated responses and shows that the LOV2 domain and residues in the C-terminal

region of the kinase domain are necessary for the chloroplast avoidance response (Kagawa *et al.,* 2004). A further study of the roles of individual LOV domains in *Arabidopsis* has confirmed that LOV2 is the main light sensor not only in phot1 but also in phot2 and is sufficient to restore the phototropic response (Cho *et al.,* 2007). Surprisingly the authors also observed that plants expressing a mutated form of phot2 comprising the functional LOV1 domain and non-functional LOV2 can also induce phototropic curvature at high light intensities and this is sufficient to cause a low level of autophosphorylation (Christie *et al.,* 2002; Cho *et al.,* 2007).

It appears that LOV2 is conserved as the main light-sensing domain in both *Adiantum* and *Arabidopsis,* and is responsible for phototropin-induced responses and autophosphorylation, which poses the question of the functional role of LOV1. Given that the LOV1 sequence is highly conserved and is present in all known phototropins, this suggests that it must play an important functional role in phototropin signalling. It is possible that LOV1 is a site for phototropin dimerisation. Small-angle X-ray scattering showed that bacterially expressed polypeptides of LOV1 from both *Arabidopsis* phot1 and phot2 were homodimeric (Nakasako *et al*., 2004). In addition, a study using oat phot1 LOV1, LOV2 and LOV1+LOV2 domains expressed in bacteria as calmodulin binding peptide (CBP) fusion proteins showed that the LOV1 domain was responsible for the dimerisation shown by the CBP-LOV1+LOV2 fusion protein (Salomon *et al.,* 2004). Although it has not been demonstrated that phototropins homo- or hetero-dimerise *in planta*, the investigation of LOV domain roles in *Adiantum* showed that the presence of phot2 LOV1 was necessary to prolong the lifetime of the phototropin-mediated chloroplast avoidance signal (Kagawa *et al.,* 2004), suggesting that LOV1 may play a role in modulating the activity of LOV2. The hypothesis that LOV1 regulates LOV2 activity is supported by the finding that when individual domains of *Arabidopsis* phot2 are expressed in bacteria, kinase activity is dependent on the light-sensing properties of LOV2 which provides the molecular switch to activate kinase activity in response to light, while LOV1 seems to attenuate the role of LOV2 (Matsuoka & Tokutomi, 2005).

1.4.4 Phototropin structural changes induced by LOV2

It has been shown that light-induced autophosphorylation of phototropins requires functional LOV2 (Christie *et al.,* 2002; Cho *et al.,* 2007) and that LOV2 acts as a negative regulator of kinase activity in the dark (Matsuoka & Tokutomi, 2005). Therefore, LOV2 acts as a molecular light-switch to activate the kinase domain upon exposure of the phototropin molecule to light. However, only minor structural changes have been observed in the LOV2 domain in response to light and appear to be conserved to the immediate vicinity of the FMN-binding pocket (Crosson & Moffat, 2002). In order to transduce light perception from the immediate vicinity of LOV2 to the rest of the phototropin molecule, a larger signal than this would be required. It was later found that a conserved glutamine residue at amino acid position 1029 in LOV2 from *Adiantum* is necessary for the conformational change of the βE sheet region which is observed when the cysteinyl adduct is formed (Nozaki *et al.,* 2004). This larger conformational change is proposed to be a mechanism by which the light signal can be transduced from the flavin binding pocket of the LOV domain to the protein surface. In support of this idea, mutation of the corresponding Gln residue in *Arabidopsis* phot1 LOV2 (Gln575Leu) severely attenuates the light-induced autophosphorylation of the full-length mutated phot1 protein when expressed in insect cells (Jones *et al.,* 2007).

Further to this, nuclear magnetic resonance (NMR) studies using oat phot1 investigated structural changes of the LOV2 domain with a 40-amino acid C-terminal extension. These studies showed that the C-terminal extension included an amphipathic helical region, termed Jα-helix, of about 20 amino acids in length (Harper *et al.,* 2003). In the dark state, the apolar side of the Jα-helix docks onto the β-sheets of the FMN-binding LOV domain. After exposure to light, structural changes caused by formation of the flavin-cysteinyl adduct propagate through the LOV domain to disrupt the structure of the Jα-helix (Harper *et al.,* 2003). Furthermore, it seems that the light-induced changes cause the Jα-helix to become more susceptible to proteolysis by chymotrypsin, presumably because light-induced disruption of the Jα-helix causes proteolytic sites to become exposed. The authors propose that light-induced conformational changes convert LOV/Jα-helix from a "closed" dark state to an "open" light state, and that disruption of the Jα-helix in the light state provides a mechanism to convey light detection from the LOV domain to activate the kinase domain (Harper *et*

al., 2003). This hypothesis is supported by a further study which shows that disruption of the oat phot1 Jα-helix by mutagenesis causes constitutive kinase activity, even when the protein is kept in dark conditions (Harper *et al.,* 2004).

1.4.5 Phototropin kinase activity and autophosphorylation

Studies of the LOV2 domain have revealed that not only does it function to sense light but it also conveys the light signal to the kinase domain by means of structural changes throughout the protein. Furthermore, it appears that LOV2 acts as a dark repressor of kinase activity. This has been demonstrated by a study using bacterially-expressed domains of *Arabidopsis* phot2 (Matsuoka & Tokutomi, 2005). The kinase domain alone constitutively phosphorylates the artificial substrate casein *in vitro*, but when the LOV2 domain is added to the reaction, the phosphorylation of casein by phot2 kinase becomes light dependent, indicating that LOV2 acts as a kinase repressor in the dark. This light dependency requires photochemically active LOV2 as mutation of the conserved cysteine at position 39 within the LOV domain to alanine abolished phosphorylation in both light and dark conditions. The repression of kinase activity by LOV2 is also seen when isolated LOV2 is added to the kinase/casein reaction. Pull-down assays indicate that light activation of the LOV2 domain is sufficient to disassociate the LOV2 domain from the kinase domain in the absence of the Jα-helix (Matsuoka & Tokutomi, 2005). This is surprising because it infers that the presence of the Jα-helix is not necessary for the light sensitive repression of kinase activity by LOV2. Although this study is completely heterologous, it may indicate that there are differences in the modes of signalling when phototropins are phosphorylating a substrate compared to autophosphorylation and that the Jα-helix is not always necessary for phosphorylation activity by the phot2 kinase. Indeed, it has been shown that the LOV1 domain of *Arabidopsis* phot2 can induce a low level of autophosphorylation and is sufficient to restore some phototropic curvature (Christie *et al*., 2002; Cho *et al*., 2007).

The kinase domain of phototropins belongs to the same family of kinases as protein kinase A (PKA), and comparison of the autophosphorylation sites of phot1 extracted from oat coleoptiles with the sites of recombinant oat phot1 phosphorylated by PKA indicates that PKA and the kinase domain of oat phot1 show the same phosphorylation-site specificity (Salomon *et al.,* 2003). This has allowed eight

phosphorylated serine residues located in the N-terminal of oat phot1 to be mapped. Two of the sites (Ser^{27} and Ser^{30}) are located upstream of LOV1, while the remaining six residues (Ser^{274}, Ser^{300}, Ser^{317}, Ser^{325}, Ser^{332} and Ser^{349}) are located in the linker region between LOV1 and LOV2. Light-dependent autophosphorylation of oat phot1 appears to be tightly regulated by light intensity. The area around LOV1 (Ser^{27}, Ser^{30}, Ser^{274} and Ser^{300}) is phosphorylated at low light intensities, followed by Ser^{274} and Ser^{300} at intermediate light intensities and finally Ser^{332} and Ser^{349} are phosphorylated at high light intensities (Salomon *et al.*, 2003). Photoactivated phot1 has been shown to return to the non-phosphorylated state when incubated in the dark (Kinoshita *et al.,* 2003). This is likely due to the action of an as yet unidentified protein phosphatase as the pattern of phosphopeptides during the dark recovery phase of oat phot1 are consistent with the dephosphorylation of existing oat phot1 rather than the synthesis of new phot1. Dephosphorylation has been shown to occur in the reverse order of phosphorylation with the last sites to undergo phosphorylation becoming dephosphorylated first (Salomon *et al.,* 2003). The significance of this fluence-dependent autophosphorylation is not known at present but the authors suggest that as autophosphorylation requires more light than is necessary for phototropin-induced responses (Briggs *et al.,* 2001), phosphorylation of low-fluence sites may induce phototropin signalling while phosphorylation of high-fluence sites may serve to desensitise the receptor (Salomon *et al.,* 2003).

There is some speculation as to the role of phototropin autophosphorylation with regard to the functional roles mediated by phototropin signalling. Phot from *Chlamydomonas* lacks the N-terminal region before LOV1 and about 70 amino acids in the linker region between the LOV domains when compared to higher plant phots. Despite this, *Chlamydomonas* phot can complement phototropin-mediated responses in the *phot1-5phot2-1* double mutant of *Arabidopsis* (Onodera *et al.*, 2005). This suggests that phosphorylation of Ser^{27} and Ser^{30} is not essential for phototropin-mediated responses *in planta* and that the function of phototropins is highly conserved throughout taxa. Further evidence of the ability of phototropins to function without undergoing autophosphorylation comes from a study using *Adiantum*. This shows that a truncated protein comprising functional LOV2 and the kinase domain of phot2 is sufficient to complement the chloroplast avoidance movement in prothallia cells (Kagawa *et al.,* 2004). A protein such as this would not be expected to retain any of the

phosphorylation sites mapped using oat phot1 and must therefore signal by a method other than autophosphorylation to induce the avoidance response. When interpreting results using mutations in one phototropin in a background where another phototropin or neochrome protein is present, it must be remembered that there is evidence for intermolecular signalling between phototropin molecules. Cho *et al.* (2007) showed that functional phot2 expressed in insect cells can cross phosphorylate insect cell expressed phot1, regardless of whether the phot1 kinase was inactivated or the photochemically active cysteine in both the LOV1 and LOV2 domains of phot1 was mutated to alanine. However, a study supporting the theory that phototropin function may be a consequence of substrate phosphorylation rather than autophosphorylation demonstrated that expression of the functional kinase domain of phot2 in the *phot1phot2* double mutant of *Arabidopsis* constitutively causes phot2 responses, even in dark conditions (Kong *et al.,* 2007).

A further consequence for phototropin autophosphorylation may be to promote photoreceptor disassociation from the plasma membrane. Both phot1 and phot2 are hydrophilic proteins and yet are membrane localised (Sakamoto & Briggs, 2002; Kong *et al.,* 2006). This is thought to be a result of a post-translational modification or an interaction with a membrane protein that anchors the phototropin in place. Studies using GFP-tagged phot2 have shown that after illumination with blue light, a proportion of phot2 becomes associated with the Golgi apparatus and this movement from the plasma membrane is dependent on the kinase domain of phot2 (Kong *et al.,* 2006). Not only is the kinase domain necessary for movement to the Golgi, it is also responsible for the association of phot2 with the plasma membrane (Kong *et al.,* 2006). Similarly, phot1 is plasma membrane associated, but approximately 20% of it moves to the cytosol within minutes of blue light exposure (Sakamoto & Briggs, 2002). Therefore, activation of the kinase domain, or autophosphorylation of the phototropin may result in its disassociation from the plasma membrane although the functional significance of this movement is unknown at present.

1.5 Physiological responses mediated by phototropins and the signalling mechanisms involved

The general effects on plant physiology mediated by phototropins serve to increase plant fitness and to maximise photosynthetic efficiency. The adaptive advantage of

these responses is particularly important during seedling establishment and when filling canopy gaps. The main responses mediated by phototropins are discussed in detail below.

1.5.1 Phototropism

Phototropism is the directional curvature of a plant organ (usually the hypocotyl or a stem) in response to unilateral illumination (Wilkins, 1977). Generally, aerial plant organs show positive phototropism and grow towards the source of light whereas roots generally show negative phototropism. However, it must be considered that the majority of phototropic responses studied or casually observed are the cumulative result of both phototropism and gravitropism. For the purposes of this introduction, the effect of the gravity vector will be considered negligible since all data has been obtained with plants subjected to the same gravitational conditions.

Phototropism can be roughly divided into two growth responses. First positive phototropic curvature involves shoots bending towards very low fluence rate pulses of light. These curvatures obey the Bunsen-Roscoe laws of reciprocity in that the same degree of curvature is obtained for a given quantity of light, regardless of the fluence/time combinations used to supply the light (Bunsen & Roscoe, 1862; Christie, 2007). Second positive curvature results in larger organ curvatures and occurs in a time-dependent manner in response to long-term exposure to light (Christie, 2007).

Phototropins function redundantly to mediate phototropism under high light intensities (Sakai *et al.*, 2001), while phot1 alone mediates phototropism under low light conditions (Liscum & Briggs, 1995; Sakai *et al.*, 2000; Sakai *et al.*, 2001). The differing sensitivities to light quantity shown by each of the phototropins may in part be due to the effect of light on their gene expression in additional to the differing quantum efficiencies shown by the LOV domains of each photoreceptor (see above). *PHOT1* gene expression is high in etiolated seedlings and prolonged exposure to light results in a decrease in transcript levels (Sakamoto & Briggs, 2002). Conversely, *PHOT2* transcript levels are increased upon exposure to light (Kagawa *et al.*, 2001) through the activation of phyA (Tepperman *et al.*, 2001).

While phototropins alone provide the directional information required for phototropic curvature, phys and crys play roles in enhancing the response. *Arabidopsis* mutants lacking both phyA and phyB fail to show an enhancement in first positive

phototropic curvature in response to a red light pulse given two hours before unilateral blue light illumination (Janoudi & Poff, 1992; Janoudi *et al.,* 1997) and also require longer exposure to blue light to achieve the same degree of second positive curvature when compared to wild-type (Janoudi *et al.,* 1997). Similarly, *Arabidopsis* mutants lacking both cry1 and cry2 show reduced first positive curvature (Ahmad *et al.,* 1998b) Thus, phys and crys appear to act downstream of phototropins to modulate the phototropic response. The phy-dependent enhancement of phototropic curvature, at least in *Arabidopsis,* is a result of phyA-mediated repression of gravitropism at the same time as phototropins promote phototropism (Stowe-Evans *et al.,* 2001; Lariguet & Fankhauser, 2004). Recently, PKS1 was shown to interact with both phot1 and Non-Phototropic Hypocotyl 3 (NPH3) to play a role in first positive phototropic curvature (Lariguet *et al.,* 2006), and since phys enhance phototropism this may prove to be a point of convergence for signalling between the two photoreceptor families.

Phototropism is the result of the generation of an auxin gradient across the hypocotyl, with higher levels of auxin, or auxin responsiveness, on the shaded side of the hypocotyl. In contrast to this, the irradiated side of the hypocotyl has higher levels of autophosphorylated phototropin (Salomon *et al.,* 1997a; Salomon *et al.,* 1997b). It is still not completely understood how a gradient of phototropin activation can result in an opposing gradient of auxin but characterisation of mutants with altered phototropic responses have provided some clues as to the signalling involved in creating phototropic curvature.

The first phototropin-interacting proteins identified as having a role in phototropism were NPH3 (Liscum & Briggs, 1995; see Section 1.3.1) and Root Phototropism 2 (RPT2; Okada & Shimura, 1992; Sakai *et al.,* 2000). NPH3 and RPT2 are members of a novel, plant-specific family and are thought to act as scaffold proteins to bring members of a signalling complex together. NPH3 is vital for phototropism mediated by phot1 and phot2 (Motchoulski & Liscum, 1999; Inada *et al.,* 2004) and RPT2 is necessary for phot1-mediated phototropism (Sakai *et al.,* 2000). Recently, it has been demonstrated the NPH3 orthologue in rice is necessary for lateral auxin redistribution across the hypocotyl which is necessary to generate phototropic curvature (Haga *et al.,* 2005). Members of the NPH3/RPT2-Like (NRL) family are discussed further in Sections 3.6, 3.10.3 and Chapter 4.

Auxin transport to and from cells is mediated by a number of transporters and facilitators, as well as by the chemiosmotic gradient which also requires transporters. It is generally considered that in aerial tissue when active auxin transport is undertaken, auxin influx is mediated by AUX/LAX transporters (Bennett *et al.,* 1996; Parry *et al.,* 2001) and that efflux is mediated by PIN-FORMED (PIN) proteins and p-glycoproteins (PGP), with PIN1 being involved in polar auxin efflux (Gälweiler *et al.,* 1998) and PIN3 being involved in lateral auxin efflux (Friml *et al.,* 2002). In the root and shoot apices and in the bundle sheath cells of dark-grown tissues, PIN1 co-localises and interacts with PGP19 (Blakeslee *et al.,* 2007). PGP19 is necessary for the correct localisation of PIN1 at the basal region of vascular tissues (Blakeslee *et al.,* 2004) and plants lacking the PGP19 protein (*mdr1-1*) exhibit increased phototropism. This is considered to be the result of the mislocalisation of PIN1 in *mdr1-1* mutants leading to decreased polar auxin transport and a consequent increase in the concentration of cellular auxin available for lateral transport to the shaded side by PIN3 proteins (Noh *et al.,* 2003), but this hypothesis is now being reconsidered due to some uncertainty regarding the relationship between PIN1 and PGP19 (Blakeslee *et al.,* 2007). In addition, it has been shown that phot1 is necessary for sensing unilateral blue light which results in mislocalisation of PIN1 proteins on the shaded side of hypocotyls: again this leads to a decrease in polar auxin transport on the shaded side and consequent increase in auxin concentration leading to curvature of the hypocotyl towards the light source (Blakeslee *et al.,* 2004).

In addition to the creation of an auxin gradient, auxin responsiveness is also necessary for phototropism. Auxin-regulated transcription factors such as Non-Phototropic Hypocotyl 4 (NPH4; Stowe-Evans, *et al.,* 1998; Harper *et al.,* 2000; see Section 1.3.1) and Massugu 2 (MSG2; Tatematsu *et al.,* 2004) are required for normal tropic responses. A recent study used a transcriptomic approach to investigate the effect of tropic stimulation on the expression of genes in the close relative of *Arabidopsis, Brassica oleracea* (Esmon *et al.,* 2006). The study showed that a small subset of genes was differentially regulated on the shaded side of the hypocotyl compared to the irradiated side of the hypocotyl, and that the change in gene expression correlated with higher levels of auxin and was sensitive to auxin transport inhibitors. Interestingly, two of the genes identified encode members of the α-expansin family, EXPA1 and EXPA8, which are involved in mediating the cell wall extension

necessary for phototropic curvature as a growth response (Esmon *et al.,* 2006). RT-PCR experiments in *Arabidopsis* showed that NPH4 was necessary for increased expression of the genes homologous to those induced by tropic stimulus in *Brassica* (Esmon *et al.,* 2006).

1.5.2 Stomatal opening

Stomatal opening is necessary for gaseous exchange between plants and the surrounding atmosphere. Carbon dioxide is taken in by the plants as a substrate for photosynthesis in order to synthesise the carbohydrates required for growth and by return, oxygen and water vapour are released from the plants through the stomatal pore. The opening of the guard cells on either side of the stomatal pore is dependent on an osmotic gradient being created by an increased concentration of potassium and chloride ions (K^+ and Cl^-) in the guard cells which results in increased water uptake by the cells and subsequent swelling causing the stomatal pore to increase in size. Proton extrusion from the guard cell is necessary to achieve the influx of K^+ ions through voltage-gated K^+ channels. Protons are extruded from the cell *via* a plasma membrane localised proton-ATPase (H^+-ATPase) pump that is activated by blue light. In *Vicia faba,* activation of the H^+-ATPase results from phosphorylation of its C-terminus in response to blue light irradiation, and subsequent binding of a 14-3-3 protein (Kinoshita & Shimazaki, 1999). The 14-3-3 protein binds to a phosphorylated tyrosine residue at amino acid position 950 in order to activate the H^+-ATPase (Kinoshita & Shimazaki, 2002). The activation of the H^+-ATPase pump can also be induced by the fungal toxin, fusicoccin which stabilises the interaction between 14-3-3 and the H^+-ATPase and irreversibly activates the H^+-ATPase (Kinoshita & Shimazaki, 2001; Kinoshita & Shimazaki, 2002).

Both phot1 and phot2 act redundantly to mediate stomatal opening in response to a range of blue light intensities (Kinoshita *et al.,* 2001). In a background of red light, additional blue light was supplied and it was observed that the *phot1-5phot2-1* double mutant failed to exhibit stomatal opening nor did it show proton extrusion in response to blue light (Kinoshita *et al,* 2001). It was later found that autophosphorylated phot1 from *Vicia faba* also binds a 14-3-3 protein in response to blue light (Kinoshita *et al.,* 2003). 14-3-3 proteins are members of a multigene family (twelve are expressed in *Arabidopsis*) and are named using Greek letters. The 14-3-3 phi protein (14-3-

3φ, taken to be a typical plant 14-3-3 protein) was found to bind to Ser^{358} of Vfphot1a and Ser^{344} of Vfphot1b which are located in the linker region between the LOV domains (Kinoshita *et al.,* 2003). These sites correspond to Ser^{325} of oat phot1 which is phosphorylated in response to intermediate intensities of light (Salomon *et al.,* 2003). While it is tempting to speculate that 14-3-3s may play a role in a direct interaction between phot1 and the H^{+}-ATPase, this does not appear to be the case as fusicoccin induced 14-3-3 binding to the phosphorylated H^{+}-ATPase in the *phot1-5phot2-1* mutant which suggests that a different kinase present in both wild-type and the double mutant plants phosphorylates the H^{+}-ATPase (Ueno *et al.,* 2005). The functional significance of 14-3-3 binding to the phototropins in stomatal opening has yet to be determined, but further evidence for the role of 14-3-3 in the regulation of stomatal aperture come from a study which shows that over-expression of *Arabidopsis* 14-3-3 lambda (14-3-3λ) in cotton plants leads to an increased tolerance to mild drought stress (Yan *et al.,* 2004). A yeast two-hybrid screen using barley cDNA identified NPH3, two NPH3-like proteins and PIN1 as 14-3-3 interactors (Schoonheim *et al.,* 2006). Given that these proteins are implicated in auxin transport (Section 1.5.1) and that NPH3 interacts directly with phot1 and that 14-3-3s interact with phototropins in other species, confirmation and further investigation of the interactions between these proteins will be interesting.

Downstream of blue light sensing by the phototropins, few proteins involved in the stomatal opening response are known, other than the 14-3-3 protein described above. A novel phot1-interacting protein was recently identified as an interacting protein for Vfphot1a in guard cells of *Vicia faba* (Emi *et al.,* 2005). Yeast two-hybrid studies show that Vfphot1a interacting protein (VfPIP) interacts specifically with the C-terminal of Vfphot1a. A VfPIP-GFP fusion protein was found to be located on cortical microtubules, suggesting that VfPIP association with the microtubules may facilitate stomatal opening in response to blue light. In support of this theory, depolymerisation of microtubules with herbicides caused mislocalisation of VfPIP and partially inhibited H^{+}-ATPase pumping and stomatal opening. Although the function of the VfPIP protein is unknown, it shows some similarity to dynein light-chain proteins. Dyneins are molecular motors found ubiquitously in animals and fungi and are composed of many subunits, however, *Arabidopsis* lacks the heavy dynein chains

necessary for force production by dynein complexes and so the function of light-chain dyneins in *Arabidopsis,* like VfPIP, are currently unknown (Emi *et al.,* 2005).

Genetic and physiological analyses showed that the NRL family member RPT2 functions in phot1-mediated stomatal opening in addition to phot1-mediated phototropism. However, it does not appear that RPT2 plays any role in the phot2-mediated stomatal opening response. The role played by RPT2 in stomatal opening is yet to be elucidated, but it is proposed that members of the NRL family act as scaffold proteins to bring members of signalling complexes together. Therefore, RPT2 may provide an essential link between phot1 and another protein involved in stomatal opening, probably in the region of the plasma membrane (Inada *et al.,* 2004).

Phototropins are not the only blue light receptors involved in stomatal opening. Stomata in the *phot1phot2* double mutant can be forced to open slightly if sufficiently high levels of blue light are given and similarly, the *cry1cry2* double mutant shows limited stomatal opening in response to blue light (Mao *et al.,* 2005). However, a quadruple mutant lacking both phots and both crys shows no blue light-induced stomatal opening, indicating that phots and crys function in tandem to regulate blue light induced stomatal opening (Mao *et al.,* 2005). The study also shows that COP1 is a repressor of stomatal opening as the *cop1* mutant has stomata which were constitutively open. When the triple mutants were examined (lacking either phots or crys and COP1), the stomata of these plants were the same as *cop1,* indicating that COP1 likely functions downstream of both crys and phots in stomatal opening by direct interaction with crys and with an intermediate signalling partner for phots (Mao *et al.,* 2005).

1.5.3 Chloroplast movement

Correct positioning of chloroplasts is essential to maximise light capture for photosynthesis in low light conditions and to avoid photodamage to the organelles in high light conditions. Under low light conditions, both phot1 and phot2 are involved in the chloroplast accumulation response to promote light capture for photosynthesis (Sakai *et al.,* 2001). Phot1 is more sensitive than phot2 and will induce the accumulation response at light intensities higher than 0.4 μmol m^{-2} s^{-1}, while phot2 promotes chloroplast accumulation at light intensities from 2 μmol m^{-2} s^{-1} to between 16 and 32 μmol m^{-2} s^{-1} (Sakai *et al.,* 2001). However, phot2 alone mediates the

chloroplast avoidance response at light intensities higher than 16 μmol m^{-2} s^{-1} (Kagawa *et al.,* 2001; Jarillo *et al.,* 2001; Sakai *et al.,* 2001). When dark-adapted *Adiantum* prothallus cells are irradiated with a high intensity microbeam of blue light, chloroplasts move near to the area irradiated, but never enter it and this response persists in subsequent darkness indicating that the avoidance signal can be retained for some time in the irradiated area (Kagawa & Wada, 2000; Kagawa & Wada, 2002). In wild-type *Arabidopsis* plants at light-intensities over 32 μmol m^{-2} s^{-1} chloroplasts show the avoidance response and so while the light provides both accumulation and avoidance signals, the avoidance signal overcomes the accumulation signal and hence only the avoidance response occurs in high light conditions (Sakai *et al.,* 2001; Kagawa & Wada, 2002).

The exact nature of chloroplast movement is not fully understood at present, but is known to involve changes in the cytoskeleton (Wada *et al*., 2003). Indeed changes in the actin cytoskeleton of the aquatic angiosperm *Vallisneria gigantea* have been observed in response to high-blue light (Sakurai *et al.,* 2005). The authors propose that short, thick actin bundles anchor the chloroplasts in position in dark-adapted cells and that upon exposure to high-intensity blue light the actin fibres stretch out to provide a track for chloroplast movement away from high-intensity light (Sakurai *et al.,* 2005). A screen for mutants lacking chloroplast avoidance has identified the novel F-actin binding protein, Chloroplast Unusual Positioning 1 (CHUP1; Oikawa *et al.,* 2003), which is consistent with the theory that chloroplast movement relies on the actin cytoskeleton. CHUP1 is located at the chloroplast envelope and mutations within the protein results in loss of chloroplast movement and unusual aggregation of chloroplasts at the bottom of palisade cells, suggesting that the protein has a fundamental role in chloroplast positioning and movement (Oikawa *et al.,* 2003). Further studies have revealed that the Plastid Movement-Impaired 1 (PMI1) protein is required for chloroplast movement in response to both high- and low-intensity blue light indicating that PMI1 encodes a protein involved in both accumulation and avoidance responses (DeBlasio *et al.,* 2005). The PMI1 protein appears to be a novel, plant-specific protein which may be responsive to Ca^{2+} (DeBlasio *et al.,* 2005). Furthermore, a screen to isolate mutants impaired in the accumulation response identified a J-domain protein required for the chloroplast accumulation response 1 (JAC1; Suetsugu *et al.,* 2005a). JAC1 also acts with phot2 to

allow chloroplasts to accumulate on the bottom of dark-adapted cells, but JAC1 is not necessary for the phot2-mediated avoidance response. The C-terminal J-domain of JAC1 shows similarity to the clathrin-uncoating factor auxilin which is a protein involved in endocytosis in animal cells, but the biochemical function of JAC1 in chloroplast movement is unknown at present (Suetsugu *et al.,* 2005a).

1.5.4 Other phototropin-mediated responses
In addition to the major responses described above, phototropins are also involved in other blue-light inducible responses, and again, these serve to maximise photosynthetic efficiency and promote plant fitness. While crys mediate most blue-light induced regulation of gene expression, phots show rapidly induced blue-light regulation of some transcription factor genes, mainly in an antagonistic manner to cry regulation (Jiao *et al.,* 2003). A further study shows that phot1 is required to destabilise mRNA transcripts of *Lhcb* and *rbcL* in response to high-fluence blue light (Folta & Kaufman, 2003). Down-regulation of gene expression may be a method by which phototropins can respond to high intensity light to prevent photodamage to cellular components.

Upon exposure to blue light, hypocotyls show a rapid inhibition in the rate of elongation which is mediated by a rapid and transient response by phot1 and a longer-term response mediated by crys (Folta & Spalding, 2001). Phototropin activation leads to an increase in cytosolic Ca^{2+} concentrations (Baum *et al.,* 1999) and pharmacological experiments reveal that changes in cytoplasmic Ca^{2+} levels are required for the phototropin-mediated inhibition of hypocotyl elongation (Folta *et al.,* 2003). It has been shown that the phototropin signalling pathway activates voltage-dependent calcium-permeable channels in response to blue light (Stoelzle *et al.,* 2003). Both phot1 and phot2 can mediate an influx of Ca^{2+} from the apoplast, but only phot2 can release Ca^{2+} from internal stores (Harada *et al.,* 2003). Consistent with other phototropin-mediated responses, phot1 shows greater photosensitivity and caused changes in cytosolic Ca^{2+} levels at lower light intensities (0.1-50 μmol m^{-2} s^{-1}) than phot2 (1-250 μmol m^{-2} s^{-1}; Harada *et al.,* 2003). Changes in calcium levels have been implicated in the phototropin-mediated responses and it is therefore likely that calcium acts as a major secondary messenger after phototropin activation (Harada & Shimazaki, 2007).

Finally, recent work has shown that phototropins play a role in plant leaf orientation which again serves to maximise light capture under lower light conditions. In the leaves of kidney bean plants, movements to face incident light are controlled by a decrease in the turgor pressure of pulvinar motor cells on the irradiated side of the leaf. A recent study indicated that phototropins may function upstream of the H^+-ATPase in order to bring about these changes in turgor pressure (Inuoe *et al.,* 2005). A subsequent study showed that phot1 and NPH3 are both necessary for the blue light-induced leaf positioning and petiole orientation shown when plants grown in a red light background (25 µmol m^{-2} s^{-1}) were supplemented with additional blue light (0.1 µmol m^{-2} s^{-1} ; Inuoe *et al.,* 2007). However, when more blue light was added (5 µmol m^{-2} s^{-1}), phot2 signalling was initiated which restored leaf positioning independently of both phot1 and NPH3 (Inuoe *et al.,* 2007). Therefore, phototropins function to modulate a number of physiological responses *in planta* which promote seedling establishment, increase general fitness and maximise photosynthetic potential.

1.6 Aims of the project

While the mechanisms of phototropin photosensory perception are relatively well understood and the physiological responses mediated by phototropins are well described, there is a significant lack of knowledge in the field about the phototropin signalling that brings about these responses.

At commencement of the project, only two interacting partners had been identified for phot1, NPH3 and RPT2. As phototropins mediate a wide range of blue light-induced responses it was thought likely that many more interacting proteins remained to be identified. Therefore, yeast two-hybrid screening was chosen as a method to identify novel interacting partners for phot1 as this method had previously been used to identify signalling partners for other plant photoreceptors (Section 1.2.3).

It was also unknown whether phototropin autophosphorylation is involved in the receptor signalling pathway, or whether the kinase domain of phototropins can phosphorylate substrates other than phototropins themselves. To investigate the effects of phototropin autophosphorylation, structure/function studies were carried out by expressing a truncated version of phot1 in the double mutant background. Known phot1-mediated responses were investigated to determine the effects of expressing this

truncated region on phot1 signalling. During the course of this project, similar studies have been carried out using *Arabidopsis* phot2 and phototropins from other species which allows the function of various phototropins to be compared.
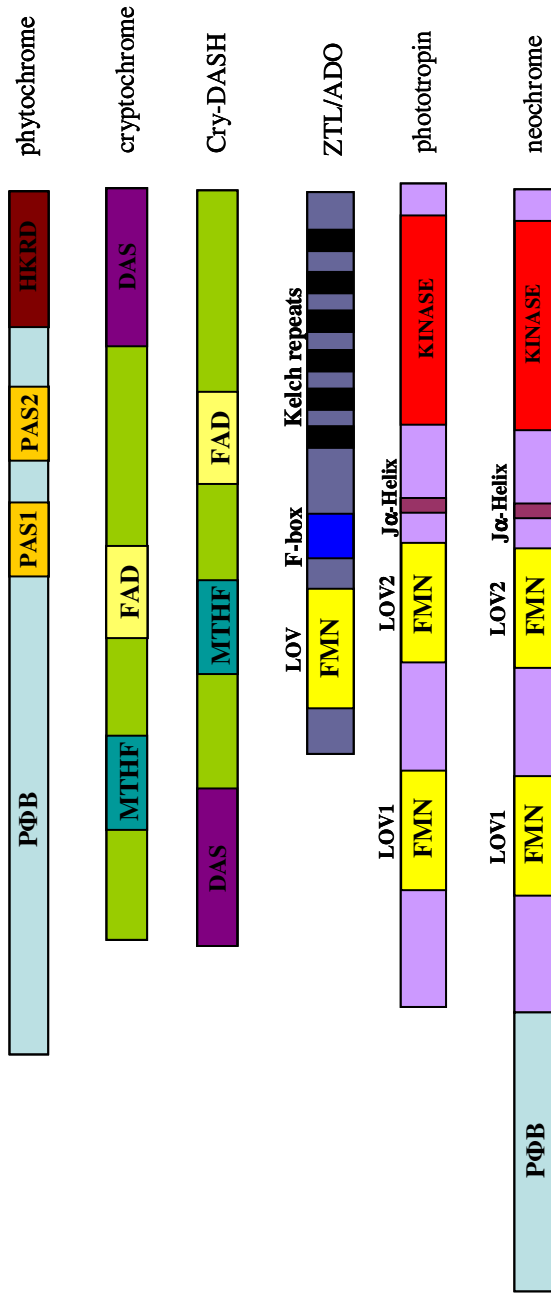
Figure 1.1 Plant photoreceptor domain structure

Schematic diagram illustrating domain structure of general plant photoreceptors. The major domains are indicated. PAS: Per, ARNT, Sim domain; HKRD: Histidine kinase-related domain; DAS: D-motif, A-motif and S-motif, conserved amino acid sequences; LOV: Light, Oxygen or Voltage-sensing domain; KINASE: serine/threonine kinase domain. The chromophores bound by the photoreceptors are also indicated. PΦB: phytochromobilin; MTHF: methenyltetrahydrofolate; FAD: flavin adenine dinucleotide; FMN: flavin mononucleotide.

A
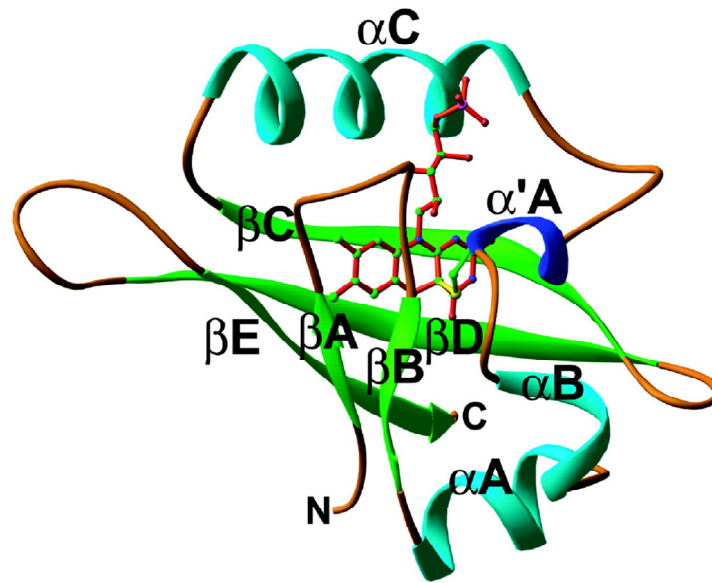
B
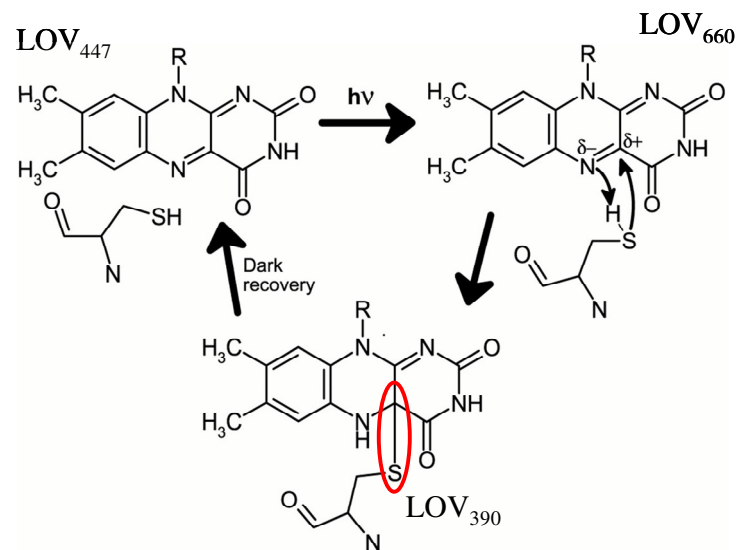
Figure 1.2 LOV domain structure and photochemistry

A) Ribbon diagram of the LOV2 structure from the *Adiantum* neo protein. The flavin mononucleotide (FMN) cofactor is shown in the chromophore-binding pocket of LOV2 as a ball and stick molecule. α-helices and β-sheets are indicated. Taken from Crosson & Moffat, (2002).

B) Schematic diagram of the proposed mechanism for adduct formation between FMN and the conserved cysteine of the LOV2 domain and the dark recovery to ground state. Absorption of blue light by the chromophore FMN held non-covalently in LOV_{447} results in an excited singlet state which decays to a flavin triplet state (LOV_{660}). Decay of LOV_{660} results in formation of the flavin-cysteinyl adduct (circled in red) between FMN and LOV_{390}. LOV_{390} subsequently decays to LOV_{447} in the dark. Taken from Crosson & Moffat, (2001).

Chapter 2: Materials and Methods

2.1 Materials

All chemicals were from Sigma-Aldrich (Poole, Dorset, UK), Fisher Scientific (Southampton) or VWR International Ltd (Poole, Dorset, UK) unless otherwise stated.

All restriction enzymes, T4 ligase, and Taq polymerase, *in vitro* transcription/translation kits and the MagneGST protein purification system were from Promega (Southampton, UK).

All DNA and protein molecular weight markers and Phusion polymerase were from New England Biolabs Ltd. (Hitchin, Hertfordshire, UK).

Radiolabelled ATP (γ-^{32}P) was from Amersham Biosciences UK Ltd. (Bucks, UK)

37.5:1 acrylamide:bis-acrylamide was from Bio-Rad Laboratories (England) Ltd., (Bramley, Kent, UK).

QIA-quick PCR purification kit, QIA-quick gel extraction kit, QIA-prep spin plasmid mini kit, DNeasy DNA isolation kit and RNeasy Plant RNA isolation kit were from Qiagen Ltd. (Crawley, UK).

TOPO® cloning kits and reagents for Gateway® cloning were from Invitrogen Ltd. (Paisley, UK)

2.2 Plant material and growth conditions

Plants of the ecotype Columbia (Col) were used in this study. Wild-type control plants were Col3 or *gl1* depending on the experiment. Glabrous (*gl1*) plants were used in addition to Col3 as wild-type because the phot-deficient mutants were created in a *gl1* background so that any contamination by Col3 plants would be easily identifiable. The parental background of *gl1* plants is Columbia, therefore making them suitable for use in conjunction with Col3 as wild-type controls. The phot-deficient mutants *phot1-5, phot2-1* and *phot1-5phot2-1* have been described previously (Liscum & Briggs, 1995; Kagawa *et al.,* 2001; Kinoshita *et al.,* 2001). Phot1-GFP (Sakamoto & Briggs, 2002), GFP-LTI6b (Culter *et al.,* 2000), *nph3-1* (Motchoulski & Liscum, 1999) have also been described previously. NPH3-L and 14-3-3λ knockout lines in a Columbia background (TAIR stock #CS60000) were obtained from the Nottingham *Arabidopsis*

Stock Centre (NASC; line #010013 and #075219, respectively). Transgenic plants over-expressing GFP-14-3-3λ, full-length phot1, active phot1 kinase, inactive phot1 kinase, phot1 LOV2-kinase, phot1 N$_2$LOV2 were created for use in this study.

Seeds were surface sterilised and grown on 0.5 X Murashige & Skoog (MS) salts containing 0.8% (w/v) agar, supplemented with antibiotic where appropriate. Alternatively, seeds were sown on soil and grown in a controlled environment room (Fititron, Weiss-Gallenkamp, Loughborough, UK) under a 16/8 hour light-dark cycle, unless otherwise described. All seeds were given a 3 day cold treatment at 4°C to induce uniform germination before being placed in the growth room. For phototropism assays germination was induced by a 6 hour white light treatment before plates were wrapped in aluminium foil and grown vertically in the dark. Light intensities used are described in the main text and in Section 2.27. The fluence rates of light sources were measured using a Li-250A and quantum sensor (LI-COR, Lincoln, NE).

2.3 Seed surface sterilisation

Seeds were surface sterilised for 6 min in 1 mL of a solution containing 50% (v/v) sodium hypochlorite (> 6% (w/v) available chlorine), 0.05% (v/v) Triton X-100. Seeds were pelleted by centrifugation at 5,000g for 30 sec before the bleach solution was removed. Seeds were washed 5 times in sterile dH$_2$O and resuspended in an appropriate volume of sterile dH$_2$O before being sown onto 0.5 X MS/0.8% (w/v) agar plates.

2.4 DNA isolation

2.4.1 Plant DNA

Plant tissue was collected and immediately frozen in liquid nitrogen to be used immediately or stored at -70°C. Genomic DNA was isolated using the DNeasy DNA isolation kit (Qiagen, UK) according to the manufacturer's protocol. The quantity and purity of all DNA was determined spectrophotometrically against a dH$_2$O blank as described in Sambrook & Russell (2001), where OD$_{260}$ of 1 = 50μg/mL DNA. The integrity of DNA was determined by 1% (w/v) agarose gel electrophoesis and visualised by ethidium bromide staining.

2.4.2 Plasmid DNA from E.coli

10 mL overnight cultures of *Escherichia coli* containing the plasmid of interest were grown overnight with shaking at 200 rpm, 37ºC. Plasmid DNA was isolated using the QIA-prep spin plasmid mini kit (Qiagen, UK) according to the manufacturer's protocol.

2.4.2 Total DNA from yeast

Total DNA was extracted from yeast by vortexing one large colony of yeast cells in a tube containing 300 µL lysis buffer (2% (v/v) 10% Triton X-100, 10% (v/v) 10% SDS, 100 mM NaCl, 10 mM Tris pH 8.0, 1 mM EDTA) and 500 µL acid-washed glass beads (#G-8772; Sigma-Aldrich) for 6 min. 200 µL of phenol:chloroform:isoamyl alchol (25:24:1 (v/v)) was added and the tubes centrifuged at maximum speed in a microcentrifuge for 5 min. 150 µL of the upper phase was removed to a fresh tube and 0.1 volume of 3 M NaOAc pH 5.2 was added with 2 volumes of ethanol. DNA was precipitated at -20ºC overnight. Samples were spun at maximum speed at 4ºC for 15 min. The supernatant was removed from the tube and the DNA pellet was washed with 70% (v/v) ethanol before centrifuging again. The resulting pellet was allowed to air dry before being resuspended in an appropriate volume of Tris-EDTA buffer (TE) (10 mM Tris-HCl pH 7.6, 1 mM EDTA).

2.5 DNA manipulation and cloning

2.5.1 Primers used in this study

Primers were designed visually or by using online Primer3 software (Rozen & Skaletsky, 2000). Table 2.1 lists the primers used for RT-PCR and identification of knockout lines in this study. Table 2.2 lists the primers used to generate the plasmid constructs used for protein expression in this study.

2.5.2 DNA digestion by restriction enzymes

The DNA to be digested (0.5 µg plasmid DNA or 2.5 µg PCR product) was prepared in 25 µL total volume containing 1 X the appropriate buffer and 2.5 U of the restriction enzyme. Reactions were incubated in a water bath at 37ºC for one hour before DNA

was re-purified using a PCR purification column (Qiagen, UK). The reactions were monitored by running an aliquot of the reaction on an agarose gel.

2.5.3 Gel extraction of DNA

Digested DNA was purified by running the remainder of the digestion reaction on an agarose gel. The appropriate band was excised from the gel and extracted from the gel slice using the Qia-quick Gel Extraction kit (Qiagen, UK) according to the manufacturer's protocol. DNA recovery from the column was monitored by running an aliquot of the reaction on an agarose gel.

2.5.4 Ligation of DNA

DNA was ligated into plasmids after digestion using T4 ligase (Promega, UK). The ratio of DNA insert:vector was 3:1. In a total reaction volume of 20 µL, buffer was added to the DNA at a final concentration of 1 X and 400 U T4 ligase was used. The reaction was allowed to proceed at room temperature for at least 2 hours. DNA was re-purified using a PCR purification column (Qiagen, UK).

2.5.5 Gateway cloning

Constructs used to over-express active phot1 kinase, full-length phot1 and phot1 N_2LOV2 in plants (pGWB17-kinase, pGWB15-phot1 and pGWB15-N_2LOV2, respectively) were created by Gateway® cloning according to the manufacturer's protocols (Invitrogen, Paisley, UK). Expression vectors containing the pGWB backbone were a gift from Dr. A. Sadanandom (University of Glasgow).

Briefly, cDNA was amplified using suitably designed primers and high-fidelity Phusion polymerase and purified to produce blunt-ended PCR products encoding the genes of interest. The PCR products were transformed into the pENTR™ TOPO® vector by TOPO® cloning according to the manufacturer's protocol. Chemically competent TOP10 *E. coli* cells were transformed according to the manufacturer's protocol with the pENTR™ vector and colonies containing the fragment of interest were selected by colony PCR. Plasmid DNA was isolated from positive transformants and used in the LR recombination reaction to insert the coding sequence of interest into the Gateway® destination vector (pGWB series). Chemically competent TOP10

E. coli cells were transformed with the pGWB vector and positive transformants were selected by colony PCR.

2.5.6 Expression vectors created for use in this study

The vectors used to express proteins in this study are described in Table 2.2, along with the primers used to amplify cDNA. Briefly, proteins were expressed in bacteria and yeast using the expression vectors pGBKT7 to generate c-Myc-tagged proteins (Clontech, Takara Bio Inc., Shiga, Japan); and pGEX to generate GST-tagged proteins (G E Healthcare, Bucks. UK). Binary vectors used for protein expression *in planta* were pEZR(K)-LC, modified to remove the GFP-tag (Christie *et al.,* 2002); and pGWB15 (HA-tag) and pGWB17 (c-Myc tag), both a gift from Dr. A Sadanandom, University of Glasgow and which were originally released by Dr Tsuyoshi Nakagawa, Shimane University, Japan.

2.6 Bacterial transformation and growth

Chemically competent *E. coli* cells were transformed with plasmid DNA according to the methods outlined in Sambrook & Russell, (2001). Transformed cells were plated onto Luria-Bertani (LB) broth plates (1% (w/v) tryptone, 0.5% (w/v) yeast extract, 1% (w/v) NaCl, 1.5% (w/v) bactoagar pH 7.5) containing antibiotics where appropriate (100 μg/mL ampicillan or 50 μg/mL kanamycin, filter sterilised and added once the LB had cooled to 50°C) and grown at 37°C overnight. Bacterial colonies containing the plasmids of interest were selected by colony PCR.

Positive transformants were rescued from the pates using a sterile pipette tip and used to inoculate 10 mL LB broth (as above, but omitting the bactoagar) containing appropriate antibiotics. The culture was grown overnight at 37°C in a shaking incubator (200 rpm). Glycerol stocks were made by mixing 500 μL of overnight culture with 500 μL 50% (v/v) sterile glycerol. The mixture was vortexed and frozen in liquid nitrogen before being stored at -70°C.

2.7 DNA sequencing

DNA sequencing was performed by The Sequencing Service (School of Life Sciences, University of Dundee, Scotland, www.dnaseq.co.uk) using Applied Biosystems Big-

Dye Ver 3.1 chemistry on an Applied Biosystems model 3730 automated capillary DNA sequencer.

2.8 RNA extraction

Plant tissue was collected and immediately frozen in liquid nitrogen to be used immediately or stored at -70ºC. Total RNA was extracted from plant tissue by the RNeasy Plant Mini Kit (Qiagen, UK) according to the manufacturer's protocol. The quantity and purity of RNA was determined spectrophotometrically as described in Sambrook & Russell, (2001), where OD_{260} of $1 = 40\mu g/mL$ RNA.

2.9 Polymersase chain reaction techniques

PCR reactions were carried out in a MJ Research DNA Engine PTC-200 Peltier Thermal Cycler (Genetic Research Instrumentation, Braintree, Essex, U.K.) machine.

2.9.1 Polymerase chain reaction (PCR)

DNA was amplified using the following basic PCR programme: 95ºC for 3 min; [95ºC for 30 sec, 50-60ºC for 1 min, and 72ºC for 1 min/kb] for 25 cycles, 72ºC for 5 min. Extension times and annealing temperatures were adjusted accordingly when specific templates or primers required it.

PCR reactions were performed using 0.2 µg DNA in a 25 µL reaction volume containing 1 X DNA polymerase buffer (10 mM Tris-HCl pH 9.0, 50 mM KCl, 0.1% Triton X-100), 1.5 mM $MgCl_2$, 1.0 µM of each primer, 200 µM each of dNTPs and 1 U Taq polymerase (M1861, Promega).

2.9.2 Reverse transcriptase PCR (RT-PCR)

To ensure the elimination of any contaminating DNA, 10 µg of RNA was treated with DNAse for 1 hour at 37ºC and the DNAse was inactivated by adding 5 µL DNAse Inactivation reagent (DNA-*free* kit; AM1906, Ambion, UK). DNAse-treated RNA was removed to a fresh tube and samples were checked for DNA contamination using actin primers. 5 µg of total DNAsed RNA was incubated with 0.4 µM oligo dT for 10 min at 70ºC and then chilled on ice.

Reverse transcription was carried out in a 25 µL reaction volume containing 1 X AMV reverse transcriptase buffer, 1 mM dNTPs, 1 U/µL RNAse inhibitor and 0.4

U/μL AMV reverse transcriptase (M5101, Promega). The reaction was carried out at 48ºC for 45 min. The enzyme was then heat-inactivated at 95ºC for 5 min before the samples were cooled to 4ºC. Samples were used immediately for PCR or stored at -20ºC until they were needed.

PCR reactions were performed using 2 μL cDNA in a 25 μL reaction volume containing 1 X DNA polymersase buffer (10 mM Tris-HCl pH 9.0, 50 mM KCl, 0.1% Triton X-100), 1.5 mM MgCl$_2$, 0.5 μM of each primer, 250 μM each of dNTPs and 1 U Taq polymerase (M1861, Promega).

2.9.3 High-fidelity PCR

For cDNA cloning, high fidelity Phusion™ polymerase (#F-530S, New England Biolabs) was used according to the manufacturer's protocol with the following PCR programme: 98ºC for 30 sec; [98ºC for 10 sec, 45-72ºC for 15 sec, and 72ºC for 15-30 sec/kb] for 25 cycles, 72ºC for 5 min. Extension times and annealing temperatures were adjusted accordingly when specific templates or primers required it.

PCR reactions were performed using 10 ng plasmid DNA or 500 ng genomic DNA in a 50 μL reaction volume containing 1 X Phusion HF buffer (10 mM Tris-HCl pH 9.0, 50 mM KCl, 0.1% Triton X-100), 1.5 mM MgCl$_2$, 0.5 μM of each primer, 200 μM each of dNTPs and 1 U Phusion polymerase.

2.10 Agarose gel electrophoresis

PCR reaction products or purified DNA samples were mixed with 5 X loading dye (30% glycerol, 0.25% bromophenol blue, 0.25% xylene cyanol FF) to a final concentration of 1 X and were resolved by electrophoresis on a 2% agarose (Roche Diagnostics, Mannheim, Germany) gel for RT-PCR products and a 1% agarose gel for all other applications. Agarose gels contained 0.1 μg/mL ethidium bromide and were run in 1 X TAE (40 mM Tris, 2 mM EDTA, 1.15% glacial acetic acid) at 100V. A 1kb or 100bp ladder (N3232S and N3231S, respectively, New England Biolabs) was used to estimate molecular mass of the DNA. Nucleic acid staining was visualised under ultra violet light using a Bio-Rad Gel-Doc 2000 connected to a computer running Quantity One software (Bio-Rad laboratories, CA).

2.11 Yeast two-hybrid screening

The Matchmaker GAL4 two-hybrid system 3 (Clontech, Takara Bio Inc., Shiga, Japan) was used for the yeast two-hybrid screen. Yeast transformation, α-galactosidase assays and pACT plasmid rescue were carried out in accordance with the manufacturer's protocol. Bait vector constructs used to screen the library are described in Table 2.2. A cDNA library derived from 3-day-old dark-grown *Arabidopsis* seedlings was obtained from the *Arabidopsis* Biological Resource Centre (#CD4-22; Kim *et al.,* 1997).

Transformed yeast were plated on non-selective medium (synthetic dropout (SD) lacking leucine and tryptophan) to select for transformation with both bait and prey vectors and on full selection medium (SD lacking adenine, histidine, leucine and tryptophan and containing 20 mg/L 5-bromo-4-chloro-3-indolyl-α-D-galactopyranoside (X-α-gal, dissolved in dimethylformamide (DMF)) per litre) to select for interacting proteins. Yeast were grown at 30ºC in a dark incubator for at least 3 days.

2.11.1 Yeast transformation

For small scale transformations to investigate specific interactions, competent AH109 yeast were prepared in the laboratory. To prepare yeast, 1 mL of Yeast Peptone Dextrose Adenine medium (YPDA; 2% (w/v) peptone, 1% (w/v) yeast extract, 5% (v/v) 40% glucose, 1.5% (v/v) 0.2% adenine hemisulphate) was inoculated with one fresh AH109 yeast colony > 2mm in diameter and vortexed vigorously. The cells were transferred to a flask containing 50 mL YPDA and incubated at 30ºC overnight with shaking (220 rpm) until $OD_{600} > 1.5$. 300 mL YPDA was inoculated with enough of the overnight culture to produce an $OD_{600} = 0.2\text{-}0.3$ and incubated as above for 3 hours until $OD_{600} = 0.5$. Cells were centrifuged in 50 mL tubes for 5 min at $1,000g$ at room temperature and washed in 50 mL sterile dH_2O. The resulting pellets were pooled and resuspended in 1.5 mL 1X TE/LiOAc (10 mM Tris pH 7.5, 1 mM EDTA, 100 mM LiOAc) solution (Clontech). 100 µL of competent cells were transformed with a molar ratio of 2:1 bait to prey vectors (0.2 and 0.1 µg, respectively) and 0.1 mg herring testes carrier DNA. 600 µL of PEG/LiOAc (40% (v/v) PEG 3350, 100 mM LiOAc) solution was added and the cells were vortexed briefly before being incubated at 30ºC for 30 min with shaking at 200 rpm. 70 µL DMSO was added to each transformation and

yeast were heat shocked at 42ºC for 15 min in a heating block. Cells were chilled on ice for 2 min and pelleted by centrifugation at 16,000g for 15 sec. The supernatant was removed and cells were resuspended in 200 µL YPDA. 100 µL of the transformation was plated on non-selective media and the remainder was plated on selective media.

For large-scale transformations used to screen the cDNA library, competent yeast were obtained from the manufacturer and the transformation described above was scaled up.

2.11.2 pACT plasmid rescue from yeast

Total DNA was isolated from yeast colonies containing putative interacting proteins as described in Section 2.4.2 and transformed into KC8 *E. coli* cells by electroporation. Cells were plated on M9 medium lacking leucine and containing ampicillin (to select for the prey vector). Single KC8 colonies containing the prey vector were selected by colony PCR and plasmid DNA was isolated from them before being sequenced to identify the putative interacting protein.

2.11.3 Alpha-galactosidase (α-gal) activity assay

Yeast were grown in 5 mL liquid cultures (SD-L/-W for non-interacting proteins, SD-H/-L/-W for interacting proteins) overnight at 30ºC with shaking. The culture was vortexed for 1 min to disperse any clumps and 1 mL of culture was transferred to a cuvette and OD_{600} was recorded. 1 mL of the culture was transferred to a a microfuge tube and the cells were pelleted by centrifugation at 16,000g for 2 min. The clear supernatant was removed to a fresh tube and stored at room temperature for use in the assay. In a fresh tube, 16 µL of cell culture supernatant was combined with 48 µL assay buffer (2 vol 0.5 M sodium acetate pH 4.5: 1 vol PNP-α-gal solution (*p*-nitrophenyl α-D-galactopyranoside, #N0877, Sigma) [2:1 (v/v) ratio]). The supernatant and assay buffer were incubated together for 2 hours at 30ºC before the reaction was terminated by adding 928 µL stop solution (1M Na_2CO_3). OD_{410} of each sample was recorded. Enzyme activity was calculated using the following equation:

α-galactosidase (milliunits) = OD_{410} x V_f x 1,000/[(ε x b) x t x V_i x OD_{600}]

where   t = time (min) of incubation

V_f = final volume of assay

V_i = volume of culture medium supernatant added

43

(ϵ X b) = *p*-nitrophenol molar absorption at 410nm X the light path (16.9 mL/μmol)

To ensure samples lay within the linear range of the assay a set of standards were created using serial dilutions of *p*-nitrophenol in place of the medium supernatant according to the manufacturer's protocol.

2.12 Protein extraction from plants and quantification

For experiments investigating the effects of light on protein, extraction was carried out under dim red safe light at 4ºC. For determining the presence of specific proteins, extraction was carried out on ice in the laboratory. Plant tissue was ground in a mortar and pestle in extraction buffer (50 mM Tris-MES pH 7.5, 300 mM sucrose, 150 mM NaCl, 10 mM potassium acetate, 5 mM EDTA, 1 mM phenylmethylsulphonyl fluoride (PMSF) and a protease inhibitor mixture (1 tablet/10 mL; Complete EDTA-free, Roche Diagnostics, Mannheim, Germany)). Total protein was clarified by centrifugation at 16,000*g* for 10 min at 4°C. For separation of soluble and membrane fractions, total protein extracts were centrifuged at 100,000*g*, 4ºC for 75 min. The resulting supernatant was used as the soluble fraction and the pellet was resuspended in extraction buffer as the membrane fraction. Quantification of protein concentrations was determined by the Bradford colourimetric method (500-0006, Bio-Rad, UK) using bovine serum albumin as a standard.

2.13 Protein expression

2.13.1 The bacterial system

Expression of GST-tagged proteins was carried out essentially as described in Christie *et al*, (1999) and Kasahara *et a.,* (2002). DNA fragments were cloned into the bacterial expression vector, pGEX4T-1 (G E Healthcare, Bucks. UK) and expressed as a fusion protein with GST. Chemically competent BL21 (DE3) pLysS *E. coli* cells (#69451-3, Novagen, Merck, Nottingham, UK) were transformed with the expression vector and colonies containing the vector were selected by colony PCR. Liquid cultures were grown at 37ºC in LB medium supplemented with ampicillin (100 μg/mL) until OD_{600} reached between 0.2-0.3. At this point, protein expression was induced by adding isopropyl β-D-galactopyranoside (IPTG) to a final concentration of 1 mM. Cells were

then grown in the dark for a further 3 hours at 30ºC to allow protein expression. Cells were pelleted by centrifugation at 5,000g, 4ºC for 10 min and resuspended in 2 mL resuspension buffer (250 mM sucrose, 4 mM KNO_3, 5 mM KH_2PO_4, 1 mM PMSF and complete protease inhibitor cocktail, pH 7.2). Cells were then lysed by sonication (MSE Soniprep) and the debris removed by centrifugation in a microfuge at 4ºC, 16,000g for 10 min. The supernatant containing the soluble protein fraction was removed to a fresh tube and used immediately or stored at -20ºC.

2.13.2 The insect cell system

Expression of phototropin proteins using the insect cell system was carried out as described previously (Christie *et al.,* 1998; Sakai *et al.,* 2001; Cho *et al.,* 2007). Recombinant baculovirus encoding *Arabidopsis PHOT1* or *PHOT2* carrying specific amino acid mutations was generated using the BaculoGold Transfection kit (BD Biosciences Pharmingen) in accordance with the manufacturer's instructions. Recombinant baculovirus was titred by end point dilution and used to infect *Spodoptera frugiperda* (Sf9) insect cells. Cells were grown in serum-free medium (SF900II, #10902-088, GIBCO® supplemented with 10% (v/v) foetal bovine serum (#S1810, Biosera, East Sussex, UK)) at 26ºC for four days in 75cm^2 culture flasks (#43072, Corning, UK) wrapped in aluminium foil. Cells were then harvested under dim red safe light by washing the cells gently off the wall of the flasks and centrifuging the resulting suspension at 1,000g for 2 min. The culture medium was removed and the cell pellet resuspended in 100 µL phosphorylation buffer (37.5 mM Tris-HCl pH 7.5, 5.3 mM $MgSO_4$, 150 mM NaCl, 1 mM EGTA, 1 mM dithiothreitol, 1 mM PMSF and 1 X EDTA-free complete protease inhibitor cocktail (Roche)). Cells were lysed by sonication and cell debris pelleted by centrifugation at 16,000g for 2 min in a microfuge. The crude soluble fraction was removed to a fresh tube and an aliquot was taken for determination of protein concentration.

2.13.3 The in vitro transcription/translation system

The TNT® Quick coupled Transcription/Translation (rabbit reticulocyte lysate) System (#L1170, Promega) was used according to the manufacturer's instruction to

generate c-Myc-tagged proteins from 2 µg circular plasmid DNA containing a T7 initiation of transcription site (pGBKT7; Clontech).

2.14 GST pull-down assays

The MagneGST™ Protein Purification System (#V8600, Promega) was used in *in vitro* GST pull-down assays. Bacterially-expressed proteins were prepared as described in Section 2.13.1 and purified by incubating 185 µL of the lysate with 20 µL of the glutathione-conjugated beads washed and resuspended in 100 µL binding/wash buffer (4.2 mM Na_2HPO_4, 2 mM K_2HPO_4, 140 mM NaCl, 10 mM KCl) and 15µL 10% (v/v) NP-40 for 30 min at room temperature on a rotating mixer. Beads were washed 3 times with binding/wash buffer and 5 µL of beads were removed from the tubes and subjected to SDS-PAGE and coomassie staining alongside known quantities of BSA to estimate the concentration of proteins bound to the beads. Varying volumes of beads with approximately equal quantities of protein attached were used in the subsequent pull-down assays. The protein-containing beads were incubated with 25 µL of *in vitro* transcribed/translated, c-Myc-tagged proteins (see Section 2.13.3) and binding/wash buffer in a total volume of 500 µL on a rotating mixer at room temperature for 1 hour. Beads were then washed 3 times with binding/wash buffer. Proteins were eluted from the beads with 1 X SDS loading dye and subjected to analysis by SDS-PAGE and western blotting. All assays were repeated a minimum of three times.

2.15 GST-protein purification

To purify proteins for use in far-western analysis and antibody testing, GST-tagged proteins were expressed as described in Section 2.13.1. The cell pellet was resuspended in purification buffer (1 X PBS (137 mM NaCl, 1.4 mM KCl, 4.3 mM Na_2HPO_4, 1.4 mM KH_2PO_4), containing 2 mg/mL aprotinin, 2 mg/µL leupeptin and 25 U benzonase (#70746, Novagen). Cells were lysed using a French Press and proteins were purified from the resulting suspension by binding to a 5 mL GST column (Bio-Rad). The column was equilibrated with 5 volumes of 1 X PBS before the protein suspension was added. GST-tagged proteins were eluted from the columns using glutathione elution buffer (50 mM glutathione, 50 mM Tris-HCl pH 8.0) and collected in 500 µL fractions. Protein concentration was quantified by Bradford assay and checked for purity and integrity by coomassie staining of an SDS-PAGE gel.

2.16 Artificial phosphorylation using PKA

Recombinant GST-tagged proteins attached to magnetic glutathione beads were phosphorylated using PKA (bovine protein kinase A catalytic subunit; #2645, Sigma-Aldrich) as described previously (Salomon *et al.,* 2003). 10 µg of protein was incubated with 40 U PKA dissolved in 10 µL 40 mM dithiothreitol in a total reaction volume of 40 µL containing 20 mM Tris-HCl pH 8.4, 150 mM Na Cl, 5 mM $CaCl_2$, 10 mM MgCl, 0.1 mM ATP. The reaction was allowed to proceed for 2 hours at 30ºC in a shaking incubator. After this time the reaction mixture was removed by washing 3 times with GST pull-down buffer and the proteins were used in the GST pull-down assay as described in Section 2.14.

2.17 Phototropin phosphorylation assay

The phosphorylation assay was carried out as described previously (Liscum & Briggs, 1995; Christie *et al.,* 1998; Sakai *et al.,* 2001; Cho *et al.,* 2007). 10 µg of insect cell protein was used for autophosphorylation analysis. Radiolabelled ATP (γ-^{32}P [110TBq/mmol; #AA0068, Amersham]) was diluted 1:5 with 10 µM unlabelled ATP and 1 µL was used for each 10 µL phosphorylation reaction. Upon addition of radiolabelled ATP, phosphorylation reactions were carried out under dim red safe light (dark) or by exposing the samples to high intensity white light (total fluence 30,000 µmol m^{-2} s^{-1}). Reactions were allowed to proceed for 2 min at room temperature before the reaction was terminated by adding 10 µL 2 X SDS loading dye (125 mM Tris-HCl pH 6.8, 4% SDS, 20% glycerol, 10% β-mercaptoethanol, 0.008% bromophenol blue). Samples were either frozen at -20ºC or immediately subjected to SDS-PAGE analysis.

2.18 λ-phosphatase treatment

The autophosphorylation assay was carried out as described above. Samples were dephosphorylated by adding 400 U of λ-phosphatase (# P0753S, New England Biolabs) to the reaction mixture and incubated at room temperature for 2 min before SDS loading dye was added to terminate the reaction.

2.19 Sequence alignments and phylogenetic analyses

Amino acid alignments were performed using the ClustalW algorithm supplied by www.ebi.ac.uk/ClustalW, with all parameters set to default (Protein Gap Open Penalty = 10.0, Protein Gap Extension Penalty = 0.2, Protein matrix = Gonnet; Chenna *et al.,* 2003)

Phylogenetic trees were also created using the programme supplied by www.ebi.ac.uk/ClustalW.

2.20 Antibody production

Custom-made antibodies for 14-3-3λ and NPH3-L were produced in New Zealand white rabbits by Eurogentec (Belgium), using two synthetic peptides for each protein. The peptides used for antibody production are described in the main text. Antibodies used were purified by peptide affinity purification by Eurogentec. In this process, the synthetic peptides used for antibody production are coupled to a sepharose column and the crude antibody obtained from the final bleed is run through the column. This allows the antibody to specifically bind the antigenic peptide, which is in turn bound to the sepharose column. The unbound antibodies and serum are washed off the column and finally the specific peptide antibodies are eluted from the column.

2.21 SDS-polyacrylamide gel electrophoresis (SDS-PAGE) and western blotting

Protein samples were denatured by adding 6 X SDS loading dye to achieve a final concentration of 1 X (62.5 mM Tris-HCl pH 6.8, 2% SDS, 10% glycerol, 5% β-mercaptoethanol, 0.004% bromophenol blue) and boiled for 5 min in a heating block. Proteins were separated by SDS-PAGE according to the method initially outlined by Lamelli (1970). SDS-PAGE gels used in this work contained a 7.5% or 12% polyacrylamide separating gel (as detailed in the figures) and a 5% polyacrylamide stacking gel. Protein molecular weights were determined using a prestained molecular weight marker (P7708S, New England Biolabs). Samples loaded onto the gels were electrophoresed at 200 V until the loading dye front reached the bottom of the gel. Proteins were electro-transferred at 100 V for 1 hour from the gels to nitrocellulose membrane (162-0115, Bio-Rad) in transfer buffer (25 mM Tris, 190 mM glycine, 20% methanol). Ponceau S staining (P3504, Sigma-Aldrich; 0.1% (w/v) in 1% (v/v) acetic

acid) was carried out to ensure protein transfer and equal loading by visualisation of the Rubisco large subunit for plant-derived samples.

After removing the stain, the membrane was blocked at room temperature for at least 1 hour using 8% (w/v) milk powder dissolved in 1 X TBS (25 mM Tris-HCL pH 8.0, 137 mM NaCl, 2.7 mM KCl) containing 0.1% (v/v) Triton X-100 (TBST). Primary antibodies (see below) were then incubated with the membrane at room temperature for 1 hour or overnight at 4ºC in 1 X TBST + 8% (w/v) milk powder at the dilutions indicated below. The membrane was washed three times with 1 X TBST + 8% (w/v) milk powder before the secondary antibodies were added (see below) for 1 hour at room temperature. The membrane was washed as described previously and proteins were detected using one of the methods described below.

Primary Antibodies:

Anti-phot1 (rabbit; 1/1,000; Christie *et al.,* 1998)

Anti-phot1 C-terminal (rabbit; 1/1,000; Cho *et al.,* 2007)

Anti-NPH3 (rabbit; 1/5,000; Motchoulski & Liscum, 1999)

Anti-GFP (mouse; 1/5,000; 632375, Roche Diagnostics, Mannheim, Germany)

Anti-UGPase (rabbit, 1/5,000; AS05086, Agrisera, Vännäs, Sweden)

Anti-14-3-3λ EP053407 (rabbit; 1/2,500; this study)

Anti-14-3-3κ EP053408 (rabbit; 1/2,500; this study)

Anti-NPH3-L EP053409 (rabbit; 1/2,500; this study)

Anti-Myc (mouse; 1/1000; 9E10, Roche Diagnostics, Mannheim, Germany)

Anti-GST (mouse; 1/10,000; 71097-3, Novagen)

Secondary Antibodies:

Anti-mouse-AP (1/5,000; 69266, Novagen)

Anti-rabbit-AP (1/5,000; S373B, Promega)

Anti-mouse-HRP (1/5,000; W402B, Promega)

Anti-rabbit-HRP (1/5,000; W401B, Promega)

Blots using horseradish peroxidase (HRP)-conjugated secondary antibodies were developed using the ECL+ system (RPN2132, Amersham) and visualised on medical

X-ray film (814 3059, Kodak) and alkaline phosphatase (AP)-conjugated secondary antibodies were developed using BCIP/NBT solution (B6404, Sigma-Aldrich).

2.22 Coomassie staining

The stacking gel was removed and discarded and the separating gel was stained for 15 min at room temperature in 0.1% Coomassie Brilliant Blue R250 (Bio-Rad), 40% (v/v) methanol, 10% (v/v) glacial acetic acid. The gel was destained in several changes of 40% (v/v) methanol, 10% (v/v) glacial acetic acid.

2.23 Far western blotting

Far western blotting was carried out according to Kinoshita & Shimazaki (1999). Essentially, purified GST-tagged 14-3-3 proteins or GST alone were incubated overnight at 4ºC with proteins electroblotted onto nitrocellulose membrane at a final concentration of 0.1 µM in far-western buffer (20 mM HEPES-KOH pH 7.7, 75 mM KCl, 0.1 mM EDTA, 1 mM dithiothreitol, 2% (w/v) milk powder and 0.04% Tween-20). The membranes were washed 3 times with far-western buffer. Protein-protein interactions between the proteins on the membrane and the GST-tagged proteins used as a probe were then identified by western blotting as described in Section 2.21 using anti-GST antibody as the primary antibody and anti-mouse-AP as the secondary antibody.

2.24 Immunoprecipitation

Sample preparation was carried out under a dim red safe light at 4ºC. Microsomal membranes were prepared from 3-day-old, dark-grown seedlings as described in Section 2.12. The microsomal membrane pellet was resuspended in extraction buffer containing 1.0% Triton X-100 and incubated on ice for 30 min before centrifugation at 100,000g, 4ºC for 30 min. The supernatant containing solubilised microsomal membrane proteins was removed to a fresh tube and quantified by Bradford assay.

Equal amounts of protein were incubated for 3 min on ice with 50 µL anti-GFP microbeads (µMACS GFP isolation kit, 130-901-370, Miltenyi Biotech) while microcolumns were equilibrated with 200 µL lysis buffer. The protein/microbead samples were applied to the columns and unbound material was allowed to run through. The columns were washed four times with 200 µL lysis buffer and once with

200 μL Tris-HCl pH 7.5. Bound proteins were eluted from the column by adding 20 μL elution buffer (0.1 M triethylamine pH 11.8, 0.1% (w/v) Triton X-100) and incubating for 5 min at room temperature. A further 50 μL of elution buffer was added to the column and the eluate was collected in a tube containing 3 μL of 1 M MES pH 3 to neutralise the sample. The eluates were mixed with SDS loading dye and subjected to SDS-PAGE and western blotting for analysis.

2.25 Transformation and selection of stable transgenic lines

Agrobacterium (strain GV3101 (pMP90)) was transformed with the appropriate binary expression vector and was used to transform *Arabidopsis* plants by the floral dipping method described previously by Clough and Bent (1998). Kanamycin-resistant plants containing the expression vector were selected by plating surface sterilised seed on 0.5 X MS/0.8% agar (w/v) medium containing 100 μg/mL kanamycin. Based on the segregation of kanamycin resistance, T2 lines that contained a single transgene locus were identified and homozygous T3 seed were used for physiological studies.

2.26 Microscopy

Green fluorescent protein (GFP) fluorescence and chloroplast autofluorescence were visualised using 20 X or 40 X objective lenses by confocal laser scanning microscopy (Zeiss LSM510) using an excitation wavelength of 488nm (Argon) and an emission range between 505-530 nm . Images were extracted using Zeiss LSM software and Adobe Photoshop.

2.27 Physiological measurements

2.27.1 Measurement of hypocotyl phototropic curvature

Second positive hypocotyl curvature was measured as described in Lascève *et al.,* (1999). Essentially, seedlings were surface sterilised and planted individually in horizontal lines on square petri dishes (#0575711A, Fisher) containing 0.5 X MS/0.8% agar (w/v). Plates were wrapped in aluminium foil and cold treated for 3 days at 4ºC before being given a 6 hour white light treatment to induce uniform germination. Plates were then wrapped in two layers of aluminium foil and grown vertically in the dark for 2.5 days. To induce phototropism, seedlings on the agar plates were exposed

to unilateral blue light for 24 hours before imaging at the light intensities described in the main text. Blue light at 20 µmol m^{-2} s^{-1} and below was supplied by a white fluorescent lamp (18 W/26-835, Osram) filtered through a blue Plexiglas filter (two layers for 0.1 µmol m^{-2} s^{-1}; Wade *et al.,* 2001). High intensity blue light (> 20 µmol m^{-2} s^{-1} was obtained using a slide projector (TLP-T50, Toshiba) and passing the light through a water filter and one layer of blue Plexiglas. Images were captured using an UMax PowerLook 1100 scanner. Hypocotyl curvature was measured using ImageJ software (http://rsb.info.nih.gov/ij/).

2.27.2 Observation of leaf positioning

Arabidopsis seeds were sown on soil and cold treated for 3 days at 4ºC before being grown under white light at 50 µmol m^{-2} s^{-1} for 7 days in a 16/8 hour light-dark cycle. Plants were then transferred to 10 µmol m^{-2} s^{-1} white light for a further 5 days in a 16/8 hour light-dark cycle before representative seedlings were photographed.

2.27.3 Measurement of leaf expansion

Measurement of leaf expansion was carried out as described previously (Takemiya *et al.,* 2005). *Arabidopsis* plants were grown on soil under 70 µmol m^{-2} s^{-1} white light for three weeks in a 16/8 hour light-dark cycle. The fifth rosette leaves were detached and scanned using a scanner (Umax PowerLook 1100). The leaves were then flattened manually and scanned again. Leaf area was measured using ImageJ software. The leaf expansion index was designated as the ratio of unflattened leaf area to flattened leaf area.

2.27.4 Fresh and dry weight determination

Fresh and dry weights were measured using green tissue only. Fresh weight was determined by immediately weighing excised tissue. Dry weight was determined by placing the excised tissue in 30 mL tubes and drying the tissue at 70ºC for three days.

2.27.5 Chloroplast accumulation response

The chloroplast accumulation response was measured essentially as described in Onodera *et al.* (2005). Three week-old plants grown under 50 µmol m^{-2} s^{-1} white light in a 16/8 hour light-dark cycle were given a low blue light treatment (1.5 µmol m^{-2} s^{-1})

for 3 hours or kept in the dark for three hours before chloroplasts in the palisade mesophyll cells of detached leaves were examined by confocal microscopy (see above).

2.27.6 Chlorophyll content

To determine chlorophyll *a* and *b* content, the fresh weights of five week old plants grown under 70 μmol m^{-2} s^{-1} white light in a 9/15 hour light-dark cycle was measured before chlorophyll from individual plants was extracted in 10 mL 80% actone by shaking the plant tissue in the acetone solution on a mixing platform overnight. Chlorophyll *a* and *b* levels were determined spectroscopically and mg of chlorophyll/L was determined using MacKinney's coefficients (MacKinney, 1941) and the equation:

$$\text{Chlorophyll}_{a+b} = 7.15 \times OD_{660nm} + 18.71 \times OD_{647nm}$$

as described by Fankhauser and Casal, (2004). The fresh weight of each plant was then used to express chlorophyll content as μg Chl$_{a+b}$/mg fresh weight

2.27.7 Gas exchange measurements

Arabidopsis plants were grown for eight weeks under 70 μmol m^{-2} s^{-1} white light in a 9/15 hour light-dark cycle to achieve leaf areas large enough to clamp the measuring apparatus (LCpro+, ADC BioScientific Ltd., Herts, UK) on to. Plants were either well watered or subjected to drought stress by terminating irrigation for 8 days. The differences in humidity and CO_2 caused by transpiration and photosynthesis were used to calculate steady state stomatal conductance (gs), rate of net photosynthesis (A) and water use potential (A/gs).

2.27.8 Determination of relative water content

Plant water status was evaluated by determining the relative water content (RWC) of plants as described in Cominelli *et al*, (2005). *Arabidopsis* plants were grown individually on soil under 70 μmol m^{-2} s^{-1} white light in 16/8 hour light-dark cycle for 24 days. On day 24, all pots were wrapped with cling film to reduce water evaporation from the soil and irrigation was terminated to induce drought stress. RWC was determined for at least 8 plants from each line on day 0, day 8 and day 12 of the drought stress treatment. RWC was determined by excising all tissues above the cotyledons and separating leaves and shoot apices (containing the leaf primordia) with

a razor blade and weighing immediately to determine the fresh weight. Tissues were then rehydrated for 24 hours in the dark by placing them, cut side down, onto tissue paper saturated with water in a petri dish. After blotting dry, the tissues were then re-weighed to determine the turgid weight. Finally, the dry weight of excised tissues was determined and the RWC calculated, as described in Ascenzi & Gantt (1999), using the following equation:

RWC = [(fresh weight – dry weight) / (turgid weight – dry weight)]

Table 2.1 Primers used for RT-PCR and the identification of knockout lines.

Primers used in the study to characterise transcript expression are shown in the top part of the table. Primers used to identify knockout lines are shown in the bottom part of the table. All primers are 5' – 3'.

Primer Name	Sequence (5' – 3')
Primers for RT-PCR	
At1g30440U (NPH3-L)	CTG AAG AAC ATG GGG AAG GA
At1g30440L (NPH3-L)	GTC CAC CAC GTC GTC TTT TT
At5g10450U (14-3-3λ)	AGG CGC TAC TCC AGC GGA
At5g10450L (14-3-3λ)	CAA AGG TTA TGG GGA TTT TGA GAT
L2K U	AAC TCA TTT GTT GGC ACT GAA
L2K L	GTA ATC TGG TAC GTC AAA AAC
Actin U	CTT ACA ATT TCC CGC TCT GC
Actin L	GTT GGG ATG AAC CAG AAG GA
Primers for Identification of Knockout Lines	
NPH3- L P1	ATTGAGCAGACTTTGGTCTGG
NPH3-L P2	TTATTAGAAGCAAGGCATTGCC
14-3-3λ P1	AGAGTGTCAAGCTCAGCTATG
14-3-3λ P2	TCTCTTGAGAGTTTGCTTCTGT
LBa	GTTCACGTAGTGGGCCATCG
LBb	GTGGACCGCTTGCTGCAACT
Vector 1	TTGTAAAACGACGGCCAGTG
Vector 2	GACGTAAGGGATGACGCACA

Table 2.2 Generation of constructs used for protein expression in this study.
The expression vectors constructed for use in this study are described in the table above. The vector used along with the location and description of any epitope tag are shown in the first two columns. The third column details the protein encoded in the expression vector. The column on the right indicates the primers used to create the constructs. The forward primers are shown in the top row and the reverse primers are shown on the bottom row. All primers are 5' – 3'.

Construct Name	Tag	Encodes (amino acid residues)	Primers used (5'-3'; upper then lower)
Constructs for protein expression in bacteria and yeast			
pGBKT7-phot1	c-Myc (N-term)	Phot1 (1-996)	EcoR1-ATGGAACCAACAGAAAAACCA
			Sal1-AAAAACATTTGTTTGCAG
pGBKT7-N₂LOV2	c-Myc (N-term)	Phot1 (1-627)	EcoR1-ATGGAACCAACAGAAAAACCA
			BamH1-GTTTGCCCATAAATCCTCTG
pGBKT7-N₂LOV2 Del1	c-Myc (N-term)	Phot1 (1-463)	EcoR1-ATGGAACCAACAGAAAAACCA
			Pst1-ATACCCTTTCTCATTTCCTTT
pGBKT7-N₂LOV2 Del2	c-Myc (N-term)	Phot1 (1-307)	EcoR1-ATGGAACCAACAGAAAAACCA
			Pst1-GGCCCCTTCAGTGTGCTTCGT
pGBKT7-N₂LOV2 Del3	c-Myc (N-term)	Phot1 (1-202)	EcoR1-ATGGAACCAACAGAAAAACCA
			Pst1-CTGAGACCACAAACGTTT
pGBKT7-Kinase	c-Myc (N-term)	Phot1 (612-996)	EcoR1-CGAGAACTTCCTGATGCCAACAT
			Sal1-AAAAACATTTGTTTGCAG
pGBKT7-Kinase Del1	c-Myc (N-term)	Phot1 (612-996)	EcoR1-CGAGAACTTCCTGATGCCAACAT
			BamH1-CGAATCAGAGCCCAATTT
pGBKT7-Kinase Del2	c-Myc (N-term)	Phot1 (612-662)	EcoR1-CGAGAACTTCCTGATGCCAACAT
			BamH1-GCTTCAAACCAATCGGT
pGBKT7-NPH3-L	c-Myc (N-term)	NPH3-L (243-433)	EcoR1-GAAGACATCATCGCTGGCTCC
			Pst1-GCTTGGAACTTTGGAAGCTTA
pGBKT7-14-3-3λ	c-Myc (N-term)	14-3-3λ (1-249)	EcoR1-ATGGCGGCGACATTAGGCAGA
			Pst1-TCAGGCCTCGTCCATCTGCTC
pGEX4T-1-N2LOV2	GST (N-Term)	Phot1 (1-627)	BamH1-ATGGAACCAACAGAAAAACCA
			EcoR1-GGTTTGCCCATAAATCCTCTG
pGEX4T-1-N₂LOV1	GST (N-Term)	Phot1 (1-307)	BamH1-ATGGAACCAACAGAAAAACCA
			EcoR1-GGCCCCTTCAGTGTGCTTCGT
pGEX4T-1-LOV Link	GST (N-Term)	Phot1 (305-473)	BamH1-GAAGGGGCCAAAGAAAAGGCT
			EcoR1-CTCGATACGTTCGAGTGTAGT
pGEX4T-1-LOV1	GST (N-Term)	Phot1 (304-197)	EcoR1-CAAACGTTTGTGGTCTCAG
			Not1-AGTGTGCTTGCTCACCTCC

Construct Name	Tag	Encodes (amino acid residues)	Primers used (5'-3'; upper then lower)
pGEX4T-1-Kinase	GST (N-Term)	Phot1 (612-996)	EcoR1-CGAGAACTTCCTGATGCCAACAT
			Sal1-AAAAACATTTGTTTGCAG
pGEX4T-1-14-3-3λ	GST (N-Term)	14-3-3λ (1-249)	EcoR1-ATGGCGGCGACATTAGGCAGA
			Sal1-TCAGGCCTCGTCCATCTGCTC
pGEX4T-1-14-3-3κ	GST (N-Term)	14-3-3κ (1-249)	EcoR1-ATGGCGACGACCTTAAGCAGAGATC
			Sal1-TCAGGCCTCATCCATCTGCTCCTGC
pGEX4T-1-14-3-3ε	GST (N-Term)	14-3-3ε (1-246)	EcoR1-ATGGAGAATGAGAGGGAAAAGCAGG
			Sal1-TTAGTTCTCATCTTGAGGCTCATCA

Constructs for protein expression in plants

Construct Name	Tag	Encodes (amino acid residues)	Primers used (5'-3'; upper then lower)
pEZR(K)-LC-14-3-3λ	GFP (N-Term)	14-3-3λ (1-249)	EcoR1-ATGGCGGCGACATTAGGCAGA
			Sal1- TCAGGCCTCGTCCATCTGCTC
pEZR(K)-LC-L2K	None	Phot1 (448-996)	EcoR1- CCTGAGAGTGTGGATGAT
			Sal1-TCAAAAAACATTTGTTTGCAG
pEZR(K)-LC - inactive kinase	None	Phot1 (612-996; Asp806Asn)	EcoR1-CGAGAACTTCCTGATGCCAACAT
			Sal1-AAAAACATTTGTTTGCAG
pGWB17-kinase	4 X c-Myc (C-Term)	Phot1 (612-996)	CACC-CGAGAACTTCCTGATGCCAACAT
			AAAAACATTTGTTTGCAG
pGWB15-phot1	3 X HA (N-Term)	Phot1 (1-996)	CACC-ATGGAACCAACAGAAAAACCA
			TCAAAAAACATTTGTTTGCAG
pGWB15-N₂LOV2	3 X HA (N-Term)	Phot1 (1-627)	CACC-ATGGAACCAACAGAAAAACCA
			TCAGTTTGCCCATAAATCCTCTG

Chapter 3: Isolation of phot1-interacting proteins

3.1 Introduction

Phototropins have been shown to mediate a variety of physiological responses in plants upon exposure to light. As discussed in Chapter 1, many studies have been carried out into the mechanisms of phototropin light sensing, their activation and their resulting autophosphorylation in response to blue light. In addition to these biochemical studies, there is wealth of data describing the physiological responses that are mediated by phototropins in various light conditions. In comparison, however, there is a significant lack of knowledge in the field about how phototropins signal to bridge the gap between sensing light and eliciting a specific physiological response.

As discussed in Chapter 1, only a few phototropin interacting partners have been identified to date. Indeed, the responses mediated by phototropins are extremely varied and are likely to be complex, involving many different signalling partners, the majority of which remain to be identified. To this end, a yeast-two hybrid screen was employed in order to identify further interacting partners for *Arabidopsis* phot1. This chapter describes the yeast two-hybrid approach that was used for screening an *Arabidopsis* cDNA library and presents the results obtained.

3.2. Yeast two-hybrid screening

To identify proteins that interact with the *Arabidopsis* phot1 protein, the Clontech Matchmaker GAL4 Two-hybrid System 3 was used to screen a cDNA library derived from *Arabidopsis* seedlings. The yeast two-hybrid system concurrently expresses the "bait" gene as a fusion protein attached to the GAL4 DNA-binding domain (DNA-BD) and the cDNA library "prey" gene as a fusion protein attached to the GAL4 activation domain (AD). If these two proteins interact within the nuclei of yeast, the domains of the GAL4 transcription factor are brought into close proximity to induce expression of four reporter genes that allow the yeast strain AH109 to grow on nutritionally deplete media and to produce and excrete α-galactosidase. The enzyme α-galactosidase hydrolyses the colourless substrate 5-bromo-4-chloro-3-indolyl-α-D-galactopyranoside (X-αGal) to produce an indigo-coloured precipitate, which results in a blue colony colour (Fields & Song, 1989, Chien *et al.,* 1991).

The afore-mentioned yeast two-hybrid system was used to carry out a number of screens. Initially, a cDNA library derived from light-grown *Arabidopsis* tissue (CD4-10) was used but this was discontinued because very few colonies were obtained, and those that were recovered all contained concatamers of the empty prey vector. Subsequent screens were therefore carried out using a cDNA library derived from 3-day-old dark-grown *Arabidopsis* seedlings (Kim *et al.,* 1997; *Arabidopsis* Biological Resource Centre (ABRC) DNA Stock Centre, #CD4-22). Two phot1 bait constructs were generated to screen the library: full-length phot1 (pGBKT7-phot1), and the N-terminal region of phot1, containing the two LOV domains (pGBKT7-N$_2$LOV2). The proteins encoded by these constructs are shown schematically in Figure 3.1A. Full-length phot1 bait was used to isolate proteins that interact with the entire phot1 protein. However, because phot1 is a relatively large protein (120kDa) and is plasma membrane-associated in plants (Sakamoto & Briggs, 2002), it was not known at the start of the screening process whether these factors would be problematic for screening, so the N-terminal portion of phot1 was also used as bait. The N-terminal region was chosen preferentially to the C-terminal kinase domain because the two LOV domains present are members of the PAS domain super family that is known to be involved in mediating protein-protein interactions (Taylor & Zhulin, 1998). Hence, this property was thought to increase the likelihood of identifying genuine phot1-interacting proteins.

3.3 Auto-activation determination of phot1 bait proteins

Prior to screening, auto-activation tests were performed to ensure that the bait proteins generated did not auto-activate the yeast two-hybrid system in the presence of the empty prey vector. Chemically competent AH109 yeast was co-transformed with the bait constructs described above in addition to the empty prey vector, pACT2. While the cDNA library was cloned into the pACT vector (Kim *et al.,* 1997), this vector was not available in the laboratory. However, pACT2 is an updated version of the pACT vector, and was therefore used for auto-activation analysis of the phot1 bait proteins.

Figure 3.1B shows the results obtained from the auto-activation tests. Yeast growing on media lacking leucine and tryptophan (-L/-W) indicates that the colony contains both vectors; the bait vector, pGBKT7, contains the Trp[+] reporter gene which allows yeast containing this vector to grow on media lacking tryptophan, while the

prey vector, pACT2, contains the Leu$^+$ reporter gene allowing yeast to grow on media lacking leucine. Fully selective media lacks adenine, histidine, leucine and tryptophan and contains X-αgal (-A/-H/-L/-W+α-gal), and can only sustain yeast growth when yeast express proteins that interact and activate the yeast two-hybrid system. As a reference, positive controls that express murine p53 fused to the GAL4 DNA-BD and the SV40 large T-antigen fused to the GAL4 AD were also used (Li & Fields, 1993; Iwabuchi *et al.*, 1993). The auto-activation analysis confirmed that neither of the phot1 bait vectors (pGBKT7-phot1 and pGBKT7-N$_2$LOV2) auto-activate the yeast two-hybrid system as no growth was observed on full selection media, thus making them suitable for further screening alongside the cDNA library.

In addition to the baits used for yeast two-hybrid screening, the kinase domain of *Arabidopsis* phot1 (Fig. 3.1A) was also generated as a bait construct and tested for auto-activation. As found for the other baits, pGBKT7-kinase did not auto-activate the yeast two-hybrid system in the presence of the empty prey vector (Fig. 3.1B). Because of time constraints, the kinase region of phot1 was not used for screening. Many putative interacting proteins were obtained with the two other baits described (see below). The kinase domain was, however used for subsequent domain mapping analyses described in the results sections below.

3.4 Putative phot1-interacting proteins identified

The transformation efficiencies of the yeast two-hybrid screens were determined to ensure that a suitable number of transformed colonies were screened. For each large-scale yeast co-transformation with the bait vector and cDNA library, an aliquot of the transformed yeast was plated on non-selective media to assess the transformation efficiency obtained. Yeast were grown in the dark, in a temperature-controlled incubator at 30ºC for 1 week. By counting the number of yeast colonies that grew on non-selective media, the number of colonies screened in a particular transformation could be extrapolated, indicating the transformation efficiency of each screen. The results obtained are shown in Table 3.1. Yeast screened for interacting proteins were also grown in the dark for 1 week. Using the full-length phot1 bait, a total of 7.8 x 10^4 colonies were screened and 2.4 x 10^5 colonies were screened using the N$_2$LOV2 bait, resulting in a total of 3.18 x 10^5 colonies. Of the colonies transformed and screened, the phot1 bait resulted in 57 colonies growing on full selection media and the N$_2$LOV2

bait resulted in 73 colonies growing on full-selection media, giving a total of 130 colonies that contained putative phot1-interacting proteins.

All colonies were re-streaked onto fresh plates containing full selection media to confirm genuine growth. Total DNA was extracted from the freshly grown yeast, and the prey vector containing the library cDNA insert was rescued. The cDNA regions in the vectors obtained were sequenced and the resulting library cDNA sequences obtained were compared with the sequenced *Arabidopsis* genome using the search engine, NCBI BLAST 2.2.8 (Altschul *et al.,* 1990). Results of all the sequences obtained are presented in Appendix 1. Sequences were analysed and the frame of the cDNA was checked to ensure it was in the correct open reading frame. Potentially interesting interacting proteins were also checked for their ability to auto-activate when transformed with the empty bait vector, pGBKT7. Both these processes were used to eliminate a large number of false positives, details of which are shown in Appendix 1. As a result, six potential phot1-interacting clones were chosen for further investigation and are shown in Table 3.2.

3.5 Phot1 interacts with ADP-ribosylation factors (ARFs)

3.5.1 Function of ARF and ARF-like proteins in Arabidopsis

ADP-ribosylation factors (ARFs) are members of a subfamily of the Ras superfamily of GTP-binding proteins which are involved in the assembly and disassembly of the coat proteins involved in driving vesicle budding and fusion (Gebbie *et al.,* 2005). ARFs were first identified in mammalian systems as cofactors required for cholera toxin-mediated ADP-ribosylation of a trimeric G protein α-chain (Kahn & Gilman, 1984), but most work in plants has focussed on their role in Golgi-to-ER and intra-Golgi transport (Pimpl *et al.,* 2000; Ritzenthaler *et al.,* 2002).

There is widely differing opinion in the literature as to the nomenclature of these proteins (Gebbie *et al.,* 2005; Nielsen *et al.,* 2006): from this point the nomenclature suggested by Neilsen *et al.* (2006) will be used since it is more recent and simpler to follow. There are 18 genes in the *Arabidopsis* genome potentially encoding members of this family. Based on sequence characteristics and their potential to functionally complement the lethal yeast mutation *arf1-arf2* described by Kahn *et al.* (1991), Neilsen *et al*. (2006) have categorised ARFs into two groups: ADP-

ribosylation factors (ARFs) and ADP-ribsoylation factor-like (ARLs). The ARFs comprise a subset of 6 proteins which are highly homologous and are assigned to Class 1 of ARF proteins based on mammalian nomenclature, and three other proteins which are thought to be genuine ARFs based on sequence similarity (Nielsen *et al.,* 2006), but which may prove to be functionally differentiated when fully characterised and as such are not assigned to Class 1 (Gebbie *et al.,* 2005). The ARL family are named ARL1-5 and ARL8a-d, based on their similarities to mammalian ARL proteins (Neilsen *et al.,* 2006).

From the yeast two-hybrid screens that were carried out, two ARF proteins were identified. Full-length ARF2 (a Class 1 ARF, At3g62290) was isolated from the screen using full-length phot1 as bait (Fig. 3.2A). Auto-activation studies in yeast show that ARF2 does not auto-activate the yeast two-hybrid system in the absence of the phot1 bait (Fig. 3.2B). By growing AH109 yeast expressing the interacting proteins in liquid media, the relative strength of the interaction can be quantified by monitoring α-galacactosidase activity. This method was used to determine the strength of the phot1/ARF2 interaction relative to positive and negative controls. Figure 3.2C shows that the interaction between phot1 and ARF2 is weaker than the interaction observed for the positive controls (murine p53 and SV40). The strength of the phot1/ARF2 interaction was approximately one half of that detected for the positive controls. As a negative control, yeast were transformed with one of the interacting proteins and the corresponding empty vector, and the α−galactosidase activity measured. The activity of the phot1/ARF2 interaction was found to be significantly greater than the negligible activity shown by both negative controls used (Fig. 3.2B).

Full-length ARF7 (non-Class 1, At5g17060) was also identified from the yeast two-hybrid screen using full-length phot1 bait (Fig. 3.2D). Again, the auto-activation experiment shows that the prey protein, ARF7 does not auto-activate the yeast two-hybrid system in the absence of the phot1 bait protein (Fig. 3.2E). The strength of the phot1/ARF7 interaction was quantified as described for ARF2. Figure 3.2F shows that the interaction between phot1 and ARF7 is weaker than that observed for the phot1/ARF2 interaction, as only a quarter of the α−galactosidase activity was detected in comparison to that measured for the positive controls.

3.5.2 Further characterisation of the phot1/ARF interactions in yeast

Since full-length phot1 interacts with both ARF2 and ARF7, we went on to establish which regions of phot1 interacted with the ARF proteins. To determine the region of phot1 necessary for the interaction with ARF2 in yeast, domain mapping was carried out. Using the baits described in Figure 3.1, yeast were co-transformed with the bait vectors, pGBKT7-N$_2$LOV2 or pGBKT7-KINASE, and the prey vector, pACT-ARF2, to assess whether the N-terminal region or C-terminal kinase domain of phot1 is required for the interaction. However, Figure 3.3A shows that full-length phot1 is necessary for the interaction as no yeast growth on full selection medium is apparent when ARF2 is transformed with either the N- or C-terminal region of phot1.

Yeast plates containing the proteins under investigation were then grown in the dark or under 20 μmol m^{-2} s^{-1} white light to establish whether light had any effect on the phot1/ARF2 interaction. Under these conditions it was observed that the phot1/ARF2 interaction is light sensitive. That is, the interaction between full-length phot1 and full-length ARF2 does not occur in the presence of white light (Fig. 3.3A).

As described for ARF2, the phot1/ARF7 interaction in yeast was also characterised further by domain mapping the region of phot1 necessary for the interaction. Again, yeast were co-transformed with pGBKT7-N$_2$LOV2 or pGBKT7-KINASE bait vectors and the pACT-ARF7 prey vector to determine the region of phot1 involved in the interaction with ARF7. Figure 3.3B shows that as found for ARF2, full-length phot1 is necessary for the interaction as no yeast growth was apparent on full selection medium when ARF7 is transformed with either the N- or C-terminal region of phot1. The effect of light on the phot1/ARF7 interaction was also investigated. Yeast plates containing the interacting proteins under investigation were grown in either darkness or under white light. The results obtained, shown in Figure 3.3B, demonstrate that, as found for ARF2, the interaction between phot1 and ARF7 is light sensitive and is severely attenuated in response to 20 μmol m^{-2} s^{-1} white light treatment (Fig. 3.3B).

3.5.3 The phot1 interaction with ARF2 and ARF7 is blue light sensitive

The light effect on the phot1/ARF interactions described above was of particular interest. Given that phot1 is a blue light receptor, it was important to determine whether these wavelengths of light specifically affected the interaction. In order to

63

determine if the light sensitivity demonstrated in the interactions between phot1 and ARF2 and ARF7 was specifically blue light sensitive, yeast colonies co-transformed with the interacting proteins were grown under a variety of different light conditions. Yeast grown in dark conditions were wrapped in aluminium foil, while those grown in blue or red conditions were wrapped in transparent, coloured filters and placed in white light. Yeast grown in white light conditions were left uncovered. Yeast were grown in a temperature controlled incubator and an equal light intensity (10 μmol m^{-2} s^{-1}) for all plates was achieved by adjusting the proximity of the plates to the light source. Figure 3.3C shows that the attenuation of both the phot1/ARF interactions occurs specifically in response to blue light. Therefore, these findings indicate that the interactions between phot1 and ARF proteins are abolished upon photoexcitation of phot1 by blue light within the yeast cell. It should be noted that some residual growth on full selection medium was observed under blue and white light for the phot1/ARF7 interaction.

3.6 Phot1 interacts with members of the NPH3/RPT2-Like (NRL) family

3.6.1 NRL function in Arabidopsis

The NPH3/RPT2 like (NRL) family is a novel, plant specific gene family comprising 32 members in *Arabidopsis* (Celaya & Liscum, 2005), and at least 24 in rice (Kimura & Kagawa, 2006). Non-Phototropic Hypocotyl 3 (NPH3) was the first member of the family to be identified (Liscum & Briggs, 1995), and is essential for phototropism (Motchoulski & Liscum, 1999, Haga *et al.*, 2005). Root Phototropism 2 (RPT2) was the second member of the family to be characterised, and was isolated in a screen for mutants with defects in root phototropism (Okada & Shimura, 1992; Sakai *et al.,* 2000). RPT2 is involved in phot1-mediated phototropism and stomatal opening (Inada *et al.,* 2004).

The N-terminal region of RPT2 (At2g30520; amino acids 1-187) was isolated from the yeast two-hybrid screen using full-length phot1 as bait (Fig. 3.4A). This region includes the BTB/POZ domain (amino acids 32-128), which has been shown to be important for mediating the RPT2 interaction with phot1 and NPH3 in yeast (Inada *et al.,* 2004). Auto-activation studies in yeast show that the N-terminal region of RPT2 identified from the screen does not auto-activate the yeast two-hybrid system in the

64

absence of the phot1 bait (Fig. 3.4B). The interaction between phot1 and the N-terminal region of RPT2 was quantified in liquid culture using the α-galactosidase assay described earlier. Figure 3.4C shows that the degree of interaction between phot1 and the N-terminal region of RPT2 is comparable to that measured for the positive controls in terms of the interaction strength.

A novel member of the NRL family was also identified from the yeast two-hybrid screen. This protein, designated NPH3-like (NPH3-L; At1g30440) was isolated using the N_2LOV2 region of phot1 as bait (Fig. 3.4D) and comprised a truncated region of the protein (amino acids 243-433). This central region of NPH3-L is downstream of the BTB/POZ domain (amino acids 28-126 http://www.ebi.ac.uk.InterProScan), but is entirely within the NPH3 signature region (IPR004249; PF03000) which lies from amino acids 213 to 484 in NPH3-L. RPT2 and NPH3 also contain the NPH3 signature domain: encoded between amino acids 186-445 and 267-583, respectively. Neither http://www.expasy.org/prosite nor http://www.ebi.ac.uk.InterProScan could identify a coiled coil region at the C-terminal of NPH3-L, as has been reported for both NPH3 and RPT2 (Motchoulski & Liscum, 1999; Sakai *et al.,* 2000). Further analysis of the central region of NPH3-L showed that this protein does not auto-activate the yeast two-hybrid system in the absence of the phot1 bait (Fig. 3.4E). Quantification of the interaction between the N_2LOV2 region of phot1 and the central region of NPH3-L showed that this interaction is relatively robust, approximately seven times stronger that that determined for the positive controls, as obtained by measuring α-galactosidase activity in liquid cultures (Fig. 3.4F).

3.6.2 Further characterisation of the interactions between phot1 and RPT2/NPH3-L in yeast

As performed with the ARF proteins, it was important to establish the regions of phot1 that interact with the RPT2 and NPH3-L proteins isolated from the yeast two-hybrid screens. Domain mapping was therefore used to identify the phot1 region involved in the interaction with RPT2. Yeast were co-transformed with pGBKT7-N_2LOV2 or pGBKT7-KINASE bait vectors (Fig. 3.1) and the prey vector, pACT-RPT2, to assess whether the N-terminal region or C-terminal kinase domain of phot1 is required for the interaction. Figure 3.5A shows that the LOV domain-containing, N-terminal region of

phot1 is sufficient for the interaction, while the kinase domain does not interact with RPT2. These findings are in agreement with the results of Inada *et al.* (2004), demonstrating that the N-terminal region of phot1 is required to interact with RPT2 in yeast.

Since the N-terminal region containing the LOV photosensors was required for the interaction with the N-terminal region of RPT2, the effect of light on the interaction was investigated. Yeast plates containing the interacting proteins under investigation were grown in the dark or under 20 μmol m^{-2} s^{-1} white light conditions. The results obtained showed that the interaction between phot1 and the N-terminal region of RPT2 was unaffected by light (Fig. 3.5A).

The central region of NPH3-L was isolated from the yeast two-hybrid screen using the N-terminal region of phot1 as bait. It was therefore important to establish whether the region of NPH3-L isolated could also interact with full-length phot1. To determine if the NPH3-L fragment interacts with full-length phot1, yeast were transformed with the bait vector, pGBKT7-phot1 and the prey vector, pACT-NPH3-L. Figure 3.5B shows that the NPH3-L fragment identified from the screen also interacts with full-length phot1 in yeast. In order to determine the specificity of the interaction with the N-terminal region of phot1, yeast were transformed with the bait vector, pGBKT7-kinase and the prey vector, pACT-NPH3-L. Yeast containing these vectors grew on full selection medium, indicating that the NPH3-L fragment identified from the yeast two-hybrid screen interacts with both the N-terminal and C-terminal regions of phot1. Furthermore, growing yeast expressing phot1 and the central region of NPH3-L under dark and light conditions demonstrated that the interaction is not affected by light (Fig. 3.5B).

3.7 Phot1 interacts with 14-3-3λ

3.7.1 14-3-3 protein function in Arabidopsis

14-3-3 proteins were first identified as acidic, soluble proteins ~30kDa in size, from bovine brain tissue, and were named after their elution and gel migration pattern (Moore & Perez, 1967). Since then, they have been identified in all eukaryotic organisms tested as a highly conserved, multigene family. The number of 14-3-3 isoforms varies according to species: yeast has two, humans have seven, rice has eight

and *Arabidopsis* has fifteen (Mackintosh, 2004; Schoonheim *et al.,* 2007). The proteins encoded by these genes are highly conserved, with regions of variation at both the N- and C-termini and in smaller internal regions (Paul *et al.,* 2005). The first 14-3-3 protein identified in *Arabidopsis* was a constituent of a protein/G-box complex and implicated to be involved in regulation of gene transcription; this was 14-3-3-omega (GF14 (G-box factor 14-3-3) omega) (Lu *et al.,* 1992).

The fifteen *grf* (G-box regulating factor) genes in *Arabidopsis* can be split into two groups according to exon structure: *grf1-8* form the non-epsilon group and *grf9-15* form the epsilon group. To date, no expression has been proven for *grf13-15* and so the proteins putatively encoded by these genes have not been named (Rosenquist *et al.,* 2001).

Full-length 14-3-3-lambda (14-3-3λ; *grf6*; At5g10450) was isolated from the yeast two-hybrid screen using full-length phot1 as bait (Fig. 3.6A). Further analysis demonstrated that 14-3-3λ does not auto-activate the yeast two-hybrid system, showing that the interaction detected is dependent on phot1 (Fig. 3.6B). In addition, quantification of the phot1/14-3-3λ interaction from yeast grown in liquid cultures showed that this interaction is approximately half as strong, relative to the α-galactosidase activity observed for the positive controls used.

3.7.2 Further characterisation of the phot1/14-3-3λ interaction in yeast

Since full-length phot1 was found to interact with 14-3-3λ, we went on to investigate which regions of phot1 were required for this interaction. Domain mapping analysis in yeast demonstrated that 14-3-3λ interacts with the N_2LOV2 region of phot1 (Fig. 3.7). By contrast, no interaction was observed between the C-terminal kinase domain of phot1 and 14-3-3λ (Fig. 3.7). Since 14-3-3 proteins typically bind phospho-serine/threonine motifs, it was thought likely that the interaction between phot1 and 14-3-3λ would be light dependent as only the N-terminal region of phot1 has been reported to be auto-phosphorylated in response to blue light (Salomon *et al.,* 2003). However, when yeast expressing both phot1 and 14-3-3λ were grown on full selection medium in dark conditions their growth was comparable to those grown under white light conditions (Fig. 3.7). These initial findings would appear to indicate that the binding of 14-3-3λ to phot1 is not dependent on the phosphorylation status of the receptor.

3.8 Phot1 interacts with p-glycoprotein 19 (PGP19)

3.8.1 PGP protein function in Arabidopsis

ATP-binding cassette (ABC) proteins are found in all organisms and share a highly conserved ATP-binding cassette (ABC) domain which binds and hydrolyses ATP to produce energy for a number of fundamental biological processes (Schneider & Hunke, 1998; Higgins, 2001; Garcia *et al.,* 2004). There are 120 ABC-type proteins in *Arabidopsis* (Garcia *et al.,* 2004). Class I ABC transporters carry ABC and Integral Membrane (IM) domains on the same polypeptide chain, and are either composed of one copy of the ABC and IM (half transporters), or two tandemly repeated copies of the domains (full transporters). Within this class are four families: Drugs, Peptide and Lipid Export (DPL) is one of these families and within it is the p-glycoprotein (PGP) subfamily (Garcia *et al.,* 2004). There are 22 genes in the PGP subfamily in *Arabidopsis,* 21 of which are transcribed (Geisler & Murphy, 2005).

P-glycoprotein 19 (PGP19) is a member of the PGP subfamily of ABC-type transporters found in *Arabidopsis.* PGP19 is also known as Multi-drug Resistance 1 (MDR1), and shares 52% amino acid identity with its closest homologue, PGP1 (Noh *et al.,* 2001). PGP19 is predicted to comprise six membrane spanning domains followed by an ATP-binding site located in the cytosol of the cell, followed by another six transmembrane domains and cytosolic ATP-binding site (Noh *et al.,* 2001). Both PGP19 and PGP1 bind the auxin transport inhibitor naphthylphthalamic acid (NPA) and PGP19 is responsible for some basipetal polar auxin transport in *Arabidopsis* (Noh *et al.,* 2001).

Initially, the C-terminal cytoplasmic tail of PGP19 (At3g28860; amino acids 1121-1252) was isolated from the yeast two-hybrid screen using the N_2LOV2 region of phot1 as bait and additional transformations of yeast revealed that the kinase domain of phot1 interacted consistently with the C-terminal region of PGP19 (Fig. 3.8A). Moreover, auto-activation studies in yeast showed that the prey protein (PGP19) does not auto-activate the yeast two-hybrid system in the absence of the phot1 bait (Fig. 3.8B). Quantification of the interaction between the kinase domain of phot1 and the C-terminal region of PGP19 showed that this interaction is approximately one and a half times as strong as that detected for the positive controls used, as measured by assessing the degree of α-galactosidase activity in liquid cultures (Fig.3.8C).

The initial identification of PGP19 as an N_2LOV2 -domain interacting partner was potentially exciting. Given the known role of auxin transport in phototropism, we wished to study this interaction in more detail, particularly with respect to the effect of light on the interaction. Figure 3.9A shows that yeast expressing the phot1 N_2LOV2 and the C-terminal of PGP19 showed a light sensitive interaction while the interaction between the kinase domain and PGP19 was light insensitive. Yeast co-expressing functional N2LOV2 and the C-terminal of PGP19 do not grow on full-selection media grown under 20μmol m^{-2} s^{-1} but do grow on full-selection media grown in darkness. Deletion series analysis demonstrated that the light sensitivity of the interaction was dependent on the presence of the LOV2 domain (Fig. 3.9B). When the C-terminus of PGP19 is expressed in yeast only with regions of phot1 upstream of LOV2, the light sensitivity of the interaction was lost and yeast continued to grow under light conditions. The importance of functional LOV2 is further demonstrated in Figure 3.9C. By creating a bait vector encoding N_2LOV2 with a mutation that converts the light-sensing cysteine at position 39 of the LOV2 to alanine allows expression of a functionall "blind" N_2LOV2 domain (N_2LOV2C39A). When this bait vector is co-expressed with a prey vector encoding the C-terminus of PGP19, the light sensitivity of the interaction is abolished, although yeast growth remains strong on plates grown in darkness (Fig. 3.9C) However, this interaction was subsequently found to be inconsistent upon further characterisation until eventually it could not be reproduced. Therefore, no further work on this interaction is presented in this thesis, although the interaction is confirmed *in vitro* (Fig. 3.10B).

3.8.2 Further characterisation of the phot1/PGP19 interaction

As the interaction between phot1 and PGP19 was consistently specific to the kinase domain of phot1 (Fig. 3.8B), a deletion series was used to determine the specific region of the kinase domain necessary for the interaction. Yeast were co-transformed with either pGBKT7-Kinase or two further bait vectors containing deletions in this region, and pACT-PGP19, the prey vector. Protein regions encoded by these additional vectors are illustrated in Figure 3.10A. The bait vector containing Kinase Deletion 1 (pGBKT7-Kinase Del.1) lacks the extreme C-terminal region outside the phot1 kinase domain and comprises the region C-terminal of the Jα-helix and the kinase domain. The second bait vector in the deletion series (pGBKT7-Kinase Del.2) consists only of

the region between the Jα-helix and the kinase domain of phot1. Figure 3.10A shows that the PGP19 fragment identified from the screen interacts with the phot1 kinase bait only when the functional kinase domain is present. PGP19 does not interact with the region between the Jα-helix and the kinase domain of phot1. Likewise, the extreme C-terminal region of phot1 outside the kinase domain is not necessary for the interaction with PGP19.

No effect of light was observed on the interaction between the kinase domain of phot1 and the C-terminal region of PGP19 (data not shown). However, this is to be expected since the kinase region of phot1 does not contain the light-sensing LOV domains.

The phot1/PGP19 interaction was further confirmed by *in vitro* pull-down assays. Domains of phot1 were tagged with glutathione-S-transferase (GST) by subcloning the respective *PHOT1* cDNA regions into the bacterial expression vector pGEX4T-1 to produce constructs encoding GST-kinase (encoding the C-terminal kinase region of phot1), and GST-N$_2$LOV1 (encoding the N-terminal of phot1 through to the LOV1 domain). GST-tagged proteins were synthesised in BL21 *E. coli* and purified after lysis by attaching the proteins to glutathione-magnetic beads via the GST tag. The C-terminal region of PGP19 was subcloned into the yeast two-hybrid vector, pGBKT7, which, in addition to the GAL4 DNA-binding domain, contains a T7 initiation of transcription site that allows *in vitro* transcription/translation of the protein of interest with an N-terminal c-Myc epitope tag. The c-Myc-tagged C-terminal region of PGP19 was synthesised using rabbit reticulocyte lysate by *in vitro* transcription/translation and was incubated with glutathione-magnetic beads containing either GST-kinase, GST-N$_2$LOV1 or GST alone, purified from *E. coli*. After washing, proteins were eluted from the beads and subjected to SDS-PAGE. Proteins were then transferred to nitrocellulose membrane and probed with anti-c-Myc antibody. The results obtained are shown in Figure 3.10B. The C-terminal region of PGP19 was found to bind to both GST-kinase and GST-N$_2$LOV1. The interaction between PGP19 and the phot1-GST fusions was specific, as the C-terminal region of PGP19 did not bind to beads with only GST attached or to the magnetic beads alone. These findings confirm that the kinase domain of phot1 interacts with the C-terminal of PGP19. In addition, the *in vitro* pull-down analysis demonstrates that the N-terminal region of phot1 can also interact with the C-terminal region of PGP19. This is in

agreement with the initial interaction studies performed in yeast, which showed an interaction between the C-terminal region of PGP19 and the N_2LOV2 region of phot1 (Fig.3.9).

3.9 Do the phot1-interacting proteins interact with phot2?

Phot1 and phot2 exhibit functional redundancy for high-light-mediated phototropism (Sakai *et al.*, 2001), stomatal opening at all light intensities (Kinoshita *et al.,* 2001) and chloroplast accumulation in response to low light (Sakai *et al.*, 2001). It was therefore important to establish whether the phot1-interacting proteins identified from the yeast-two hybrid screen also interacted with phot2. To determine if phot1 and phot2 share interaction partners, all the phot1-interacting partners described above were co-transformed into yeast with the bait vector pGBKT7-phot2. The results of these co-transformations are presented in Figure 3.10 along with representative images of the ability of the yeast obtained to grow on full selection medium. The results show that ARF2, ARF7 and RPT2 are also able to interact with full-length phot2 in yeast, while NPH3-L, 14-3-3λ and PGP19 do not. The interaction between phot2 and ARF2 and ARF7 is stronger than the interactions between phot1 and ARF2 or ARF7, but weaker than the phot2/ RPT2 interaction which is comparable in strength to the phot1/RPT2 interaction. These findings suggest that while phot1 and phot2 may share some interacting partners, they also bind specific partners to mediate signalling.

3.10 Discussion

In an attempt to identify proteins involved in phot1 signalling, yeast two-hybrid screens were carried out. The results of these screens have been presented in this chapter, and the proteins identified from the screens have been subjected to initial characterisation with regards to their interaction with phototropins.

3.10.1 The yeast two-hybrid screen

Full-length phot1 and the light-sensing N-terminal region of phot1 (N_2LOV2) were used as baits to screen a cDNA library derived from 3-day-old, etiolated *Arabidopsis* seedlings. A total of 130 yeast colonies containing putative phot1-interacting proteins were obtained from the yeast two-hybrid screens. After eliminating false positives, six proteins were chosen for further investigation in this study.

Confidence in the efficacy of the screens was improved upon isolation of known phot1-interacting partners such as RPT2. However, other known phot1-interacting proteins such as NPH3 and Phytochrome Kinase Substrate 1 (PKS1) were not isolated from the screen. This may be due to low representation of certain genes in the cDNA library, or simply that an insufficient number of yeast colonies were screened to identify every phot1-interacting partner.

Had time allowed, the extent of the screen could have been expanded by carrying out the initial screens in both dark and light growth conditions or by carrying out an additional screen using the kinase domain of phot1 as bait. Screening a cDNA library derived from light-grown tissue using all three baits described above would allow identification of any light-induced phot1-interacting proteins which would definitely have been unidentifiable in a cDNA library derived from dark grown tissue, but would have been outside the time constraints of this project. However, the conditions used for screening identified a manageable number of putative interacting proteins for a study of this magnitude. Two of the phot1-specific-interacting proteins isolated from the yeast two-hybrid screens will be investigated in greater detail in subsequent chapters.

3.10.2 Members of the ARF family interact with phot1

Two members of the ARF family were isolated from the yeast two-hybrid screen using full-length phot1 as bait. Interestingly, ARF2 and ARF7 were found to interact with full-length phot1 in a blue-light-sensitive manner. Neither ARF2 nor ARF7 could interact with truncated regions of phot1 (N_2LOV2 and the kinase regions), so the major domain of phot1 that is involved in the interaction with ARFs could not be identified. This may indicate that correct folding of the full-length phot1 protein is necessary for the interaction, or that steric effects inherent to the yeast two-hybrid system mask a binding site necessary for the interaction between the ARFs and one of the truncated phot1 proteins. Quantification of the interactions between phot1 and the ARFs indicated that both interactions were weak compared to the positive controls. It should be noted however, that the interaction between the ARFs and phot1 is light sensitive and that ambient light present during the growth of the liquid culture may have negatively affected the strength of the interaction. Given that both ARF2 and ARF7

interact with phot2, it would be interesting to investigate the effect of light on the interactions to determine if these are also blue-light sensitive.

ARF proteins are involved in the regulation of vesicle trafficking and organelle structure by undergoing a GDP/GTP nucleotide exchange cycle that involves conformational changes in the ARF protein and the client protein to which it is bound (Gebbie *et al.,* 2005; Neilsen *et al.,* 2006). It is possible to "lock" ARF proteins in their GTP- (active) or GDP- (inactive) bound forms (Berón *et al.,* 2001), and it would be interesting to use these locked isoforms in the yeast two-hybrid system to determine the activity of ARFs when they are bound to phot1.

Because of the high degree of similarity between the ARF proteins in *Arabidopsis*, it is likely that they exhibit functional redundancy. A recent study has created an antisense *Arabidopsis* line that greatly reduces or abolishes expression of all Class1 ARF proteins (Gebbie *et al.,* 2005). Plants from this line show reduced cell division, reduced cell expansion, delayed flowering and reduced apical dominance, which indicate changes in hormonal pathways (Gebbie *et al.,* 2005). Indeed, the ARF GEF (Guanine Exchange Factor), GNOM is at least partially responsible for the polar localisation at the plasma membrane of the auxin efflux carrier, PIN-FORMED 1 (PIN1) (Steinmann *et al.,* 1999). As phot1 has been shown to disassociate from the plasma membrane in response to blue light, it is interesting to speculate that either of the ARFs may be involved in maintaining the plasma membrane localisation state of phot1 in the dark, and that as the phot1/ARF interaction is lost upon exposure to blue light, phot1 delocalises from the plasma membrane. Although the phot1 interaction with ARFs could yield exciting results, it was not pursued because it was a relatively weak interaction and the extreme light-sensitivity posed potential problems for verifying the interactions.

3.10.3 Members of the NRL family interact with phot1

Two members of the NRL family were identified from the yeast-two hybrid screen. The isolation of the N-terminal region of RPT2 using full-length phot1 as bait is a good indication that the screen is effective as this protein has already been identified previously as a phot1-interacting partner (Inada *et al.,* 2004). Domain mapping showed that the N-terminal region of phot1 is necessary for the interaction with the RPT2 fragment isolated from the screen, and that the kinase domain of phot1 does not

interact with the RPT2 fragment. These findings are in agreement with the results described by Inada *et al.* (2004). In addition to the interaction with phot1, this study also shows that the N-terminus of RPT2 (amino acids 1-187) interacts strongly with full-length phot2. These findings are in contrast to the results of Inada *et al.*, who showed that when the N-terminus of phot2 (amino acids 1-537) is co-transformed in yeast with the either the N-terminus (amino acids 1-257) or the C-terminus (amino acids 284-593) of RPT2 there is no significant interaction. Since the region of RPT2 used in our screen and the region of RPT2 used in the screen carried out by Inada *et al.* (2004) overlap, the data indicate that the N-terminus of RPT2 interacts with a region of phot2 downstream of amino acid 537.

The interaction between phot1 and RPT2 has been verified *in vivo* (Inada *et al.*, 2004), and although an absolute function for RPT2 has not been identified, it is thought likely that it acts as a scaffold to form a functional phot1 receptor complex. RPT2 also interacts with NPH3 in yeast (Inada *et al.*, 2004), but while NPH3 is essential for phot1- and phot2-mediated phototropism, RPT2 is only involved in phot1-mediated phototropism. Unlike NPH3, RPT2 is involved in phot1-mediated stomatal opening. If phot1, NPH3 and RPT2 are all part of a complex involved in signal transduction, it would appear that the initial phot1 signal results in a highly regulated signalling pathway. Members of the phot1 signalling pathway can also be involved with phot2 signalling (NPH3, for example); or may be phot1 specific, but not the only signalling partner required for phot1 to mediate a specific response (for example, RPT2 plays a role in, but is not essential for phot1-mediated phototropism).

A novel member of the NRL family, NPH3-L, was also identified from the yeast two-hybrid screen using the N-terminal region of phot1 as bait. Subsequent analysis demonstrated that the central region of the NPH3-L protein identified in the screen could interact with both the N_2LOV2 and kinase regions of phot1. Similarly to RPT2, there was no effect of light on the interaction between phot1 and NPH3-L. One of the puzzling observations about the NPH3-L interaction with phot1 was that the central region of NPH3-L interacts with both the extreme N-terminus and the kinase domain of phot1. This finding is investigated in greater detail and discussed in Chapter 4. As NPH3-L is a novel member of a family known to be involved in phototropin-mediated responses and the interaction between the N-terminus of phot1 and the central region of NPH3-L was extremely robust and phot1-specific, NPH3-L was

chosen to be investigated in more detail. Further analysis of this interaction is detailed in Chapter 4.

3.10.4 14-3-3λ interacts with phot1

Our yeast two-hybrid screening identified the full length 14-3-3λ isoform as an interacting partner for full-length *Arabidopsis* phot1. Domain mapping demonstrated that the N-terminal region of phot1 was necessary for the interaction with 14-3-3λ, and not the kinase domain. There was no effect of light on the phot1/14-3-3λ interaction in yeast, which would appear to indicate that the interaction is not dependent on the phosphorylation status of phot1. However, Kinoshita *et al.* demonstrated that the 14-3-3 interaction with phot1 from *Vicia faba* was dependent on blue light-induced autophosphorylation of phot1 (Kinoshita *et al.,* 2003). In their study, bacterially expressed 14-3-3-phi (14-3-3ϕ) was used as a typical plant 14-3-3. 14-3-3ϕ is a member of the non-epsilon group of *Arabidopsis* 14-3-3 proteins, as is 14-3-3λ and therefore it is possible that phot1 binding is a functional property shared by all members of the group. The function of 14-3-3 binding to phot1 is as yet undetermined, however a previous study has shown that 14-3-3ϕ also binds to the phosphorylated C-terminus of the H^+-ATPase in *Vicia faba* guard cell protoplasts (Kinoshita & Shimizaki, 1999). Blue light-induced phosphorylation and activation of the H^+-ATPase results in increased H^+ pumping and, consequently, increased stomatal opening. Given that phototropins are known to play a functionally redundant role in blue-light induced stomatal opening (Kinoshita *et al.,* 2001), it is possible that 14-3-3s may play a role in transducing a signal from blue-light activated phototropins which later results in activation of the H^+-ATPase with the physiological consequence that the stomatal pore opens in response to blue light. However, the functional redundancy shown by phototropins with regard to stomatal opening and the lack of interaction between 14-3-3λ and phot2 suggests that there are two independent signalling pathways, which result in phototropin-mediated blue-light induced stomatal opening. The phot1/14-3-3λ interaction is investigated in more detail and discussed further in Chapter 5.

3.10.5 PGP19 interacts with phot1

Initially, the C-terminal cytoplasmic tail of PGP19 was identified from the yeast two-hybrid screen using the N-terminus of phot1 as bait. Preliminary characterisation

indicated that the interaction was dependent on the LOV2 domain of phot1 and was blue light-sensitive (Fig.3.9). However, this interaction was found to be inconsistent. Subsequent investigation revealed that the interaction between the C-terminal kinase region of phot1 and the C-terminal tail of PGP19 was reliable. Pull-down analysis confirmed the interaction of the C-terminal fragment of PGP19 with both the N-terminal and C-terminal regions of phot1. To date, no plant protein other than phototropins themselves has been identified as a phototropin substrate, although phototropins have been shown to phosphorylate the artificial substrate, casein, (Matsuoka & Tokotumi, 2005). Mammalian PGPs are regulated by phosphorylation of the linker domain adjoining the first nucleotide-binding fold by protein kinases A and C (Castro *et al.,* 1999; Ambudkar *et al.,* 2003; Geisler & Murphy, 2005). Therefore, it is intriguing to postulate that phot1 regulates the activity of PGP19 by phosphorylating the C-terminal nucleotide-binding fold in response to light. It is possible that when phot1 is in its dark state the folded protein structure allows interaction of both the kinase and N_2LOV2 domains with the C-terminal of PGP19. Light-induced conformational changes in the phot1 protein structure could result in attenuation of the N_2LOV2/PGP19 interaction and phosphorylation of the C-terminus of PGP19 by the now active phot1 kinase domain providing a possible means for either activating or deactivating PGP19.

This interaction was of particular interest, given that PGP19 is required for auxin transport and that phot1-mediated phototropism is the result of an auxin gradient across the hypocotyl, with higher auxin levels or responsiveness on the shaded side of the hypocotyl. Identification of PGP19 from the yeast two-hybrid screen as a phot1–interacting protein therefore provides a potential link between phototropins and the auxin transport necessary for phototropism. Additional yeast studies showed that the interaction was specific to the C-terminal kinase domain of phot1 as no interaction was seen in yeast co-transformed with the C-terminal of PGP19 and full-length phot2 or the kinase domain of phot2 (data not shown). As the interaction was specific to phot1, the possibility that the interaction was generic with all PGP proteins was investigated. Yeast were co-transformed with the closest homologue to PGP19, PGP1, and the C-terminal kinase domains of both phot1 and phot2. However, none of these proteins appeared to interact in the yeast two-hybrid system, (data not shown), indicating that the interaction is specific to the C-termini of phot1 and PGP19. Because of the exciting

possibilities suggested by this interaction, further work was carried out in the laboratory to investigate it in more detail. Unfortunately, extensive attempts to confirm the interaction of full-length PGP19 with full-length phot1 *in planta* have proven unsuccessful to date (S. Sullivan and J.M. Christie, unpublished data). Therefore, no further work on the phot1/PGP19 interaction is presented in this study.

A) Schematic representation of the baits used for yeast two-hybrid screening and domain mapping. Major domains of the full-length phot1 protein are indicated. Amino acid positions are indicated numerically.

B) Auto-activation tests of the baits used in the yeast-two hybrid system. Vectors encoding murine p53 and the SV40 large T-antigen were included as a positive control. Yeast were plated on non-selective medium lacking leucine and tryptophan (-L/-W) for plasmid selection and on full selection medium lacking adenine, histidine, leucine and tryptophan and including 5-bromo-4-chloro-3-indolyl-α-D-galactopyranosidase (X-α-Gal) (-A/-H/-L/-W+α-gal) to select for an interaction between two proteins, or to identify auto-activation in the absence of bait or prey proteins.

Figure 3.1 Baits used in the yeast two-hybrid system

Table 3.1 Transformation efficiencies obtained from yeast two-hybrid screening

Using the two different baits indicated to screen the *Arabidopsis* cDNA library, a total of 1.2 x 10^6 yeast colonies were screened. From the colonies screened, 130 grew on fully selective media.

Bait Used	Library Used	Number of colonies screened	Number of colonies growing on selective media
Full-length phot1	Dark	7.8 x 10^4	57
N$_2$LOV2	Dark	2.4 x 10^5	73
Total	**Dark**	**3.18 x 10^5**	**130**

Table 3.2 Phot1-interacting proteins identified from the yeast two-hybrid screen

Six proteins identified from the yeast two-hybrid screen were chosen for further investigation. The bait protein used to identify the phot1-interacting proteins is shown in the table along with their TAIR accession number and predicted function.

Bait Used	Interacting Protein Obtained	TAIR Accession Number	Predicted Protein Function
phot1	ARF2	At3g62290	GTP binding, vesicle trafficking
phot1	ARF7	At5g17060	GTP binding, vesicle trafficking
phot1	14-3-3λ	At5g10450	Cellular signalling, phosphoprotein binding
phot1	RPT2	At2g30520	Phototropism, stomatal opening, protein binding
N_2LOV2	NPH3-L	At1g30440	Signal transducer activity, novel member of NPH3/RPT2-Like family
N_2LOV2	PGP19	At3g28860	Photomorphogenesis, polar auxin transport, response to blue light
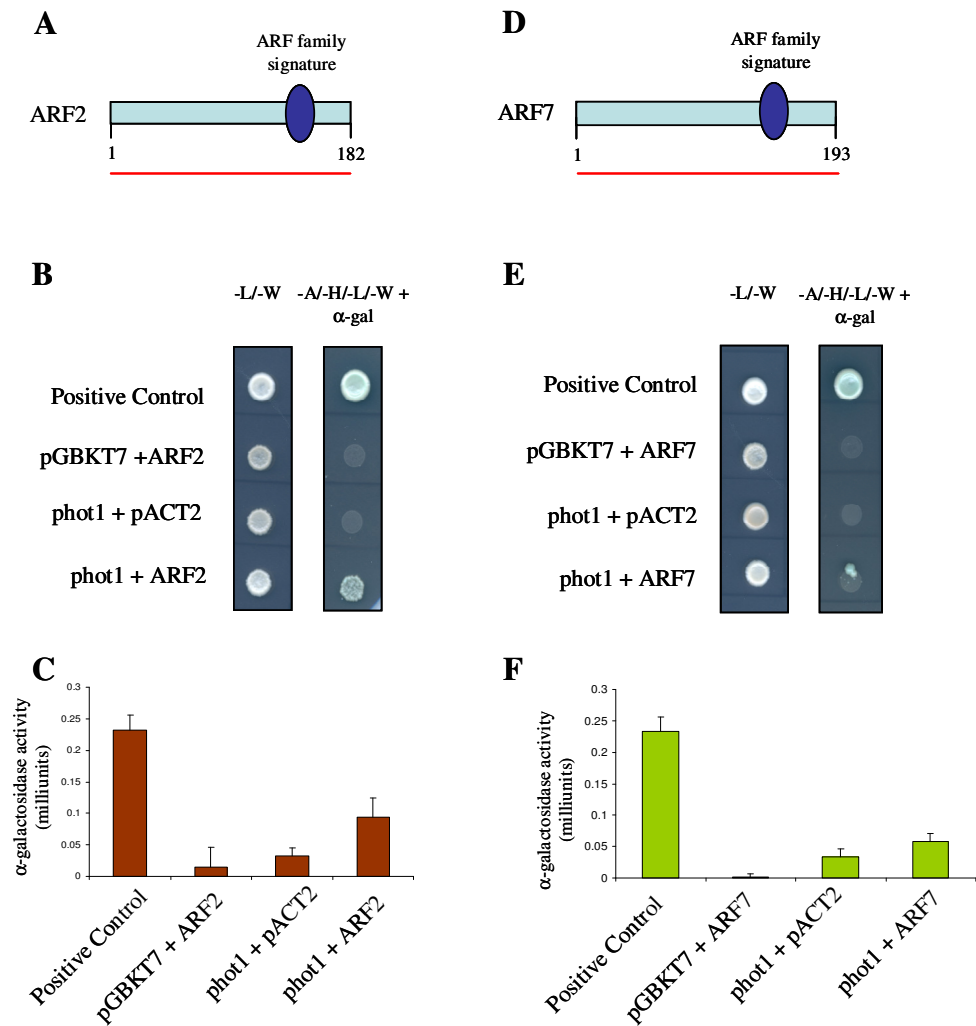
Figure 3.2 Phot1 interacts with ARF2 and ARF7 in yeast

A + D) Using full-length phot1 as bait, the entire coding sequences of ARF2 (A) and ARF7 (D) were isolated from the yeast two-hybrid screen. The underline denotes the regions identified and amino acid positions are indicated. ARF family signature: Pfam PF00244.

B + E) Auto-activation analysis of ARF2 (B) and ARF7 (E) in yeast. Yeast were co-transformed with bait and prey vectors encoding phot1 and ARF2/ARF7, respectively to confirm the interaction between these proteins. Co-transformation of vectors encoding the phot1 bait and ARF2/ARF7 prey proteins with the corresponding empty prey and bait vectors were also included as a test for auto-activation of the yeast two-hybrid system. Yeast were grown on media as described in Figure 3.1A. Positive controls used are as described in Figure 3.1A.

C + F) Quantification of the phot1/ARF2 (C) and phot1/ARF7 (F) interaction using the α-galactosidase assay. Yeast co-transformed with the bait and prey vectors (outlined in B and E) were grown in liquid culture and the activity of α-galactosidase secreted into the media was measured as described in the Materials and Methods. Error bars indicate standard error (n=3).
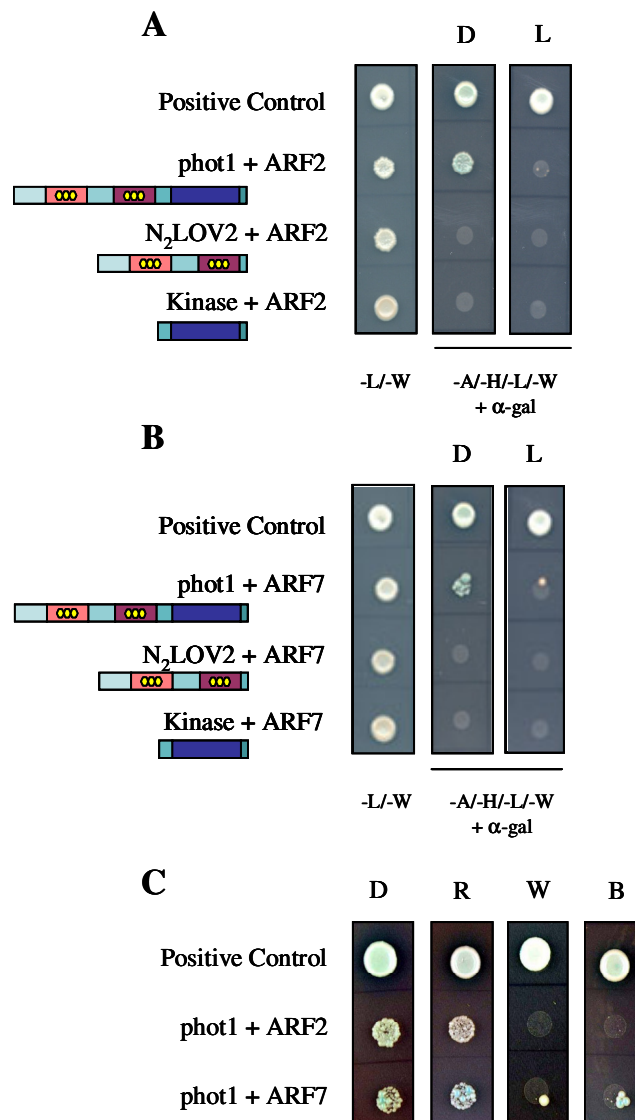
Figure 3.3 Domain mapping and the effect of light on the interaction between phot1 and ARFs

A + B) ARF2 and ARF7 only interact with full-length phot1. Yeast were co-transformed with bait vectors encoding full-length phot1 or the phot1 domains (N$_2$LOV2, Kinase) and the prey vector encoding ARF2 (A) or ARF7 (B). The domains of phot1 expressed are shown schematically. Yeast were plated on non-selective media (-L/-W) for plasmid selection, and on full selection medium (-A/-H/-L/-W+α-gal) to select for interacting proteins. Yeast were grown in the dark (D) or under 20 μmol m^{-2} s^{-1} white light (L). Positive controls used are as described in Figure 3.1A.

C) The phot1 interaction with ARF2 and ARF7 is blue light sensitive. Yeast co-transformed with the bait vector encoding phot1 and a prey vector encoding either ARF2 or ARF7, and were plated on full selection medium. Yeast were grown in dark (D) conditions or under 10 μmol m^{-2} s^{-1} red (R), white (W) or blue (B) light.
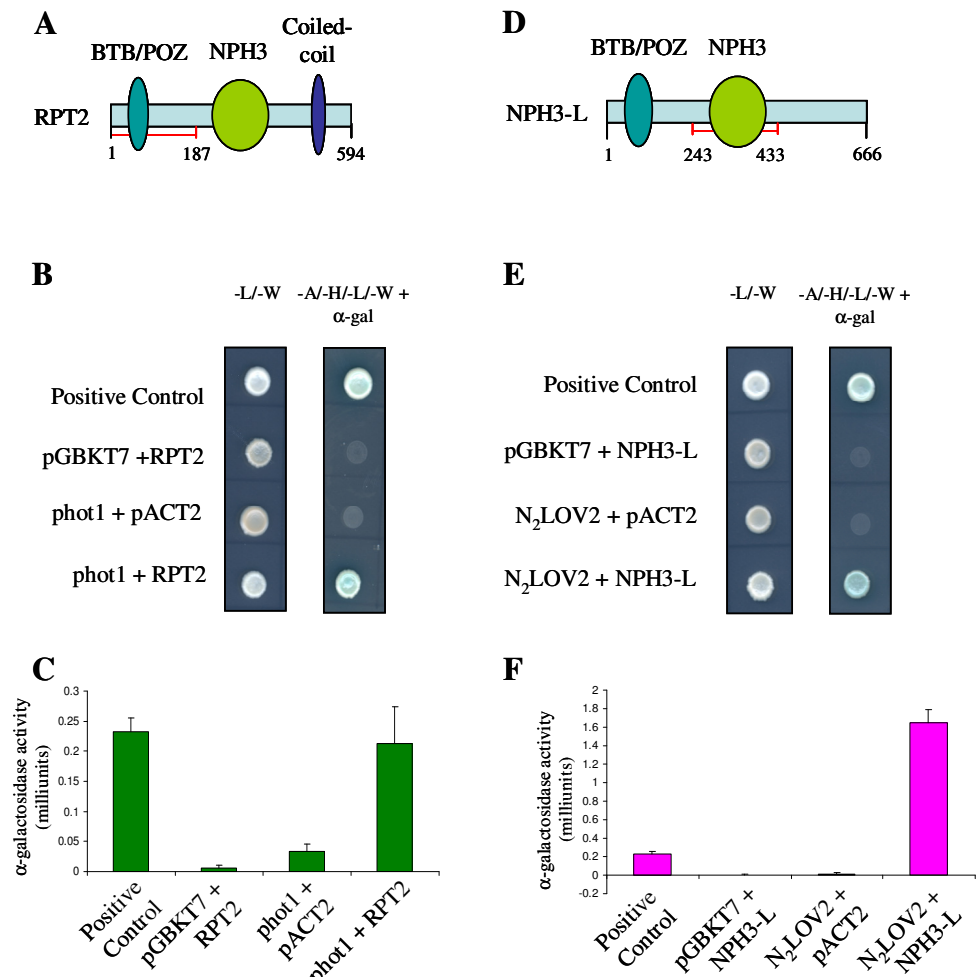
Figure 3.4 Phot1 interacts with RPT2 and NPH3-L in yeast

A) Using full-length phot1 as bait, the N-terminal region of RPT2 was isolated from the yeast two-hybrid screen (amino acids 1-187). The underline denotes the region identified and amino acid positions are indicated numerically. Domains are described in main text.

B + E) Auto-activation analysis of RPT2 and NPH3-L in yeast. Yeast were co-transformed with bait and prey vectors encoding phot1 and the N-terminal region of RPT2, respectively (B) or bait and prey vectors encoding N_2LOV2 and the NPH3-L fragment, respectively to confirm the interactions. Co-transformation of bait and prey vectors with the corresponding empty vectors were included as a test for auto-activation of the yeast two-hybrid system. Positive controls used are as described in Figure 3.1A.

C + F) Quantification of the phot1/RPT2 (C) and N_2LOV2/NPH3-L (F) interactions using the α-galactosidase assay. Yeast co-transformed with the bait and prey vectors outlined in (B) and (E) were grown in liquid culture and the activity of α-galactosidase secreted into the media was measured as described in the Materials and Methods. Error bars indicate standard error (n=3).

D) The N-terminal region of phot1 (N_2LOV2) was used as bait to isolate the central region of NPH3-L (amino acids 243-433) from the yeast two-hybrid screen. The region of NPH3-L identified is underlined and amino acid positions are indicated.
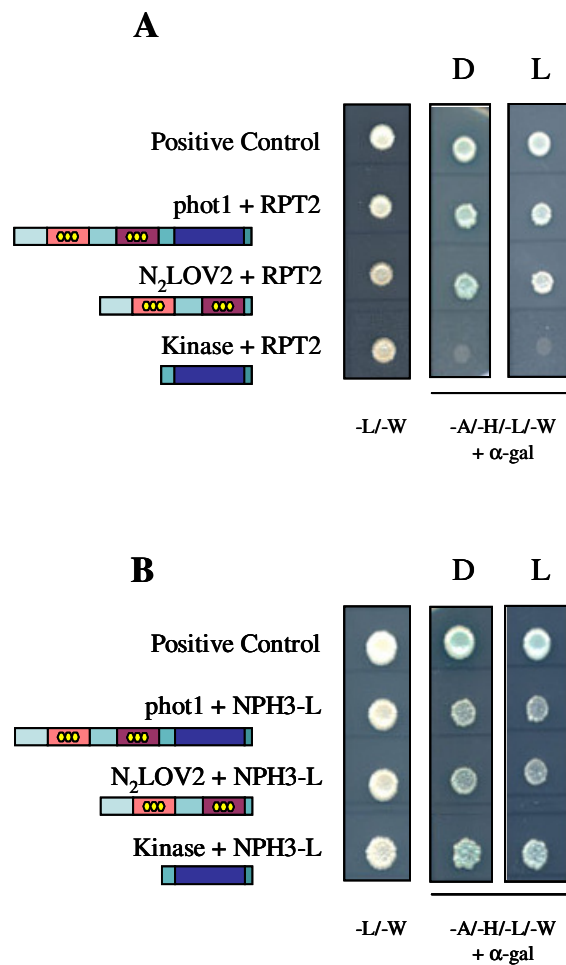
Figure 3.5 Domain mapping the phot1/RPT2 and phot1/NPH3-L interactions

A) Domain mapping analysis of the phot1/RPT2 interaction. Yeast were co-transformed with bait vectors encoding phot1 or the phot1 domains (N_2LOV2 and Kinase) and the prey vector encoding the N-terminal region of RPT2. Non-selective media (-L/-W) selects for both vectors, while full selective media (-A/-H/-L/-W+α-gal) selects for interacting proteins. Yeast were grown in darkness (D) or under 20 μmol m^{-2} s^{-1} white light (L). Positive controls used are as described in Figure 3.1A.

B) Domain mapping analysis of the phot1/NPH3-L interaction. As described for RPT2, yeast were co-transformed with a bait vector encoding either full-length phot1 or one of the phot1 domains, and the NPH3-L fragment encoded in the prey vector. Yeast were then grown with positive controls as described in (A).

84
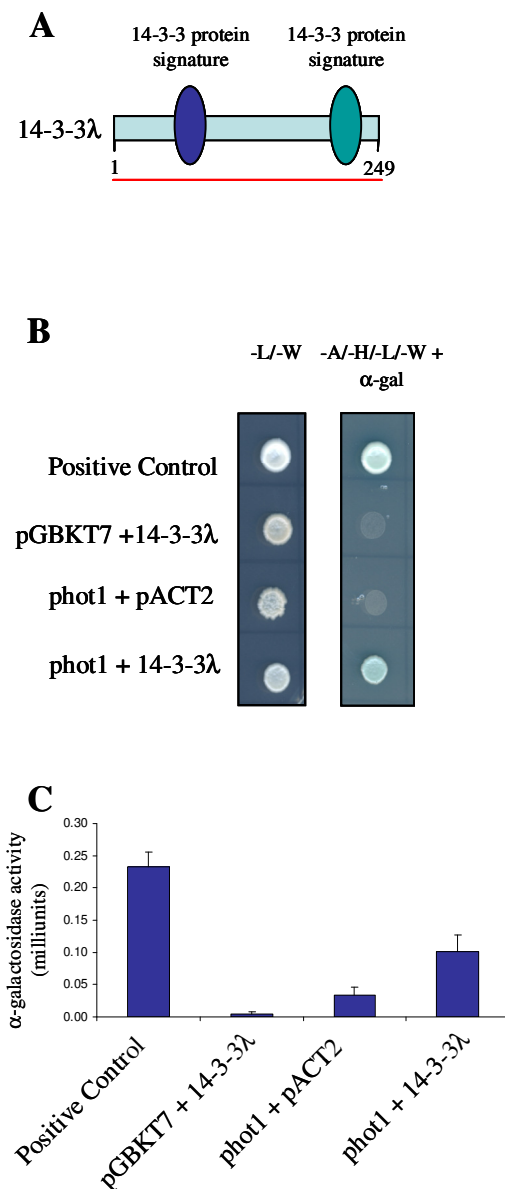
Figure 3.6 Phot1 interacts with 14-3-3λ in yeast

A) Using the full length phot1 bait, the entire coding sequence of 14-3-3λ was isolated from the yeast two-hybrid screen, this is denoted by the red underline. Amino acid positions are indicated. Two different signature domains determined by InterPro as being indicative of 14-3-3 proteins are indicated on the diagram: Interpro IPR006689, IPR006688.

B) Auto-activation analysis of 14-3-3λ. To confirm the interaction, yeast were co-transformed with the bait vector encoding full-length phot1 and the prey vector which encodes 14-3-3λ. Yeast were also co-transformed with either the bait (phot1) or the prey (14-3-3λ) and the corresponding empty vector. Non-selective media (-L/-W) selects for yeast transformed with both vectors while full-selection media (-A/-H/-L/-W+α-gal) selects for interacting proteins. Positive controls used are as described in Figure 3.1A.

C) Quantification of the phot1/14-3-3λ interaction in yeast. Yeast were co-transformed with the constructs described in (B) and α-galactosidase activity was measured as described in the Materials and Methods. Error bars indicate standard error (n=3).

85
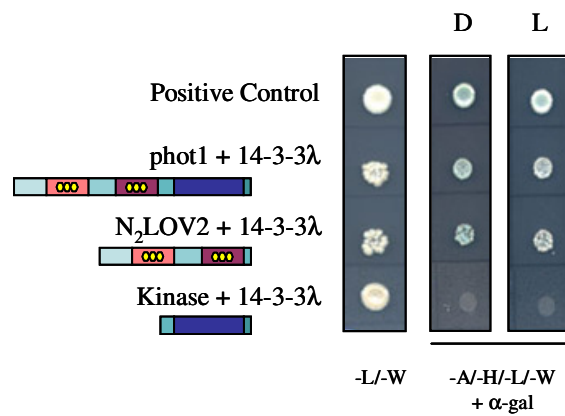
Figure 3.7 Domain mapping and the effect of light on the phot1/14-3-3λ interaction

Yeast were co-transformed with a bait vector encoding either full-length phot1 or one of the phot1 domains (N$_2$LOV2 or Kinase), and the prey vector encoding 14-3-3λ. Non-selective media (-L/-W) selects for yeast transformed with both vectors while full-selection media (-A/-H/-L/-W+α-gal) selects for interacting proteins. Yeast were grown in dark (D) or 20 μmol m^{-2} s^{-1} white light (L) conditions. Positive controls used are as described in Fig. 3.1A.
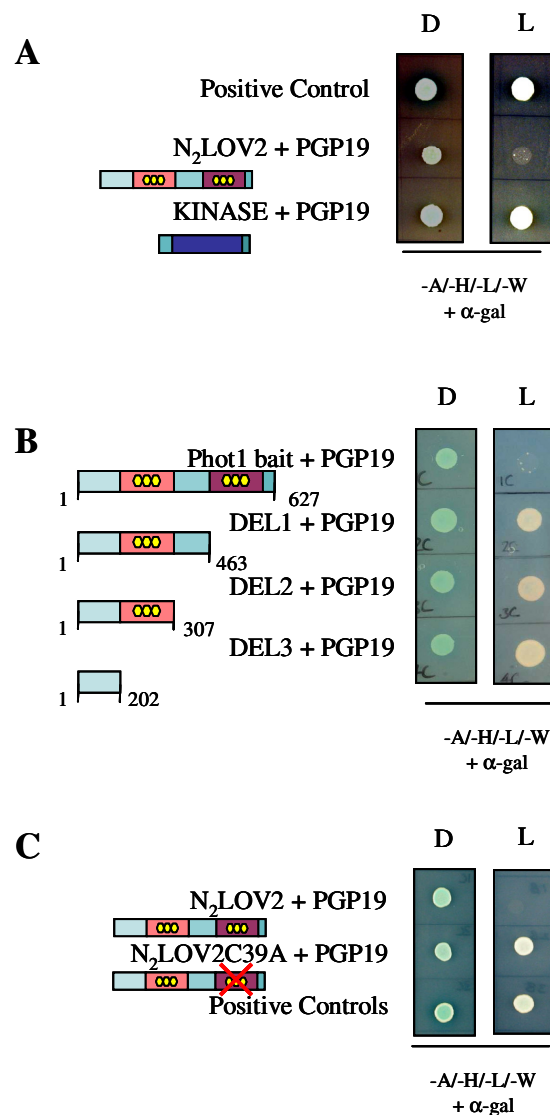
Figure 3.9 Domain mapping and the effect of light on the interaction between N₂LOV2 and PGP19.

A) Domain mapping analysis of the N₂LOV2/PGP19 interaction. Yeast were co-transformed with bait vectors encoding the kinase or N₂LOV2 domains of phot1, and the prey vector encoding the C-terminal region of PGP19. Full-selection media (-A/-H/-L/-W+α-gal) selects for interacting proteins. Yeast were grown in darkness (D) or 20 μmol m^{-2} s^{-1} white light (L). Positive controls used are as described in Figure 3.1A.

B) Deletion analysis of the phot1 N₂LOV2 regions required for interaction with PGP19. Yeast were co-transformed with a bait vector encoding phot1 N₂LOV2 deletions, and the prey vector encoding the C-terminal region of PGP19. Yeast were grown as described in (A).
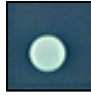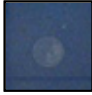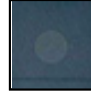
C) Analysis of the effect of a point mutation in the LOV2 domain on the interaction between N₂LOV2 and PGP19. Yeast were co-transformed with a bait vector encoding functional phot1 LOV2 (N₂LOV2), or phot1 containing a mutation at position 39 of the second LOV domain (N₂LOV2C39A) and a prey vecor encoding the C-terminal region of PGP19. The mutation is indicated by a red cross. Yeast were grown as described in (A).
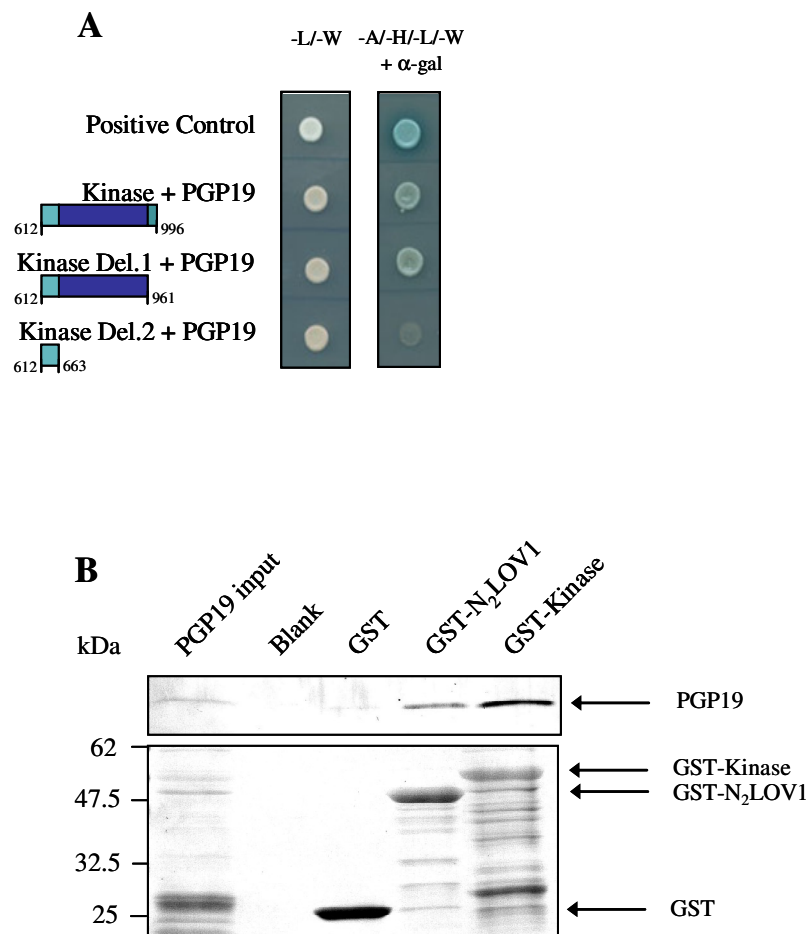
Figure 3.10 Characterisation and confirmation of the phot1/PGP19 interaction

A) Deletion analysis of the phot1 kinase domain region required for the interaction with the C-terminal region of PGP19. Yeast were co-transformed with a bait vector encoding the kinase domain of phot1, or deletions of that region as indicated by the amino acids positions above, and the prey vector encoding the C-terminal region of PGP19. Non-selective media (-L/-W) selects for yeast transformed with both vectors while full-selection media (-A/-H/-L/-W+α-gal) selects for interacting proteins. Positive controls used are as described in Figure 3.1A.

B) *In vitro* binding of PGP19 to phot1. Approximately equal amounts (indicated in the lower panel by Ponceau S staining) of bacterially-synthesised GST-tagged phot1 proteins (GST-N$_2$LOV1 and GST-Kinase) were incubated with the c-Myc-tagged C-terminal region of PGP19, synthesised by *in vitro* transcription/translation. Western blotting using anti-c-Myc antibody was used to visualise c-Myc-PGP19 (upper panel). One twenty-fifth (2μL) of the transcription/translation reaction was loaded as a size marker for PGP19 (PGP19 input). GST protein alone (GST), and empty magnetic beads (Blank) were included as negative controls to show specific binding. Size markers (kDa) are indicated on the left.

	ARF2	ARF7	RPT2	NPH3-L	14-3-3λ	PGP19
phot2	++	++	+++	-	-	-

Figure 3.11 Determination of the interaction of phot2 with the phot1-interacting proteins

All phot1-interacting proteins were transformed into yeast with full-length phot2 to determine if they were common phototropin-interacting proteins, or if they were phot1-specific. The strength of the interaction (as measured by yeast growth) relative to the growth shown by the positive controls is indicated above a representative picture of the transformed yeast.

+++ indicates a strong interaction, - indicates there is no interaction.

Chapter 4: Investigation of the phot1-interacting protein, NPH3-L

4.1 Introduction

As described in Chapter 1 the NPH3/RPT2-like (NRL) proteins belong to a novel plant-specific family. The proteins are characterised by an N-terminal broad complex, tram-track, bric à brac/pox virus and zinc finger, (BTB/POZ) domain, a NPH3 domain (Pfam: PF03000) in the middle of the protein, and most have a coiled-coil domain at the C-terminus (Motchoulski & Liscum, 1999, Sakai *et al.,* 2000, Pedmale & Liscum, 2007). Both the BTB/POZ and coiled-coil domains are thought to be involved in protein-protein interactions (Stogios *et al.,* 2005), although the function of these domains in NRL proteins is not fully understood at present. To date, only two members of the family have been characterised: NPH3 and RPT2. NPH3 is essential for phototropism (Motchoulski & Liscum, 1999, Inada *et al*., 2004), and is also involved in leaf positioning (Inuoe *et al.,* 2007). RPT2 functions in phot1-mediated phototropism and stomatal opening (Sakai *et al.,* 2000; Inada *et al*., 2004). This chapter aims to confirm and characterise the interaction between phot1 and a novel member of the NRL family, designated NPH3-like (NPH3-L), which was initially identified from the yeast two-hybrid screen described in Chapter 3.

4.2 Results

4.2.1 Further characterisation of the phot1/NPH3-L interaction

As described in Section 3.6.1, the N-terminal region of phot1 was used as bait to isolate the central region of NPH3-L from a yeast two-hybrid screen. Figure 3.5 demonstrates that both the N-terminal (N_2LOV2) and the C-terminal (Kinase) domains of phot1 interact with the NPH3-L fragment isolated. To identify in more detail the regions of phot1 involved in the interaction, a phot1 deletion series was constructed in the yeast two-hybrid bait vector pGBKT7 and co-transformed into yeast with the prey vector pACT2 encoding the NPH3-L fragment. The regions of phot1 encoded in these constructs are shown schematically in Figure 4.1. Using the deletion series, Figure 4.1A shows that all phot1 N-terminal regions interact with the NPH3-L fragment. The extreme N-terminus of phot1 does not encode any LOV domains, which are part of the larger PAS domain superfamily and are thought to be involved in protein-protein

interactions, but is still sufficient for the interaction with the truncated NPH3-L protein. Figure 4.1B shows that the C-terminal region of phot1 also interacts with the NPH3-L fragment. However, for the interaction to occur it is imperative that the phot1 kinase domain is present: when removed, the interaction is attenuated (Kinase Del.2). These results indicate that the regions of phot1 involved in the interaction with the central region of NPH3-L are the kinase domain and extreme N-terminal region of phot1.

To confirm the results of the yeast two-hybrid analyses, an *in vitro* pull-down assay was used. Bacterially-expressed GST-tagged domains of phot1 (GST-N$_2$LOV1 and GST-Kinase) were purified using glutathione-magnetic beads. The cDNA region encoding the central NPH3-L fragment was sub-cloned into the yeast two-hybrid vector, pGBKT7, which allows *in vitro* transcription/translation of the protein with an N-terminal c-Myc epitope tag. The c-Myc-tagged NPH3-L fragment and GST-tagged proteins were incubated together. Beads were then extensively washed and proteins bound to the beads were eluted and then separated by SDS-PAGE. Figure 4.2 shows that the NPH3-L fragment interacts with both the N-terminus (GST-N$_2$LOV1) and C-terminus (GST-Kinase) of phot1. Although the signals obtained were relatively weak, the *in vitro* pull-down assay confirms the yeast two-hybrid data.

4.2.2 Phylogenetic analysis of the NRL family and antibody production

Members of the large *Arabidopsis* NRL family have five regions of primary amino acid sequence conservation, (designated DIa, DIb, DII, DIII and DIV), separated by regions of non-conserved amino acid sequence which exhibits predicted secondary structure conservation throughout the family (Motchoulski & Liscum, 1999, Sakai *et al,* 2000, Inada *et al.,* 2004; Celaya & Liscum, 2005). Phylogenetic analysis was carried out to compare the NPH3-L protein identified in this study to the known members of the family, NPH3 and RPT2. A phylogenetic tree of all members in the *Arabidopsis* NRL family shows that NPH3-L is located in a separate branch from either of the described members of the family (Fig. 4.3A). Amino acid alignment by ClustalW indicates that NPH3-L shows 37% amino acid identity to NPH3 and 33% amino acid identity to RPT2 (www.ebi.ac.uk/ClustalW). Proteins from the NPH3-L clade (boxed in green in Figure 4.3A) were aligned using the ClustalW algorithm and the C-terminal region of this alignment is shown in Figure 4.3B. Within the NPH3-L

clade, At5g03250 is the closest family member to NPH3-L and shows 54% amino acid identity, while the least similar member within the clade, At3g44820, shows 40% amino acid identity. Although there is some amino acid sequence conservation in the NRL family (see above), the extreme C-termini of these proteins are particularly divergent. The amino acid alignment was used to identify two NPH3-L-specific regions (EP053409 and EP053410) that were used for peptide antibody production, and these regions are indicated in Figure 4.3B. The antibodies produced were initially characterised by another laboratory member (S. Sullivan and J.M. Christie, unpublished data). In subsequent studies, the antibody used to measure NPH3-L protein levels was that raised against the antigenic region encoded by peptide EP053409.

4.2.3 Identification of an NPH3-L knockout line

In order to determine the function of the NPH3-L protein *in planta*, a knockout line was identified. A T3-generation, segregating SALK T-DNA insertional line in the Columbia (Col) background was obtained from the National *Arabidopsis* Stock Centre (NASC; line SALK_010013). NASC sequences online showed that the T-DNA insertion was located in the second intron of NPH3-L (www.arabidopsis.org). All seeds obtained from the stock centre were sown on soil and grown for three weeks under constant white light at a fluence rate of 70 μmol m^{-2} s^{-1}. Under these conditions, no obvious phenotypic difference could be distinguished from wild-type seedlings.

The approach used to identify potential knockout lines is represented in Figure 4.4. As described at www.arabidopsis.org, genomic DNA (gDNA) was extracted from leaf tissue and primers were designed to the borders of the T-DNA insertion and to gene-specific regions of NPH3-L (see Table 2.1 and Appendix 2 for primer details and location). This is preferable to screening for kanamycin resistance as often the kanamycin resistance gene is lost and it is recommended that genomic screening is carried out instead. gDNA from each plant was subjected to four polymerase chain reactions (PCR). Using primer set one, comprising the internal primer on the left border (LB) of the T-DNA insertion (LBa) and a gene specific reverse primer (P2: NPH3-L P2), generation of a PCR product indicates that the insertion is in the correct site. To confirm this, and to ensure that the entire left border is present, primer set two (the external primer on the left border of the T-DNA insertion (LBb) and the gene-

specific reverse primer) was used to generate a slightly smaller PCR product. True homozygous knockout lines did not produce a PCR product when using the two gene-specific primers (Primer set three: P1: NPH3-L P1 and P2: NPH3-L P2) because of the presence of the T-DNA insertion in the expected region of gDNA. Primer set four comprises two primers (Vector 1 and Vector 2) on the right border (RB) of the insertion to confirm that the entire T-DNA insertion is present. Figure 4.4 exemplifies how the pattern of bands from these PCR reactions can identify possible knockout lines. Bands generated from primers sets one, two and four indicate that the entire T-DNA insertion is present in the expected region of gDNA and the absence of a band from primer set three indicates that the insertion prevents formation of a PCR product. This banding pattern indicates a homozygous knockout line for NPH3-L. Bands produced from primers sets one and/or two, as well as three represent an insertion in the correct region of the gDNA, but only one copy i.e. the plant is heterozygous for the T-DNA insertion. Bands produced by primers sets three and four indicate that there is an insertion in the lines, but that it is not in the expected region of genomic DNA. Images of the genomic PCR screening are shown in Appendix 2. Two potential knockout plants were identified in this way: 010013_10 and 010013_16.

The two plants identified were grown to maturity and seed were collected from them. Further investigation of the NPH3-L knockout line in this study uses seed and tissue derived from these two knockout plants (010013_10 and 010013_16).

Figure 5.4A shows schematically the location of the T-DNA insertion in the second intron of the gene At1g30440. RNA was extracted from the potenetial knockout plants and used to generate cDNA. Specific primers (shown in Fig.5.4A) were designed to the exon immediately downstream of the T-DNA insertion. RT-PCR analysis showed that neither of the plants produced any NPH3-L transcript, but both wild-type (Col3) and *phot1-5phot2-1*plants produced transcript of the expected size (~500bp; Fig. 5.4B). Actin was used to show equal loading of all samples.

Generation of specific peptide antibodies for NPH3-L allowed confirmation that the knockout plants did not express the NPH3-L protein (Fig. 4.5C). Total protein was extracted from 3-day old, T4-generation, etiolated seedlings and probed with anti-NPH3-L antibody (EP053409). Western blotting shows that both wild-type (Col3) and the *phot1-5phot2-1 double mutant* express a protein of the expected size of 72kDa, while the suspected NPH3-L knockout lines do not (Fig. 4.5C). No other bands were

present on the blot in this region, which confirms that the antibody is specific for NPH3-L. The NPH3-L protein band is of the same intensity in both the wild-type and *phot1-5phot2-1* double mutant seedlings, indicating that NPH3-L expression is not dependent on the presence of phototropins. In addition, immunoblotting also confirms that the line is homozygous for the insertion: if the T4 line was not homozygous, heterozygous or knockout-null plants would express protein and this would be visible on the Western blot.

Taken in conjunction with the RT-PCR data, this confirms that the knockout line does not express NPH3-L protein. As the peptide antibody is raised against the very C-terminal of the protein, it is possible that a truncated version of the protein would not be identified in the manner, but the RT-PCR data which uses primers closer to the T-DNA insertion confirms that no transcript is produced.

4.2.4 In vivo confirmation of the phot1/NPH3-L interaction by co-immunoprecipitation

The work described in the following paragraph was carried out in conjunction with Stuart Sullivan. To confirm the interaction between full-length phot1 and full-length NPH3-L *in vivo,* Triton X-100 solubilised membrane fractions were prepared from etiolated seedlings that were either kept in the dark or given a 2 hour white light treatment. Genotypes used were phot1-GFP (*phot1-5* expressing phot1-GFP under control of the PHOT1 promoter), Col3 (wild-type) and 726-GFP. This latter line expresses the membrane-bound protein LTI6b tagged with GFP, under control of the *35S* promoter (Cutler et al., 2000). Membrane extracts were immunoprecipitated with anti-GFP antibody attached to magnetic beads and washed extensively. Specifically-bound proteins were eluted, separated by SDS-PAGE and subjected to western blotting using the antibodies indicated in Figure 4.6. The GFP antibody shows that GFP-tagged proteins were eluted from the beads and were effectively immunoprecipitated. The smaller bands in the phot1-GFP lanes are likely to be degradation products of phot1-GFP. Probing the membrane with the NPH3-L antibody revealed that NPH3-L co-immunoprecipitates with phot1-GFP in both light and dark conditions, confirming results obtained in the yeast two-hybrid study. Using an antibody against NPH3 showed that NPH3 also co-immunoprecipitates with phot1-GFP. The expected increase in mobility caused by blue-light dependent dephosphorylation of NPH3 was also observed (Motchoulski & Liscum, 1999, Pedmale & Liscum, 2007). These

interactions are likely to be phot1-specific as neither NPH3 nor NPH3-L co-immunoprecipitated using the negative controls Col3 or 726-GFP. Previous investigations of the interaction between phot1 and NPH3-L in this study have used the truncated region of NPH3-L isolated from the yeast two-hybrid screen and have been carried out in non-plant systems. The co-immunoprecipitation experiment demonstrates that full-length phot1 and NPH3-L interact *in vivo*.

4.2.5 Characterisation of NPH3-L expression and sub-cellular localisation

In order to gain insights into possible functions of NPH3-L, it was important to determine the transcript and protein spatial expression patterns and the subcellular localisation of the NPH3-L protein. Analysis of NPH3-L transcript levels was carried out using RNA extracted from rosette leaves, cauline leaves, stems, siliques and flowers of 5-week-old, wild-type (Col3) plants grown under constant white light (70 μmol m^{-2} s^{-1}). NPH3-L-specific primers were designed for RT-PCR analysis of transcripts and actin transcripts were monitored as a loading control (details of the primers are described in Table 2.1). RT-PCR products for NPH3-L transcripts were identified from rosette leaves, cauline leaves, stems and flowers (Fig. 4.7A). NPH3-L transcripts were not identified in siliques, but the actin loading control shows that the levels of cDNA from this tissue sample were low, making it difficult to determine expression in this tissue. For later studies using RT-PCR, a different method of RNA extraction was used which allowed more accurate RNA quantification, thereby reducing the variation between actin levels of samples.

To determine whether NPH3-L protein expression correlated with the transcript expression, total protein was extracted from wild-type (Col3) plants grown under the same conditions and probed by western blotting using the NPH3-L antibody. The results confirm that NPH3-L was present in flowers and siliques (Fig. 4.7B, top panel). Low levels of protein were detectable in rosette and cauline leaves. Protein was detected in stems but the size of the band observed was of slightly higher molecular mass. The membrane was stripped and re-probed with an antibody raised against the soluble protein marker UDP-glucose pyrophosphorylase (UGPase) antibody as a loading control. Low levels of UGPase were also detected in rosette and cauline leaves. The UGPase antibody cross-reacts slightly with the large subunit of rubsico as can be seen in Figure 4.7. The results indicate that NPH3-L is likely to be expressed

ubiquitously throughout the mature plant tissue at both mRNA and protein levels. NPH3-L transcript and protein was also detected in root tissue (data not shown).

To determine the sub-cellular localisation of NPH3-L, soluble and membrane protein fractions were extracted from 3-day-old etiolated seedlings and probed with the NPH3-L antibody. The results shown in Figure 4.7C indicate that NPH3-L is localised in the membrane fraction. There is a band in the soluble fraction, which is slightly larger than the NPH3-L band in the membrane fraction. It is possible that this band is a different protein which cross-reacts with the NPH3-L antibody, although Figure 4.5 shows no such cross reaction from total protein extracted from seedlings grown in the same conditions as described above. Therefore, another possibility is that a smaller proportion of the NPH3-L protein is present in the soluble protein fraction and that this pool of NPH3-L is modified in someway to account for the slower gel migration pattern shown.

4.2.5 Preliminary characterisation of the NPH3-L knockout line

The biological relevance of the phot1/NPH3-L interaction is unknown, and no function of the NPH3-L protein has been identified. The NPH3-L knockout line identified previously (Fig. 4.5) was used to investigate possible phenotypes caused by a lack of the NPH3-L protein. Since phot1 interacts with NPH3-L *in vivo*, some of the known responses mediated by phot1 were investigated. Both NPH3 and RPT2 function in phot1-mediated phototropism, so initially the phototropic response of the knockout lines was examined. Etiolated seedlings were grown on vertical agar plates for two-and-a-half days before being exposed to unilateral blue light (1 μmol m^{-2} s^{-1}) for 24 hours. The plates were then scanned and the angle of curvature was measured using ImageJ software (http://rsb.info.nih.gov/ij/). Wild-type (Col3) seedlings showed curvature of approximately 83º, while *phot1-5phot2-1* seedlings showed only random bending of less than 10º. Seedlings of the NPH3-L knockout line showed normal phototropic curvature comparable to wild-type seedlings (Fig. 4.8A). Therefore NPH3-L does not appear to be involved in phototropism under the conditions examined.

Phot1 activity and NPH3 are also required for light-regulated leaf positioning in *Arabidopsis* (Inuoe *et al*., 2007). When wild-type seedlings are grown under 100 μmol m^{-2} s^{-1} white light in long days for one week and then transferred to 10 μmol m^{-2} s^{-1} for a further week, the first leaves and cotyledons flatten and petioles move

obliquely upwards so they are orientated perpendicular to the incident light from above (Fig. 4.8B). This response has been described, albeit under different light conditions and results in enhanced plant growth under low blue light conditions (Inoue *et al.,* 2007). The NPH3-L knockout lines in addition to *phot2-1* show normal leaf positioning under these conditions, whereas *phot1-5* and *phot1-5phot2-1* show downward-pointed leaves and flattened petioles indicative of a disruption in the NPH3-mediated phot1-signalling pathway necessary for this response (Fig. 4.8B).

NPH3-L knockout lines show no visible phenotype as young or mature plants when grown in constant light or long days (data not shown). Similarly, when grown in short day conditions, NPH3-L knockout plants look similar to wild-type (Col3) plants. In contrast, abnormal phenotypes of the *phot1-5* single and *phot1-5phot2-1* double mutant are much more apparent; plants show poor establishment and a general lack of growth and general fitness in young seedlings (data not shown). In addition, leaves of mature plants are epinastic in the *phot1-5phot2-1* double mutant, and in the *phot1-5* single mutant; petioles are elongated and leaf area reduced when compared to wild-type (Fig. 4.9A). An interesting observation is the early flowering phenotype exhibited by *nph3-1* plants when grown in short day conditions. After 11 weeks of short day growth, *nph3-1* plants were flowering and beginning to set seed, whereas all other lines had not yet initiated flowering (Fig. 4.9A).

To investigate if there were more subtle differences between the NPH3-L knockout lines and wild-type, the number of leaves produced during the 11-week growth period were counted. No significant difference in leaf number was detected (Fig. 4.9B). However, the *phot1-5, phot1-5phot2-1* and *nph3-1* plants showed reduced leaf number compared to wild-type plants (Fig. 4.9B). The average dry weight of plants grown under these conditions was calculated for each line. No difference in dry weight was observed for NPH3-L knockout plants compared to wild-type. Again, *phot1-5, phot1-5phot2-1* and *nph3-1* plants showed a decrease in dry weight compared to wild-type (Fig. 4.9C).

Interestingly, *phot1-5* and *phot1-5phot2-1* plants grown under 70 μmol m^{-2} s^{-1} in long days or constant light do not show the same severity of phenotype as plants grown under short days. The enhanced phenotype when grown in short days is apparent at all stages of development (see Fig. 4.8 and Fig. 4.9 for examples of seedlings and mature plants, respectively). This suggests that the enhanced growth

promoted by phototropins is dependent not only on the fluence rate of light, but also on the total fluence received within a 24-hour period.

4.3 Discussion

4.3.1 Biochemical analysis of the phot1/NPH3-L interaction

Results from this chapter show that the NPH3-L fragment identified from the yeast two-hybrid screen interacts with both the extreme N-terminal region and the kinase domain of phot1 in yeast (Fig. 4.1), and this was confirmed by *in vitro* pull-down assays (Fig. 4.2). The *in vivo* interaction of full-length phot1 and NPH3-L proteins in both light and dark conditions was confirmed by co-immunoprecipitation. It is unusual that at least in yeast and *in vitro* the central region of NPH3-L can interact with two different regions of the phot1 protein. The significance of this is difficult to interpret. Another possibility is that there may be more than one phot1-binding site in the central region of NPH3-L identified from the yeast two-hybrid screen. Domain mapping of the central region of NPH3-L similar to the approach used in this study would determine exactly which part of the NPH3-L fragment is necessary for the interaction with each of the two interacting regions of phot1 identified. Given that the kinase domain of phot1 interacts with the central region of the NPH3-L protein, this region could serve as a substrate for phot1. Further work is now required to test this hypothesis.

Another possibility is that two independent molecules of NPH3-L can interact with one molecule of phot1, and may explain why NPH3-L can bind to different regions of phot1. Alternatively, the region of phot1 that NPH3-L binds to is regulated by light. This hypothesis is plausible, given that the phot1/NPH3-L interaction is not disrupted in light or dark conditions *in planta* (Fig. 4.6). It is possible that NPH3-L is the substrate for light-induced phot1 kinase activity but no change in electrophoretic mobility was observed in NPH3-L co-immunoprecipitated with light- treated phot1-GFP (Fig. 4.6). Likewise, in contrast to NPH3 (Pedmale & Liscum, 2007), NPH3-L does not appear to be dephosphorylated in response to phot1 activation. RPT2 is also not dephosphorylated following illumination (Inada et al., 2004). These findings, along with those presented here, indicate that there is likely to be variability in the regulation and function of members of the NRL family. Furthermore, the situation is likely to be complex as members of the NRL family have been shown to form heterodimers as

well as homodimers (Inada et al., 2004). Like NPH3 and RPT2, NPH3-L was localised to the membrane fraction (Fig. 4. 7C). Members of the NRL family are not membrane spanning proteins, therefore the mode of membrane attachment is not known. This is also the case for the phototropins. However, the kinase domain of phot2 has been shown to localise to the membrane fraction indicating that regions important for this process are located within this domain of the protein (Kong *et al.*, 2006; 2007).

4.3.2 Functional analysis of the phot1/NPH3-L interaction in planta

Having identified NPH3-L as a novel interacting partner for phot1 *in vivo,* we tried to determine a function for the protein. Tissue expression analyses showed that NPH3-L was expressed in most mature plant tissues tested at both the mRNA and protein level and gave no clue as to its function. Western blotting using the NPH3-L antibody EP053407 produced multiple bands when probing tissue derived from light grown plants (Fig 4.7B) compared to etiolated seedlings (Fig. 4.5). It is possible that there are light-induced members of the NRL family that cross-react with the antibody to produce these extra bands. Indeed, it has been shown that mRNA levels of RPT2 are up-regulated in response to light (Sakai *et al.,* 2000). While the NPH3-L band identified by western analysis coincides with the correct molecular mass of the protein (Fig. 4.7B) it would be prudent to repeat the experiment using both wild-type and the NPH3-L knockout line to ensure that the correct band has been identified. Given that RPT2 is induced by light it would also be important to look at the effect of light on NPH3-L protein and transcript levels.

Identification of an NPH3-L knockout line allowed a preliminary investigation to identify a function for the NPH3-L protein. There was no difference between the wild-type plants and the knockout lines when phototropism and leaf positioning was investigated in immature plants (Fig. 4.8). Mature plants grown under a variety of light intensities and day length also showed no visible phenotype (Fig. 4.9). While the studies carried out have not allowed identification of a function for the NPH3-L protein, this may be because NPH3-L shares functional redundancy with another member of this large, plant-specific family. It would be interesting to create lines that do not express multiple NPH3-L clade members to try to identify a function for proteins within this clade. Of the two members of the NRL family that have been characterised, both NPH3 and RPT2 function in phot1-mediated phototropism

(Motchoulski & Liscum, 1999; Sakai *et al.,* 2000), RPT2 is also involved in stomatal opening (Inada *et al.,* 2004) and NPH3 is necessary for leaf positioning (Inuoe *et al.,* 2007). This study has determined that NPH3-L does not function in phot1-mediated phototropism or leaf positioning at least under the conditions examined. If time allowed it would be worthwhile to investigate other responses mediated by phot1 such as stomatal opening and chloroplast movement. NPH3 is not required for the rapid inhibition of hypocotyl growth mediated by phot1 upon transfer of dark-grown seedlings to light (Folta *et al*., 2001). It would therefore be worth testing whether the NPH3-L knockout lines established here show altered hypocotyl growth inhibition. However, a high resolution imaging system is needed to measure this response. NPH3-L does not function in phototropin-mediated leaf expansion because NPH3-L knockout lines show normal leaf growth as both immature and mature plants (Fig. 4.8B and Fig. 4.9).

Further work to characterise the NPH3-L protein further should include creating GFP-tagged-NPH3-L lines, driven by the native promoter, to investigate the sub-cellular localisation of the protein, and to determine if there is any sub-cellular movement as is the case for phot1 (Sakamoto & Briggs, 2002) and phot2 (Kong *et al*., 2007). This could also be investigated by western blotting, but given the multiple bands produced when light grown tissue is analysed with the NPH3-L antibody, it might be easier to determine changes in localisation visually using fluorescence microscopy. Generation of NPH3-L over-expressing lines is currently underway in the laboratory and will provide a useful tool that could be used to investigate protein function, either by investigation of known phot1-responses, or in-depth characterisation of plant growth under a variety of light conditions if there is no immediately visible phenotype.

A
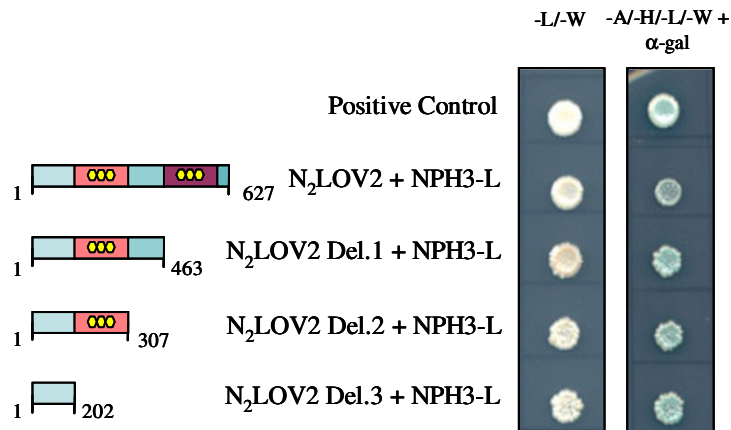
B
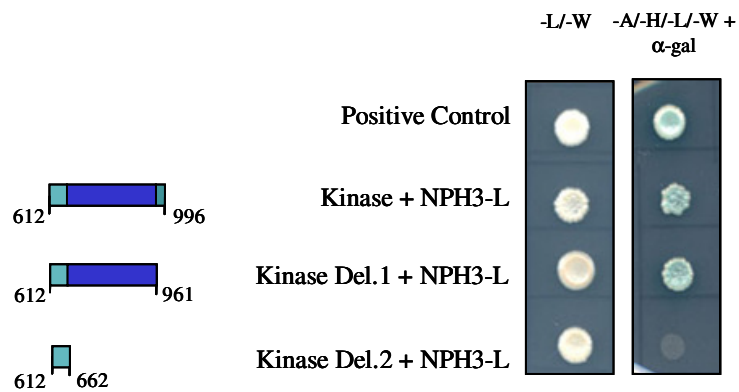
Figure 4.1 Further domain mapping of the phot1/NPH3-L interaction

A + B) Deletion analysis of the phot1 regions required for the interaction with the central region of NPH3-L. Yeast were co-transformed with bait vectors encoding phot1 N_2LOV2 deletions (A) or kinase deletions (B) and with the prey vector encoding the central region of NPH3-L. Yeast were plated on non-selective media (-L/-W) for plasmid selection and on full selection media (-A/-H/-L/-W+α-gal) to select for interacting proteins. Yeast were grown in darkness (D) or 20 μmol m^{-2} s^{-1} white light (L). Positive controls used are as described in Figure 3.1A.
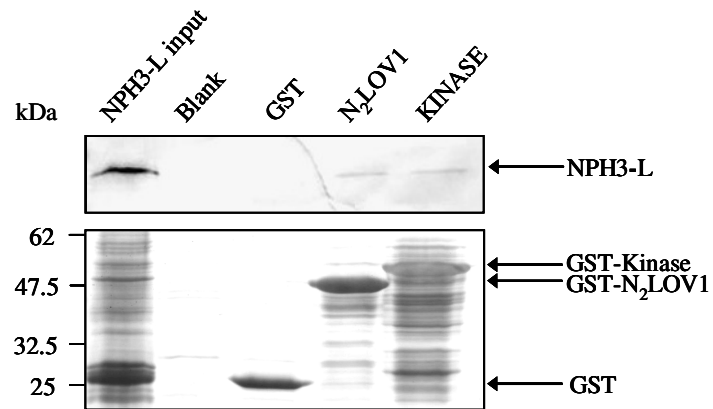
Figure 4.2 *In vitro* **confirmation of the phot1/NPH3-L interaction**

In vitro binding of the NPH3-L fragment to the phot1 N_2LOV1 and kinase domains. Approximately equal amounts (indicated in the lower panel by Ponceau S staining) of bacterially-expressed GST-N_2LOV_2, GST-Kinase and GST were incubated with the c-Myc-tagged NPH3-L fragment synthesised by *in vitro* transcription/translation.Western blotting using anti-c-Myc antibody was used to detect c-Myc-NPH3-L (upper panel). One-twenty-fifth (2μL) of the *in vitro* transcription/translation reaction was loaded as a size reference for NPH3-L (input). GST protein alone (GST), and empty magnetic beads (Blank) were included as negative controls to show specific binding. Molecular weight size markers are indicated on the left. Proteins were run on a 12.5% polyacrylamide gel.

A)

B)

```
At5g03250    -----------LLKPRGENVRERVSELEKECMNMKQELHKLVRTKRS-----------W
At5g13600    -----------NANMVMHGMRERVFELEKECMSMKQDLDKLVKTKEG-----------R
NPH3-L       -GWATAVRENQVLKVGMDSMRMRVCELEKECSNMRQEIEKLGKTTKGGGSASNGVGSKTW
At3g44820    DGWVTVVRQNQVLKVDMQKMRSRVGELEEEFQSIKQEMKKRVSKSSS-----------S
At3g50840    GRWKEAVKENQVLRLDMDTMRTRVNQLEKECLYLKKVIAKIDKE--SLLKAKHG-----A
At5g66560    GKWKKTVRENQVLRLDMDTMRTRVHRLERECSNMKKVIAKIDKEGSSPATTTDR-----P
                     .   . :* ** .**.*    ::: : *        .
At5g03250    KNFTRKLNFK---KKSECCKPKDQATPAI----------------------------
At5g13600    NFFSKIFGSRSKTKTSPCGKGGEDALVIPETKN------------------------
NPH3-L       ENVSKKLGFGFKLKSHQMCSAQEGSVSKSNNENVKIEKLKDVKERRGKHKKASSISSER-
At3g44820    MSSPRLVKLGCKFLLPRASDAKNDTVQNSVSSTPRSATADHTLPRSSRHSKHRKSFSFFG
At3g50840    GKWSIGKKFGCKFSAQVCDSQEATMVDRRSRRFLS----------------------
At5g66560    RSWSITKKFGCKFKTQVCDSHEATMVDHRSRRS-----------------------
                     .              .
```

Figure 4.3 Phylogentic analysis of the NRL family in *Arabidopsis*

A) A phylogenetic tree of the *Arabidopsis* NRL family based on amino acid sequences. The NPH3-L clade is boxed in green. RPT2 and NPH3 are boxed in red and blue, respectively.

B) Alignment of the C-terminal peptide sequences of the NPH3-L clade. Identical amino acids are shaded grey and indicated underneath by an asterisk. The two peptide regions used to generate antibodies are boxed and shaded. The green box represents the peptide region used to generate antibody EP053409 and the purple box and underline denotes the partially overlapping region used to generate antibody EP053410.

A

Primer Set	Primers Used
1	LBa + P2
2	LBb + P2
3	P1 + P2
4	V1 + V2

B

Possible Knockout   Heterozygous   Multiple Insertion/ Mislocalised Insertion
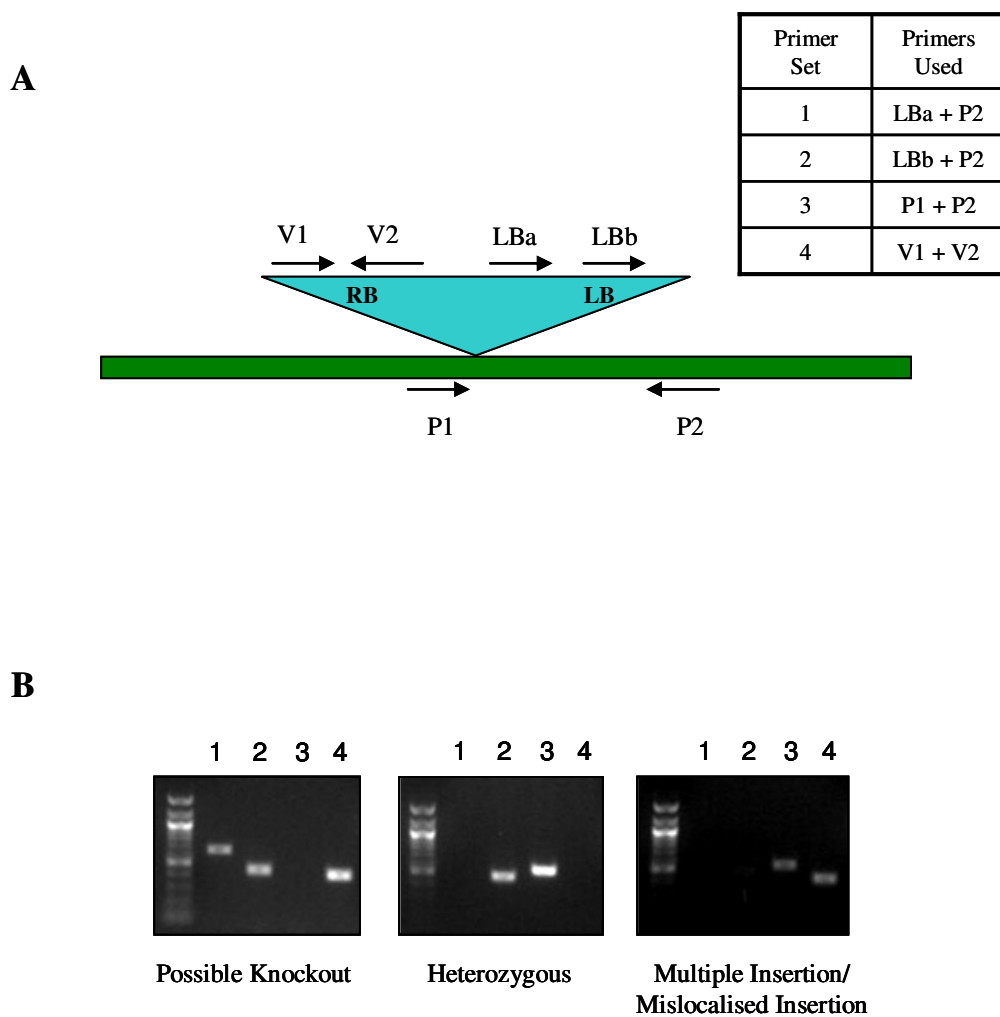
Figure 4.4 Genomic screening of knockout lines

A) Schematic representation of a knockout line with a T-DNA insertion. Plant genomic DNA is represented by the green rectangle and the T-DNA insertion is represented by the blue triangle (RB- right border; LB- left border). Primers used to identify knockout lines are indicated on the figure and primer sets are described in the table.

B) Genomic DNA was extracted from leaf tissue and subjected to PCR using the four sets of primers described in the table in (A) and in the main text. Band patterns resulting from the four PCR reactions indicated the status of each plant for the presence of the T-DNA insertion.
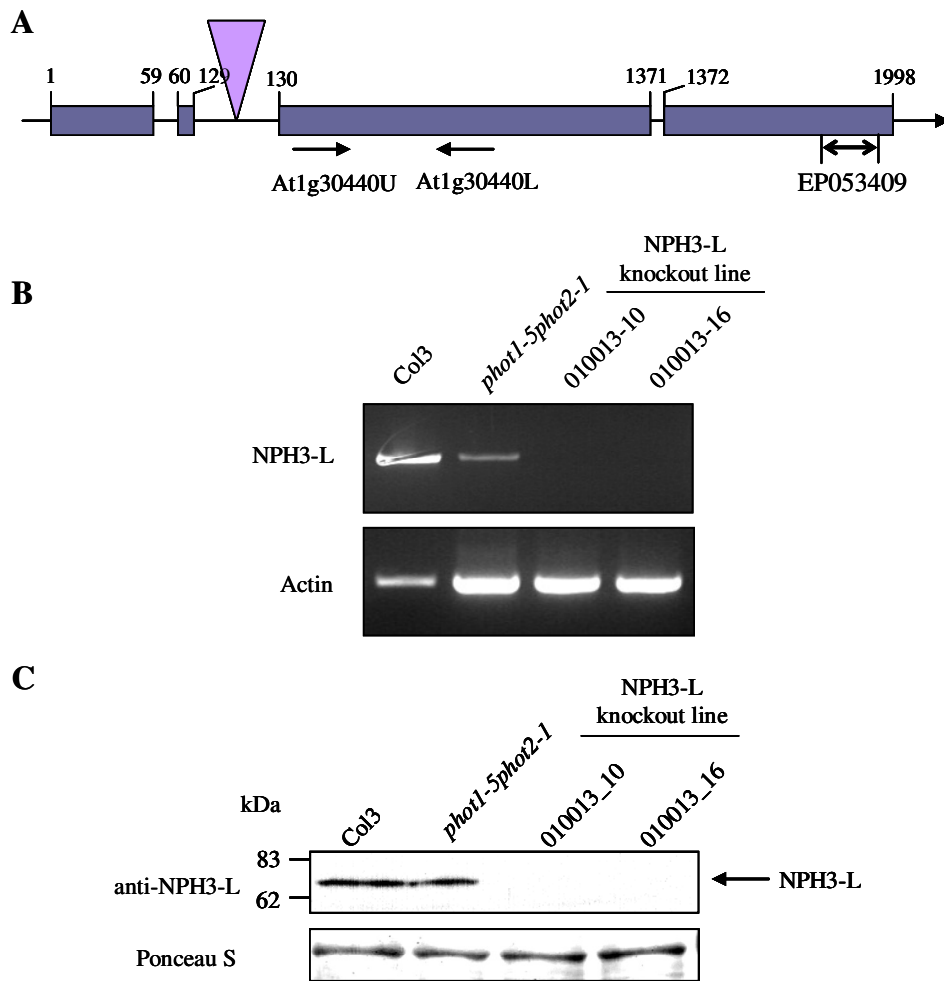
Figure 4.5 Identification of an NPH3-L knockout line

A) Schematic diagram showing location of the T-DNA insertion (lilac triangle) in the second intron of the NPH3-L gene. Introns are shown as a black line and exons are shown as blue boxes. Nucleotide positions are indicated above the gene. Locations of NPH3-L specific primers (At1g30440U and At1g30440L) are indicated by block arrows. The region used for antibody production (EP053409) is shown by unfilled arrows.

B) RT-PCR analysis of NPH3-L transcript levels in 3 week old putative knockout plants (010013_10 and _16), wild-type (Col3) and *phot1-5phot2-1* plants. PCR products generated using the NPH3-L specific primers shown in (A) are shown in the top panel. PCR products using actin primers as a loading control are shown in the lower panel

C) Western blot showing the level of NPH3-L protein in wild-type (Col3), the phot1-5phot2-1 mutant and potential NPH3-L knockout seedlings (010013_10 and 010013_16). Total protein (20 μg) was extracted from etiolated T4 seedlings and used for western analysis. with an antibody (EP053409) raised against the C-terminus of NPH3-L (upper panel). The lower panel shows Ponceau S staining of the membrane as a loading control. Size markers on the left show protein molecular mass. Proteins were run on a 7.5% polyacrylamide gel.
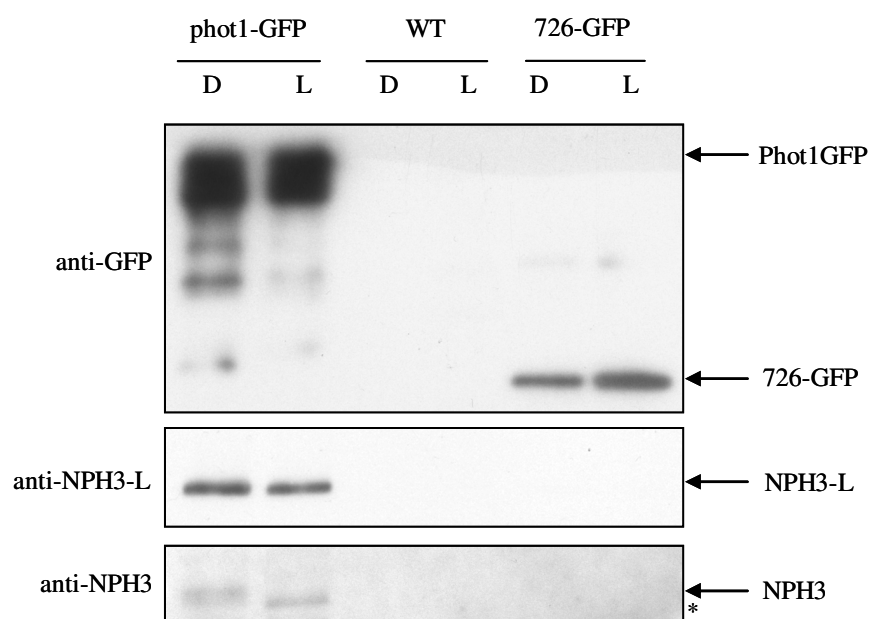
Figure 4.6 Phot1 interacts with NPH3-L *in vivo*

In vivo co-immunoprecipitation of NPH3-L with phot1. Dark grown seedlings of phot1-GFP, wild-type (WT) and 726-GFP were either kept in the dark (D) or given a two hour treatment with 100 μmol m^{-2} s^{-1} white light (L) before the microsomal fraction from the seedlings was extracted under red safe light conditions. Membrane protein fractions were incubated with anti-GFP-beads and subjected to sequential washes before eluting the specifically bound proteins. Antibodies used to probe the nitrocellulose membrane are indicated on the left of the corresponding panel. (Co-)Immunoprecipitated proteins are indicated by arrows on the right hand side of the panels. The asterisk indicates the dephosphorylated form of NPH3. Proteins were run on a 12.5% polyacrylamide gel.

107
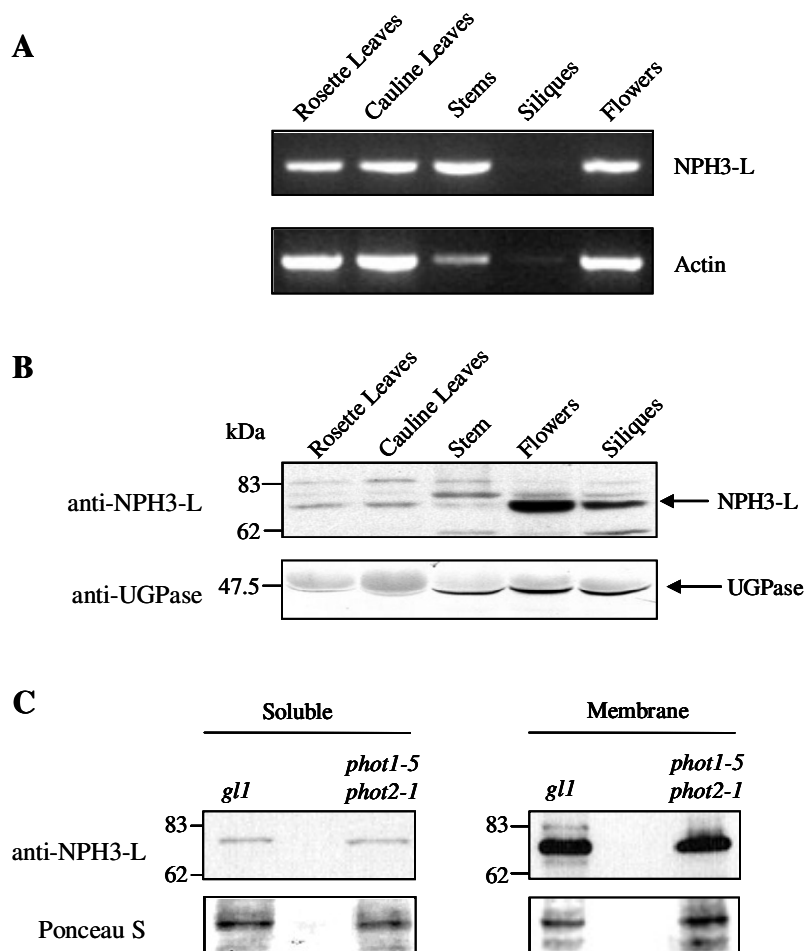
Figure 4.7 Tissue and sub-cellular localisation of NPH3-L

A) RT-PCR analysis on 5 week-old tissue grown under 70 μmol m^{-2} s^{-1} white light. The top panel shows PCR products generated using NPH3-L specific primers, and the lower panel shows PCR products generated using actin primers as a loading control. The results are representative of three RT-PCR experiments on the same RNA samples.

B) Western blotting of NPH3-L protein levels in extracts from different tissues. Ten μg of protein extracted from different tissues of wild-type plants grown for 5 weeks under 70 μmol m^{-2} s^{-1} white light were probed with EP053409 (anti-NPH3-L, upper panel) and re-probed with UDP-glucose pyrophosphorylase (UGPase) antibody as a loading control (lower panel). The NPH3-L band is indicated by the arrow. Molecular mass (kDa) size markers are indicated on the left. Proteins were run on a 12.5% polyacrylamide gel.

C) Western blotting of NPH3-L protein levels in soluble protein and membrane extracts. Ten μg of protein extracted from dark-grown wild-type (*gl1*) or *phot1-5phot2-1* seedlings were probed with anti-NPH3-L antibody (upper panel). The membrane was stained with Ponceau S as a loading control (lower panel). Molecular mass (kDa) size markers are indicated on the left. Proteins were run on a 12.5% polyacrylamide gel.

A
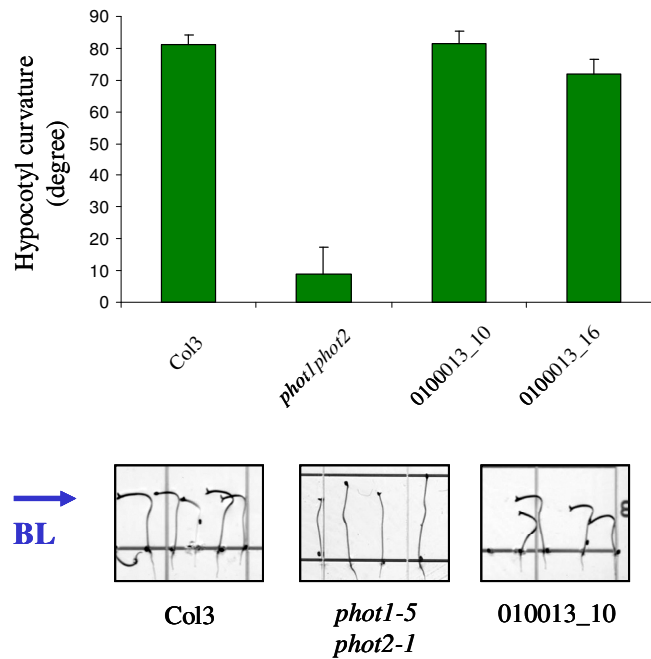
B

Figure 4.8 Characterisation of NPH3-L knockout line seedling phenotype

A) Phototropism of wild-type (Col3), *phot1-5phot2-1* and the NPH3-L knockout lines (010013-10 and 010013-16). Two-and-a-half day old dark-grown seedlings were placed in unilateral blue light (1 μmol m^{-2} s^{-1}) for 24 hours before measuring the angle of curvature. Representative seedling are pictured. The arrow indicates the direction of blue light (BL). Error bars indicate standard error (n>20).

B) Leaf orientation by light in the NPH3-L knockout lines. Seedlings described in (A) were grown under 100 μmol m^{-2} s^{-1} white light for one week then transferred to 10 μmol m^{-2} s^{-1} for a further week. Scale bar represents 0.5cm.

109

A)

Col3

phot1phot2

phot1-5

010013-10

nph3-1

1cm

010013-16

B

number of leaves

Col3 *phot1-phot2* 010013_10 010013_16 *phot1-5* *nph3-1*

C

Average dry weight (g)

Col3 *phot1-phot2* 010013_10 010013_16 *phot1-5* *nph3-1*
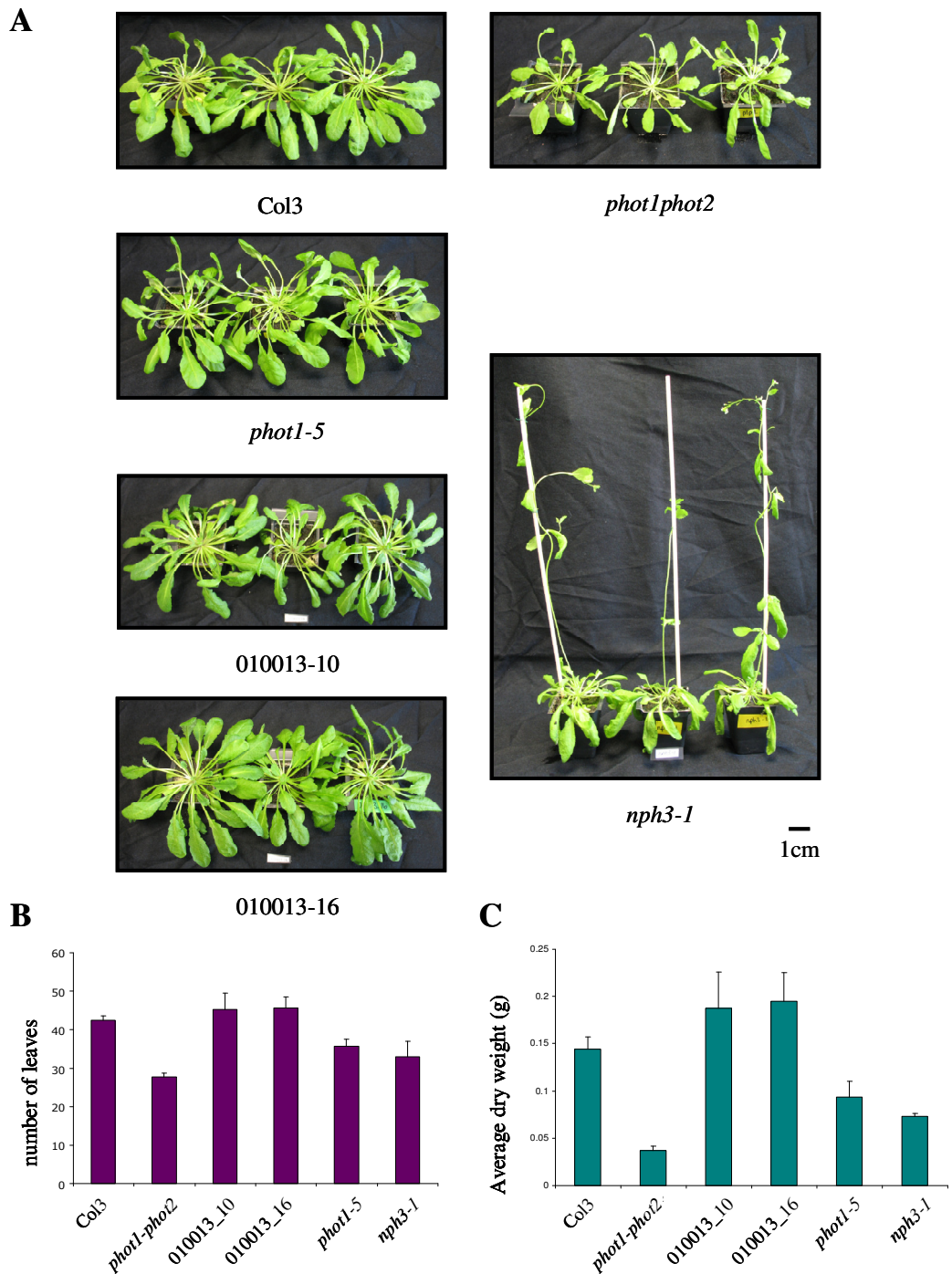
Figure 4.9 Characterisation of mature NPH3-L knockout lines

A) Growth phenotypes of NPH3-L knockout lines (010013_10 and 010013_16) compared to wild-type (Col3), *phot1-5phot2-1, phot1-5, nph3-1* plants. Plants were grown in 70 μmol m^{-2} s^{-1} white light in short day conditions (9 h light, 15 h dark) for 11 weeks.

B) Bar chart showing average leaf number per plant as described in (A). Error bars indicate standard error (n=5).

C) Bar chart showing average dry weight per plant as described in (A). Error bars indicate standard error (n=5).

Chapter 5: Characterisation of the phot1/14-3-3 interaction

5.1 Introduction

Chapter 3 showed that full-length phot1 isolated full-length 14-3-3λ from a yeast two-hybrid screen, and that the light-sensing N-terminal region of phot1 (N_2LOV2) is necessary for this interaction. The N-terminal region of oat phot1 is heavily phosphorylated in response to blue light (Salomon *et al.,* 2003). The sites of phosphorylation in oat phot1 have been mapped to two sites upstream and two sites immediately downstream of LOV1 in response to low fluence light (1 μmol m^{-2} s^{-1}) and four sites within the linker region between the LOV domains in response to mid- to high-intensities of light (10 and 50 μmol m^{-2} s^{-1}, respectively; Salomon *et al.,* 2003). Therefore, this chapter aims to characterise the phot1/14-3-3λ interaction in more detail, particularly with regard to the effect of phot1 phosphorylation status on the interaction. Despite the fact that a 14-3-3 protein has been shown to bind to phototropin in *Vicia faba* (Kinoshita *et al.,* 2003), no physiological function for the interaction has been described. Work in this chapter will attempt to elucidate a function for 14-3-3λ *in planta* by investigating 14-3-3λ knockout and over-expressing lines.

5.2 Results

5.2.1 Further investigation of the phot1/14-3-3λ interaction in yeast

In order to elucidate the specific region of phot1 necessary for the interaction with 14-3-3λ, in-depth domain mapping was employed. For this, the deletion series of phot1 bait vectors described in Section 4.2.1 were used. These included N_2LOV2 Deletion 1 (N_2LOV2 Del.1) which encodes the extreme N-terminal of phot1, the LOV1 domain and the LOV linker region; N_2LOV2 Deletion 2 (N_2LOV2 Del.2) which encodes the N-terminus of phot1 and the LOV1 domain; and finally N_2LOV2 Deletion 3 (N_2LOV2 Del.3) which encodes only the extreme N-terminal region of phot1. The constructs and the amino acids encoded within them are shown schematically in Figure 5.1A. Yeast were co-transformed with bait vectors encoding the phot1 deletion series and the prey vector encoding 14-3-3λ. The results of these co-transformations are shown in Figure 5.1A and indicate that the linker region between LOV1 and LOV2 (LOV Link) is

necessary for the interaction of phot1 with 14-3-3λ. When yeast were co-transformed with 14-3-3λ and full-length phot1, N₂LOV2 or N₂LOV2 Del.1 (which all contain the LOV Link region) the interaction between the proteins was sustained and yeast could grow on full selection media (-A/-H/-L/-W+α-gal). When the LOV Link region was removed from the phot1 bait (N₂LOV2 Del.2 and N₂LOV2 Del.3) the interaction was abolished and yeast could not grow on full selection media. As shown in Section 3.7.2, interactions between all phot1 baits and 14-3-3λ are not light sensitive (Fig.5.1A).

Yeast containing the bait and prey vector combinations described above were grown in liquid culture in order to quantify the strength of the interaction relative to the positive controls by measuring α-galactosidase activity, as described in Section 2.11.3. Quantification showed that the interaction between full-length phot1 protein and 14-3-3λ is approximately half as strong as the positive controls. When yeast were transformed with N₂LOV2 and 14-3-3λ, the interaction strength increased to around two-thirds the α-galactosidase activity shown by the positive controls. The interaction of N₂LOV2 Del.1 and 14-3-3λ was comparable to the positive controls in terms of α-galactosidase activity. Removal of the interacting LOV Linker domain resulted in yeast containing proteins (N₂LOV2 Del.2 and N₂LOV2 Del.3) that did not interact with 14-3-3λ. Quantification of the α-galactosidase activity of yeast containing these non-interacting proteins was comparable in strength to that shown by the negative controls, where the yeast were co-transformed with 14-3-3λ vector and the corresponding empty bait vector (Figure 5.1B).

5.2.2 In vitro verification of the phot1/14-3-3λ interaction

To confirm the yeast data regarding the phot1/14-3-3λ interaction, *in vitro* pull-down analyses were performed. This was particularly important because, although 14-3-3λ has been shown not to auto-activate the GAL4-based yeast two-hybrid system (Fig. 3.6B), it has been reported that an *Arabidopsis* 14-3-3 protein commonly auto-activates transcription of reporter genes in a LexA-based yeast two-hybrid system (Zhang *et al.,* 1995).

Figure 5.2 shows three pull-down experiments carried out to investigate and confirm the phot1/14-3-3λ interaction. For proteins that were transcribed and translated *in vitro,* the respective cDNA sequences were sub-cloned into the yeast two-hybrid bait

112

vector, pGBKT7. This vector contains a T7 initiation of transcription site (in addition to the GAL4 DNA-binding domain), which allows *in vitro* transcription/translation of the protein of interest with an N-terminal c-Myc epitope tag, using rabbit reticulocyte lysate. In addition to this, the corresponding interacting protein was sub-cloned into the bacterial expression vector, pGEX4T-1. BL21 *E. coli* were transformed with this vector and used to express the protein of interest with an N-terminal glutathione-S-transferase (GST) epitope tag. Western blotting using anti-Myc-antibody visualised interacting proteins. Bacterially expressed GST was used as a negative control to determine whether an interaction was specific. Figure 5.2A demonstrates that *in vitro* transcribed and translated N_2LOV2 binds to bacterially-expressed GST-tagged 14-3-3λ, thus confirming the interaction shown in yeast. 14-3-3λ interacts specifically with the N_2LOV2 region of phot1, as there is no binding of N_2LOV2 to GST alone.

Yeast data indicated that the LOV Link region of phot1 was necessary for the interaction with 14-3-3λ. *In vitro* confirmation of the interaction between N_2LOV2 and 14-3-3λ (Fig. 5.2A) prompted further investigation of the interaction between the LOV Link region of phot1 and 14-3-3λ using the pull-down system. 14-3-3 proteins are known to bind to phosphorylated serine/threonine motifs (Ferl, 2004) and sites of oat phot1 autophosphorylation have been mapped using artificial phosphorylation by purified bovine protein kinase A (PKA; Salomon *et al.,* 2003). Therefore, experiments were carried out to determine if the phosphorylation status of the LOV Link region had any effect on 14-3-3λ binding. In this instance, the GST-tagged LOV Link region of phot1 was expressed in bacteria, and 14-3-3λ was expressed with a c-Myc tag by *in vitro* transcription/translation. When GST-LOV Link was phosphorylated (GST-LOV Link (P)) using PKA (as described in Salomon *et al.,* 2003 and Section 2.16), this interaction remained as strong as the interaction between non-phosphorylated LOV Link and 14-3-3λ (upper panel), given the relative amounts of protein (as shown in the lower panel) (Fig. 5.2B). Considering that 14-3-3 proteins usually bind to phosphorylated proteins, it was expected that phosphorylation of the interacting LOV Link domain would increase the binding capacity for 14-3-3λ, but this did not appear to be the case.

To ensure that the heterologous expression systems were expressing functional 14-3-3λ, a known response was investigated. 14-3-3 proteins are known to form both homo- and hetero-dimers *in vivo* and function in this dimeric form (Ferl, 2004; Paul *et al.,*

2005). To investigate the ability of 14-3-3λ to dimerise, 14-3-3λ was expressed as a GST-fusion in bacteria and with a c-Myc-tag by *in vitro* transcription/translation. Figure 5.2C shows that c-Myc-14-3-3λ interacts with GST-14-3-3λ, thus indicating that the protein is functional, with regard to dimerisation, when expressed in these systems.

5.2.3 Characterisation of the phot1/14-3-3λ interaction using the insect cell system

To further investigate the phot1/14-3-3λ interaction, phototropin proteins were expressed in Sf9 insect cells and a far-western approach was used to examine their ability to bind 14-3-3λ. Previously, insect cells infected with recombinant baculovirus containing phototropin coding sequence have been used successfully to express functional phototropin proteins (Christie *et al.,* 1998, Sakai *et al.,* 2001, Onodera *et al.,* 2005). Far-western blotting uses a purified tagged-protein as a probe to identify interacting proteins bound to a nitrocellulose membrane, and has been used previously to show 14-3-3 binding to phototropins from V*icia faba* (Kinoshita *et al.,* 2003).

Yeast data in Chapter 3 indicated that the interaction between phototropin and 14-3-3λ is specific to phot1, so the insect cell/far-western system was used initially to confirm this result. Total soluble protein was extracted from insect cells expressing full-length phot1 and phot2 under red safe light conditions. It is known that insect cell-expressed phot1 and phot2 become autophosphorylated *in vitro* after exposure to a short pulse of light in the presence of radiolabelled ATP (Christie *et al.,* 1998, Sakai *et al.,* 2001, Onodera *et al.,* 2005; Jones et al., 2007). Protein extracts treated in this manner were used for far-western analysis. Nitrocellulose membranes were incubated with 0.1 μM purified GST or GST-14-3-3λ and probed for 14-3-3 binding with anti-GST antibodies. The results are shown in Figure 5.3. Far-western blotting using GST-14-3-3λ as the probe shows that GST-14-3-3λ binds specifically to phot1 and does not bind to phot2 (Fig. 5.3A). Binding of GST-14-3-3λ to phot1 is dependent on the presenceof phot1, as GST alone does not bind to either phot1 or phot2 (Fig. 5.3B). Both phot1 and phot2 expressed in insect cells are functional, as shown by the radiolabelled phosphate incorporated in the *in vitro* autophosphorylation assay (Fig. 5.3C). While 14-3-3λ binding is specific to phot1 expressed in insect cells, it does not appear to be dependent on the phosphorylation status of phot1 as 14-3-3λ binds to phot1 which has not been

light treated and therefore shows only minimal levels of phosphorylation, as well as to light-treated, autophosphorylated phot1.

One explanation for this apparently anomalous result was that the red safe light was sufficient to cause some autophosphorylation of phot1. To test this possibility, the experiment was repeated using wild-type phot1 and phot1 expressing a mutation in the kinase domain (Asp806Asn) which renders the kinase inactive (phot1 kinase dead) (Christie *et al.,* 2002). Using the same far-western approach, Figure 5.4A shows that GST-14-3-3λ binds to phot1 kinase dead, although the level of binding is decreased compared to wild-type phot1. Again, this binding is due to the presence of 14-3-3λ since GST alone does not bind either phot1 or phot1 kinase dead (Fig. 5.4B). The effect of the kinase mutation is shown by the minimal incorporation of radiolabelled phosphate, which is less than the basal level shown in dark-treated wild-type phot1 (Fig. 5.4C). The decreased level of 14-3-3λ binding to phot1 kinase dead is not due to lower levels of protein expression as the Ponceau S stain shows equal protein loading (Fig. 5.4D) and western blotting using anti-phot1 antibody shows that equal levels of wild-type phot1 and phot1 kinase dead are expressed in insect cells (Fig. 5.5C).

The data shown in Figure 5.4 lend weight to the alternative hypothesis that there is an endogenous kinase present within the insect cells, which phosphorylates phot1 at the site necessary for 14-3-3λ binding. To investigate this possibility, the experiment was carried out as described above with the modification that λ-phosphatase was used to de-phosphorylate the phot1 samples before they were resolved by SDS-PAGE. Figure 5.5A shows that GST-14-3-3λ does not bind to phot1 or phot1 kinase dead if they have been treated with λ-phosphatase. The autoradiographs shown in Figure 5.5B demonstrate that treatment with λ-phosphatase removes all radiolabelled phosphate incorporated in the samples as a result of phot1 autophosphorylation or as a result of phosphorylation by the unknown endogenous insect cell kinase in the case of phot1 kinase dead. Treatment of the samples with λ-phosphatase does not result in degradation of phot1, and lack of GST-14-3-3λ binding is not due to a lack of phot1 protein as western blotting using anti-phot1 antibody (Christie *et al.,* 1998) shows equivalent levels of phot1 protein in all samples (Fig. 5.5C).

5.2.4 14-3-3λ interaction with plant-derived phot1 is light-dependent

The data obtained from characterising the phot1/14-3-3λ interaction using the insect cell system indicate that 14-3-3λ binding is dependent on the phosphorylation status of phot1. To explore this light-dependency in more detail and to avoid confusion caused by artificial phosphorylation of phot1 in the insect cell system, it was thought prudent to investigate the interaction using plant-derived phot1. *In vitro* autophosphorylation analysis performed on microsomal membranes prepared from etiolated wild-type (Col3) and *phot1-5phot2-1* seedlings gave an inconclusive result when subjected to far western analysis using GST-14-3-3λ (data not shown), so an alternative approach was used.

A transgenic line created in the *phot1-5* null mutant background expresses phot1-GFP under the control of the native *PHOT1* promoter (Sakamoto & Briggs, 2002). This line, used in Chapter 4 to verify the phot1/NPH3-L interaction, was used to immunoprecipitate phot1-GFP from 3-day-old etiolated seedlings using anti-GFP antibody conjugated to magnetic beads. Prior to this, seedlings were either kept in the dark or given a two hour white light treatment to induce *in vivo* phosphorylation of phot1. Far-western analysis using 0.1 µM GST-14-3-3λ or GST alone showed that 14-3-3λ only binds to light-treated phot1 (Fig. 5.6A). This interaction is dependent on 14-3-3λ since GST alone does not bind to phot1 (Fig. 5.6A). Moreover, autophosphorylation of phot1 is shown by the reduced electrophoretic mobility of phot1 in light treated samples, when immunoblotted with the phot1 antibody (Fig. 5.6B).

5.2.5 14-3-3λ as a phot1 phosphorylation substrate

Despite having a serine/threonine kinase at the C-terminal end no plant proteins, other than phototropins themselves, have been shown to be phosphorylated by phototropins (Matsuoka & Tokotumi, 2005). 14-3-3 proteins are known to function as dimers, and their dimerisation state can be affected by the phosphorylation status of the 14-3-3-protein (Gu *et al.,* 2006). It has been demonstrated previously that *Arabidopsis* somatic embryogenesis receptor-like kinase (*At*SERK1) can phosphorylate *Arabidopsis* 14-3-3λ *in vitro* (Rienties *et al.,* 2005). Therefore, the possibility that phot1 can phosphorylate 14-3-3λ was investigated. GST-14-3-3λ was incubated with phot1 expressed in insect cells in the presence of radiolabelled ATP. The samples were either

given a brief pulse of white light or kept in the dark and the reaction allowed to proceed for 5 minutes before glutathione-magnetic beads were added to the samples. Proteins bound to the beads were washed repeatedly before being eluted. As a positive control for autophosphorylation, phot1-only samples were included. The upper panel of Figure 5.7 shows that insect cell phot1 becomes autophosphorylated in response to light and that phot1 can be pulled-down via GST-14-3-3λ attached to the magnetic beads. However, no radiolabelled band was observed where GST-14-3-3λ would appear if it incorporated radiolabel as a result of phot1 phosphorylation. To increase the likelihood of visualising proteins with low levels of autophosphorylation, both $\gamma-^{32}$P-ATP diluted 1:5 with non-radiolabelled ATP, and undiluted $\gamma-^{32}$P-ATP were used in the assay. Equal amounts of GST-14-3-3λ were recovered from the magnetic beads and equal amounts of phot1 were used, as shown by coomassie staining in the lower panel of Figure 5.7. Nevertheless, the results indicate that 14-3-3λ is not a phosphorylation substrate for phot1.

5.2.6 Phylogenetic analyses of the 14-3-3 family and antibody production

Phylogenetic analysis was carried out to compare 14-3-3λ to other members of the *Arabidopsis* 14-3-3 family. A phylogenetic tree of the *Arabidopsis* 14-3-3 family shows that the members can be separated into two evolutionary branches: the epsilon and non-epsilon groups. 14-3-3λ is closely linked to 14-3-3-kappa (14-3-3κ) in a sub-branch of the non-epsilon group (Fig. 5.8A). The family member least similar to 14-3-3λ is 14-3-3-epsilon (14-3-3ε; Fig 5.8A). Alignment of the 14-3-3λ and 14-3-3κ proteins by ClustalW shows 93% amino acid identity (Fig.5.8B), while 14-3-3λ and 14-3-3ε show only 43% amino acid identity.

Because of the high degree of identity shown by 14-3-3λ and 14-3-3κ, it was difficult to identify suitably antigenic regions specific to the 14-3-3λ isoform therefore, peptide antibodies were designed against regions of 14-3-3λ and 14-3-3κ (Fig. 5.8B). To test the specificity of the antibodies produced, 14-3-3κ and 14-3-3ε were also subcloned into the bacterial expression vector pGEX4T-1. One μg of the GST-tagged 14-3-3 proteins, and GST as a negative control, were probed with each of the peptide antibodies produced. The upper panel of Figure 5.9A shows that both peptide antibodies recognise all three GST-14-3-3 proteins, but they do not bind to GST alone.

Both antibodies show greater reactivity with 14-3-3λ and 14-3-3κ than with 14-3-3ε. The lower panel shows equal loading of the GST and GST-14-3-3 proteins (Fig. 5.9A). To test if the antibodies showed specificity for the 14-3-3λ or 14-3-3κ isoform, a dilution series of each of the GST-tagged 14-3-3 proteins was spotted onto nitrocellulose membrane. Western blotting using the antibodies showed that EP053407 is more specific for the 14-3-3λ isoform and can recognise as little as 50 ng of GST-14-3-3λ protein compared to 500 ng of GST-14-3-3κ protein. However, the EP053408 antibody is more specific for 14-3-3κ and can recognise 5 ng of GST-14-3-3κ protein compared to 50 ng of GST-14-3-3λ protein. Therefore, for all further analyses using antibodies to 14-3-3λ, the more lambda-specific peptide antibody EP053407 was used.

5.2.7 Specificity of the phot1 interaction with 14-3-3λ

The high amino acid identity of the 14-3-3λ and 14-3-3κ isoforms gave rise to the question of whether both proteins were capable of interacting with phot1. To test this hypothesis, GST-tagged 14-3-3κ was used in far-western experiments. Ten μg of insect cell-expressed phot1 was probed with GST-14-3-3λ, GST-14-3-3κ, GST-14-3-3ε or GST alone as a negative control. Figure 5.10 shows that both GST-14-3-3λ and GST-14-3-3κ bind to phot1, but GST-14-3-3ε and GST alone do not, indicating that 14-3-3 binding the phot1 is limited to specific family members.

5.2.8 Identification and characterisation of 14-3-3λ knockout lines

Having determined that 14-3-3λ binds to phot1 *in vitro* by a variety of techniques, it was considered important to identify a functional consequence for this interaction *in planta*. In order to do this, a 14-3-3λ knockout line was identified. A T3-generation, segregating SALK T-DNA insertional line in Columbia background was obtained from NASC (line SALK_075219). NASC sequences online showed that the T-DNA insertion was located in the second intron of the 14-3-3λ gene (www.arabidopsis.org). Seeds obtained from NASC were sown on soil and subjected to the same screening process used to identify NPH3-L knockout lines (described in Section 4.2.3 and in the Materials and Methods). The primers used for screening are detailed in Table 2.1. Using this method, three plants were identified as potential homozygous knockout plants and were used for further investigation.

Figure 5.11A shows a schematic diagram that represents the location of the T_DNA insertion within the 14-3-3λ gene (At5g10450). RNA was extracted from the potential knockout plants and used to generate cDNA. Primers were designed specifically to 14-3-3λ and are shown in Figure 5.11A and Table 2.1. RT-PCR analysis showed that none of the three plants produced any 14-3-3λ transcript, but both wild-type (Col3) and *phot1-5phot2-1* produced PCR products of the expected size (Fig. 5.11B). Actin was used to show equal loading of all samples.

Generation of the peptide antibodies allowed confirmation that the knockout plants did not produce 14-3-3λ protein. Total protein extracted from etiolated seedlings of the three knockout plants, and from wild-type (Col3) and *phot1-5phot2-1* were probed with EP053407 antibody. Figure 5.11C shows that both wild-type and *phot1-5phot2-1* seedlings produced a band of the expected size of 27kDa, while the 14-3-3λ knockout plants did not. No other bands were present on the blot in this region, which indicates that this antibody can be used to specifically identify 14-3-3λ.

Preliminary characterisation of the knockout plants was carried out to try to identify a function for the 14-3-3λ protein with regard to phot1 signalling. Initially, phototropism was investigated. Etiolated seedlings of wild-type (Col3), *phot1-5phot2-1* and the knockout plants were grown vertically on agar plates for two-and-a-half days before being exposed to unilateral blue light (1 μmol m^{-2} s^{-1}) for 24 hours. Figure 5.12A shows that wild-type seedlings exhibit normal curvature and bend on average 80º towards the light source, while *phot1-5phot2-1* seedlings show random curvature of less than 10º towards the source of blue light. The 14-3-3λ knockout seedlings do not show any inhibition of curvature under these conditions and show average bending of approximately 80º towards the blue light source, comparable to wild-type seedlings (Fig. 5.12A).

The leaf positioning response of the 14-3-3λ knockout plants was also investigated. A recent study has shown that signalling via phot1 and NPH3 results in cotyledons and leaves that are orientated perpendicular to the light source from above (Inuoe *et al.,* 2007). Seedlings were grown as described in Section 2.27.2. Figure 5.12B shows that *phot1-5phot2-1* and *phot1-5* seedlings do not exhibit correct leaf positioning under these light conditions, whereas the 14-3-3λ knockout seedlings are comparable to wild-type and show normal leaf positioning.

The only unusual phenotype noticed for mature 14-3-3λ knockout plants was observed when plants were treated with the fungicide, mycobutanil. After spraying with mycobutanil, it was observed that often the mid-vein became bifurcated (Fig. 5.13A) and that leaves grew from the mid-vein on the upper surface of otherwise apparently normal rosette leaves of 14-3-3λ knockout plants, and some of these leaflets went on to produce shoots from their base and to set seed (Fig. 5.13B). This was not observed on wild-type or *phot1-5phot2-1* plants grown and treated in the same way. No visible phenotype was observed for mature 14-3-3λ knockout plants grown without fungicide treatment in a variety of light conditions and day lengths.

5.2.9 14-3-3λ expression and localisation in planta

Since there was no obvious phenotype for the 14-3-3λ knockout line, it was important to determine the expression pattern and tissue localisation of 14-3-3λ in wild-type plants to try to gain an insight into the possible function of the protein. RNA was extracted from a variety of tissues and used to determine 14-3-3λ transcript levels in these tissues. Primers used were those designed for RT-PCR analysis of the knockout plants (see Table 2.1). Figure 5.14A shows that 14-3-3λ transcript was identified in all tissues tested (flowers, roots, stems, cauline leaves and rosette leaves). Again, actin was used as a control for equal loading.

To determine the tissues expressing the 14-3-3λ protein, total protein extracted from 5-week-old wild-type (Col3) plants was probed with the 14-3-3λ antibody, EP053407. Figure 5.14B (upper panel) shows that 14-3-3λ protein was identified in all tissues examined. The membrane was stripped and reprobed with UGPase as a loading control, as described in Section 4.2.4 (Fig. 5.14B, lower panel).

If 14-3-3λ interacts with phot1 *in planta,* it would be expected that at least some of the 14-3-3λ protein would co-localise with phot1 at the plasma membrane. To explore this idea, soluble and membrane protein fractions were extracted from etiolated seedlings and probed with the 14-3-3λ antibody. The results of this experiment are shown in Figure 5.14C and indicate that 14-3-3λ is present in both membrane and soluble protein fractions. Therefore, at least a proportion of the total 14-3-3λ protein is found in the microsomal membrane fraction along with phot1. Nonetheless, the presence of 14-3-3λ in the membrane fraction is not dependent on phototropins as 14-3-3λ is still

present in the membrane fraction in extracts from the *phot1-5phot2-1* double mutant (Fig 5.14C, right panel).

5.2.10 Preliminary characterisation of 14-3-3λ over-expressing lines

14-3-3λ knockout plants do not show any visible phenotype and the ubiquitous expression of the protein throughout the plant does not give any clues as to 14-3-3λ function. To try to identify a role for 14-3-3λ *in planta*, over-expressing lines were created in wild-type (*gl1*) and *phot1-5phot2-1* backgrounds. Plants were transformed with a construct encoding 14-3-3λ with an N-terminal GFP tag under the control of the cauliflower mosaic virus *35S* promoter. T2 plants were observed using confocal microscopy to visualise the subcellular localisation of GFP-14-3-3λ and to determine if there were differences in the localisation when phototropins were absent. Plants were grown in light conditions (Fig. 5.15A, upper panels) or dark-adapted for two hours (Fig. 5.15A, lower panels). GFP-14-3-3λ is localised at the plasma membrane and in the cytosol of epidermal cells in both wild-type and *phot1-5phot2-1* backgrounds. Higher magnification reveals that GFP-14-3-3λ is present in the nuclei of both epidermal cells and guard cells, regardless of whether phototropins are present (Fig. 5.15A). While there is no major change in 14-3-3λ localisation between the two light treatments, the GFP-14-3-3λ localised to the plasma membrane in the wild-type background appears to be more punctuate when kept in light than the dark-adapted plants. This punctuate staining is not visible in the *phot1-5phot2-1* background.

It is known that phot1 is apically and basally localised in cortical cells of the root and hypocotyl of phot1-GFP plants, and that a fraction of it moves to the cytosol after treatment with blue light (Sakamoto & Briggs, 2002). Therefore, T2 plants over-expressing GFP-14-3-3λ in the wild-type background were used to visualise GFP-14-3-3λ localisation in the hypocotyl. Figure 5.15B shows that when plants are dark-adapted for two hours GFP-14-3-3λ is evenly distributed throughout these cells and no particularly strong signal is apparent at the basal or apical regions of the cells (left panel). If plants are kept in the light, however, the membrane localised GFP-14-3-3λ appears more punctuate and the signal at the apical and basal region of the cells is stronger (Fig. 5.15B, right panel).

There was insufficient time to generate homozygous lines in order to fully characterise the effect of over-expressing GFP-14-3-3λ *in planta*, however T1 and T2 plants showed a number of unusual phenotypes. In both the *gl1* and *phot1-5phot2-1* backgrounds, over-expressing plants were generally smaller than non-transformed plants and the leaves were shinier, darker green and more brittle than non-transformed plants, however this did not become apparent until plants were about three weeks old. In T1 over-expressing plants, the time taken to reach senescence varied among transformants in both backgrounds. Approximately one-quarter of plants rescued from kanamycin plates flowered within the normal timescale of about four weeks after transfer to soil, and after setting seed began to die back as normal. Around half of the plants took a further two weeks to begin senescence, while the remaining quarter persisted in flowering for an abnormally long time, therefore delaying normal senescence. This group of plants remained green and continued to initiate new flowering stems for up to twelve weeks after transfer to soil, when finally water was withheld and they began to die. The senescence phenotype appeared to correlate with the other phenotypes. Those that took longer to die were shorter, greener and had more flowering stems than plants which completed a more normal life cycle. The senescence and size phenotypes also correlated with T2 kanamycin-resistance segregation ratios of 3:1, i.e. one quarter of T2 plants were kanamycin sensitive and the remainder which survived on kanamycin were smaller, greener and showed increased longevity when compared to wild –type (Col3) plants.

T2 plants over-expressing GFP-14-3-3λ in the *gl1* background are pictured alongside non-transformed *gl1* plants in Figure 5.15. The variation in size between segregating lines is clearly visible; presumably the smaller plant is homozygous and the larger plant is heterozygous for GFP-14-3-3λ, given the segregation ratio of phenotypes shown by T1 plants. However, both transformed plants are smaller than the *gl1* plant shown on the left. There is a visible necrotic region shown on the apical meristem of the smaller transformed plant, these were also observed on some of the T1 plants. Death of this region of the plants would result in altered auxin homeostasis and may partially account for the increased number of flowering stems shown by some of the lines. Figure 5.15 also shows plants over-expressing GFP-14-3-3λ in the *phot1-5phot2-1* background. Essentially, these plants show similar phenotypes to those in the

gl1 background but in addition to this, they also maintain the phenotype of the *phot1-5phot2-1* background (epinastic leaves and slightly reduced overall growth).

5.3 Discussion

5.3.1 Biochemical analysis of the phot1/14-3-3λ interaction

In this chapter, investigation of the phot1/14-3-3λ interaction in yeast showed that the LOV Link region of phot1 is necessary for the interaction with 14-3-3λ. This was confirmed by *in vitro* pull-down assay and showed that this region is not only necessary but is sufficient for the interaction. This region of phot1 is phosphorylated in oat phot1 (Salomon *et al.,* 2003) and it is known that 14-3-3s usually bind phosphorylated proteins (Ferl, 2004). However, artificial phosphorylation of the LOV Link region by PKA did not result in an increase of *in vitro* 14-3-3λ binding. Kinoshita *et al.* (2003) determined that the sites of phosphorylation-dependent 14-3-3 binding in *Vicia faba* were Ser^{358} in *Vf*phot1a and Ser^{344} in *Vf*phot1b, and amino acid sequence alignment shows that these sites correspond to Ser^{325} in oat and Ser^{387} in *Arabidopsis.* Therefore, a mutated form of phot1 (S387A) was created for use in yeast two-hybrid analysis. When yeast were co-transformed with phot1 S387A and 14-3-3λ, the interaction persisted and was not affected by this mutation (data not shown). This suggests that the 14-3-3 binding site is not conserved among phototropins from different species and that 14-3-3λ must bind to an alternative phosphorylated site in *Arabidopsis* phot1.

The effect of light and the resulting autophosphorylation of phot1 was investigated using phot1 expressed in insect cells. However, while this confirmed the specificity of 14-3-3λ binding to phot1 and not phot2, it was found that a kinase endogenous to the expression system artificially phosphorylated phot1 at the 14-3-3λ binding site. This is in agreement with a previous study, which found that *Vicia faba* phot1 was phosphorylated by an insect cell kinase (Kinoshita *et al.,* 2003). While this posed problems for investigating the effect of light on 14-3-3λ binding to phot1, it would prove a useful tool for determining the precise site that is required for 14-3-3λ binding. Each of the phosphorylation sites in the LOV Link region could be mutated to alanine and far-western blotting used to determine the effect of mutagenesis on the ability of the mutated phot1 to bind 14-3-3λ. By using phot1-GFP immunoprecipitated from

light or dark treated plants, it was shown that 14-3-3λ binding is dependent on light-induced autophosphorylation of phot1. This is in contrast to the lack of effect of light on the interaction between phot1 and 14-3-3λ in insect cells and yeast. Thus, the the site of 14-3-3-interaction in yeast, as in insect cells, appears to be phosphorylated by an endogenous yeast protein kinase enabling the interaction to occur in the absence of light. This may be a common occurrence, as the *Arabidopsis* plasma membrane H$^+$ATPase AHA2 is also phosphorylated by an endogenous yeast protein kinase (Fuglsang *et al.,* 1999)

5.3.2 Analysis of 14-3-3λ expression, localisation and function in planta

A variety of techniques were employed to try to identify a function for 14-3-3λ *in planta*. RT-PCR analysis and western blotting showed that 14-3-3λ was present in all tissues tested. Although this does not give any clue as to the function of 14-3-3λ, it does at least demonstrate that a proportion of 14-3-3λ is localised at the plasma membrane where phot1 is also found (Sakamoto and Briggs, 2002). 14-3-3 proteins are not membrane spanning proteins so how they are attached to the membrane is not known at present. A previous study showed that mRNA levels of *Arabidopsis* 14-3-3λ were down-regulated in response to light (Zhang *et al.,* 1995) and as phot1 protein levels decrease in response to light (Sakamoto & Briggs, 2002), this indicates that both proteins show some light regulation and are present at the highest levels in dark grown tissues.

A 14-3-3λ knockout line was identified, but preliminary characterisation did not show any immediately obvious phenotypes that were different to wild-type. If time allowed, it would be worthwhile investigating the knockout lines responses to blue-light induced chloroplast movement, stomatal opening or other responses mediated by phototropins. However, phylogenetic analysis revealed that 14-3-3λ is highly homologous to 14-3-3κ at the amino acid level. It is therefore possible that the proteins exhibit functional redundancy, indeed far-western analysis indicates that both 14-3-3λ and 14-3-3κ bind to phot1. Investigating the ability of other members of the non-epsilon group to bind to phot1 would determine the extent of the phot1 interaction with 14-3-3s. If phot1 binding is specific to the lambda and kappa isoforms, creation of a double knockout line could give clues as to the function of the proteins. It is possible,

however, that the role of 14-3-3λ in phototropin signalling is not involved in one of the visible responses such as phototropism or chloroplast movement. Previous studies using antisense technology to knockout 14-3-3ε and 14-3-3μ function in *Arabidopsis* resulted in increased starch accumulation in leaves (Sehnke *et al.,* 2001), and potato plants over- or under-expressing 14-3-3 proteins showed changes in the composition of amino acids, lipids and minerals (Presha *et al.,* 2002; Swiedrych *et al.,* 2002; Szopa 2002).

Confocal imaging of plants over-expressing GFP-14-3-3λ showed that GFP-14-3-3λ is located in a variety of subcellular regions: nucleus, cytoplasm and at the plasma membrane of epidermal, hypocotyl and guard cells. The localisation of 14-3-3λ in the nucleus of guard cells is in contrast to a previous study which demonstrated that although a 14-3-3λ-GFP fusion was located in the nucleus of *Arabidopsis* trichomes, when guard cells were examined 14-3-3λ-GFP was detected on the inner surface of guard cells and not in the nucleus (Paul *et al.,* 2005). The authors of the study point out that the 14-3-3λ-GFP visualised is comprised of not only homo-dimers, but also hetero-dimers with native 14-3-3 proteins. The localisation of the GFP tag on the N-terminal of 14-3-3λ in our study may have an effect on the ability of 14-3-3λ to form dimers resulting in localisation differences between the two studies. In order to definitively determine the subcellular localisation of 14-3-3λ however, the fluorescent construct would ideally be under control of the native promoter and expressed in the 14-3-3λ knockout line.

When dark-adapted plants were compared with plants kept in the light, it was noticeable that GFP-14-3-3λ showed more punctate distribution in light-maintained plants when functional phototropins were present (*gl1* background). Hypocotyl cells expressing GFP-14-3-3λ showed increased localisation at the apical and basal region of the cells when kept in the light compared to dark-adapted plants. One plausible explanation for these observations is that in dark-adapted plants, 14-3-3λ is evenly distributed across the plasma membrane, but after light exposure, the ability of 14-3-3λ to bind to autophosphorylated phot1 results in the movement of 14-3-3λ to areas where phot1 is localised. A recent study shows that barley 14-3-3 proteins can interact with a barley protein homologous to *Arabidopsis* PIN1 and barley NPH3, both of which are involved in auxin transport (Noh *et al.,* 2003; Haga *et al.,* 2005; Schoonheim *et al.,*

2007). It is intriguing to hypothesise that perhaps light-dependent 14-3-3λ binding to phot1 results in a complex that also comprises an NRL family member and/or auxin transporters to result in phototropism. Chapters 3 and 4 indicated that phot1 interactions with NPH3-L and RPT2 did not appear to be light-sensitive or light-dependent, and while NPH3 is modified in response to light it interacts with phot1 in both light and dark conditions (Pedmale & Liscum, 2007; Fig. 4.6). It is possible that phot1 interacts with NRL proteins in all light conditions, but light-dependent binding of 14-3-3λ to phot1 results in activation of this hypothetical complex and "switches on" phot1 signalling via NRL proteins to mediate responses to light.

Over-expression of 14-3-3λ in wild-type (*gl1*) and *phot1phot2* backgrounds resulted in a variety of phenotypes in mature plants; however, these must be interpreted with caution. It is thought that 30-40% of proteins in *Arabidopsis* possess Mode-1 (R/KxxpS/TxP) or Mode-2 (R/KxxxpS/TxP) 14-3-3 target peptides (Sehnke *et al.,* 2002) and so over-expressing a 14-3-3 protein is likely to have wide spread implications on plant growth. A previous study over-expressing *Arabidopsis* 14-3-3λ in cotton plants resulted in delayed leaf senescence and a "stay-green" phenotype when subjected to mild drought stress (Yan *et al.,* 2004). The 14-3-3λ over-expressing plants described in this chapter displayed prolonged flowering and hence, delayed senescence. Although the drought tolerance of our 14-3-3λ over-expressing plants was not investigated, it has been shown that phot1 enhances fitness and drought tolerance when compared to *phot1-5* through enhanced root efficiency as measured by root orientation and depth (Galen *et al.,* 2007). If 14-3-3λ over-expression does result in changes in the composition of lipids and starch accumulation as shown in other studies (see above), this may explain the increased brittleness observed in the leaves of our transgenic plants.

Identification of homozygous lines which over-express GFP-14-3-3λ would allow further characterisation to build on the preliminary work described in this chapter. It would be worthwhile investigating known phot1-mediated responses in the *gl1* background over-expressing line to determine if these are altered as a result of 14-3-3λ over-expression. These lines could also be used to immunoprecipitate GFP-14-3-3λ which could then be probed with the phot1 antibody to confirm the interaction *in planta.* The reciprocal co-immunoprecipitation experiment (probing phot1-GFP with the 14-3-3λ antibody) has so far proved unsuccessful as a means for confirming the

interaction *in planta*. It would also be useful to have homozygous lines to carry out further confocal microscopy studies to determine in more detail the effect of light and dark on 14-3-3λ localisation. At present, the plants must be selected on kanamycin to ensure they are transformed with the GFP construct and consequently are two weeks old and have been subjected to prolonged exposure to light by the time they are imaged. A homozygous line could be grown in the dark and visualised as seedlings with or without light treatment, which may result in clearer determination of the effect of light on GFP−14−3−3λ localisation.
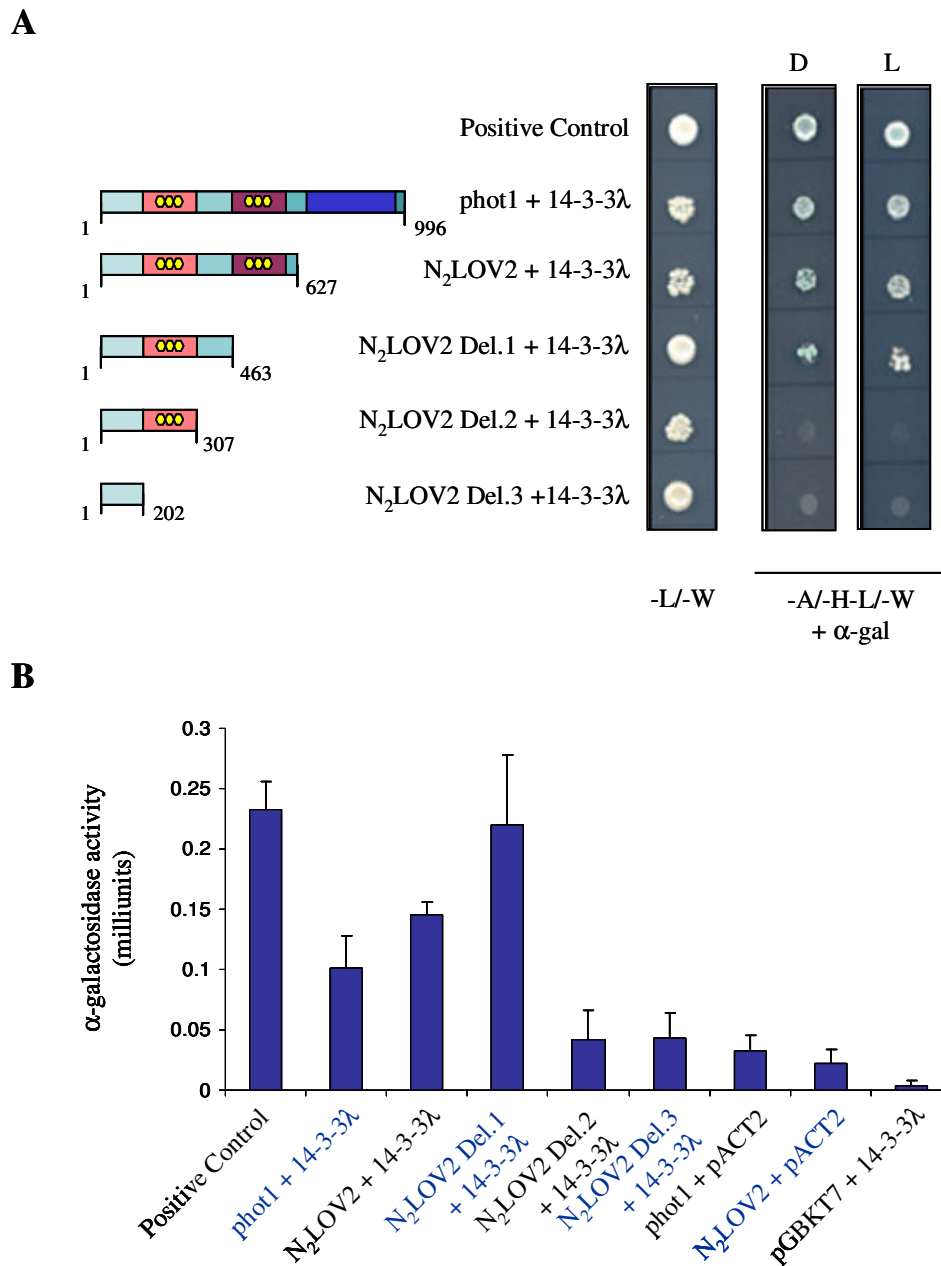
Figure 5.1 Further domain mapping of the phot1/ 14-3-3λ interaction in yeast

A) Deletion analysis of the phot1 N$_2$LOV2 regions required for the interaction with 14-3-3λ. Yeast were co-transformed with bait vectors encoding phot1 N$_2$LOV2 deletions and with the prey vector encoding full-length 14-3-3λ. Yeast transformed with both vectors were selected on non-selective media (-L/-W), and interacting proteins were selected for on full selection media (-A/-H/-L/-W+α-gal). Yeast were grown in the dark (D) or in 20 μmol m^{-2} s^{-1} white light (L).

B) Quantification of the phot1/14-3-3λ interaction using the α-galactosidase assay. Yeast co-transformed with the bait and prey vectors indicated were grown in liquid culture and the activity of α-galactosidase secreted into the media was measured as described in the Materials and Methods. Error bars indicate standard error (n=3)
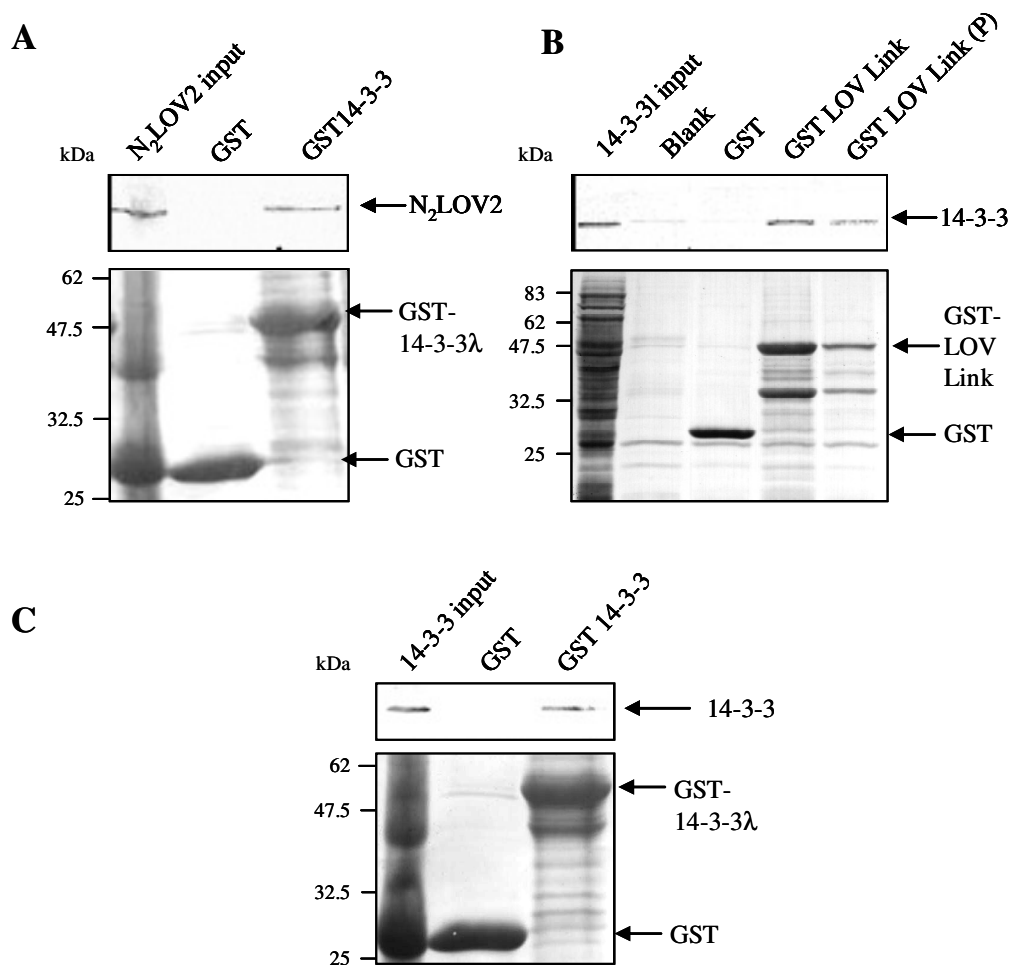
Figure 5.2 Confirmation of the phot1/14-3-3λ interaction by *in vitro* pull-down assay

A) *In vitro* binding of N₂LOV2 to 14-3-3λ. Approximately equal amounts (indicated in the lower panel by Ponceau S staining) of bacterially-expressed GST-14-3-3λ and GST were incubated with c-Myc-tagged N₂LOV2 synthesised by *in vitro* transcription/translation. Western blotting using anti-c-Myc antibody was used to detect c-Myc-N₂LOV2 (upper panel). One-twenty-fifth (2μL) of the *in vitro* transcription/translation reaction was loaded as a size reference for N₂LOV2 (input). Molecular mass markers are indicated on the left.

B) *In vitro* binding of 14-3-3λ to LOV Link. Approximately equal amounts (indicated in the lower panel by Ponceau S staining) of bacterially-expressed GST-LOV Link, GST or magnetic beads alone (blank) were incubated with c-Myc-tagged 14-3-3λ. GST-LOV Link (P) was artificially phosphorylated using PKA. Western blotting using anti-c-Myc antibody was used to detect c-Myc-14-3-3λ (upper panel). One-twenty-fifth (2μL) of the *in vitro* transcription/ translation reaction was loaded as a size reference for 14-3-3λ (input).

C) 14-3-3λ dimerises *in vitro*. Approximately equal amounts (indicated in the lower panel by Ponceau S staining) of bacterially-expressed GST-14-3-3λ was incubated with c-Myc-tagged 14-3-3λ. Western blotting using anti-c-Myc antibody was used to detect c-Myc-14-3-3λ (upper panel) as in (B).

All proteins were run on 12.5.5% polyacrylamide gels.

129
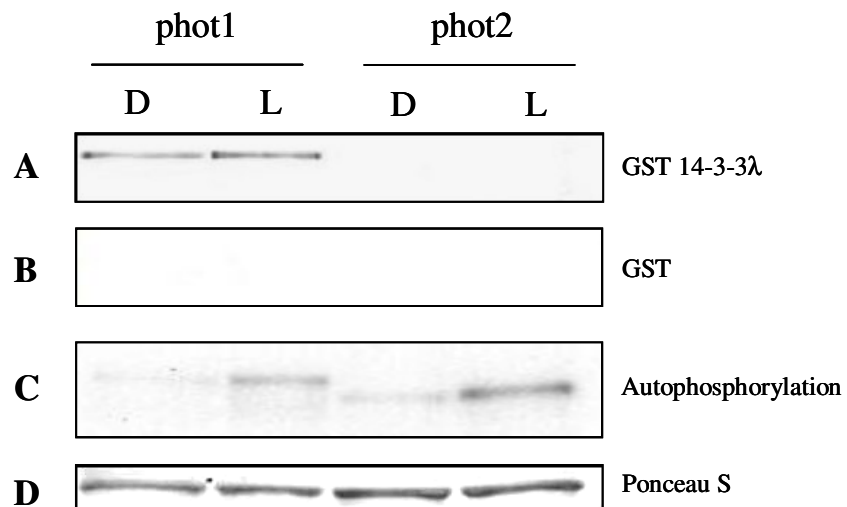
Figure 5.3 14-3-3λ binds specifically to phot1 expressed in insect cells

In vitro binding of bacterially-expressed 14-3-3λ to phot1 expressed in insect cells. Sf9 insect cells were used to express phot1 and phot2. The phototropins were incubated with radiolabelled ATP and kept in the dark (D) or given a brief pulse of high intensity white light (L) before being separated by SDS-PAGE and transferred to nitrocellulose membrane. Proteins were run on 7.5% polyacrylamide gels.

A) Specific binding of GST-14-3-3λ to phot1. The membrane was subjected to far western blotting using GST-14-3-3λ as a probe.

B) GST alone does not bind to phototropins. The membrane was subjected to far western blotting using GST as a probe.

C) Autoradiogram showing light-dependent autophosphorylation of phot1 and phot2.

D) Ponceau S staining of the membrane shows equal loading of samples.
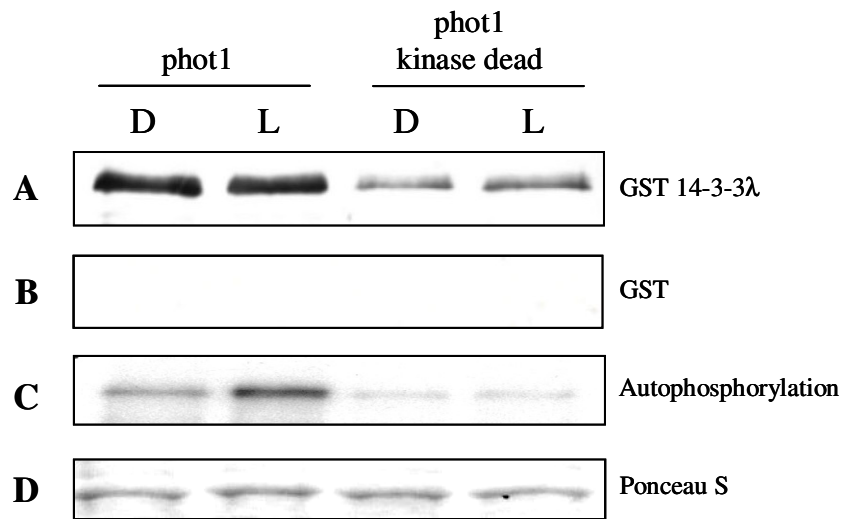
Figure 5.4 14-3-3λ binds to a kinase inactive mutant of phot1 expressed in insect cells

In vitro binding of bacterially-expressed GST-14-3-3λ to phot1 with a mutation in the kinase domain. Sf9 insect cells were used to express phot1 and the mutated phot1 (phot1 kinase dead). The phototropins were incubated with radiolabelled ATP and kept in the dark (D) or given a brief pulse of high intensity white light (L) before being separated by SDS-PAGE and transferred to nitrocellulose membrane. Proteins were run on 7.5% polyacrylamide gels.

A) Specific binding of GST-14-3-3λ to phot1 and phot1 kinase dead. The membrane was subjected to far western blotting using GST-14-3-3λ as a probe.

B) GST alone does not bind to phot1. The membrane was subjected to far western blotting using GST as a probe.

C) Autoradiogram showing results of the autophosphorylation assay on phot1 and phot1 kinase dead.

D) Ponceau S staining of the membrane shows equal loading of samples.
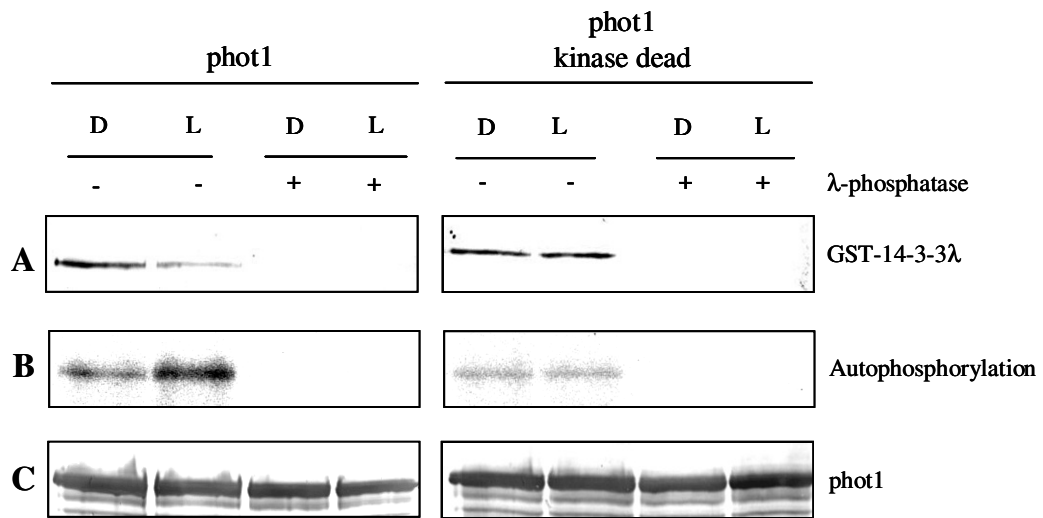
Figure 5.5 14-3-3λ binding to phot1 is abolished upon λ-phosphatase treatment

The effect of λ-phosphatase treatment on GST-14-3-3λ binding to phot1. Insect cells were used to express phot1 and phot1 kinase dead. Protein extracts were incubated with radiolabelled ATP and kept in the dark (D) or given a brief pulse of high intensity white light (L). λ-phosphatase was added to samples (indicated by +) before the proteins were separated by SDS-PAGE and transferred to nitrocellulose membrane. Far western blotting using GST-14-3-3λ as a probe is shown in the top panels. The middle panels show autoradiograms from the *in vitro* autophosphorylation assay. The lower panels show a western blot using phot1 antibody as a loading control for phot1 protein. Proteins were run on 7.5% polyacrylamide gels.
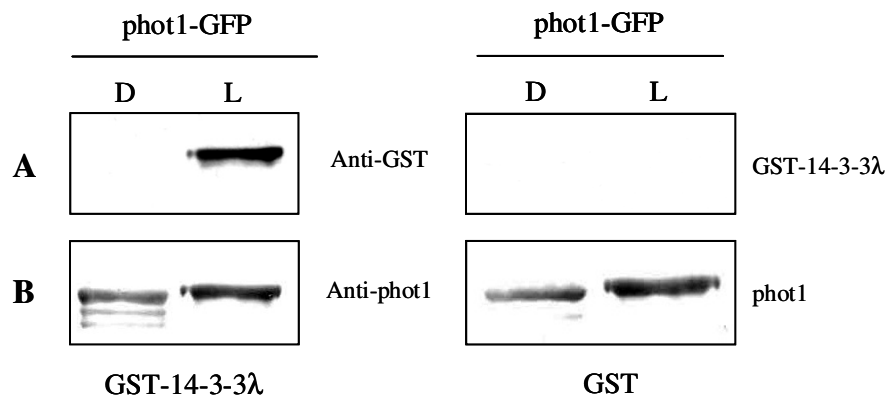
Figure 5.6 14-3-3λ binds specifically to plant-derived, light-treated phot1

Far western analysis of 14-3-3λ binding to plant-derived phot1-GFP. Three-day-old, etiolated seedlings were treated with white light (70 μmol m^{-2} s^{-1}) for 2 hours (L) or kept in the dark (D). Phot1-GFP was immunoprecipitated using anti-GFP antibody. Proteins were run on 7.5% polyacrylamide gels.

A) Far western analysis was carried out using bacterially-expressed GST-14-3-3λ or GST alone.

B) The membrane was stripped and reprobed with anti-phot1 antibody as a loading control for phot1 protein and to visualise *in vivo* autophosphorylation.
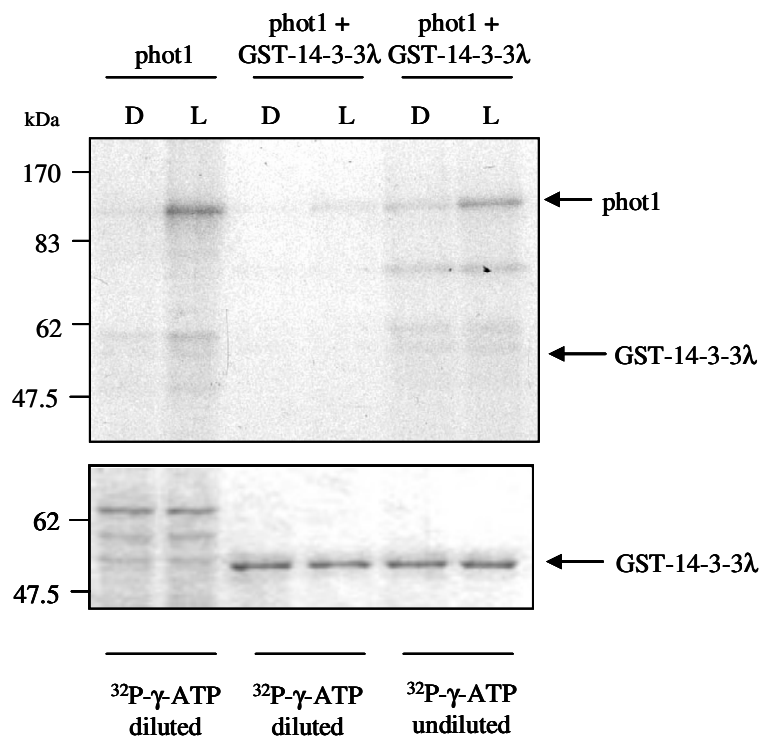
Figure 5.7 Insect cell expressed phot1 does not appear to phosphorylate 14-3-3λ

14-3-3λ as a phosphorylation substrate for phot1. Phot1 expressed in insect cells was incubated, where indicated, with bacterially-expressed GST-14-3-3λ in the presence of radiolabelled ATP. The ATP was either diluted 1:5 with unlabelled ATP or used undiluted. Samples were either kept in the dark (D) or given a brief pulse of white light (L). Phot1-only samples were loaded directly onto the gel after the autophosphorylation assay. Samples containing GST-14-3-3λ were purified by attaching to glutathione-magnetic beads. The upper panel shows the autoradiogram of the phosphorylation assay. The lower panel shows the coomassie stain of the gel and shows equal loading of phot1 protein (as determined by a visible protein from the insect cell system; first two lanes) and that equal amounts of GST-14-3-3λ were recovered from the beads (last four lanes). Molecular weight markers are indicated on the left. Proteins were run on 12.5% polyacrylamide gels.

Figure 5.8 Phylogeny of the *Arabidopsis* 14-3-3 family

A) Phylogenetic tree of the *Arabidopsis* 14-3-3 family. The epsilon group is shaded in blue and the non-epsilon group is shaded in pink. Lambda, kappa and epsilon isoforms are indicated.

B) Amino acid alignment of *Arabidopsis* 14-3-3-lambda (At5g10450) and kappa (At5g65430) proteins by ClustalW. The peptide regions used to generate antibodies EP053407 and EP053408 are coloured purple and red, respectively.
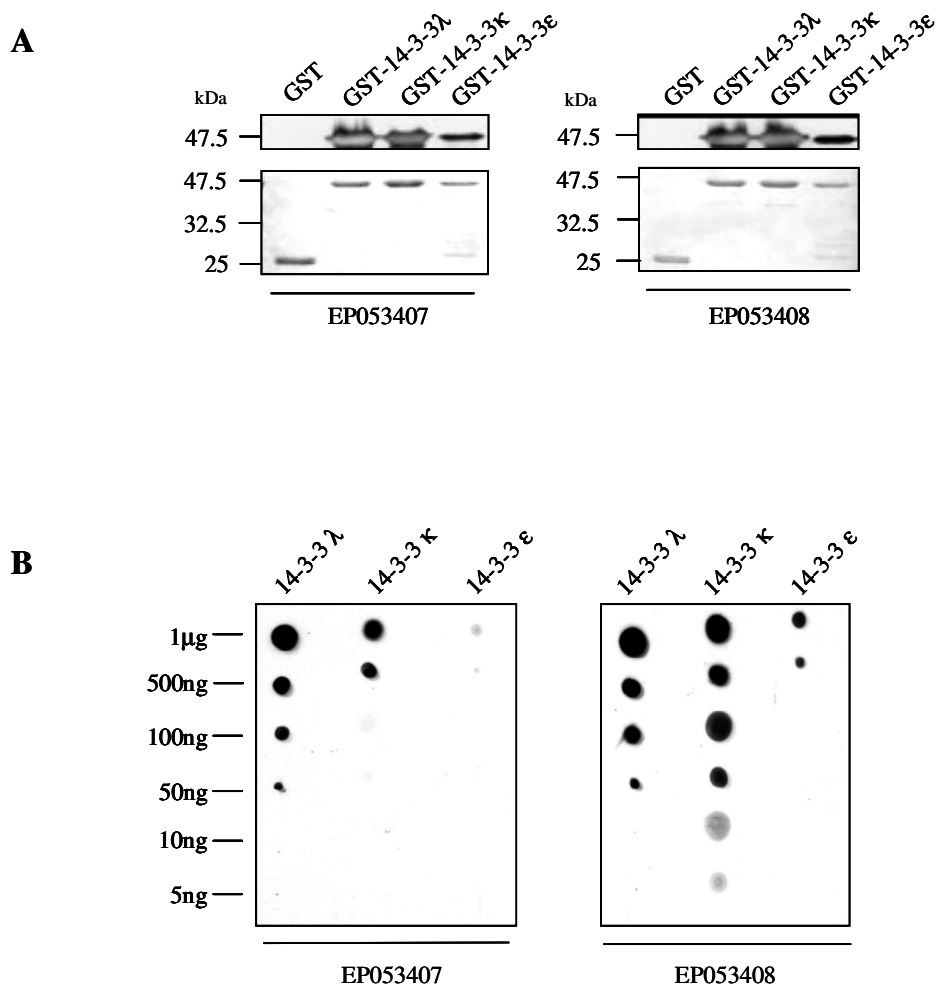
Figure 5.9 14-3-3 antibody characterisation

A) Western blotting of GST-tagged 14-3-3 proteins using peptide antibodies. Bacterially-expressed GST, GST-14-3-3λ, GST-14-3-3κ and GST-14-3-3ε were detected by western blotting using the peptide antibodies EP053407 and EP053408 (upper panel). Ponceau S staining shows equal loading of all proteins (lower panel). Molecular mass markers are indicated on the left. Proteins were run on 12.5% polyacrylamide gels.

B) Analysis of antibody specificity for different 14-3-3 isoforms. Decreasing amounts of GST-14-3-3λ, GST-14-3-3κ and GST-14-3-3ε were spotted onto nitrocellulose membrane and probed with the antibodies EP053407 and EP053408.
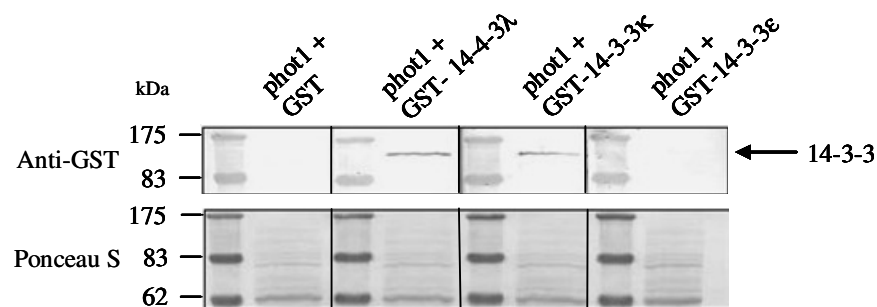
Figure 5.10 Phot1 binds members of the non-epsilon group of *Arabidopsis* 14-3-3 proteins

Far western analysis of the phot1 interaction with different 14-3-3 isoforms. Insect cell-expressed phot1 was subjected to far western analysis by probing with bacterially-expressed GST, GST-14-3-3λ, GST-14-3-3κ and GST-14-3-3ε. Interacting proteins were visualised using anti-GST antibody (upper panel). Ponceau S staining of the membrane shows equal loading (lower panel). Molecular weight markers are indicated on the left. Proteins were run on 12.5% polyacrylamide gels.
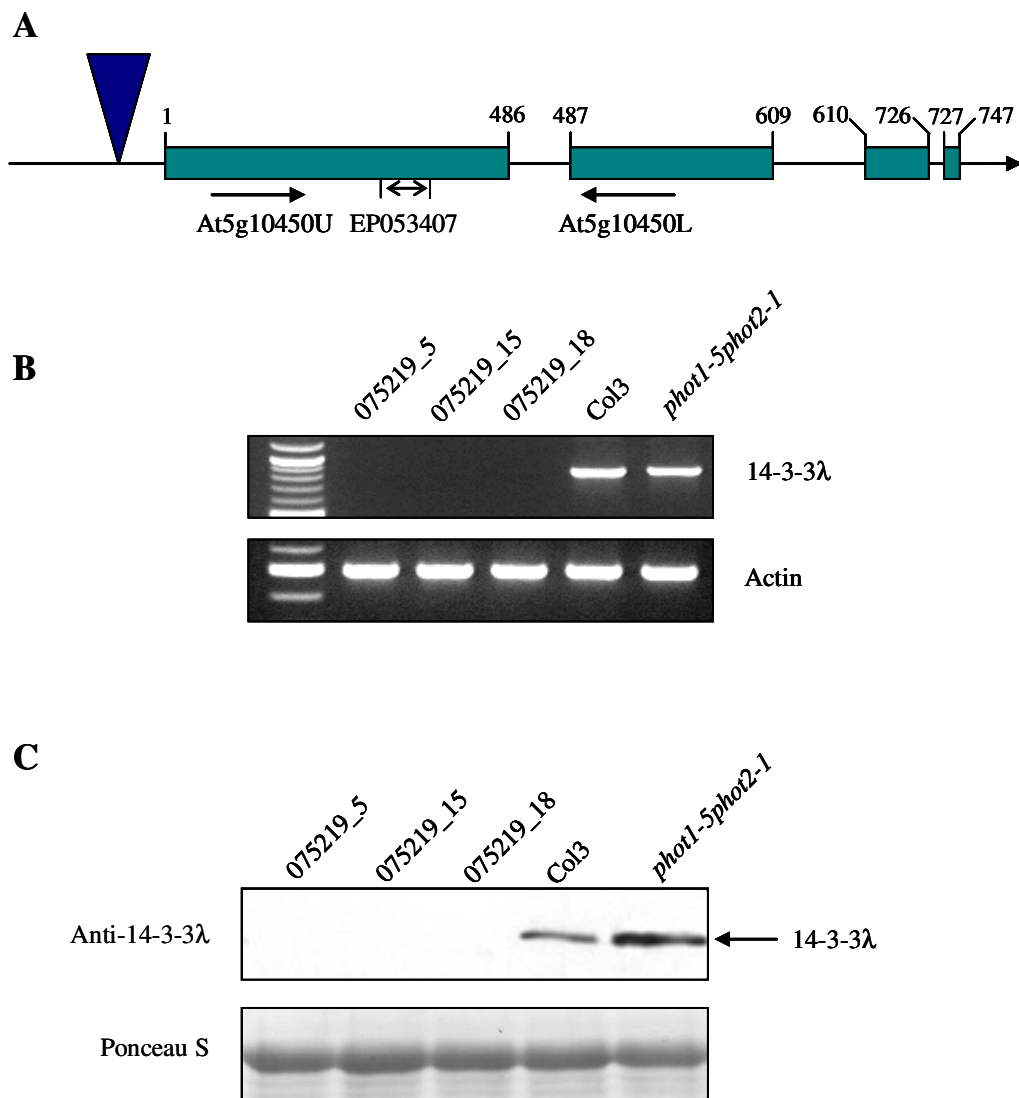
Figure 5.11 Identification of a 14-3-3λ knockout line

A) Schematic diagram showing location of the T-DNA insertion (navy triangle) in the second intron of the 14-3-3λ gene. Introns are shown as a black line and exons are shown as teal boxes. Nucleotide positions are indicated above the gene. Locations of NPH3-L specific primers (At5g10450U and At5g10450L) are indicated by block arrows. The region used for antibody production (EP053407) is shown by unfilled arrows.

B) RT-PCR analysis of 14-3-3λ transcript levels in 3 week old putative knockout plants (075219_5, 075219_15 and 075219_18) and wild-type (Col3) and *phot1-5phot2-1* plants. PCR products generated using 14-3-3λ specific primers are shown in the top panel. PCR products generated using actin primers as a loading control are shown in the bottom panel.

C) Western blot showing the levels of 14-3-3λ protein in wild-type (Col3), *phot1-5phot2-1* and putative knockout plants (075219_5, 075219_15 and 075219_18). Fifty μg of total protein extracted from etiolated seedlings was probed using the 14-3-3λ antibody EP053407. Equal loading is shown in the lower panel by Ponceau S staining of the membrane. Proteins were run on 12.5% polyacrylamide gels.
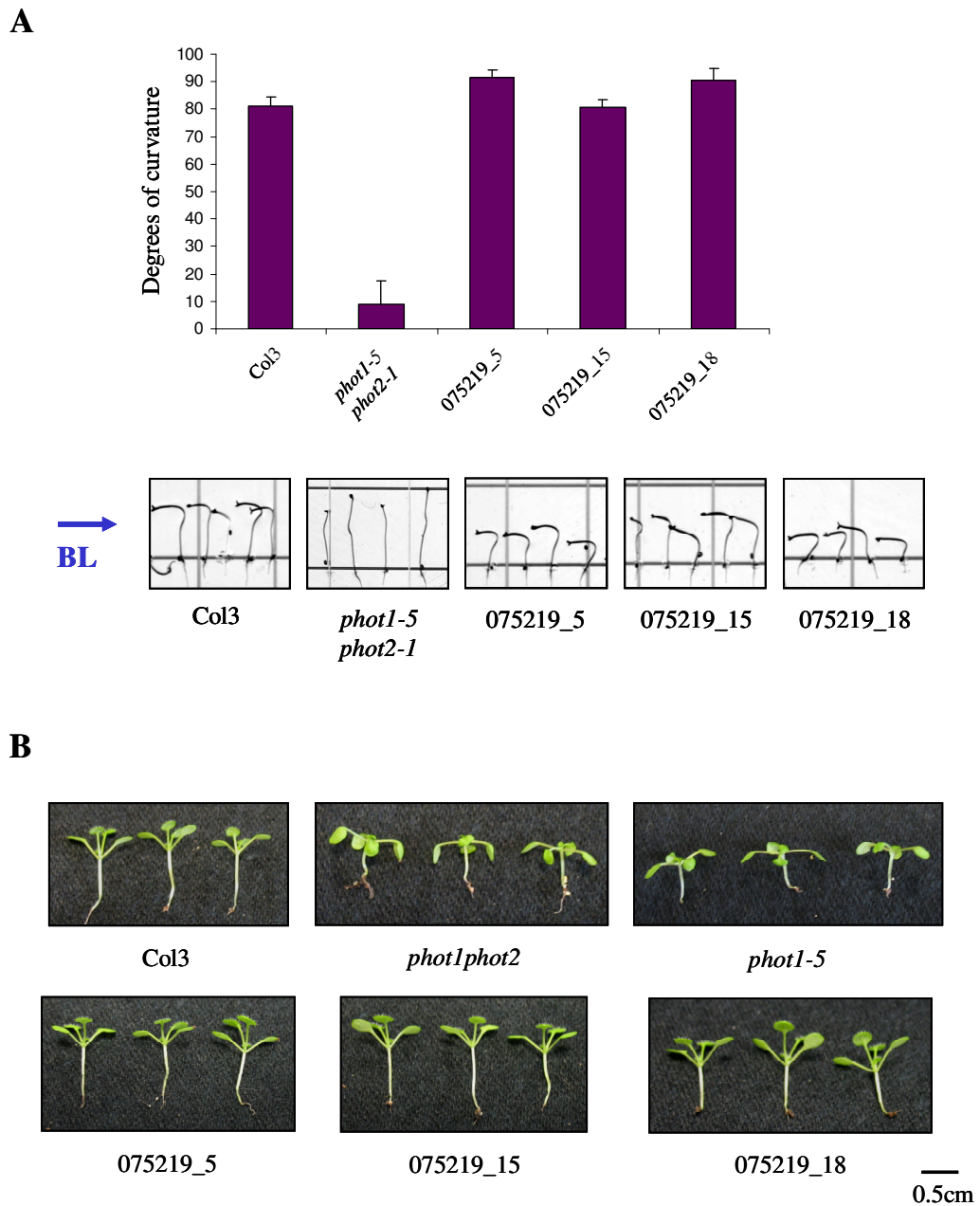
A) Phototropism of wild-type (Col3), *phot1-5phot2-1* and the 14-3-3λ knockout line (075219_5, 075219_15 and 075219_18). Two-and-a-half day old dark-grown seedlings were placed in unilateral blue light (1 μmol m^{-2} s^{-1}) for 24 hours before the angle of curvature was measured. Representative seedlings are pictured. The arrow indicates the direction of blue light (BL). Error bars indicate standard error (n>20)

B) Leaf orientation by light of the 14-3-3λ knockout line. Seedlings described in (A) were grown under 100 μmol m^{-2} s^{-1} white light for one week then transferred to 10 μmol m^{-2} s^{-1} white light for a further week. Scale bar represents 0.5cm.

A

Col3   075219_15

B

075219_18

Figure 5.13 Unusual phenotypes of 14-3-3λ knockout plants sprayed with mycobutanil

A) Bifurcation of the mid-vein of 14-3-3λ knockout plants sprayed with mycobutanil. Wild-type (Col3) and knockout plants (075219_15) were grown for 3 weeks under constant white light (70 μmol m^{-2} s^{-1}). A commercially available preparation of mycobutanil was sprayed weekly before representative images were taken.

B) Leaf growths of 14-3-3λ knockout plants sprayed with mycobutanil. Plants were grown and treated as described in (A). The image is of a 5 week old knockout plant (075219_18).
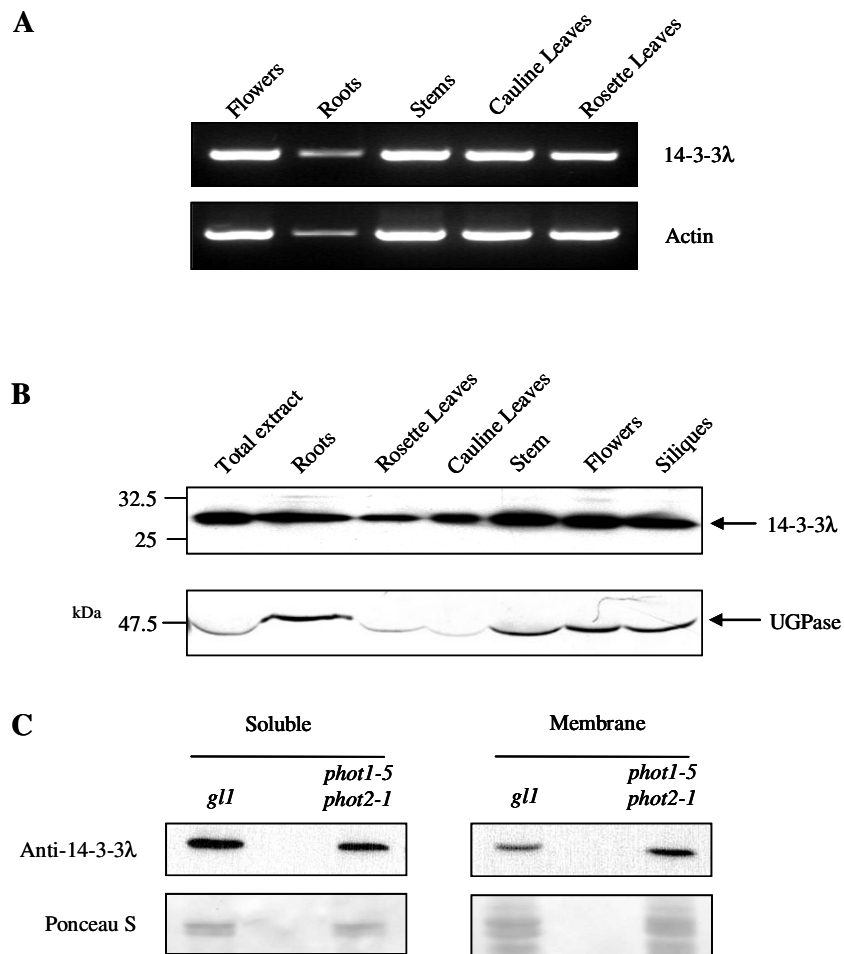
Figure 5.14 Expression and localisation of 14-3-3λ in *Arabidopsis*

A) RT-PCR analysis on 5 week old tissue grown under 70 μmol m^{-2} s^{-1} white light. RNA was extracted from flowers, roots, stems, cauline leaves and rosette leaves of wild-type (Col3) plants. PCR products generated using 14-3-3λ specific primers are shown in the top panel. The lower panel shows PCR products generated using actin primers as a loading control.

B) Western blotting of 14-3-3λ protein levels in extracts from different tissues. Ten μg of total protein extracted from the tissues of 5 week old wild-type (Col3) plants was probed with the 14-3-3λ antibody, EP053407 (upper panel). The membrane was reprobed with the UGPase antibody as a loading control (lower panel). Proteins were run on a 12.5% polyacrylamide gel.

C) Western blotting of 14-3-3λ protein levels in soluble protein and membrane extracts. Ten μg of membrane or soluble protein extracted from wild type (*gl1*) or *phot1-5phot2-1* etiolated seedlings was probed with the 14-3-3λ antibody, EP053407 (upper panel). Ponceau S staining of the membrane is shown as a loading control (lower panel). Proteins were run on 12.5% polyacrylamide gels

141

A

phot1phot2
35S :: GFP-14-3-3λ

gll
35S ::GFP-14-3-3λ

Light

Dark

epidermis   stomata   epidermis   stomata

B

gll
35S ::GFP-14-3-3λ

Dark   Light
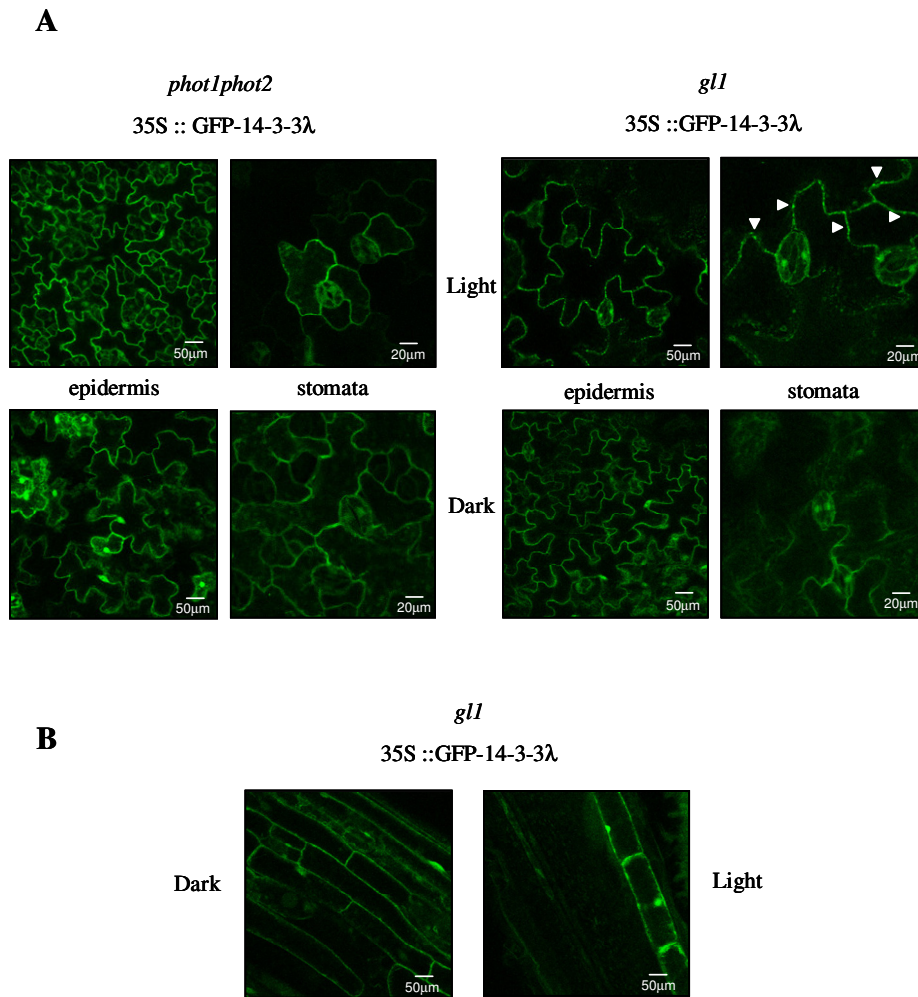
Figure 5.15 GFP-14-3-3λ localisation

A) Sub-cellular localisation of GFP-14-3-3λ. Wild-type (*gll*) or *phot1-5phot2-1* expressing 35S::GFP-14-3-3λ grown in light (Light) or dark-adapted (Dark) for 2 hours. Confocal images show GFP fluorescence of epidermal and guard cells. Scale bars represent 20 or 50 μm.

B) GFP-14-3-3λ localisation in hypocotyl cells. Wild-type (*gll*) expressing 35S::GFP-14-3-3λ dark-adapted for 2 hours (Dark) or kept in the light (Light). Confocal images show GFP fluorescence in hypocotyl cells. Scale bars represent 50 μm.

142

gl1

gl1
35S ::GFP-14-3-3λ

phot1phot2

phot1phot2
35S :: GFP-14-3-3λ

1cm
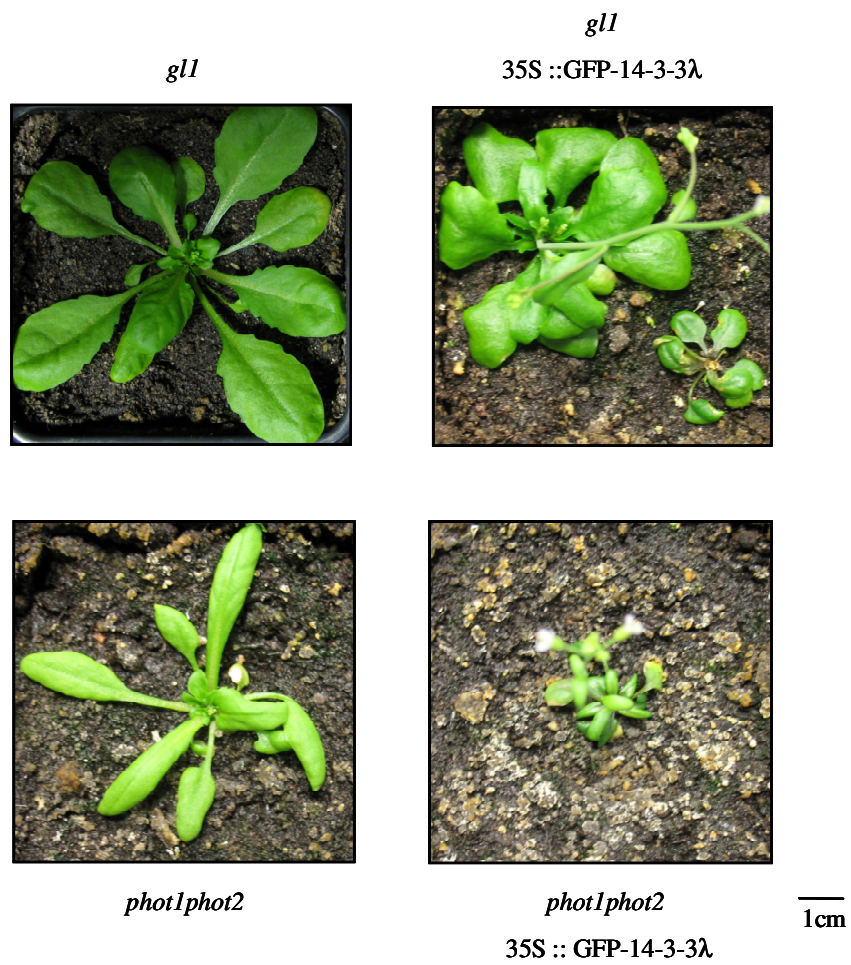
Figure 5.16 Phenotypes of 14-3-3λ over-expressing lines

Phenotypes resulting from over-expression of GFP-14-3-3λ in *gl1* and *phot1-5phot2-1* backgrounds. Wild-type (*gl1*) and *phot1-5phot2-1* were grown on agar plates for 2 weeks then transferred to soil and grown under 70 μmol m^{-2} s^{-1} long day white light for 2 weeks. T2 transgenic plants were selected on agar plates containing kanamycin for 2 weeks then transferred to soil and grown under 70 μmol m^{-2} s^{-1} long day white light for 2 weeks. Scale bar represents 1cm.

143

Chapter 6: Structure/function studies of phot1

6.1 Introduction

As little is known about the early events associated with phototropin signalling, structure/function analyses were carried out using regions of the phot1 protein expressed in a variety of plant backgrounds. The approach of over-expressing photoreceptor domains *in planta* to try to identify a function for them has previously been used successfully; for example, over-expression of the C-terminal domains of cry 1 and cry2 resulted in a COP phenotype (see Section 1.2.6; Yang *et al.,* 2000).

In this study, particular attention was paid to the effect of receptor autophosphorylation and the role this plays in phototropin signalling *in planta.* Initially, the phototropin double mutant was transformed with a truncated version of phot1 which lacked the sites for receptor autophosphorylation upstream of LOV2 and the functional consequences of truncated phot1 expression in the transgenic lines were investigated.

6.2 Results

6.2.1 Expression of LOV2-kinase in the phot double mutant background

To investigate the necessity of phot1 autophosphorylation in phot1 signalling, the *phot1-5phot2-1* double mutant was transformed with a construct encoding the regions of the *PHOT1* cDNA downstream from phosphorylation sites mapped previously (Salomon *et al.,* 2003). Under the control of the cauliflower mosaic virus 35S promoter, the LOV2-kinase (L2K) region of phot1 (Fig. 6.1A) was stably transformed into the double mutant. Four independent homozygous lines were obtained and the data from two representative lines are described in this chapter.

RT-PCR analysis using primers designed specifically against the region encoding L2K showed that transcript corresponding to this region was only identified in cDNA extracted from transgenic plants (Fig. 6.1B). Western analysis using an antibody raised against the extreme C-terminal region of phot1 demonstrated that L2K protein of the expected size (~70 kDa) was expressed in the transgenic lines, but not in the double mutant line (Fig. 6.1C). The L2K band sometimes appeared as a doublet on western blots; however, a band of the same size as the lower doublet band is observed

in extracts from wild-type seedlings and likely represents degradation of the phot1 protein, which also occurs in the L2K protein (data not shown).

6.2.2 Subcellular localisation of L2K

Native phot1 protein is membrane localised in dark conditions and upon exposure to light a proportion of the protein moves to the cytosol (Sakamoto & Briggs, 2002; Lariguet *et al.,* 2006). To investigate the subcellular localisation of L2K, total protein was extracted from etiolated seedlings that had either been kept in the dark or given two hours of white light treatment. The protein was fractionated into membrane and soluble fractions and subjected to western blotting using the phot1-kinase antibody (Fig. 6.2A). The results show that L2K is localised in the membrane fraction, indicating that this region alone is sufficient for membrane localisation of phot1 in *Arabidopsis.* Unlike phot1 however, there does not appear to be any re-localisation of L2K to the soluble fraction after exposure to light (Fig. 6.2A). The membrane was subsequently probed with anti-NPH3 antibody as a marker for membrane localisation and with an antibody raised against the cytosolic protein, UDP-glucose pyrophosphorylase (UGPase), to monitor membrane purity.

In addition to the subcellular movement shown by phot1, western blot analysis shows that phot1 irradiated *in vivo* undergoes autophosphorylation which results in a decrease in electrophoretic mobility (Knieb *et al.,* 2005). Functional phot1 is also required for the increase in electrophoretic mobility shown when NPH3 is dephosphorylated after exposure to blue light (Motchoulski & Liscum, 1999; Pedmale & Liscum, 2007). To determine if the L2K region of phot1 is sufficient to complement either of these responses, proteins extracted from dark and light-treated etiolated seedlings were subjected to western blot analysis. Figure 6.2B (top panel) shows that there is no decrease in electrophoretic mobility of L2K after *in vivo* light treatment consistent with the conclusion that autophosphorylation of the N-terminal region of phot1 is necessary for this shift. Probing the nitrocellulose membrane with the NPH3 antibody showed that there was no increase in NPH3 electrophoretic mobility in response to *in vivo* light treatment. This indicates that the region of phot1 upstream of amino acid 448 is required for the post-translational modification of NPH3.

6.2.3 L2K mediates phototropism under moderate light conditions

As discussed in Chapter 1, phot1 is the primary photoreceptor for phototropism in *Arabidopsis* and can mediate phototropism at light intensities as low as 0.1 µmol m^{-2} s^{-1} blue light (Sakai *et al.,* 2001). To investigate the role played by L2K in the phototropic response, etiolated transgenic seedlings were exposed to unilateral blue light for 24 hours over a range of fluence rates. As expected, wild-type seedlings showed phototropic curvature over a wide range of light intensities while *phot1-5phot2-1* seedlings showed minimal curvature (Fig. 6.3A). At light intensities up to 1 µmol m^{-2} s^{-1} L2K seedlings behaved as the double mutant, but at higher light intensities (> 10 µmol m^{-2} s^{-1}) they showed strong phototropic curvature (Fig. 6.3A). Representative images of phototropically stimulated seedlings are shown in Figure 6.3B. Although the phototropic response was slightly weaker than in wild-type seedlings, the results show that L2K is sufficient to mediate phototropism at intermediate light intensities.

6.2.4 L2K mediates leaf positioning under moderate light conditions

It has been shown that *Arabidopsis* seedlings orientate their leaves in response to blue light in order to optimise light harvesting for photosynthesis resulting in enhanced growth. The response is dependent on phot1 and NPH3 at low fluences of blue light (Inoue *et al.,* 2007). We have observed that leaf positioning under white light is also dependent on phot1 activity. Wild-type seedlings grown under 50 µmol m^{-2} s^{-1} white light for 1 week before being transferred to 10 µmol m^{-2} s^{-1} white light for a further week show petioles that point upwards towards the light source and flattened leaves perpendicular to the incident light, whereas *phot1-5phot2-1* and *phot1-5* seedlings show flat petioles and downward-pointing leaves (Fig. 6.4A). L2K lines grown in this manner respond like the *phot1-5phot2-1* and *phot1-5* lines and do not show correct leaf positioning. However, if L2K seedlings are kept under 50 µmol m^{-2} s^{-1} for the second week, L2K lines respond like wild-type and position their leaves to face upward (Fig. 6.4B). Therefore, the L2K lines can complement this response, but as for phototropism, it appears that they require higher intensities of light for functionality. The photographs for Figure 6.4B were taken by Stuart Sullivan.

6.2.5 L2K promotes leaf expansion and increases fresh weight

Leaves of *phot1-5phot2-1* plants are epinastic and curled underneath themselves resulting in a long, narrow shape compared to the wide, flat shape shown by wild-type leaves (Fig. 6.5 A). Genetic analysis has shown the either phot1 or phot2 is sufficient to promote leaf expansion in *Arabidopsis* (Sakamoto & Briggs, 2002; Takemiya *et al.,* 2005). As mature rosette leaves of the L2K lines looked like the leaves of wild-type plants (Fig. 6.5B), it can be concluded that the L2K region of phot1 is sufficient to complement the leaf expansion response. By calculating the ratios of the area of unflattened and artificially flattened leaves, the leaf expansion index (LEI) can be calculated, where an LEI of 1 indicates a completely flat leaf (Takemiya *et al.,* 2005). Figure 6.5B shows that transformation of the double mutant line with L2K results in a leaf expansion index similar to that of wild-type (LEI ~ 0.85) and almost twice that of the *phot1-5phot2-1* double mutant (LEI ~ 0.5).

Phototropin-mediated responses collectively increase the photosynthetic potential of plants. Flatter leaves result in an increased area available for interception of light for photosynthesis, and phototropins promote increases in fresh weight, especially under low light conditions (Takemiya *et al.,* 2005). Therefore, the fresh weight of plants grown under 50 μmol m^{-2} s^{-1} for three weeks was determined. Figure 6.5 C shows that plants lacking phototropins can only achieve about half the fresh weight of wild-type plants. However, expression of L2K results in plants that weigh as much as wild-type plants. These data indicate that L2K can completely restore the growth responses promoted by phot1.

6.2.6 L2K expression results in decreased chlorophyll levels

When growing L2K transgenic lines, it was observed that plants looked less green than their parental background, the *phot1-5phot2-1* line (Fig. 6.6A). During early light development, the steady state level of light-harvesting complexes of photosystem II (Lhcb) transcript is closely correlated with greening and fresh weight (Horwitz *et al.,* 1988). Phot1 has been shown to mediate the destabilisation of *Lhcb* transcript levels and differences in *Lhcb* transcript accumulation correspond with the greening of cotyledons in white light where *phot1* seedlings exhibit increased chlorophyll accumulation (Folta & Kaufman, 2003). Similarly, seedlings in a *Ler* background grown under 60 μmol m^{-2} s^{-1} white light stop accumulating LHCB and ribulose-1,5-

bisphosphate carboxylase/ oxygenase (Rubisco) large subunit (RBCL) proteins when transferred to 600 μmol m^{-2} s^{-1} white light (Weston *et al.,* 2000). This decrease in protein accumulation is less pronounced for *phot1-5* seedlings, (though this may be due in part to genotypic differences) and could represent a phot1-mediated influence on chloroplast protein abundance (Folta & Kaufman, 2003; Weston *et al.,* 2000). Therefore, the chlorophyll content of L2K plants was compared to wild-type and *phot1-5phot2-1* plants. The results shown in Figure 6.6 indicate that L2K lines have wild-type levels of chlorophyll and this is less than the level of chlorophyll found in the double mutant. If phot1-mediated destabilisation of transcripts is reflected in the abundance of chloroplast proteins, then L2K is sufficient to mediate this response. However, the possibility remains that the double mutant line does in fact contain the same level of chlorophyll as the wild-type and L2K lines, but the double mutant cell size is smaller. Therefore, even by expressing the chlorophyll levels in units of μg/mg,more *phot1-5phot2-1* cells would be included in the analysis making it appear that the line contains increased levels of chlorophyll.

6.2.7 L2K restores the phot1-mediated chloroplast accumulation response

Under low light conditions, phot1 and phot2 mediate the movement of chloroplasts to the upper face of palisade mesophyll cells in order to maximise light capture for photosynthesis (Kagawa *et al.,* 2001). Since L2K can restore phot1-mediated growth responses which likely result from increased photosynthesis, it was decided to investigate the effect of L2K on the chloroplast accumulation response. Three-week-old plants grown in low light conditions were subjected to three hours dark treatment or three hours of low intensity blue light (1.5 μmol m^{-2} s^{-1}; Onodera *et al.,* 2005) before detached leaves were imaged by confocal microscopy. Both wild-type plants and L2K lines accumulated chloroplasts at the upper face of the mesophyll cells when subjected to low blue light compared to dark treated plants or *phot1-5phot2-1* plants (Fig. 6.7A and B). Figure 6.7B shows that L2K almost fully restores the accumulation response under low blue light conditions. Further work in the laboratory has shown that the accumulation response persists in the L2K lines in response to high intensity blue light (10 μmol m^{-2} s^{-1}) whereas phot2 present in wild-type plants initiates the avoidance response (Thomson *et al.,* 2007). The higher number of chloroplasts detected in L2K and double mutant lines under dark conditions is due to the lack of

phot2 which is required to localise chloroplasts to the anticlinal walls in darkness (Fig. 6.7; Suetsugu *et al.,* 2005; Tsuboi *et al.,* 2007).

6.2.8 L2K plants display different responses to drought stress compared to wild-type or the double mutant.

Recently, it has been demonstrated that phot1 promotes tolerance to drought stress by promoting root growth into the soil and away from the soil surface which is more likely to become desiccated in times of limited rainfall (Galen *et al.,* 2007). However, phototropins also function redundantly, and in tandem with cryptochromes, to promote stomatal opening in response to blue light (Kinoshita *et al.,* 2001; Mao *et al.,* 2005). Mao *et al*. (2005) reported that a lack of cryptochromes results in increased tolerance to drought stress as a result of reduced stomatal opening (Mao *et al.,* 2005). Therefore, the effect of phototropins on the ability to tolerate drought stress was investigated by gas exchange measurements. Wild-type and *phot1-5phot2-1* double mutant plants were grown under 70 μmol m^{-2} s^{-1} white light in short day conditions for eight weeks in order to achieve leaf areas large enough to clamp the apparatus onto. The rate of photosynthesis (A) and stomatal conductance (gs, as an indicator of transpiration) were measured before and after 8 days of drought stress caused by a complete termination of irrigation. The results of this experiment are shown in Figure 6.8. There was no difference in A between either of the genotypes in either watered or unwatered conditions (Fig. 6.8A), although it must be noted that the rate of photosynthesis measured is low and is probably due to insufficient light levels required to saturate photosynthesis. In wild-type plants, gs was reduced in response to drought, whereas in the double mutant gs remained more or less constant (Fig. 6.8B). The decrease in stomatal conductance shown by wild-type plants in response to drought stress resulted in a 50% increase in water use efficiency (WUE) under drought conditions compared to well-watered conditions (Fig. 6.8C). Conversely, the WUE of *phot1-5phot2-1* plants decreased in response to drought stress, presumably because of the maintenance of stomatal conductance.

It was decided to use the physiological responses to drought as an indication of stomatal opening and to determine the effect of L2K in promotion of stomatal opening. Plants were grown on soil in individual pots for three weeks before drought stress was

initiated by termination of irrigation. On the last day of watering, pots were wrapped in cling film to prevent evaporation of water from the soil. After 8 days without water, the *phot1-5phot2-1* plants remained green and turgid, while wild-type plants were wilted and senescing. The L2K plants were flaccid, but still green and could certainly have been rescued by watering (Fig. 6.9A). Measurement of the relative water content (RWC) is a useful indicator of plant water status as it closely reflects the balance between water supply and transpiration rate (Cominelli *et al.,* 2005). After 8 days of drought stress, wild-type plants showed a decrease in RWC to around 50% of the initial value at Day 0, whereas the *phot1-5phot2-1* double mutant showed a decrease in RWC of around 20% compared to the initial RWC value. The L2K lines showed an intermediate reduction in RWC of around 25-30%. After 12 days of water stress, all plants showed an approximately 75% reduction in RWC (Fig. 6.9B). As L2K lines appeared to have an intermediate drought stress phenotype when compared to wild-type and *phot1-5phot2-1* mutant, this suggests that L2K can only partially restore stomatal opening in the double mutant background.

6.2.9 Over-expression of phot1 kinase results in a dwarf phenotype

The kinase domain of phot2 has been shown to be constitutively active *in vitro* unless LOV2 is present to repress its activity in the dark (Matsuoka & Tokotumi, 2005). In addition the kinase domain of phot2 has been shown to constitutively mediate phototropin responsiveness *in vivo* (Kong *et al.,* 2007). To determine the effect of phot1 kinase expression *in vivo*, transgenic plants were created. Wild-type (Col3) plants were transformed with an expression construct harbouring the *PHOT1* cDNA region encoding amino acids 612 to 996 of phot1, comprising a small region N-terminal of the kinase domain, the functional kinase domain and the extreme C-terminal, under the control of the cauliflower mosaic virus *35S* promoter (Fig. 6.10A). The phot1 kinase region was expressed as a C-terminal c-Myc epitope fusion (Fig. 6.10A). Homozygous lines are currently being selected, but the image in Figure 6.10B shows the phenotype of a mature T2 plant. Compared to wild-type, over-expression of the kinase domain results in a dwarf plant with darker leaves, similar to that shown when phot2 kinase is over-expressed in the wild-type background (Kong *et al.,* 2007).

6.2.10 Over-expression of inactive phot1 kinase

The *phot1-5* null allele has previously been shown to be complemented when transformed with full-length phot1 fused to green fluorescent protein (phot1-GFP) under the control of the native *PHOT1* promoter (Sakamoto & Briggs, 2002). Wild-type plants have been successfully transformed with the active or inactive kinase domain of phot2 tagged with GFP under the control of the *35S* promoter (Kong *et al.,* 2007). To investigate the effects of the inactive phot1 kinase domain, phot1-GFP plants (see above) were transformed with the inactive kinase domain of phot1 (Fig. 6.11A). Transcript was identified in three of the lines which showed homozygous segregation ratios (Fig. 6.11B). Despite many attempts, detection of the inactive kinase protein was unsuccessful, probably because a major degradation product of phot1-GFP is the same size (~ 50kDa; data not shown). However, further investigations were carried out on the two lines that showed high transcript levels (1H and 36D).

Because the parental background of the transgenic lines was phot1-GFP, the effect of the inactive kinase domain on the localisation of phot1-GFP could be easily determined using confocal microscopy. Figure 6.11C shows that etiolated phot1-GFP seedlings kept in the dark showed fluorescence exclusively at the plasma membrane region but after exposure to light for 3 hours, a proportion of phot1-GFP was found to become localised in the cytosol (left panels). However, phot1-GFP seedlings expressing the inactive phot1 kinase domain showed constitutive localisation of phot1-GFP in the cytosol and at the plasma membrane in both light and dark conditions (Fig. 6.11C, right panels). This was consistent for all lines examined, regardless of the level of transcript identified by RT-PCR analysis.

Initial investigations of phototropism in seedlings over-expressing the inactive kinase domain were made. Non-uniform germination made it difficult to determine statistically if there was an effect, but observation and measurements of bending over a variety of time scales indicated that there was no difference between the transgenic plants and Col3 wild-type, or the parental background phot1-GFP seedlings (data not shown).

It was observed that transgenic plants over expressing inactive phot1 kinase were more tolerant to drought stress than the parental background, phot1-GFP (Fig.6.12). After 10 days without watering, phot1-GFP plants were wilting and becoming yellow, whereas the inactive kinase over expressing plants were still turgid

and looked healthy. This is consistent with the observations of Kong *et al.* (2007) who showed recently that inactive over-expression of the C-terminal kinase region of phot2 produced a dominant negative effect on native phot2 activity with regard to stomatal opening.

6.2.11 Over-expression of phot1 results in a phenotype reminiscent of altered auxin homeostasis

It has been shown that phot2 can cross phosphorylate phot1 *in vitro* and *in vivo* (Cho *et al.,* 2007). To investigate the effects of full-length phot1 being constitutively expressed in the presence of native phots, wild-type (Col3) plants were transformed with full-length phot1 under control of the *35S* promoter and fused to an N-terminal haemagluttinin (HA) epitope tag (Fig. 6.13A). T2 plants expressing phot1 (as determined by western blotting, data not shown) showed a variety of phenotypes (Fig. 6.13B, plants 2, 3 and 4). These plants were smaller and bushier than those that did not express HA-tagged phot (Fig. 6.13B, plant 1). The leaves of phot1 over-expressing plants had non-symmetrical margins and did not form normal, flat rosettes. Apical dominance was reduced and the amount of seed produced was greatly increased compared to wild-type plants. These phenotypes are indicative of altered auxin homestasis and are similar to the phenotypes shown by plants lacking PGP19 (*mdr1-1*). Further characterisation of homozygous lines is currently underway in the laboratory. Wild-type (Col3) plants were also transformed with the N_2LOV2 region of phot and over-expressed by the *35S* promoter in addition to being tagged with the HA epitope sequence. These lines are still being selected but show no visible phenotype. They will, however, prove a useful tool for further investigation of the effects of the photosensory region when over-expressed in *Arabidopsis,* and also act as a negative control since the vector backbone of the kinase, phot1 and N_2LOV2 is the same and phenotypes caused by the vector can be ruled out if one of the lines fails to display a phenotype.

6.3 Discussion

6.3.1 Structure/function analysis of L2K

Phototropins are autophosphorylating blue light receptor kinases. Sites of *in vitro* receptor autophosphorylation in oat phot1 have been mapped to the N-terminal region of phot1 upstream of LOV1 and in the linker region between LOV1 and LOV2 (Salomon *et al.,* 2003). Recent work in the laboratory has identified four autophosphorylation sites in *Arabidopsis* phot1 *in vivo* by using a mass spectrometry approach. Two sites are upstream of LOV1 (Ser^{58} and Ser^{185}) and two are located in the linker region (Ser^{350} and Ser^{410}; Thomson *et al.,* 2007,). To determine the necessity of phot1 autophosphorylation to elicit responses to light, *phot1-5phot2-1* plants were transformed with a truncated version of the phot1 protein encoding the regions downstream of the autophosphorylation sites (LOV2-kinase, amino acids 448-996).

Investigation of the subcellular localisation of L2K revealed that the protein is located at the membrane. The mechanism by which phototropins associate with the plasma membrane is unknown, however our data indicate that the regions involved in membrane localisation are conserved in the truncated protein. This is in agreement with the results of Kong *et al.* (2006, 2007) which show that the kinase domain alone is sufficient for membrane localisation. A proportion of phot1 disassociates from the plasma membrane within minutes of exposure to light (Sakamoto & Briggs, 2002; Lariguet *et al.,* 2006). However, this disassociation was not observed when seedlings expressing L2K were exposed to light (Fig. 6.2). L2K was expressed at lower levels than native phot1 (data not shown), so it is possible that the cytosolic portion of L2K was below the levels of detection. Another possibility is that regions of phot1 protein upstream of LOV2 are necessary for the movement of phot1 from the plasma membrane. It has been shown that inactivation of the kinase domain of phot2 prevents light-stimulated association of phot2 with the Golgi apparatus (Kong *et al.,* 2006) therefore it is also possible that receptor autophosphorylation may result in changes of the subcellular localisation.

Investigation of the physiological responses to light that could be mediated by L2K indicated that lack of autophosphorylation sites does not abolish protein function. Therefore, this strongly indicates that phot1 autophosphorylation is not the primary signalling event. A study using the L2K region of phot2 in *Adiantum* shows that the

153

region is sufficient to mediate the chloroplast avoidance movement (Kagawa *et al.,* 2004), and is consistent with the results presented here that indicate L2K is sufficient to mediate phot1 responses. As the light levels required for phot1 autophosphorylation are much higher than those required to induce phot-mediated responses (Briggs *et al.,* 2001), it has been postulated that phot1 autophosphorylation leads to receptor desensitisation (Salomon *et al.,* 2003; Christie, 2007). If this was the case, the inability of L2K to desensitise itself would be expected to lead to increased responsiveness to light. However, these studies suggest that the opposite is true. Higher light intensities were required to induce phototropism and leaf orientation in L2K lines compared to wild-type. It has been suggested previously that the LOV1 domain of phot1 is required to prolong the lifetime of the photoreceptor in the active state by slowing its dark recovery (Christie *et al.,* 2002; Kagawa *et al.,* 2004). A potentially faster dark recovery for L2K compared to full-length phot1 may account for the observation that higher light intensities are to needed to reach an equivalent photostationary equilibrium to bring about phototropic responsiveness (Fig. 6.3).

It has also been proposed that LOV1 mediates receptor dimerisation (Salomon *et al.,* 2004). The functional studies of L2K presented here indicate that receptor dimerisation via the LOV1 domain is not required for phot1-mediated responses s the LOV1 domain is not present in the transgenic plants. However, artificial phosphorylation of phot1 peptides by PKA results in a decrease in dimerisation mediated by the LOV1 domain (data not shown), suggesting the possibility that autophosphorylation of the regions around LOV1 could attenuate dimerisation.

A particularly interesting observation was that L2K could mediate phototropism (Fig. 6.3), yet light treatment did not result in dephosphorylation of NPH3 (Fig. 6.2B). Dephosphorylation of NPH3 has previously been reported as a signalling event essential for phot1-mediated phototropism (Pedmale & Liscum, 2007). However, these data show that L2K is sufficient to mediate phototropism without NPH3 being dephosphorylated and suggest that autophosphorylation of phot1 is necessary for the dephosphorylation of NPH3. It has been shown that NPH3 is necessary for phot1-mediated leaf positioning (Inoue *et al.,* 2007), and as L2K can mediate leaf positioning under sufficiently high intensities of light, it appears that post-translational modification of NPH3 is not required for this response.

L2K was sufficient to complement phot1-mediated leaf expansion, fresh weight gain and chloroplast accumulation. The ability of L2K to restore stomatal opening was investigated by using tolerance to drought stress as an indication of stomatal opening (Mao *et al.,* 2005). Gas exchange measurements showed there was a difference in the way the wild-type and double mutant plants responded to drought stress (Fig. 6.8), in that wild-type plants showed an increase in WUE whereas the double mutant showed a decrease in WUE. This was reflected in the RWC of wild-type and double mutant plants subjected to drought stress (Fig. 6.9). Thus, in contrast to the other phot1-mediated responses, it appears that L2K can only partially complement stomatal opening. The lack of stomatal opening might be accounted for by the likely inability of L2K to bind 14-3-3λ. A 14-3-3 protein binds to autophosphorylated Vfphot1 after light exposure and also regulates the activity of the guard cell H^+-ATPase required for stomatal opening (Kinoshita & Shimizaki, 2002). The binding site for 14-3-3s on phot1 is proposed to be situated in the linker region and autophosphorylation of phot1 is necessary for 14-3-3 binding. As the L2K lines do not contain this region, stomatal opening via the 14-3-3/H^+-ATPase pathway would be expected to be abolished. However, it appears that there is more than one way for phototropins to mediate stomatal opening, given that the L2K lines are more drought sensitive than the parental double mutant background. It is possible that this pathway involves phosphorylation of an unidentified protein. Over-expression of phot2 kinase results in constitutive stomatal opening, even in dark conditions (Kong *et al.,* 2007), consistent with the idea that phot kinases phosphorylate a protein involved in the activation of H^+-ATPases, and that activity of the kinase is negatively regulated by LOV2 (Matsuoka & Tokotumi, 2005; Shimazaki *et al.,* 2007). The partial complementation of the stomatal opening response is actually quite exciting because it appears to result in plants that can maintain wild-type growth (as determined by fresh weight), yet require less water to do so. Therefore, L2K can function to promote responses that increase photosynthetic potential and plant fitness to near wild-type levels and yet do not require the same amount of water due to their inability to open stomata to the same degree.

6.3.2 Structure/function analysis of phot1 kinase

If, as has been proposed, the kinase domains of phototropins are, in the absence of LOV2, constitutively active, it would be expected that plants over-expressing this domain would constitutively show phototropin-mediated phenotypes. To investigate this, wild-type plants transformed with phot1 kinase are currently being selected for. Initial observations of T1 and T2 lines show that plants over-expressing the active kinase domain have reduced leaf size and are greener than wild-type plants (Fig.6.10). This phenotype is similar to that seen when wild-type plants over-express phot2 kinase (Kong *et al.,* 2007). Work is underway in the laboratory to determine if homozygous lines display phenotypes that suggest phot1 kinase is constitutively activated, such as open stomata in dark conditions, as has been observed for over-expression of the kinase domain of phot2.

Homozygous lines have been obtained for phot1-GFP plants over-expressing the inactivated kinase domain of phot1 (Fig. 6.11). Expression of this domain results in movement of phot1-GFP to the cytosol in dark conditions. Dissociation of phot1 from the plasma membrane is normally seen when plants are exposed to light (Sakamoto & Briggs, 2002; Lariguet *et al.,* 2006). This suggests that inactive phot1 kinase somehow causes phot1-GFP to behave as if it has been exposed to light. It has been shown that the kinase domain of phot2 is located at the plasma membrane, regardless of its ability to function, and that inactivation of phot2 kinase reduces the re-localisation of phot2 from the membrane to the Golgi apparatus (Kong *et al.,* 2006). In contrast, our results suggest that inactive phot1 kinase promotes phot1-GFP disassociation from the membrane. The biological implications of this dissociation are not known, but analysis of phototropism in kinase dead seedlings does not appear to be significantly different from wild-type or phot1-GFP (data not shown). However, there is the suggestion of a reduction in stomatal opening of plants that over-express inactive phot1 kinase. These plants are more tolerant to drought stress than wild-type or phot1-GFP plants which suggests a dominant negative role for the inactive phot1 kinase. This concurs with the results reported by Kong *et al.* (2007) who observed that inactive phot2 kinase inhibited the stomatal opening mediated by endogenous phototropins. It is possible that the inactive kinase competes with endogenous phototropins for binding to target proteins required for activation of the H^+-ATPase.

6.3.2 Over-expression of full-length phot1

Over-expression of full-length phot1 in a wild-type background has not been reported before. Homozygous lines over-expressing full-length phot1 with an HA tag are currently being selected for in the laboratory. Preliminary investigation of T1 and T2 lines shows that an auxin-related phenotype correlates with the over-expression of phot1 protein. Specifically, transgenic plants are smaller and bushier compared to wild-type. The mid veins of leaves are often bifurcated resulting in heart-shaped leaves. These are all indicative of alterations in auxin homeostasis. There is some similarity in phenotype between phot1-over-expressing plants and PGP19-null mutants (*mdr1-1*; Noh *et al.,* 2001; Lin & Wang, 2005). This suggests that over-expression of phot1 may inactivate PGP19 resulting in a phenotype that resembles plants lacking PGP19. Given that the yeast two-hybrid screen described in Chapter 3 identified PGP19 as a phot1-interacting protein and that PGP19 mediates polar auxin transport (Lin & Wang, 2005), it is possible that constitutive over-expression of phot1 results in altered polar auxin transport which would account for the loss of apical dominance that is observed. Identification of homozygous lines will doubtless prove an invaluable tool to investigate further the consequences of phot1 over-expression. Responses that directly involve auxin transport, such as phototropism, should be investigated as *mdr1-1* seedlings exhibit increased phototropism as a result of PIN1 mislocalisation (Noh *et al.,* 2003) and show hypersensitivity to blue light-induced inhibition of hypocotyl elongation (Lin & Wang, 2005). Phot1 is also necessary for the mislocalisation of PIN1 on the shaded side of hypocotyls illuminated with unilateral blue light (Blakeslee *et al.,* 2004), therefore it is likely that constitutive over-expression of the phot1 protein would have an effect on PIN1-mediated polar auxin transport.
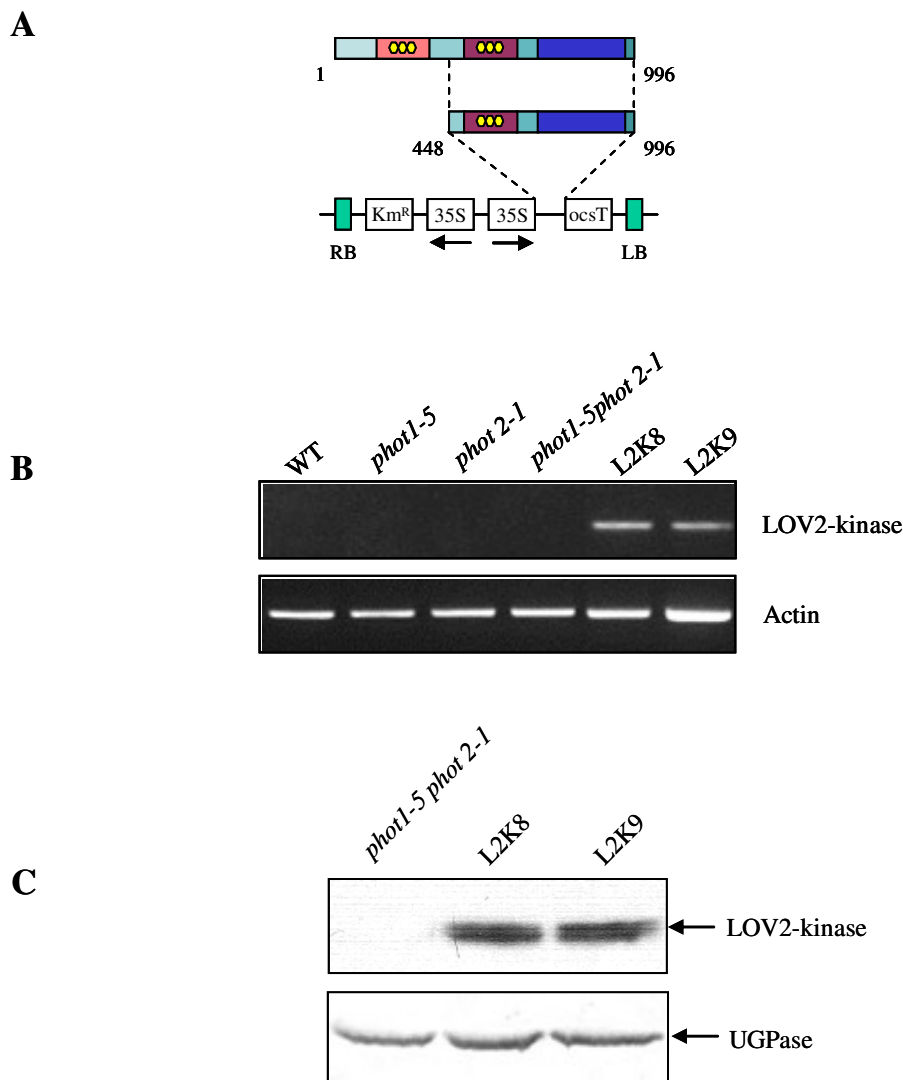
Figure 6.1 Expression of phot1 LOV2-kinase in transgenic plants

A) Schematic diagram showing the expression vector used to transform *phot1-5phot2-1* plants. The LOV domains are shown with the chromophore FMN bound to them. Amino acid positions are indicated.

B) RT-PCR analysis of L2K transcript levels in wild type (Col3), *phot1-5, phot2-1, phot1-5phot2-1*, L2K8 and L2K9 plants. PCR products generated using L2K specific primers are shown in the top panel. PCR products generated using actin primers as a loading control are shown in the bottom panel.

C) Western blot analysis of total protein extracted from *phot1-5phot2-1*, L2K8 and L2K9 plants. 10µg of total protein extracted from three week old leaf tissues was probed with an antibody raised against the C-terminal kinase region of phot1 (top panel). As a loading control, the blots were probed with the UDP-glucose pyrophosphorylase (UGPase) antibody (bottom panel). Proteins were run on a 7.5% polyacrylamide gel.

158

A

L2K8 (Dark)   L2K9 (Light)

T   S   M   T   S   M

← Kinase

← UGPase

B

L2K8 (Dark)   L2K9 (Light)   L2K8 (Dark)   L2K9 (Light)

← Kinase

← NPH3

← UGPase

Total protein   Membrane fraction
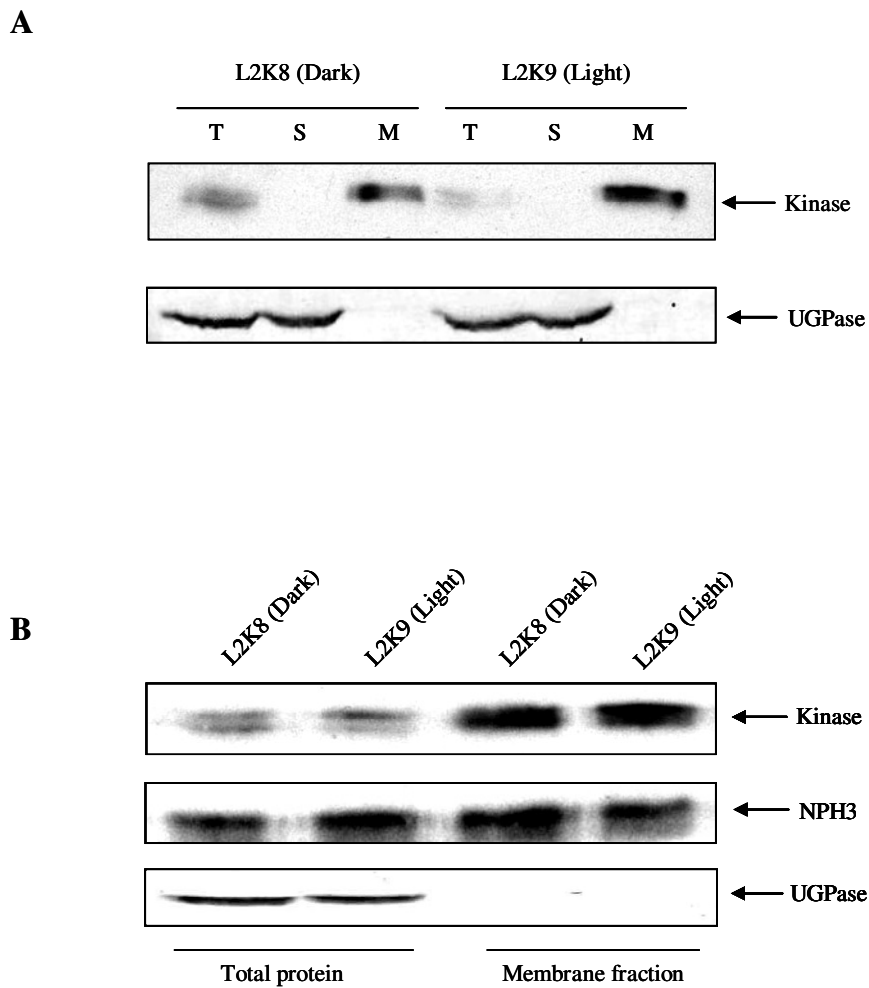
Figure 6.2 The effect of light on the subcellular localisation of phot1 L2K

A) Western blot analysis of L2K localisation in 3-day old etiolated seedlings kept in the dark (L2K8, Dark) or given 20 μmol m^{-2} s^{-1} white light treatment for 1 hour (L2K9, Light). Total protein extract (T) was fractionated into soluble (S) or membrane (M) fractions by ultra centrifugation. Equal volumes of each fraction was probed with the phot1 kinase antibody (top panel). The blot was probed with an antibody against the cytosolic UGPase protein as a control for equal loading and as a marker of membrane fraction purity. Proteins were run on a 7.5% polyacrylamide gel.

B) Western blot analysis of L2K localisation in 3-day old etiolated seedlings kept in the dark (L2K8, Dark) or given 20 μmol m^{-2} s^{-1} white light treatment for 1 hour (L2K9, light). Total protein (T) and membrane fractions (M) were probed with the phot1 kinase antibody (top panel), the NPH3 antibody (middle panel), or the UGPase antibody as a control for equal loading (bottom panel). Proteins were run on a 7.5% polyacrylamide gel.

159

A) Phototropism fluence rate response curves for wild type, *phot1-5phot2-1,* L2K8 and L2K9 two-and-a-half-day-old etiolated seedlings. Seedlings were exposed to unilateral blue light at the indicated fluence rates for 24 hours before curvature was measured. Error bars indicate standard error (n > 15).
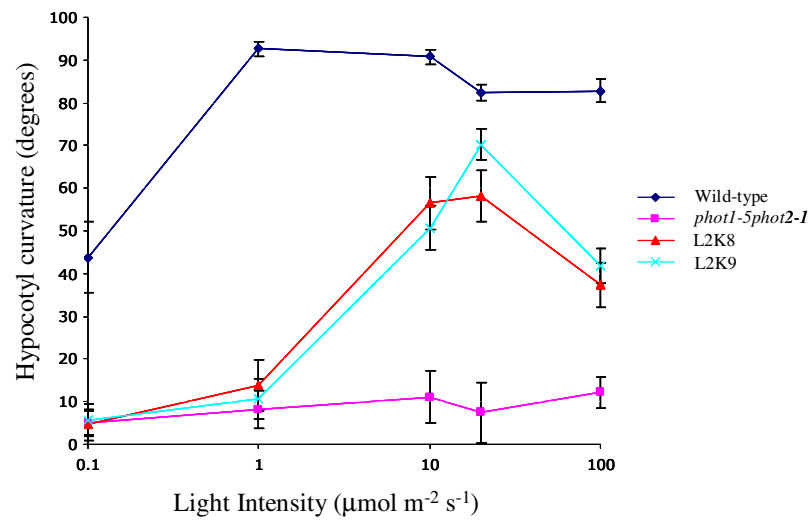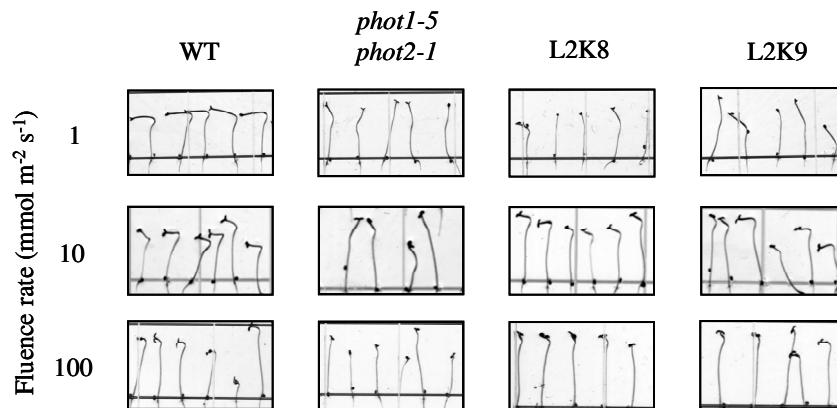
Figure 6.3 Hypocotyl phototropism in L2K seedlings

A) Phototropism fluence rate response curves for wild type, *phot1-5phot2-1,* L2K8 and L2K9 two-and-a-half-day-old etiolated seedlings. Seedlings were exposed to unilateral blue light at the indicated fluence rates for 24 hours before curvature was measured. Error bars indicate standard error (n > 15).

B) Images of representative wild type, *phot1-5phot2-1,* L2K8 and L2K9 seedlings after 24 hours exposure to unilateral blue light, as indicated on the left hand side.

A
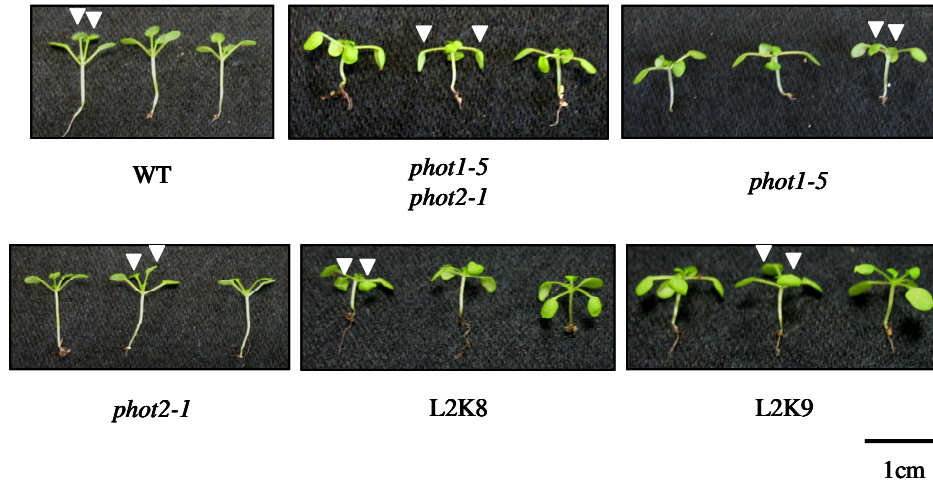
B
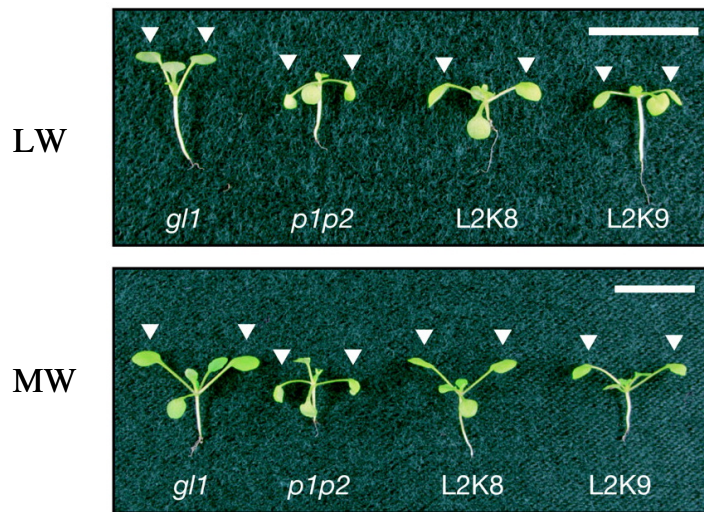
Figure 6.4 Leaf positioning of L2K seedlings under low and medium light conditions

A) Leaf positioning of wild type, *phot1-5phot2-1, phot1-5, phot2-1,* L2K8 and L2K9 seedlings grown for one week under 50 µmol m^{-2} s^{-1} 16/8 hour light-dark cycle white light then transferred to 10 µmol m^{-2} s^{-1} 16/8 hour light-dark cycle white light for a further week. White arrowheads show the first true leaves. Scale bar represents 1 cm.

B) Leaf positioning of wild-type (*gl1*), *phot1phot2* double mutant (*p1p2*) and two independent transgenic lines expressing the LOV2-kinase construct (L2K8 and L2K9) in response to 10 (LW) or 50 µmol m^{-2} s^{-1} (MW) continuous white light. White arrowheads show the first true leaves. The scale bar represents 1 cm. (Figure taken from Thomson *et al.,* 2008)

A
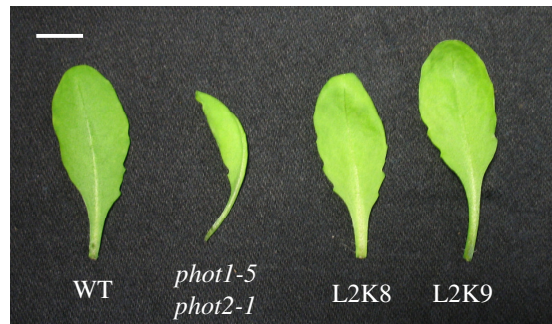
B
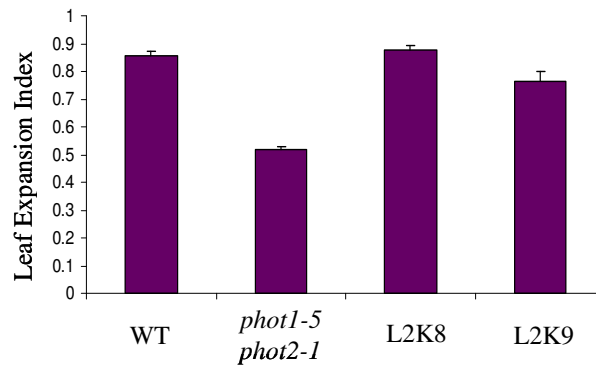
C
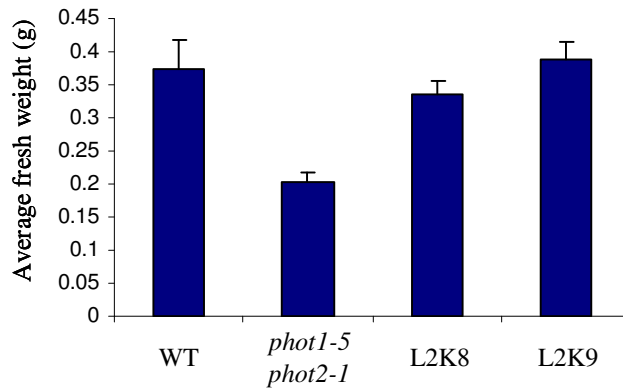
Figure 6.5 Leaf expansion and fresh weight measurements of L2K plants

A) Representative fifth rosette leaves of wild type, *phot1-5phot2-1,* L2K8 and L2K9 plants grown on soil for 3 weeks under 70 μmol m^{-2} s^{-1} 16/8 hour light-dark cycle white light. The leaf from the *phot1-5phot2-1* plants is curled and is therefore lying on its side. Scale bar represents 1 cm.

B) The leaf expansion index of the fifth rosette leaves from the plants described in (A). The leaf expansion index is expressed as the ratio of leaf area before and after artificial flattening. Error bars indicate standard error (n = 5).

C) Fresh weight of green tissue from three week-old plants grown on soil under 70 μmol m^{-2} s^{-1} 16/8 hour light-dark cycle white light. Error bars indicate standard error (n = 19).

162

A

phot1-5
phot2-1

L2K8

B
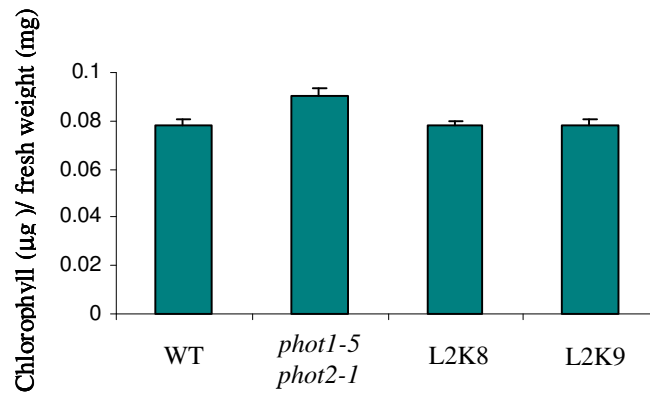
Figure 6.6 Chlorophyll content of L2K plants

A) *Phot1-5phot2-1* and L2K8 seedlings grown on soil for 2 weeks under 70 μmol m^{-2} s^{-1} 16/8 hour light-dark cycle white light.

B) Measurement of chlorophyll a and b expressed as mg chlorophyll per mg fresh weight. Plants were grown as described in (A). Error bars indicate standard error (n = 3).
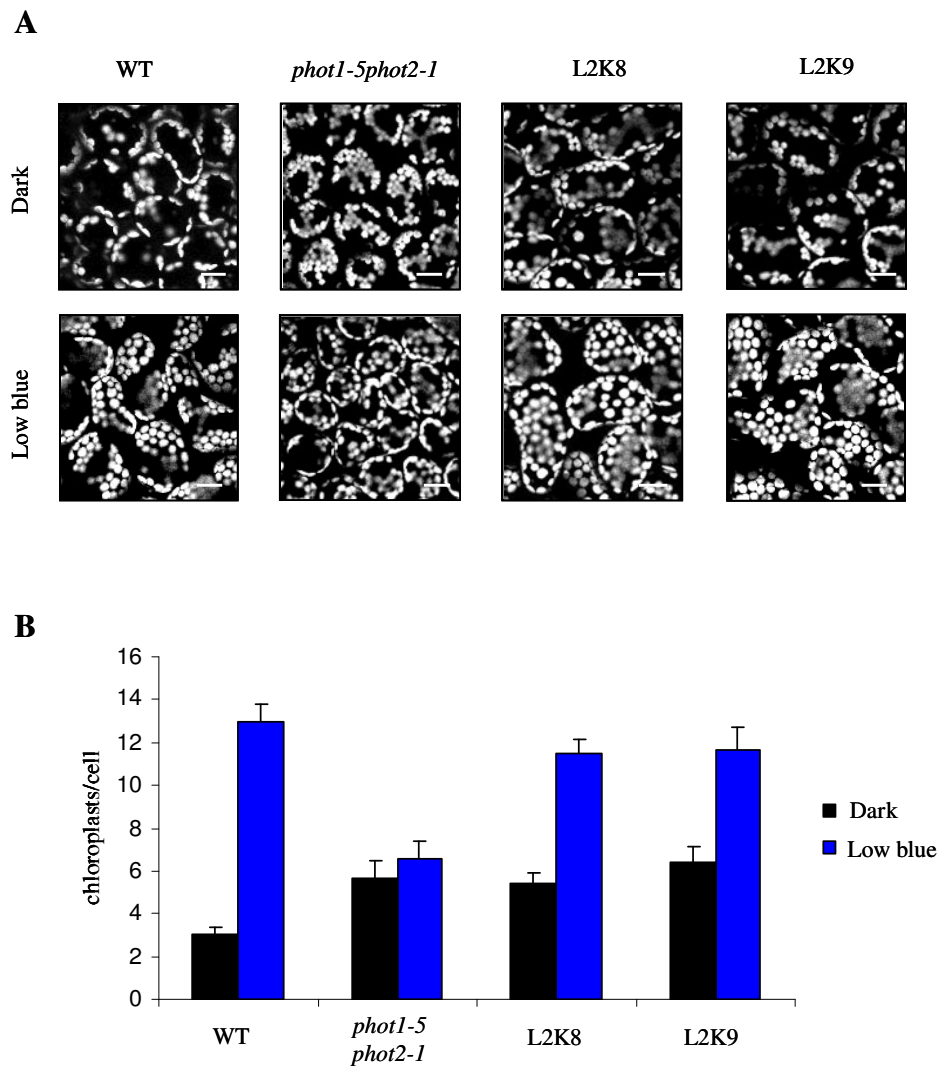
Figure 6.7 Chloroplast movement in L2K plants

A) Chloroplast positioning of wild type, *phot1-5phot2-1*,L2K8 and L2K9 plants were grown on soil for 3 weeks under 70 μmol m^{-2} s^{-1} 16/8 hour light-dark cycle white light. Rosette leaves were detached and treated with blue light (1.5 μmol m^{-2} s^{-1}) for 3 hours (Low blue; blue) or kept in the dark for 3 hours (Dark; black) before observation of chloroplast autofluorescence by confocal microscopy. Scale bar represents 20 μm.

B) Quantification of the number of chloroplasts at the upper face of palisade mesophyll cells of the plants described in (A). Error bars indicate standard error of the mean of 16 cells per line.
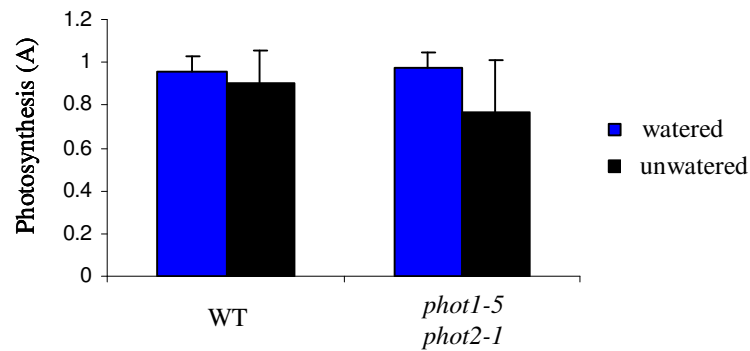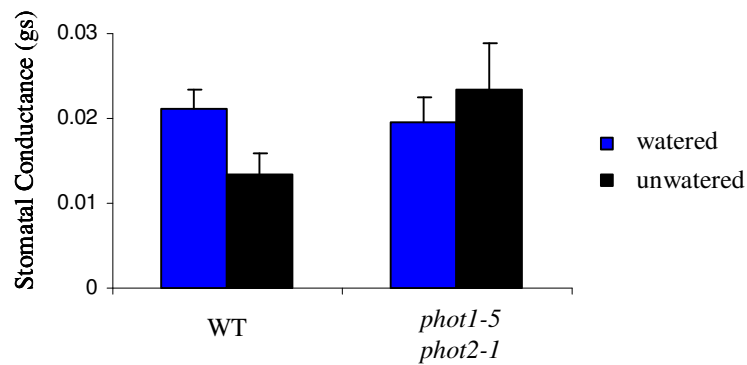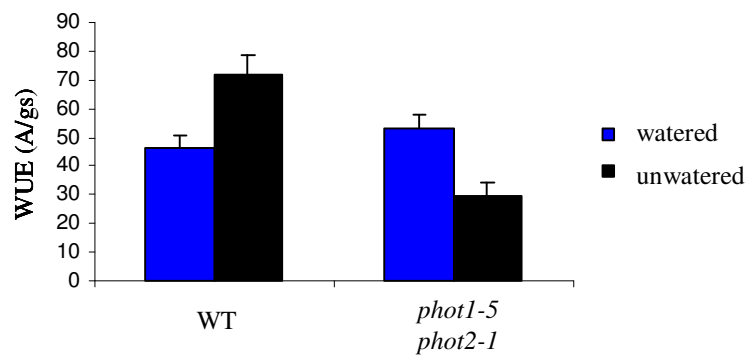
Figure 6.8 Steady state rate of photosynthesis, stomatal conductance and water use efficiency in wild-type and *phot1-5phot2-1* plants subjected to drought stress.

A) The rate of photosynthesis (A; μmol m^{-2} s^{-1}) of wild type (Col3) and *phot1-5phot2-1* plants grown on soil for 8 weeks under 70 μmol m^{-2} s^{-1} 9/15 hour light-dark cycle white light. Well watered plants are indicated in blue. Plants subjected to 8 days of drought stress are indicated in black.

B) The stomatal conductance (gs; mmol m^{-2} s^{-1}) of wild type and double mutant plants grown as described in (A).

C) Water use efficiency (WUE; A/gs) of wild type and *phot1-5phot2-1* plants grown as described in (A). Error bars indicate standard error (n = 5)

A
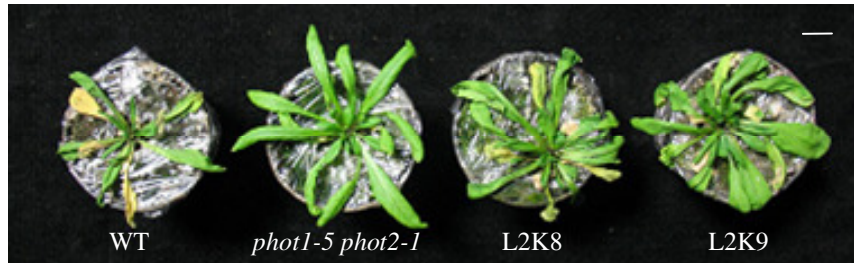
B
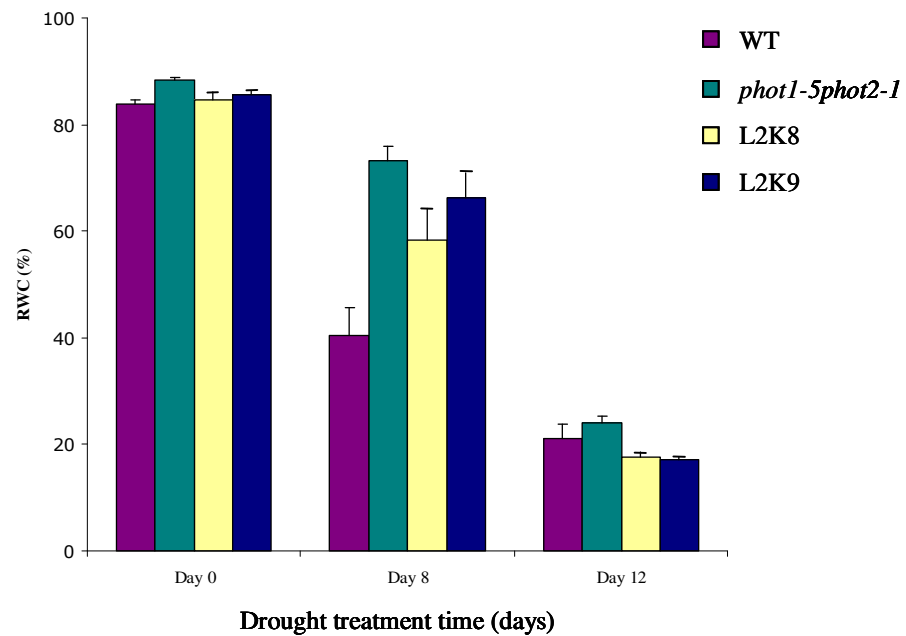
Figure 6.9 Increased tolerance to drought stress shown by L2K plants

A) Representative wild type, *phot1-5phot2-1*, L2K8 and L2K9 plants 8 days after cessation of irrigation. Plants were grown with normal watering for 24 days and then drought stressed by complete termination of irrigation. Scale bar represents 1 cm.

B) Changes in relative water content (RWC) of wild type, *phot1-5phot2-1*, L2K8 and L2K9 plants during drought stress. Plants were grown as described in (A). Error bars indicate standard error (n = 8).

166

A
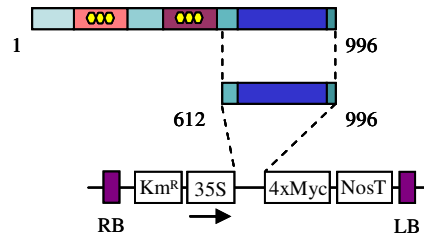
B

WT   Kinase over-
expressor

Figure 6.10 Overexpression of the phot1 kinase domain causes a dwarf phenotype

A) Schematic diagram showing the expression vector used to transform wild-type (Col3) plants. Amino acid positions of the region of phot1 encoded in the construct are indicated.

B) Wild type (*gl1*) and a representative T2 kinase over-expressing plants grown on soil for 3 weeks under 70 μmol m^{-2} s^{-1} 16/8 hour light-dark cycle white light. Scale bar represents 1 cm.
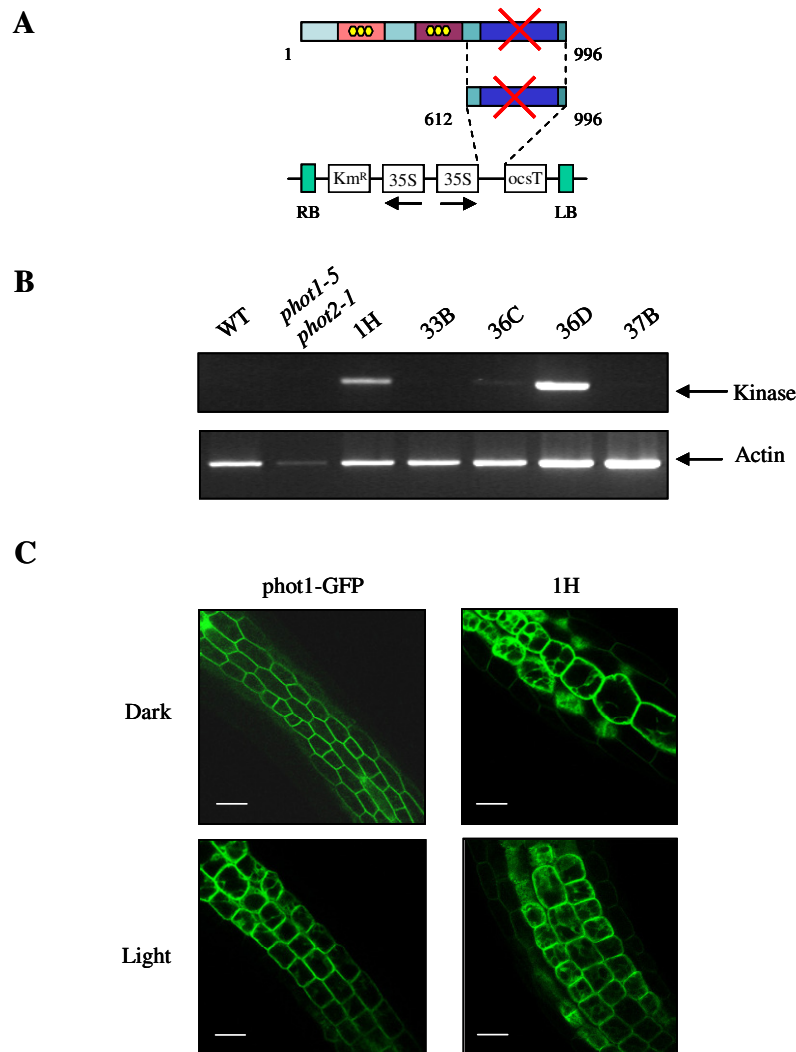
Figure 6.11 Overexpression of inactive phot1 kinase in the phot1-GFP background

A) Schematic diagram showing the expression vector used to transform phot1-GFP plants. Amino acid positions of the region of phot1 encoded in the construct are indicated. The red cross represents the amino acid substitution Asp806Asn used to render the kinase domain inactive (Christie *et al.,* 2002).

B) RT-PCR analysis of inactive kinase transcript levels in wild type (Col3), *phot1-5phot2-1*, and kinase dead transgenic lines (1H, 33B, 36C, 36D, and 37B). PCR products generated using inactive kinase specific primers are shown in the top panel. PCR products generated using actin primers as a loading control are shown in the bottom panel.

C) Phot1-GFP localisation in phot1-GFP and inactive kinase overexpressing line 1H. 3-day-old etiolated seedlings were kept in the dark (Dark) or exposed to 20 μmol m^{-2} s^{-1} white light for 3 hours (Light). Confocal images show GFP fluorescence in hypocotyl cells. Scale bar represents 50 μm.

Figure 6.12 Overexpression of phot1 inactive kinase increases tolerance to drought stress

Five phot1-GFP and inactive kinase (36D) plants were grown per pot for three weeks under 70 μmol m^{-2} s^{-1} continuous white light. After four weeks of normal watering (upper panels), water was withheld for 10 days (lower panels). Scale bar represents 1 cm.

A
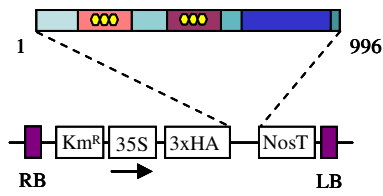
B
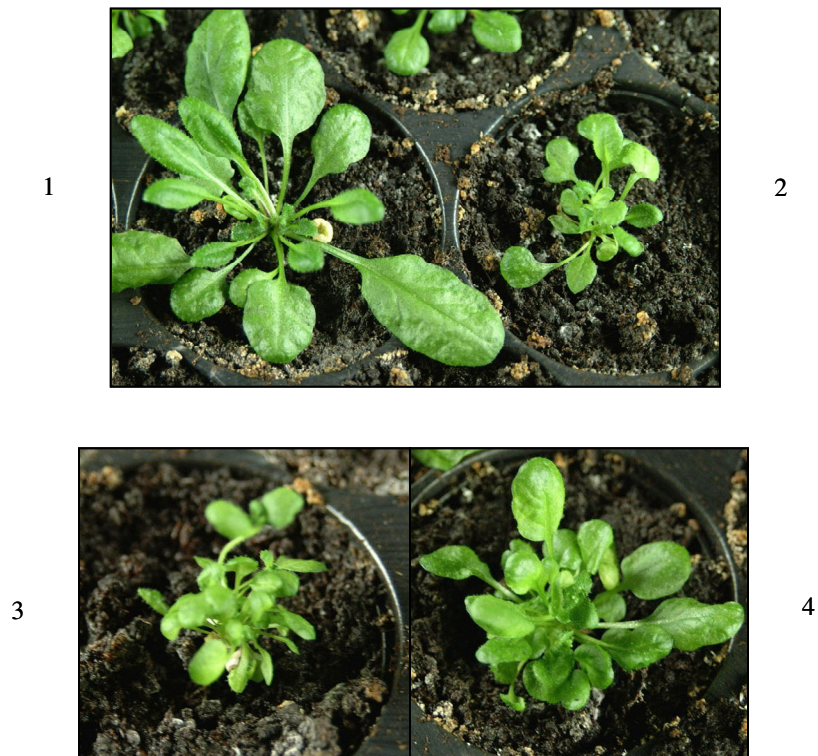
Figure 6.13 Over-expression of phot1 in wild-type background

A) Schematic diagram showing the expression vector used to transform Col0 plants. Amino acid positions of the region of phot1 encoded in the construct are indicated.

B) Images of T1 transgenic plants transformed with full-length phot1. Plant 1 did not express transgenic phot1 protein as detected by western blot. Plants 2, 3 and 4 expressed transgenic phot1.

Chapter 7: Final Discussion

7.1 Introduction

Phototropins are blue light receptor kinases that have been shown to mediate a variety of physiological responses in plants. Much is known about the modes of receptor activation and the responses elicited by them; however, there is a significant lack of knowledge in the field about the signalling mechanisms employed by phototropins to mediate these responses. Therefore, the aims of this thesis were to identify novel phot1-interacting partners by yeast two-hybrid screening and to carry out structure/function studies to investigate the methods of phot1 signalling. In this final chapter, the results of the preceding chapters are summarised and prospects for future research discussed.

7.2 Identification of novel phot1-interacting proteins by yeast two-hybrid screening

When this project was initiated only NPH3 and RPT2 had been identified as phot1-interacting proteins. Given the wide variety of physiological responses mediated by phototropins it was thought likely that many more interacting proteins remained to be identified. To identify novel phot1-interacting proteins, a yeast two-hybrid screen was carried out. Yeast two-hybrid screens have previously been used successfully to identify proteins that interact with other plant photoreceptors. For example, PIF3 was isolated from a yeast two-hybrid screen to identify proteins that interact with phytochrome B and was subsequently found to interact with phytochrome A (Ni *et al.,* 1998, Ni *et al.,* 1999). PKS1 was also identified using a yeast two-hybrid screen for proteins that interact with phytochrome A (Fankhauser *et al.,* 1999), and has subsequently been shown to interact with phot1 (Lariguet *et al.,* 2006).

7.2.1 The yeast two-hybrid screen

Chapter 3 described how full-length phot1 and the N_2LOV2 region of phot1 were used as baits to screen a cDNA library derived from dark-grown *Arabidopsis* seedlings. A total of 1.02×10^6 yeast colonies were screened resulting in 130 colonies containing putative phot1-interacting proteins. The cDNA sequences obtained from these colonies

are listed in Appendix 1. Six proteins were chosen for further investigation and these are detailed in Chapter 3.

The identification of ARF2 and ARF7 as blue-light sensitive phot1-interacting proteins and as phot2-interacting proteins (Sections 3.5 and 3.9) is potentially exciting as ARFs are involved in the regulation of membrane traffic by undergoing a GDP/GTP nucleotide exchange cycle that involves conformational changes in two highly conserved regions of the ARF protein, which can result in subsequent conformational changes in the protein that ARF is bound to (Gebbie *et al.,* 2005; Neilsen *et al.,* 2006). While the GDP/GTP cycle is common with other GTPases, ARF proteins are unique in having an N-terminal myristolated α-helix involved in GTP-dependent interaction with membranes. Currently, the mechanism by which phototropins are associated with the plasma membrane is unknown, the blue light-induced delocalisation of phot1 from the plasma membrane (Sakamoto & Briggs, 2002) is also not understood and there is little data about the movement of phot2 to the Golgi in response to blue light (Kong *et al.,* 2006; 2007). It is possible that an ARF is involved in anchoring phot1 at the membrane resulting in its delocalisation as the interaction between phot1 and ARFs is lost upon blue light exposure, or involved in the transport of phot2 to the Golgi. Recent preliminary results in the laboratory add weight to the notion that there is a physiological consequence for the interaction between phot1 and the ARFs. A member of the Class 1 ARF family has been cautiously identified by mass spectrometry as a phot1-GFP-interacting protein after purifiation from dark-grown microsomal membrane preparations, consistent with the idea that ARFs and phot1 interact in the dark (S. Sullivan & J.M. Christie, unpublished data).

In addition to the proteins described in Chapter 3, a number of other potentially interesting interacting proteins were identified from the yeast two-hybrid screen but these were not pursued because the amino acid sequences were out of frame or the proteins auto-activated the yeast two-hybrid system. However, yeast can allow translational frameshifts resulting in expression of a protein from a large open reading frame in the wrong reading frame; and auto-activation of the system can result not only from transcriptional activation domains within the prey protein, but also because of acidic amphipathic domains within the protein (Matchmaker GAL4 Two-Hybrid System 3 User Manual, Clontech, 1999; Ruden, 1991; Ruden, 1992). Therefore, the

possibility of a prey protein that autoactivates the system being a true phot1-interacting protein cannot be ruled out.

Proteins excluded from further analysis because of the reasons mentioned above include a number of proteins involved in cell wall synthesis and maintenance, including Expansin 8A (EXP8A; At2g40610; auto-activated the yeast two-hybrid system). *EXP8A* was identified as a gene that is up-regulated on the shaded side of tropically stimulated *Brassica* hypocotyls and is necessary for the cell wall extension required for curvature (Esmon *et al.,* 2006). Auxin-induced up-regulation of *EXP8A* is genetically dependent on activation of the auxin-regulated transcription factor NPH4 (Esmon *et al.,* 2006). The authors propose that as the activity of EXP8A is stimulated by low pH and as auxin is known to rapidly stimulate activation of a plasma membrane H^+-ATPase which results in acidification of the apoplastic space, an increase in auxin concentration could both stimulate expression and regulate activity of EXP8A (Esmon *et al.,* 2006). Isolation of EXP8A from the yeast two-hybrid screen suggests that not only are phototropins necessary for the perception of light which results in an auxin gradient across the hypocotyl, phot1 at least may interact at a protein level with the products of auxin-induced gene regulation. However, it is considered that expansins are located within the cell wall (Sampedro & Cosgrove, 2005) so it is difficult to understand how a direct interaction between the proteins would occur.

Another protein of interest identified from the screen that was not pursued was Nitrilase 1 (NIT1; At3g44310; auto-activated the system). NIT1 hydrolyses indole-3-acteonitrile (IAN) to indole-3-acetic acid (IAA; Normanly *et al.,* 1997). A subsequent study has shown that levels of endogenous IAN increase in phototropically-stimulated wild-type seedlings, but not in *nph3-101* seedlings which led the authors to suggest that IAN is an inhibiting substance responsible for phototropism (Hasegawa *et al.,* 2004). The authors propose that IAN plays a role in phototropism of *Arabidopsis* seedlings by inhibiting growth on the illuminated side of the hypocotyl, but note that the relative concentrations of IAN on the irradiated and shaded sides of the hypocotyl could not be determined because of the small size of the organ being studied. However, it has been reported that IAN is found at a higher concentration on the illuminated side of cabbage hypocotyls when compared to the shaded side (Kosemura *et al.,* 1997). In the study by Hasegawa *et al.* (2004) IAN applied exogenously to *nph3-101* seedlings inhibited their growth prompting the authors to propose that the

173

failure of *nph3*-101 seedlings to bend towards light is because NPH3 is involved in IAN biosynthesis, and that IAN is a negative growth regulator. Yet, there is no difference in the phototropic response of *nit1* mutant seedlings when compared to wild-type (Hasegawa *et al.,* 2004). However, this is not unexpected as although NIT1 is the predominant member, it belongs to a small, functionally redundant family where more than one member can cause hydrolysis of IAN to IAA (Normanly *et al.,* 1997). In addition, non-functional NIT1 would be expected to lead to an increase in IAN, the proposed growth inhibitor, which should alter phototropism at some level and it seems unlikely that a precursor of IAA would have such an opposite effect on plant growth to its successor. Therefore, the possibility remains that phot1 negatively regulates the activity of NIT1 in an NPH3-dependent manner when the hypocotyl is light treated, resulting in a relative build up of IAN on the irradiated side of the hypocotyl. This would explain the fact that no difference is seen in IAN levels of light-treated *nph3-101* seedlings when compared to dark-grown seedlings despite exogenously-applied IAN having a biological effect on *nph3-101* growth. If this were the case then it would add another layer of complexity to phot1 signalling, where phot1 actively regulates levels of biologically active auxins in the hypocotyl.

It may prove worthwhile to try to determine the true interacting potential of proteins identified in the yeast two-hybrid screen by some other means. Potentially interesting putative phot1-interacting proteins such as EXP8A and NIT1 could be sub-cloned into a different expression vector and subjected to pull-down analysis with regions of phot1 to determine if the interaction is real before pursuing them further, analogous to the approaches employed with the phot1-interacting proteins further analysed throughout this study.

7.2.2 Members of the NRL family as phot1-interacting proteins

RPT2 and a novel member of the NRL family, NPH3-L, were identified from the yeast two-hybrid screen as phot1-interacting proteins (Section 3.6). Isolation of RPT2 from the screen was a good indication that the screen was effective, as this is a known phot1-interacting protein (Inada *et al.,* 2004). The isolation of NPH3-L from the screen prompted further investigation into the role of the protein *in planta* (Chapter 4). Disappointingly, NPH3-L knockout plants failed to show any disruption in the phot1-signalling responses investigated. However, because NPH3-L is a member of a large

family, there may be functional redundancy between members of the family, and in addition there was insufficient time to investigate all phot1-mediated responses in the knockout lines, leaving the possibility that a biological function for NPH3-L has been overlooked. Our studies show that the interaction is specific to phot1 as NPH3-L does not interact with phot2 (Section 3.9). Therefore, further investigation of phot1-specific responses in the NPH3-L knockout line such as the inhibition of hypocotyl elongation would be prudent.

Searching a database of phosphorylation site mapping experiments in *Arabidopsis* (http://www.plantenergy.uwa.edu.au/applications/phosphat/index/html) shows that NPH3-L becomes phosphorylated when cell cultures are treated with flg22 (a conserved domain of the bacterial elicitor, flagellin, which promotes plant defence mechanisms) or xylanase. Two sites within NPH3-L have been identified as phosphorylated peptides: amino acids 273 – 290; and amino acids 527 – 553, where Ser^{533} has been mapped as the phosphorylated residue (Benschop *et al.,* 2007). The first peptide region (amino acids 273 – 290) lies within the region of NPH3-L identified from the yeast two-hybrid screen (amino acids (243 – 433), while the second peptide region lies C-terminal of the region identified from the screen. The region of NPH3-L identified from the yeast two-hybrid screen has been shown experimentally as a domain that can be phosphorylated (Benschop *et al.,* 2007) and we have shown in this study that this region of NPH3-L interacts with the kinase domain of phot1 (Section 4.2.1). Our structure/function studies have shown that autophosphorylation of phot1 is not necessary for phot1-signalling to mediate responses to blue light which suggests that activation of the kinase domain by light perception in the N-terminal photosensory region of the protein results in phosphorylation of an as yet unidentified substrate (Chapter 6). Therefore, it is possible that NPH3-L is a phosphorylation substrate for phot1. Co-immunoprecipitation studies have shown that NPH3-L interacts with phot1-GFP *in vivo.* However, co-immunoprecipitated NPH3-L showed no change in electrophoretic mobility in the samples when etiolated seedlings were treated with light (Section 4.2.4). It is possible that phosphorylation on only one or two residues of NPH3-L by phot1 kinase activity would not result in an increase in molecular mass large enough to be visualised on the SDS-PAGE gels that were used for this experiment.

The hypothesis that NPH3-L is a substrate for phot1 could be tested experimentally using some of the tools described in this project. The yeast two-hybrid system could be used to determine if the kinase domain must be functional for the interaction to occur as it is possible that the phosphorylation status of NPH3-L is not altered in response to light, but is constant after an initial phosphorylation event that promotes the interaction with the kinase domain of phot1. Transformation of yeast with NPH3-L and the inactive kinase domain of phot1 (containing the mutation Asp806Asn) would determine if kinase activity is necessary for the interaction.

The insect cell system could be used to investigate phot1 phosphorylation of NPH3-L in the same way that 14-3-3 phosphorylation was investigated (Section 5.2.5). We can already express active phot1 in insect cells and creation of a GST-NPH3-L protein expression vector would allow NPH3-L to be purified via the GST tag (as for GST-14-3-3λ). A phosphorylation assay would reveal if bacterially-expressed full-length NPH3-L could be phosphorylated by insect cell-expressed full-length phot1 *in vitro,* using kinase-inactive phot1 as a negative control.

In addition, the GFP-tagged NPH3-L over-expressing lines currently being generated in the laboratory could be used to immunoprecipitate NPH3-L from dark- and light-treated seedlings. Higher levels of NPH3-L protein could be obtained and purification of the protein via the GFP tag would allow better resolution of the protein by SDS-PAGE. This would also provide a means for purification of NPH3-L to map phosphorylation sites by phosphopeptide mapping using mass spectrometry as has been done in the laboratory for phot1-GFP derived from *Arabidopsis* (Thomson *et al.,* 2007), to determine if there is a difference between light and dark-treated seedlings. Further investigation of the NPH3-L protein *in planta* should also be carried out using the knockout line described in Chapter 4 and the over-expressing line that is currently being generated to try to identify a functional role for NPH3-L.

7.2.3 14-3-3λ as a phot1-interacting protein

Full-length 14-3-3λ was identified from the yeast two-hybrid screen as a phot1-interacting protein (Section 3.7). Previously, in broad bean, *Arabidopsis* 14-3-3ϕ has been shown to bind to phosphorylated Vfphot1 and also to a phosphorylated H^+-ATPase (Kinoshita & Shimazaki, 2002; Kinoshita *et al.,* 2003). 14-3-3 binding to phototropin precedes 14-3-3 binding to the H^+-ATPase and the subsequent opening of

stomata (Kinoshita *et al.,* 2003). The site of 14-3-3 binding was identified as Ser^{358} for Vfphot1a and Ser^{344} for Vfphot1b, both within the linker regions between the LOV domains (Kinoshita *et al.,* 2003). Yeast two-hybrid analysis showed that the LOV linker region of *Arabidopsis* phot1 was required for 14-3-3λ binding (Sections 5.2.1 and 5.2.2). Structure/function studies using a truncated version of phot1 which lacks the majority of the LOV linker region (LOV2-kinase (L2K); Section 6.2.1 - 6.2.8) showed that this region of phot1 was sufficient to complement most phot1-mediated responses. However, stomatal opening appeared to be only partially complemented in the transgenic lines suggesting the possibility that the phot1 interaction with 14-3-3λ is involved in the stomatal opening response. Far western analysis confirmed that L2K expressed in insect cells does not bind 14-3-3λ (data not shown). The hypothesis that 14-3-3λ binding to phot1 is necessary for full stomatal movement could be investigated by measuring the stomatal opening responses of the 14-3-3λ knockout lines identified in Section 5.2.8 and comparing these to wild-type responses. However, the results shown in Sections 5.2.6 and 5.2.7 imply that there is likely to be functional redundancy between 14-3-3λ and 14-3-3κ which may prove problematic. Creation of a double mutant for 14-3-3λ and 14-3-3κ may prove a useful tool in determining the function of these proteins with regard to phototropin signalling.

Further knowledge on the importance of the phot1/14-3-3λ interaction is likely to be gained from studies using the GFP-14-3-3λ over-expressing lines. Far western analysis has shown that the interaction between GST-14-3-3λ and phot1-GFP from seedlings was light dependent (Section 5.2.4). Confocal microscopy showed punctate staining at the membrane in GFP-14-3-3λ seedlings that had been exposed to light, but only in the parental background where phototropins were present (Section 5.2.10). The movement of GFP-14-3-3λ in response to light in the wild-type (*gl1*) background but not in the double mutant background suggests that there is a biological role for the interaction *in planta* in response to light stimulus and that it is likely to be dependent on phot1 as studies in yeast showed no interaction between 14-3-3λ and phot2. Isolation of homozygous GFP-14-3-3λ over-expressing lines in both backgrounds will prove a useful tool for further studies comparing 14-3-3λ localisation in plants in which native phototropins are either present or absent. Phototropic stimulation of etiolated homozygous seedlings would allow 14-3-3λ localisation to be monitored

across a gradient of active phototropins and an opposing auxin gradient, as well as in phototropic-responsive tissues (near the apical hook) and non-phototropic-responsive tissues (at the base of the hypocotyl) to determine the effects on 14-3-3λ localisation caused by active phot1. However, some caution would have to be exercised as GFP-14-3-3λ expression is driven by the *35S* promoter. Further experiments should also involve mapping the 14-3-3λ binding site in *Arabidopsis* phot1. Our phosphopeptide mapping experiments have identified three sites located in the LOV linker region that are autophosphorylated in response to light (Thomson *et al.,* 2007). Site directed mutagenesis of these sites and expression of the resulting phot1 mutant proteins in insects cells would allow determination of which site is involved in 14-3-3λ binding by far-western analysis.

7.3 Structure/function studies of phot1

7.3.1 L2K over-expression

Chapter 6 described the structure/function studies carried out to try to identify the functions of different domains in phot1 signalling. Particular attention was paid to the role of phot1 autophosphorylation in mediating phot1-induced responses. Our studies show that for the majority of responses investigated (phototropism, leaf positioning and expansion, promotion of growth as measured by fresh weight and chloroplast movement), the LOV2-kinase (L2K; amino acids 448-996) region of phot1 is sufficient to complement the double mutant. This study shows that increased light intensities are required to induce some of these responses (phototropism and leaf positioning) in L2K transgenic plants compared to wild-type. It is noticeable that the responses that require higher light intensities also require functional NPH3 (Motchoulski & Liscum, 1999; Inuoe *et al*., 2007) and are a consequence of differential growth in response to auxin. Our studies indicate that L2K is not sufficient to cause the phot1-mediated dephosphorylation of NPH3 that is observed in dark-grown wild-type seedlings upon exposure to light (Pedmale & Liscum, 2007). It has been shown that the N-terminal of phot1 (amino acids 7-622) interacts with the coiled-coil domain of NPH3 (Motchoulski & Liscum, 1999), therefore it is possible that a region of phot1 upstream of amino acid 448 is involved promoting the dephosphorylation of NPH3, while the region between amino acids 448 and 622 is

involved in signalling via NPH3 to mediate responses. As discussed in Section 6.3.1, the LOV1 domain may be responsible for prolonging receptor activation which could also explain why L2K plants needed higher intensities of light for some responses. Therefore, it appears that neither the LOV1 domain of phot1 nor autophosphorylation of phot1 is necessary for phot1-mediated responses to blue light. This strongly suggests that the kinase domain of phot1 phosphorylates unidentified substrates and the search for *bona fide* phot1 phosphorylation substrates must now be undertaken. The search could be initiated by yeast two-hybrid screening using the phot1 kinase domain as bait, however kinase/substrate interactions can be transient which may result in substrates being overlooked (Maly *et al*., 2004).

7.3.2 Kinase and phot1 over-expression

Wild-type plants over-expressing the active phot1 kinase domain (Section 6.2.9) result in small, dark-green plants similar to those observed when phot2 kinase is over-expressed, suggesting that functional phot1 kinase may also be constitutively active (Kong *et al.,* 2007). In contrast, plants over-expressing the inactive kinase domain look like wild-type plants (Section 6.2.10). How expression of functional kinase results in this phenotype is not understood, although it is likely to be a result of constitutive activation of the kinase domain in the absence of the proposed repressor, LOV2 (Matsuoka & Tokotumi, 2005) Isolation of homozygous c-Myc-tagged kinase over-expressing plants will provide a useful tool for further investigations. Co-immunoprecipitation of proteins that interact with the kinase domain *in vivo* may provide a means to identify possible phosphorylation substrates for the kinase domain, and could provide further confirmation of the phot1/NPH3-L and phot1/PGP19 interactions *in planta*, this time specifically with the kinase domain.

Given that the kinase domain of phot1 interacts with the C-terminal of PGP19 in yeast and in *in vitro* pull-down assays (Section 3.8), and that *mdr1-1* plants display increased phototropic responses, it will be interesting to investigate the effects of kinase over-expression on phototropism in homozygous lines and to compare these results with phototropism data from L2K and inactive kinase lines to determine the actual effect of the active kinase domain. It would also be prudent to investigate the possibility that PGP19 is a substrate for kinase activity using the insect cell and bacterial expression systems in the manner suggested for NPH3-L.

179

Over-expression of full-length phot1 strongly suggests that phot1 has a direct effect on auxin homeostasis within the plant, given the auxin-related phenotypes seen in T2 transgenic lines (Section 6.2.11). As discussed in Section 6.3.2, identification of phot1 over-expressing homozygous lines is currently underway. This will provide a tool to investigate the effects of over-expressing phot1 in a background of native phototropins. From the phenotypes observed so far, it seems likely that transgenic phot1 will have a dominant effect on native phototropins, particularly in responses involving auxin transport. A study investigating the effects of broad spectrum kinase inhibitors have shown that treatment of tobacco cell suspension cultures with staurosporine and K252a results in an inhibition of auxin efflux, suggesting a role for tyrosine- and serine/threonine-kinases in auxin regulation (Delbarre *et al.,* 1998). In addition the serine/threonine kinase, PINOID (PID) has been shown to positively regulate auxin transport (Benjamins *et al.,* 2001) and plays a role in the localisation of PIN proteins (Friml *et al.,* 2004). Like phototropins, PID is a member of the plant-specific ACG group VIII family of serine/threonine kinases (Benjamins *et al.,* 2001) and undergoes autophosphorylation (Zegzouti *et al.,* 2006) Therefore, it is possible that phosphorylation of a substrate involved in auxin transport by phot1 could also have a regulatory effect.

7.4 Conclusions

The aims of this project were to identify novel phot1-interacting proteins by yeast two-hybrid screening and to investigate the modes of phot1 signalling by structure/function analysis. The interaction between phot1 and a novel member of the NRL family identified from the yeast two-hybrid screen has been confirmed *in vivo* and work is underway to try to identify a role for NPH3-L in phot1 signalling. A second phot1-interacting protein identified from the yeast two-hybrid screen, 14-3-3λ, has been subject to extensive biochemical analysis to determine that its interaction with the LOV linker region of phot1 is dependent on light. Although a physiological role for this protein remains to be determined *in planta*, over-expressing, GFP-tagged lines and knockout lines have been obtained in this study to facilitate further investigation of the protein. Preliminary data suggest that the light-dependent movement of GFP-14-3-3λ at the plasma membrane depends on the presence of endogenous phototropins, suggesting a physiologically important role for the interaction. Structure/function

studies indicate that autophosphorylation of phot1 is not essential for signalling to mediate blue light responses, but suggests instead that the kinase domain of phot1 phosphorylates as yet unidentified substrates. They also show that the LOV1 domain of phot1 and autophosphorylation of the protein are both dispensable for signalling. The suite of transgenic plants created during the course of this study and described in Chapter 6 will provide a useful tool for further investigation of the responses mediated by specific region of the phot1 protein. Therefore, the aims set out at the beginning of the study have largely been achieved.

References

Ahmad, M & Cashmore, A. R. (1993) *HY4* gene of *A. thaliana* encodes a protein with characteristics of a blue-light photoreceptor. *Nature.* **366**: 162-166

Ahmad, M., Jarillo, J. A. & Cashmore, A. R. (1998a) Chimeric proteins between cry1 and cry2 Arabidopsis blue light receptors indicate overlapping functions and varying protein stability. *Plant Cell.* **10**: 197-207

Ahmad, M., Jarillo, J. A., Smirnova, O. & Cashmore, A. R. (1998b) Cryptochrome blue-light photoreceptors of *Arabidopsis* implicated in phototropism. *Nature.* **392**: 720-723

Ahmad, M., Jarillo, J. A., Smirnova, O. & Cashmore, A. R. (1998c) The CRY1 blue light photoreceptor of Arabidopsis interacts with Phytochrome A *in vivo. Molecular Cell.* **1**: 939-948

Altschul, S. F., Gish, W., Miller, W., Myers, E. W. & Lipman, D. J. (1990) Basic local alignment search tool. *J. Mol. Biol.* **215**: 403-410

Ambudkar, S. V., Kimichi-Sarfaty, C., Sauna, Z. E. & Gottesman, M. M. 2003. P-glycoprotein: from genomics to mechanism. *Oncogene.* **22**: 7468-7485

Ascenzi, R. & Gantt, J. S. (1999) Molecular genetic analysis of the drought-inducible linker histone variant in *Arabidopsis thaliana. Plant Mol. Biol.* **41**: 159-169

Banerjee, R., Schleicher, E., Meier, S., Viana, R. M., Pokorny, R., Ahmad, M., Bittl, R. & Batschauer, A. (2007) The signaling state of *Arabidopsis* cryptochrome 2 contains flavin semiquinone. *J. Biol. Chem.* **282**: 14916-14922

Batschauer, A., Banjeree, R. & Pokorny, R. (2007) In: Light and Plant Development. (Eds. Whitelam, G. C. & Halliday, K. J.) Blackwell Publishing Ltd., Oxford, U.K.

Baum, G., Long, J. C., Jenkins, G. I. & Trewavas, A. J. (1999) Stimulation of the blue light photoreceptor NPH1 causes a transient increase in cytosolic Ca^{2+}. *Proc. Natl. Acad. Sci. USA.* **96**: 13554-13559

Benjamins, R., Quint, A., Weijers, D., Hooykaas, P. & Offringa, R. (2001) The PINOID protein kinase regulates organ development in *Arabidopsis* by regulating polar auxin transport. *Development.* **128**: 4057-4067

Bennett, M. J., Marchant, A., Green, H. G., May, S. T., Ward, S. P., Millner, P. A., Walker, A. R., Schultz, B. & Feldmann, K. A. (1996) *Arabidopsis AUX1* gene: a permease-like regulator of root gravitropism. *Science.* **273**: 948-950

Benschop, J. J., Mohammed, S., O'Flaherty, M., Heck, A. J. R., Slijper, M. & Menke, F. L. H. (2007) Quantitative phosphoproteomics of early elicitor signaling in *Arabidopsis. Molecular and Cellular Proteomics.* **6**: 1198-1214

Beron, W., Mayorga, L. S., Colombo, M. I. & Stahl, P. D. (2001) Recruitment of coat-protein-complex prteins on to phagosomal membranes is regulated by a brefeldin A-sensitive ADP-ribosylation factor. *Biochem. J.* **355**: 409-415

Blakeslee, J. J., Bandyopadhyay, A., Lee, O. R., Mravec, J., Titapiwatanakun, B., Sauer, M., Makam, S. N., Cheng, Y., Bouchard, R., Adamec, J., Geisler, M., Nagashima, A., Sakai, T., Martinoia, E., Friml, J., Peer, W. A. & Murphy, A. S. (2007) Interactions among PIN-FORMED and p-glycoprotein auxin transporters in Arabidopsis. *Plant Cell.* **19**: 131-147

Blakeslee, J. J., Bandyopadhyay, A., Peer, W. A., Makam, S. N., Murphy, A. S. (2004) Relocalization of the PIN1 auxin efflux facilitator plays a role in phototropic responses. *Plant Physiology.* **134**: 28-31

Boccalandro, H. E., Mazza, C. A., Mazzella, A., Casal, J. J. & Ballare, C. L. (2001) Ultraviolet B radiation enhances a phytochrome-B-mediated photomorphogenic response in Arabidopsis. *Plant Physiology.* **126**: 780-788

Bogre, l., Okresz, L., Henriques, R., Anthony, A. R. (2003) Growth signaling pathways in *Arabidopsis* and the AGC protein kinases. *TRENDS in Plant Science.* **8**: 424-431

Bouly, J. P., Schleider, E., Dionisio-Sese, M., Vandenbussche, F., van der Straeten, D., Bakrim, N., Meier, S., Batschauer, A., Galland, P., Bittl, R. & Ahmad, M. (2007) Cryptochrome blue light photoreceptors are activated through interconversion of flavin redox states. *J. Biol. Chem.* **282**: 9383-9391

Brautigam, C. A., Smith, B. S., Ma, Z., Palntkar, M., Tomchick, D. R., Machius, M. & Deisenhofer, J. (2004) Structure of the photolyase-like domain of cryptochrome 1 from *Arabidopsis thaliana. Proc. Natl. Acad. Sci. USA.* **101**: 12142-12147

Briggs, W. R., Beck, C. F., Cashmore, A. R., Christie, J. M., Hughes, J., Jarillo, J. A., Kagawa, T., Kanegae, H., Liscum, E., Nagatani, A., Okada, K., Salomon, M., Rudiger, W., Sakai, T., Takano, M., Wada, M. & Watson, J. C. (2001) The phototropin family of photoreceptors. *Plant Cell.* **13**: 993-997

Briggs, W. R., Christie, J. M. & Salomon, M. (2001) Phototropins: a new family of flavin-binding blue light receptors in plants. *Antiox. Redox Signal.* **3**: 775-788

Brown, B. A., Cloix, C., Jiang, G. H., Kaiserli, E., Herzyk, P., Kliebenstein, D. J. & Jenkins, G. I. (2005) A UV-B specific signaling component orchestrates plant UV protection. Proc. *Natl. Acad. Sci. USA.* **102**: 18225-18230

Bunsen, R. & Roscoe, H. (1862) Photochemische Unterzuchungen. *Ann. Phys. Chem.* **117**: 529-562

Butler, W. L., Norris, K.H., Siegelman, H. W. & Hendricks, S. B. (1959) Detection, assay and preliminary purification of the pigment controlling photoresponsive development of plants. *Proc. Nat. Acad. Sci. USA* **45**: 1703-1708

Castro, A. F., Horton, J. K., Vanoye, C. G. & Altenberg, G. A. (1999) Mechanism of inhibition of p-glycoprotein-mediated drug transport by protein kinase C blockers. *Biochem. Pharmacol.* **58**: 1723-1733

Celaya, B. R. & Liscum, E. (2005) Phototropins and associated signaling: providing the power of movement in higher plants. *Photochem. Photobiol.* **81**: 73-80

Chien, C. T., Bartel, P. L., Sternglanz, R. & Fields, S. (1991) The two-hybrid system: a method to identify and clone genes for proteins that interact with a protein of interest. *Proc. Natl. Acad. Sci. USA.* **88**: 9578-0582

Cho, H-Y., Tseng, T-S., Kaiserli, E., Sullivan, S., Christie, J. M. & Briggs, W. R. (2007) Physiological roles of the light, oxygen, or voltage domains of phototropin1 and phototropin2 in Arabidopsis. *Plant Physiology.* **143**; 517-529

Christie, J. M. (2007) In: Light and Plant Development. (Eds. Whitelam, G. C. & Halliday, K. J.) Blackwell Publishing Ltd., Oxford, U.K.

Christie, J. M., Reymond, P., Powell, G. K., Bernasconi, P., Raibekas, A. A., Liscum, E. & Briggs, W. R. (1998) *Arabidopsis* NPH1: a flavoprotein with the properties of a photoreceptor for phtotropism. *Science.* **282**: 1698-1701

Christie, J. M., Salomon, M., Nozue, K., Wada, M. & Briggs, W. R. (1999) LOV (light, oxygen, or voltage) domains of the blue-light photoreceptor phototropin (nph1): binding sites for the chromophore flavin mononucletotide. *Proc. Natl. Acad. Sci. USA.* **96**: 8779-8783

Christie, J. M., Swartz, T. E., Bogomoloni, R. A. & Briggs, W. R. (2002) Phototropin LOV domains exhibit distinct roles in regulating photoreceptor function. *Plant Journal.* **32**: 205-219

Cominelli, E., Galbiati, M., Vavsseur, A., Conti, L., Sala, T., Vuylsteke, M., Leonhardt, N., Dellaporta, S. L. & Tonelli, C. (2005) A guard-cell-specific MYB transcription factor regulates stomatal movements and plant drought tolerance. *Curr. Biol.* **15**: 1196-1200

Crosson, S. & Moffat, K. (2001) Structure of a flavin-binding plant photoreceptor domain: insights into light-mediated signal transduction. *Proc. Natl. Acad. Sci. USA.* **98**: 2995-3000

Crosson, S. & Moffat, K. (2002) Photoexcited structure of a plant photoreceptor domain reveals a light-driven molecular switch. *Plant Cell.* **14**: 2-10

Cutler, S. R., Ehrhardt, D. W., Griffitts, J. S. & Somerville, C. R. (2000) Random GFP::cDNA fusions enable visualization of subcellular structures in cells of Arabidopsis at a high frequency. *Proc. Nat. Acad. Sci. USA*. **97**: 3718-3723

Darwin, C. (1881) The Power of Movement in Plants. John Murray, London, U. K.

DeBlasio, S. L., Luesse, D. L. & Hangarter, R. P. (2005) A plant-specific protein essential for blue-light-induced chloroplast movements. *Plant Physiology*. **139**: 101-114.

DeBlasio, S. L., Mullen, J. L., Luesse, D. R. & Hangarter, R. P. (2003) Phytochrome modulation of blue light-induced chloroplast movements in *Arabidopsis*. *Plant Physiology*. **133**:1471-1479.

Delbarre, A., Muller, P. & Guern, J. (1998) Short-lived and phosphorylated proteins contribute to carrier-mediated efflux, but not to influx, of auxin in suspension-cultured tobacco cells. *Plant Physiology*. **116**: 833-844

Emi, T., Kinoshita, T., Sakamoto, K., Mineyuki, Y. & Shimazaki, K. (2005) Isolation of a protein interacting with Vfphot1a in guard cells of *Vicia faba*. *Plant Physiology*. **138**: 1615-1626

Ermilova, E. V., Zalutskaya, Z. M., Huang, K. & Beck, C.F. (2004) Phototropin plays a crucial role in controlling changes in chemotaxis during the initial phase of the sexual life cycle in Chlamydomonas. *Planta*. **219**: 420-427

Esmon, C. A., Tinsley, A. G., Ljung, K., Sandberg, G., Hearne, L. B. & Liscum, E. (2006) A gradient of auxin and auxin-dependent transcription precedes tropic growth responses. *Proc. Natl. Acad. Sci. USA*. **103**: 236-241

Fankhauser, C. & Casal, J. J. (2004) Phenotypic characterization of a photomorphogenic mutant. *Plant Journal*. **39**: 747-760

Fankhauser, C., Yeh, K-C., Lagarias, J. C., Zhang, H., Elich, T. D. & Chory, J. (1999) PKS1, a substrate phosphorylated by phytochrome that modulates light signaling in *Arabidopsis*. *Science*. **284**: 1539-1541

Federov, R., Schlichting, I., Hartmann, E., Domratcheva, T., Fuhrmann, M., Hegemann, P. (2003) Crystal structures and molecular mechanism of a light-induced signaling switch: the Phot-LOV1 domain for *Chlamydomonas reinhardtii*. *Biophys. Journal*. **84**: 2474-2482

Fellner, M. Horton, L. A., Cocke, A. E., Stephens, N. R., Ford, E. D. and Van Volkenburgh, E. (2003) Light interacts with auxin during leaf elongation and leaf angle development in young corn seedlings. *Planta*. **216**: 366-376.

Ferl, R. J. (2004) 14-3-3 proteins: regulation of signal-induced events. *Physiologia Plantarum*. **120**: 173-178

Fields, S. & Song, O. (1989) A novel genetic system to detect protein-protein interactions. *Nature.* **340**: 245-247

Folta, K. M. & Maruhnich, S. A. (2007) Green light: a signal to slow down or stop. *J. Ex. Bot.* Advance Access doi: 10.1093/jxb/erm130

Folta, K. M. & Spalding, E. P. (2001) Unexpected roles for cryptochrome 2 and phototropin revealed by high-resolution analysis of blue light-mediated hypocotyl growth inhibition. *Plant Journal.* **26** (5): 471-478.

Folta, K. M. (2004) Green light stimulates early stem elongation antagonizing light-mediated growth inhibition. *Plant Physiology.* **135**: 1407-1416

Folta, K. M., Lieg, E. J., Durham, T. and Spalding, E. P. (2003) Primary inhibition of hypocotyl growth and phototropism depend differently on phototropin-mediated increases in cytoplasmic calcium induced by blue light. *Plant Physiology.* **133**: 1464-1470.

Folta, K.M. & Kaufman, L. S. (2003) Phototropin 1 is required for high-fluence blue light-mediated mRNA destabilisation. *Plant Molecular Biology.* **51**: 609-618.

Franklin, K. A. & Whitelam, G. C. (2007) In: Light and Plant Development. (Eds. Whitelam, G. C. & Halliday, K. J.) Blackwell Publishing Ltd., Oxford, U.K.

Franklin, K. A., Davis, S. J., Stoddart, W. M., Viestra, R. D. & Whitelam, G. C. (2003a) Mutant analyses define multiple roles for Phytochrome C in *Arabidopsis thaliana* photomorphogenesis. *The Plant Cell.,* **15**: 1981-1989

Franklin, K. A., Praaekelt, U., Stoddart, W. M., Billingham, O. E., Halliday, K., J. & Whitelam, G., C. (2003b) Phytochromes B, D, and E act redundantly to control multiple physiological responses in Arabidopsis. *Plant Physiology.* **131**: 1340-1346

Friml, J., Wisniewska, J., Benkova, E., Mendgen, K. & Palme K. (2002) Lateral relocation of auxin efflux regulator PIN3 mediates tropism in Arabidopsis. *Nature.* **415**: 806-809

Friml., Yang, X., Michniewicz, M., Weijers, D., Quint, A., Tietz, O., Benjamins, R., Ouwerkerk, P. B. F., Ljung, K., Sandberg, G., Hooykaas, P. J. J., Palme, K. & Offringa, R. (2004) A PINOID-dependent binary switch in apical-basal PIN polar targeting directs auxin efflux. *Science.* **306**: 862-865

Frohnmeyer, H. & Staiger, D. (2003) Ultraviolet-B radiation-mediated responses in plants. Balancing damage and protection. *Plant Physiology.* **133**: 1420-1428

Fuglsang, A. T., Visconti, S., Drumm, K., Jahn, T., Stensballe, A., Mattei, B., Jensen, O. N., Aducci, P. & Palmgren, M. G. (1999) Binding of a 14-3-3 protein to the plasma membrane H$^+$-ATPase AHA2 involves the three C-terminal residues Tyr^{946}-Thr-Val and requires phosphorylation of Thr^{946}. *J. Biol. Chem.* **274**: 36774-36780

Galen, C., Huddle, J. and Liscum, E. (2004) An experimental test of the adaptive evolution of phototropins: blue-light photoreceptor controlling phototropism in *Arabidopsis thaliana*. *Evolution*. **58**: 515-523.

Galen, C., Rabenold, J. J. and Liscum, E. (2007) Functional ecology of a blue light photoreceptor: effects of phototropin 1 on root growth enhance drought tolerance in *Arabidopsis thaliana*. *New Phytologist*. **173**: 91-99.

Gallagher, S., Short, T. W., Ray, P. M., Pratt, L. H. & Briggs, W. R. (1988) Light-mediated changes in two proteins found associated with plasma membrane fractions from pea stem sections. *Proc. Natl. Acad. Sci. USA*. **85**: 8003-8007.

Galweiler, L., Guan, C., Muller, A., Wisman, E., Mendgen, K., Yephremov, Y. & Palme, K. (1998) Regulation of polar auxin transport by AtPIN1 in *Arabidopsis* vascular tissue. *Science*. **282**: 2226-2230

Garcia, O., Bouige, P., Forestier, C. & Dassa, E. (2004) Inventory and comparative analysis of rice and Arabidopsis ATP-binding cassette (ABC) systems. *J. Mol. Biol.* **343**: 249-265

Gebbie, L. K., Burn, J. E., Hocart, C. H. & Williamson, R. E. (2005) Genes encoding ADP-ribosylation factors in *Arabidopsis thaliana* L. Heyn.; genome analysis and antisense supression. *J. Ex. Bot.* **56**: 1079-1091

Geisler, M. & Murphy, A. S. (2006) The ABC of auxin transport: the role of p-glycoproteins in plant development. *FEBS Lett*. **580**: 1094-1102

Gu, Y-M., Jin, Y-H., Choi, J-K., Baek, K-H., Yeo, C-Y. & Lee, K-Y. (2006) Protein kinase A phosphorylates and regulates dimerization of 14-3-3ζ *FEBS Lett.* **580**: 305-310

Guo, H., Mockler, T., Duong, H. & Lin, C. (2001) SUB1, an Arabidopsis Ca^{2+}-binding protein involved in cryptochrome and phytochrome coaction. *Science*. **291**: 487-490

Haga, K., Takano, M., Neumann, R. & Iino, M. (2005). The rice COLEOPTILE PHOTOTROPISM 1 gene encoding an orthologue of Arabidopsis NPH3 is required for phototropism of coleoptiles and lateral transport of auxin. *Plant Cell*. **17**: 103-115

Han, L., Mason, M., Risseeuw, E. P., Crosby, W. L. & Somers, D. E. (2004) *Plant Journal*. **40**: 291-301

Hanks, S. K. & Hunter, T. (1995) Protein kinases 6. The eukaryotic protein kinase superfamily: kinase (catalytic) domain structure and classification. *FASEB Journal*. **9**: 567-576

Harada, A. & Shimizaki, K-I. (2007) Phototropin and blue light-dependent calcium signaling in higher plants. *Photochem. Photobiol.* **83**: 102-111.

Harada, A., Sakai, T. and Okada, K. (2003) Phot1 and phot2 mediate blue light-induced transient increases in cytosolic Ca^{2+} differently in *Arabidopsis* leaves. *Proc. Nat. Acad. Sci. USA*. **100**: 8583-8588.

Hardtke, C. S., Gohda, K., Osterlund, M. T., Oyama, T., Okada, K. & Deng, X. W. (2000) HY5 stability and activity in Arabidopsis is regulated by phosphorylation in its COP1 binding domain. *The EMBO Journal.* **19**: 4997-5006

Harper, R. M., Stowe-Evans, E. L., Luesse, D. R., Muto, H., Tatematsu, K., Watahiki, M. K., Yamamoto, K. & Liscum , E. (2000) The NPH4 locus encodes the auxin response factor ARF7, a conditional regulator of differential growth in aerial *Arabidopsis* tissue. *Plant Cell.* **12**: 757-770

Harper, S. M., Christie, J. M. & Gardner, K. H. (2004) Disruption of the LOV-Jα helix interaction activates phototropin kinase activity. *Biochemistry.* **43**: 16184-16192

Harper, S. M., Neil, L. C., Gardner, K. H. (2003) Structural basis of a phototropin light switch. *Science.* **301**: 1541-1544

Hasegawa, T., Yamada, K., Shigemori, H., Goto, N., Miyamoto, K., Ueda, J. & Hasegawa, K. (2004) Isolation and identification of blue light-induced growth inhibitor from light-grown *Arabidopsis* shoots. *Plant Growth Regulation.* **44**: 81-86

Higgins, C. F. (2001) ABC transporters: physiology, structure and mechanism - an overview. *Res. Microbiol.* **152**: 205-210

Hiltbrunner, A., Viczian, A., Bury, E., Tscheuschler, A., Kircher, S., Toth, R., Honsberger, A., Nagy, F., Fankhauser, C. & Schafer, E. (2005) Nuclear accumulation of the Phytochrome A photoreceptor requires FHY1. *Current Biology.* **15**: 2125-2130

Horwitz, B. A.,Thompson, W. F. & Briggs, W. R. (1988) Phytochrome regulation of greening in *Pisum. Plant Physiology.* **86**: 299-305

Huang, K. Y. & Back, C. F. (2003) Phototropin is the blue light receptor that controls multiple steps in the sexual life cycle of the green alga *Chlamydomonas reinhadtii. Proc. Natl. Acad. Sci. USA.* **100**: 6269-6274

Huang, Y., Baxter, R., Smith, B. S., Partch, C. L., Colbert, C. L. & Deisenhofer, J. (2006) Crystal structure of cryptochrome 3 from *Arabidopsis thaliana* and its implications for photolyase activity. *Proc. Natl. Acad. Sci. USA.* **103**: 17701-17706

Huq, E. & Quail, P. H. (2002) PIF4, a phytochrome-interacting bHLH factor, functions as a negative regulator of phytochrome B signaling in Arabidopsis. *The EMBO Journal* **21**: 2441-2450

Huq, E., Al-Sady, B., Quail, P. H. (2003) Nuclear transportation of the photoreceptor phytochrome B is necessary for its biological function in seedling photomorphogenesis. *Plant Journal.* **35**: 660-664

Imaizumi, T., Schultz, T. F., Harmon, F. G., Ho, L. A. & Kay, S. A. (2005) FKF1 F-box protein mediates cyclic degradation of a repressor of CONSTANS in Arabidopsis. *Science.* **309**: 293-297

Imaizumi, T., Tran, H. G., Swartz, T. E., Briggs, W. R. & Kay, S. A. (2003) FKF1 is essential for photoperiodic-specific light signalling in Arabidopsis. *Nature.* **426**: 302-306

Inada, S., Ohgishi, M., Mayama, T., Okada, K. & Sakai, T. (2004) RPT2 is a signal transducer involved in phototropic response and stomatal opening by association with phototropin 1 in Arabidopsis thaliana. *Plant Cell.* **16**: 887-896

Inoue, S-I., Kinoshita, T. & Shimizaki, K-I. (2005) Possible involvement of phototropins in leaf movement of kidney bean in response to blue light. *Plant Physiology.* **138**: 1994-2004.

Inoue, S-I., Kinoshita, T., Takemiya, A., Doi, M. and Shimizaki, K-I. (2007) Leaf positioning of *Arabidopsis* in response to blue light. *Molecular Plant.* Advance Access doi: 10.1093/mp/ssm001

Iwabuchi, K., Li, B., Bartel, P. & Fields, S. (1993) Use of two-hybrid system to identify the domain of p53 involved in oligomerization. *Oncogene.* **8**: 1693-1696

Janoudi, A. K. & Poff, K. L. (1992) Action spectrum for enhancement of phototropism by *Arabidopsis thaliana* seedlings. *Photochem. Photobiol.* **56**: 655-659

Janoudi, A. K., Gordon, W. R., Wagner, D., Quail, P. H. & Poff, K. L. (1997) Multiple phytochromes are involved in red-light-induced enhancement of first-positive phototropism in *Arabidopsis thaliana. Plant Physiology.* **113**: 975-979

Jarillo, J. A., Ahmad, M. & Cashmore, A. R. (1998) NPL1 (Accession No. AF053941): A second member of the NPH serine.threonine kinase family of *Arabidopsis* (PGR98-100). *Plant Physiology.* **117**: 719

Jarillo, J. A., Capel, J., Tang, R-H., Yang, H-Q., Alonso, J. M., Ecker, J. R. & Cashmore, A. R. (2001) An *Arabidopsis* circadian clock component interacts with both CRY1 and phyB. *Nature.* **410**: 487-490.

Jarillo, J. A., Gabrys, H., Capel, J., Alonso, J. M., Ecker, J. R. & Cashmore, A. R. (2001) Phototropin-related NPL1 controls chloroplast relocation induced by blue light. *Nature.* **410**: 952-954.

Jiao, Y., Yang, H., Ma, L., Sun, N., Yu, H., Liu, T., Gao, Y., Gu, H., Chen, Z., Wada, M., Gerstein, M., Zhao, H., Qu, L-J. & Deng, X. W. (2003) A genome-wide analysis of blue-light regulation of Arabidopsis transcription factor gene expression during seedling development. *Plant Physiology.* **133**: 1480-1493.

Jones, M. A., Feeney, K. A., Kelly, S. M. & Christie, J. M. (2007) Mutational analysis of phototropin 1 provides insights into the mechanism underlying LOV2 signal transduction. *J. Biol. Chem.* **282**: 6405-6414

Kagawa, T. & Suetsugu, N. (2007) Photometrical analysis with photosensory domains of photoreceptors in green algae. *FEBS Lett.* **581**: 368-374

Kagawa, T. & Wada, M. (2000) Blue light-induced chloroplast relocation in *Arabidopsis thaliana* as analyzed by microbeam irradiation. *Plant Cell Physiol.* **45**: 416-426

Kagawa, T. & Wada, M. (2002) Blue light-induced chloroplast relocation. *Plant Cell Physiology.* **43**: 367-371.

Kagawa, T., Kasahara, M., Abe, T., Yoshida, S. & Wada, M. (2004) Function analysis of phototropin 2 using fern mutants deficient in blue light-induced chloroplast avoidance movement. *Plant Cell Physiol.* **41**: 84-93

Kagawa, T., Sakai, T., Suetsugu, N., Oikawa, K., Ishiguro, S., Kato, T., Tabata, S., Okada, K. & Wada, M. (2001) *Arabidopsis* NPL1: a phototropin homolog controlling the chloroplast high-light avoidance response. *Science.* **291**: 2138-2141.

Kahn, R. A. & Gilman, A. G. (1984) Purification of a protein cofactor required for ADP-ribosylation of the stimulatory regulatory component of adenylate cyclase by chloera toxin. *J. Biol. Chem.* **259**: 6228-6234

Kahn, R. A., Kern, F.G., Clark, J., Gelmann, E. P. & Rulka, C. (1991) Human ADP-ribosylation factors. A functionally conserved family of GTP-binding proteins. *J. Biol. Chem.* **266**: 2606-2614

Kanegae, T., Hayashida, E., Kuramoto, C. & Wada, M. (2006) A single chromoprotein with triple chromophores acts as both a phytochrome and a phototropin. *Proc. Natl. Acad. Sci. USA.* **103**: 17997-18001

Kasahara, M., Kagawa, T., Sato, Y., Kiyosue, T. & Wada, M. (2004) Phototropins mediate blue and red light-induced chloroplast movements in Physcomitrella patens. *Plant Physiology.* **135**: 1388-1397

Kasahara, M., Swartz, T. E., Olney, M. A., Onodera, A., Mochizuki, N., Fukuzawa, H., Asamizu, E., Tabata, S., Kanegae, H., Takano, M., Christie, J. M., Nagatani, A. & Briggs, W. R. (2002) Photochemical properties of the flavin mononucletotide-binding domains of the phototropins from *Arabidopsis*, rice and *Chlamydomonas reinhardtii*. *Plant Physiology.* **129**: 762-773

Kawai, H., Kanegae, T., Christensen, S., Kiyosue, T., Sato, Y., Imaizumi, T., Kadota, A. & Wada, M. (2003) Responses of fern to red light are mediated by an unconventional photoreceptor. *Nature.* **421**: 287-290

Kennis, J. T. M., Crosson, S., Gauden, M., van Stokkum, I. H. M., Moffat, K. & van Grondelle, R. (2003) Primary reactions of the LOV2 domain of phototropin, a plant blue-light photoreceptor. *Biochemistry.* **42**: 3385-3392.

Kevei, E., Gyula, P., Hall, A., Kozma-Bognar, L., Kim, W-Y., Eriksson, M. E., Toth, R., Hanano, S., Feher, B., Southern, M. M. Bastow, R. M., Viczian, A., Hibberd, V., Davis, S. J., Somers, D. E., Nagy, F. & Millar, A. J. (2006) Forward genetic analysis

of the circadian clock separates the multiple functions of ZEITLUPE. *Plant Physiology*. **140**: 933-945

Kiba, T., Henriques, R., Sakakibara, H. & Chua, N-H. (2007) Targeted degradation of PSEUDO-RESPONSE REGULATOR5 by a SCF^{ZTL} complex regulates clock function and photomorphogenesis in *Arabidopsis thaliana*. *Plant Cell*. Advance Access doi: 10.1105/tpc.107.053033

Kim, B. C., Tennessen, D. J. & Last, R. L. (1998) UV-B-induced photomorphogenesis in Arabidopsis thaliana. *Plant Journal*. **15**: 667-674

Kim, J., Harter, K. & Theologis, A. (1997) Protein-protein interactions among the Aux/IAA proteins. *Proc. Natl. Acad. Sci. USA*. **94**: 11786-11791

Kim, J-I., Bhoo, S-H., Han, Y-J., Zarate, X., Furuya, M. & Song, P-S. (2006) The PAS2 domain is required for dimerization of phytochrome A. *Biochem. Photobiol.* **178**:115-121

Kim, W. Y., Fujiwara, S., Suh, S. S., Kim, J., Kim, Y., Han, L., David, K., Putterill, J., Nam, H. G. & Somers, D. E. (2007) ZEITLUPE is a circadian photoreceptor stabilized by GIGANTEA in blue light. *Nature* **449**: 356-360

Kimura, M. & Kagawa, T. (2006) Phototropin and light-signaling in phototropism. *Curr. Opin. Plant Biol.* **9**: 503-508

Kinoshita, T. & Shimazaki, K. (1999) Blue light activates the plasma membrane H$^+$-ATPase by phosphorylation of the C-terminus in stomatal guard cells. *EMBO Journal*. **18**: 5548-5558

Kinoshita, T. & Shimazaki, K. (2001) Analysis of the phosphorylation level in guard-cell plasma membrane H$^+$-ATPase in response to fusicoccin. *Plant Cell Physiol*. **42**: 424-432

Kinoshita, T. & Shimazaki, K. (2002) Biochemical evidence for the requirement of 14-3-3 protein binding in activation of the guard-cell plasma membrane H$^+$-ATPase by blue light. *Plant Cell Physiol*. **43**: 1359-1365

Kinoshita, T., Doi, M., Suetsugu, N., Kagawa, T., Wada, M. & Shimazaki, K. (2001) Phot1 and phot2 mediate blue light regulation of stomatal opening. *Nature*. **414**: 656-660

Kinoshita, T., Emi, T., Tominga, M., Sakamoto, K., Shigenaga, A., Doi, M. & Shimazaki, K. (2003) Blue-light and phosphorylation-dependent binding of a 14-3-3 protein to phototropins in stomatal guard cells. *Plant Physiology*. **133**: 1453-1463

Kiyosue, T. & Wada, M. (2000) LKP1 (LOV kelch protein 1): a factor involved in the regulation of flowering time in Arabidopsis. *Plant Journal*. **23**: 807-815

Kleibenstein, D. J., Lim, J. E., Landry, L. G. & Last, R. L. (2002) Arabidopsis UVR8 regulates ultraviolet-B signal transduction and tolerance and contains sequence similarity to human regulator of chromatin condensation. *Plant Physiology*. **130**: 234-243

Kleine, T., Lockhart, P. & Batschauer, A. (2003) An Arabidopsis protein closely related to *Synechocystis* cryptochrome is targeted to organelles. *Plant Journal*. **35**: 93-103

Kleiner, O., Kircher, S., Harter, K. & Batschauer, A. (1999) Nuclear localization of the *Arabidopsis* blue light receptor cryptochrome 2. *Plant Journal*. **19**: 289-296

Kneib, E., Salomon, M. & Rudiger, W. (2005) Autophosphorylation, electrophoretic mobility, and immunoreaction of oat phototropin 1 under UV and blue light. *Photochem. Photobiol*. **81**: 177-182

Knighton, D. R., Zheng, J., TenEyck, L. F., Ashford, V. A. & Xuong, N. H. (1991) Crystal structure of the catalytic subunit of cAMP-dependent protein kinase. *Science*. **253**: 407-414

Kong, S. G., Kinoshita, T., Shimazaki, K-I., Mochizuki, N., Suzuki, T. & Nagatani, A. (2007) The C-terminal kinase fragment of phototropin 2 triggers constitutive photomorphogenic responses. *Plant Journal*. **51**: 862-873

Kong, S. G., Suzuki, T., Tamura, K., Mochizuki, N., Hara-Nishimura, I. & Nagatani, A. (2006) Blue light-induced association of phototropin 2 with the Golgi apparatus. *Plant Journal*. **45**: 994-1005

Kosemura, S., Niwa, K., Emori, H., Yokotani-Tomita, K., Hasegawa, K. & Yamamura, S. (1997) Light-induced auxin-inhibiting substance from cabbage (*Brassica oleracea* L.) shoots. *Tetrahedron Lett*. **38**: 8327-8330

Kottke, T., Heberle, J., Hehn, D., Dick, B., Hegemann, P. (2003) Phot-LOV1: photocycle of a blue-light receptor domain from the green alga *Chlamydomonas reinhartii. Biophys. Journal*. **84**: 1192-1201

Kumatani, T., Sakuri-Ozato, N., Miyawaki, N., Yokota, E., Shimmen, T., Terashima, I. & Takagi, S. (2006) Possible association of actin filaments with chloroplasts of spinach mesophyll cells *in vivo* and *in vitro. Protoplasma*. **229**: 45-52

Lariguet, P. & Dunand, C. (2005) Plant photoreceptors: phylogenetic overview. *J. Mol. Evol*. **61**: 559-569

Lariguet, P. & Fankhauser, C. (2004) Hypocotyl growth orientation in blue light is determined by phytochrome A inhibition of gravitropism and phototropin promotion of phototropism. *Plant Journal*. **40**: 826-834.

Lariguet, P., Schepens, I., Hodgson, D., Pedmale, U. V., Trevisan, M., Kami, C., de Carbonnel, M., Alonso, J. M., Ecker, J. R., Liscum ,E. & Fankhauser, C. (2006)

PHYTOCHROME KINASE SUBSTRATE 1 is a phototropin 1 binding protein required for phototropism. *Proc. Natl. Acad. Sci. USA*. **103**: 10134-10139

Li, B. & Fields, S. (1993) Identification of mutations in p53 that affect its binding to SV40 T antigen by using the yeast two-hybrid system. *FASEB Journal*. **7**: 957-963

Lin, C. & Shalitin, D. (2003) Cryptochrome structure and signal transduction. *Annu. Rev. Plant. Biol*. **54**: 469-496

Lin, C. & Todo, T. (2005) The cryptochromes. *Genome Biology*. **6**: 220

Lin, C., Ahmad, M., Chan, J. & Cashmore, A. R. (1996) CRY2: a second member of the Arabidopsis cryptochrome gene family. *Plant Physiology*. **110**: 1047

Lin, C., Robertson, D. E., Ahmad, M., Raibekas, A. A., Schuman-Jornes, M., Dutton, P. L. & Cashmore, A. R. (1995) Association of flavin adenine dinucleotide with the Arabidopsis blue-light receptor CRY1. *Science*. **269**: 968-970

Lin, C., Yang, H., Guo, H., Mockler, T., Chen, J. & Cashmore, A. R. (1998) Enhancement of blue-light sensitivity of Arabidopsis seedlings by a blue light receptor cryptochrome 2. *Proc. Natl. Acad. Sci. USA*. **95**: 2686-2690

Lin, R. & Wang, W. (2005) Two homologous ATP-binding cassette transporter proteins, AtMDR1 and AtPGP1, regulate *Arabidopsis* photomorphogenesis and root development by mediating polar auxin transport. *Plant Physiology*. **138**: 949-964

Liscum, E. & Briggs, W. R. (1995) Mutations in the NPH1 locus of Arabidopsis disrupt the perception of phototropic stimuli. *Plant Cell*. **7**: 473-485

Lu, G., DeLisle, A. J., de Vetten, N. C. & Ferl, R. J. (1992) Brain proteins in plants: An *Arabidopsis* homolog to neurotransmitter pathway activators in part of a DNA binding complex. *Proc. Natl. Acad. Sci. USA*. **89**: 11490-11494

MacKinney, G. (1941) Absorption of light by chlorophyll solutions. *J. Biol. Chem*. **140**: 315-322

MacKintosh, C. (2004) Dynamic interactions between 14-3-3 proteins and phosphoproteins regulate diverse cellular processes. *Biochem.J*. **381**: 329-342

Malhotra, K., Kim, S-T., Batschauer, A., Dawut, L. & Sancar, A. (1995) Putative blue-light photoreceptors from *Arabidopsis thaliana* and *Sinapis alba* with high degree of sequence homology to DNA photolyase contain the two photolyase cofactors but lack DNA repair activity. *Biochemistry*. **34**: 6892-6899

Maly, D. J., Allen, J. A. & Shokat, K. M. (2004) A mechanism-based cross-linker for the identification of kinase-substrate pairs. *J. Am. Chem. Soc*. **126**: 9160-0161

Mao, J., Zhang, Y-C., Sang, Y., Li, Q-H. & Yang, H-Q. (2005) A role for *Arabidopsis* cryptochromes and COP1 in the regulation of stomatal opening. *Proc. Natl. Acad. Sci. USA*. **102**: 12270-12275

Martinez-Garcia, J. F., Hug, E. & Quail, P. H. (2000) Direct targeting of light signals to a promoter element-bound transcription factor. *Science*. **288**: 859-863

Mas, P., Devlin, P. F., Panda, S. & Kay, S. A. (2000) Functional interaction of phytochrome B and cryptochrome 2. *Nature*. **408**: 207-211

Mathews, S. & Sharrock, R. A. (1997) Phytochrome gene diversity *Plant, Cell and Environment*. **20**: 666-671.

Matsuoka, D. & Tokotumi, S. (2005) Blue light-regulated molecular switch of Ser/Thr kinase in phototropin. *Proc. Natl. Acad. Sci. USA*. **102**: 13337-13342

Matsushita, T., Mochizuki, N. & Nagatani, A. (2003) Dimers of the N-terminal of phytochrome B are functional in the nucleus. *Nature*. **424**: 571-574

Moller, S. G., Kim, Y-S., Kunkel, T., Chua, N-M. (2003) PP7 is a positive regulator of blue light signaling in *Arabidopsis. Plant Cell*. **15**: 1111-1119

Monte, E., Tepperman, J. M., Al-Sady, B., Kaczorowski, K. A., Alonso, J. M., Ecker, J. R., Li, X., Zhang, Y. & Quail, P. H. (2004) The phytochrome-interacting factor, PIF3, acts early, selectively, and positively in light-induced chloroplast development. *Proc. Nat. Acad. Sci. USA*. **101**: 16091-16098

Montgomery, B. L. & Lagarias, J. C. (2002) Phytochrome ancestry: sensors of bilins and light. *TRENDS in Plant Science*. **7**: 357-366

Moore, B. W. & Perez, V. J. (1967) *Specific acidic proteins of the nervous system.* In: Physiological and Biochemical Aspects of Nervous Integration (ed F. Carlson). Prentice Hall, Woods Hole, MA

Motchoulski, A. & Liscum, E. (1999) Arabidopsis NPH3: a NPH1 photoreceptor-interacting protein essential for phototropism. *Science*. **286**: 961-964

Nakasako, M., Matsuoka, D., Zikihara, K. & Tokotumi, S. (2005) Quaternary structure of LOV-domain containing polypeptide of Arabidopsis FKF1 protein. *FEBS Lett*. **579**: 1067-1071

Nelson, D. C., Lasswell, J., Rogg, L. E., Cohen, M. A. & Bartel, B. (2000) FKF1, a clock-controlled gene that regulates the transition to flowering in Arabidopsis. *Cell*. **101**: 331-340

Ni, M., Tepperman, J. M., Quail, P. H. (1998) PIF3, a phytochrome-interacting factor necessary for normal photo-induced signal transduction, is a novel basic helix-loop-helix protein. *Cell*. **95**: 657-667

Ni, M., Tepperman, J. M., Quail, P. H. (1999) Binding of phytochrome B to its nuclear signalling partner PIF3 is reversibly induced by light. *Nature*. **400**: 781-784

Nielsen, M., Albrethsen, J., Larsen, F. H. & Skriver, K. (2006) The *Arabidopsis* ADP-ribosylation factor (ARF) family and ARF-like (ARL) system and its regulation by BIG2, a large ARF-GEF. *Plant Science.* **171**: 707-717

Noh, B., Bandyopadhyay, A., Peer, W. A., Spalding, E. P. & Murphy, A. S. (2003) Enhanced gravi- and phototropism in plant *mdr* mutants mislocalising the auxin efflux protein PIN1. *Nature.* **423**: 8373-8379

Noh, B., Murphy, A. S. & Spalding, E. P. (2001) Multidrug-resistance-like genes of Arabidopsis required for auxin transport and auxin-mediated development. *The Plant Cell.* **13**: 2441-2454

Normanly, J., Grisafi, P., Fink, G. R. & Bartel, B. (1997) *Arabidopsis* mutants resistant to the auxin effects of indole-3-acetonitrile are defective in the nitrilase encoded by the *NIT1* gene. *Plant Cell.* **9**: 1781-1790.

Nozaki, D., Iwata, T., Ishikawa, T., Todo, T., Tokotumi, S. & Kandori, H. (2004) Role of Gln1029 in the photoactivation processes of the LOV2 domain in Adiantum phytochrome 3. *Biochemistry.* **43**: 8373-8379

Nozue, D., Kanagae, T., Imaizumi, T., Fukuda, S., Okamoto, H., Yeh, K. C., Lagarias, J. C. & Wada, M. (1998) A phytochrome from the fern *Adiantum* with the properties of the putative photoreceptor NPH1. *Proc. Natl. Acad. Sci. USA.* **95**: 15826-15830

Oikawa, K., Kasahara, M., Kiyosue, T., Kagawa, T., Suetsugu, N., Takahashi, F., Kanegae, T., Niwa, Y., Kadota, A. & Wada, M. (2003) Chloroplast unusual positioning 1 is essential for proper chloroplast positioning. *Plant Cell.* **15**: 2805-2815

Okada, K. & Shimura, Y. (1992) Mutational analysis of root gravitropism and phototropism of *Arabidopsis thaliana* seedlings. *Aust. J. Plant. Physiol.* **19**: 439-448

Onodera, A., Kong, S. G., Doi, M., Shimazaki, K., Christie, J., Mochizuki, N. & Nagatani, A. (2005) Phototropin from *Chlamydomonas reinhardtii* is functional in *Arabidopsis thaliana.* *Plant Cell Physiol.* **46**: 367-374

Osterlund, M. T. & Deng, X-W. (1998) Multiple photoreceptors mediate the light-induced reduction of GUS-COP1 from Arabidopsis hypocotyl nuclei. *Plant Journal.* **16**: 201-208

Ozgur, S. & Sancar, A. (2006) Analysis of autophosphorylating kinase activities of *Arabidopsis* and human cryptochromes. *Biochemistry.* **45**: 13369-13374

Palmer, J. M., Short, T. W., Gallagher, S., Briggs, W. R. (1993) Blue light-induced phosphorylation of a plasma membrane-associated protein in *Zea mays* L. *Plant Physiology.* **102**: 1211-1218

Parry, G., Delbarre, A., Marchant, A., Swarup, R., Napier, R., Perrot-Rechenmann, C. & Bennett, M. J. (2001) Novel auxin transport inhibitors phenocopy the auxin influx carrier mutation *aux1*. *Plant Journal.* **25**: 399-406

Paul, A-L., Sehnke, P. C. & Ferl, R. J. (2005) Isoform-specific subcellular localization among 14-3-3 proteins in *Arabidopsis* seems to be driven by client interactions. *Mol. Biol. Cell.* **16**: 1735-1743

Paul, N. D. & Gwynn-Jones, D. (2003) Ecological roles of solar UV radiation: towards an integrated approach. *TRENDS in Ecology and Evolution.* **18**: 48-55

Pedmale, U. V. & Liscum, E. (2007) Regulation of phototropic signaling in *Arabidopsis* via phosphorylation state changes in the phototropin 1-interacting protein NPH3. *J. Biol. Chem.* **282**: 19992-20001

Pimpl, P., Movafeghi, A., Pacoda, D. & Dalessandro, G. (2000) *In situ* localization and *in vitro* induction of plant COPI-coated vesicles. *Plant Cell.* **12**: 2219-2236

Presha, A., Biernat, J. & Szopa, J. (2002) Quantitative and qualitative analysis of lipids in genetically modified potato tubers with varying rates of 14-3-3 protein synthesis. *Nahrung.* **46**: 179-183

Quail, P. H. (2007) In: *Light and Plant Development.* (Eds. Whitelam, G. C. & Halliday, K. J.) Blackwell Publishing Ltd., Oxford, U.K.

Quail, P. H. (1997) An emerging map of the phytochromes. *Plant, Cell and Environment.* **20**: 657-665

Quail, P. H., Boylan, M. T., Parks, B. M., Short, T. W., Xu, Y., Wagner, D. (1995) Phytochromes: phototsensory perception and signal transduction. *Science.* **268**: 675-680

Reymond, P., Short, T. W. & Briggs, W. R. (1992) Blue light activates a specific protein kinase in higher plants. *Plant Physiology.* **100**: 655-661

Reymond, P., Short, T. W., Briggs, W. R., Poff, K. L. (1992) Light-induced phosphorylation of a membrane protein plays an early role in signal transduction for phototropism in *Arabidopsis thaliana. Proc. Natl. Acad. Sci. USA.* **89**: 4718-4721

Rientes, I. M., Vink, J., Borst, J. W., Russinova, E. & de Vries, S. C. (2005). The *Arabidopsis* SERK1 protein interacts with the AAA-ATPase *At*CDC48, the 14-3-3 protein GF14λ and the PP2C phosphatase KAPP. *Planta.* **221**: 394-405

Ritzenthaler, C., Nebenfuhr, A., Movafeghi, A., Stussi-Garauda, C., Behniac, L., Pimpl, P., Staehelin, L. A. & Robinson, D. G. (2002) Re-evaluation of the effects of brefeldin A on plant cells using tobacco Bright Yellow 2 cells expressing Golgi-targeted green fluorescent protein and COPI antisera. *Plant Cell.* **14**: 237-261

Rosenquist, M., Alsterfjord, M., Larson, C. & Sommarin, M. (2001) Data mining the *Arabidopsis* genome reveals fifteen 14-3-3 genes. Expression is demonstrated for two out of five novel genes. *Plant Physiology.* **127**: 142-149

Rozen, S. & Skaletsky, H. S. (2000) Primer 3 on the WWW for general users and for biologist programmers. In: Bioinformatics, Methods and Protocols: Methods in Molecular Biology (Eds.. S. Krawetz & S. Misner). Humana Press, Totowa, NJ

Ruden, D. M. , Ma, J., Li, Y., Wood, K. & Ptashne, M. (1991) Generating yeast transcriptional activators containing no yeast protein sequences. *Nature.* **350**: 250-251

Ruden, D. M. (1992) Activating regions of yeast transcription factors must have both acidic and hydrophobic amino acids. *Chromosoma* **101**: 342-348

Sakai, T., Kagawa, T., Kasahara, M., Swartz, T. E., Christie, J. M., Briggs, W. R., Wada, M. & Okada, K. (2001) *Arabidopsis* nph1 and npl1: blue light receptors that mediate both phototropism and chloroplast relocation. *Proc. Nat. Acad. Sci. USA.* **98**: 6969-6974.

Sakai, T., Wada, T., Ishiguro, S. & Okada, K. (2000) RPT2: A signal transducer of the phototropic response in *Arabidopsis. Plant Cell.* **12**: 225-236

Sakai, Y & Takagi, S. (2005) Reorganised actin filaments anchor chloroplasts along the anticlinal walls of *Vallisneria* epidermal cells under high-intensity blue light. *Planta.* **221**: 823-830.

Sakamoto, K. & Briggs, W. R. (2002) Cellular and subcellular localization of phototropin 1. *Plant Cell.* **14**: 1723-1735

Sakurai, N., Domoto, K. & Takagi, S. (2005) Blue-light-induced reorganization of the actin cytoskeleton and the avoidance response of chloroplasts in epidermal cells of *Vallisneria gigantea. Planta.* **221**: 66-74.

Salomon, M., Christie, J. M., Knieb, E., Lempert, U., Briggs, W. R. (2000) Photochemical and mutational analysis of the FMN-binding domains of the plant blue light receptor, phototropin. *Biochemistry.* **39**: 9401-9410

Salomon, M., Knieb, E., von Zepplin, T. & Rudiger, W. (2003) Mapping of low- and high-fluence autophosphorylation sites in phototropin 1. *Biochemistry.* **42**: 4217-4225

Salomon, M., Lempert, U. & Rudiger, W. (2004) Dimerization of the plant photoreceptor phototropin is probably mediated by the LOV1 domain. *FEBS Lett.* **572**: 8-10

Salomon, M., Zacherl, M., Luff, L. & Rudiger, W. (1997a) Exposure of oat seedlings to blue light results in amplified phosphorylation of the putative photoreceptor for phototropism and in higher sensitivity of the plants to phototropic stimulation. *Plant Physiology.* **115**: 493-500

Salomon, M., Zacherl, M., Rudiger, W. (1997b) Asymmetric, blue light-dependent phosphorylation of a 116-kilodalton plasma membrane protein can be correlated with

the first- and second-positive phototropic curvature of oat coleoptiles. *Plant Physiology.* **115**: 485-491

Sambrook, J. & Russell, D. W. (2001) Molecular Cloning: A Laboratory Manual. 3rd Edition. Cold Spring Harbor Laboratory Press, Cold Spring Harbor, NY

Sampedro, J. & Cosgrove, D. J. (2005) The expansin superfamily. *Genome Biology.* **6**: 242

Sancar, A. (1994) Structure and function of DNA photolyase. *Biochemistry.* **33**: 2-9

Sang, Y., Li, Q-H., Rubio, V., Zhang, Y-C., Mao, J., Deng, X-W. & Yang, H-Q. (2005) N-terminal domain-mediated homodimerization is required for photoreceptor activity of *Arabidopsis* CRYPTOCHROME 1. *Plant Cell.* **17**: 1569-1584

Schepens, I., Duek, P. & Fankhauser, C. (2004) Phytochrome-mediated light signalling in *Arabidopsis. Curr. Opin. Plant Biol.* **7**: 564-569

Schinkle, J. R., Derickson, D. L. & Barnes, P. W. (1999) Comparative photobiology of growth responses to two UV-B wavebands and UV-C in dim-red-light- and white-light-grown Cucumber (*Cucumis staivus*) seedlings: physiological evidence for photoreactivation. *Photochem. Photobiol.* **81**: 1069-1074

Schmidt, W., Marme, D., Quail, P. & Schafer, E. (1973) Phytochrome: first-order phototransformation kinetics *in vivo*. *Planta.* **111**: 329-336

Schneider, E. & Hunke, S. (1998) ATP-binding-cassette (ABC) transport systems: functional and structural aspects of the ATP-hydrolyzing subunits/domains. *FEMS Microbiol. Rev.* **22**: 1-20

Schoonheim, P. J., Veiga, H., Pereira, D., da C., Friso, G., van Wijk, K. J. & de Boer, A. H. (2007) A comprehensive analysis of the 14-3-3 interactome in barley leaves using a complementary proteomics and two-hybrid approach. *Plant Physiology.* **143**: 670

Schultz, T. W., Kiyosue, T., Yanovsky, M., Wada, M. & Kay, S. A. (2001) A role for LKP2 in the circadian clock of Arabidopsis. *Plant Cell.* **13**: 2659-2670

Sehnke, P. C., Chung, H. J., Wu, K. & Ferl, R. J. (2001) Regulation of starch accumulation by granule-associated plant 14-3-3 proteins. *Proc. Natl. Acad. Sci. USA..* **98**: 765-770

Sehnke, P. C., DeLille, J. M. & Ferl, R. J. (2002) Consummating signal transduction: the role of 14-3-3 proteins in the completion of signal-induced transitions in protein activity. *Plant Cell.* **14**: S339-S354

Selby, C. P. & Sancar, A. (2006) A cryptochrome/photolyase class of enzymes with single-stranded DNA-specific photolyase activity. *Proc. Natl. Acad. Sci. USA..* **103**: 17696-17700

Seo, H., S., Watanabe, E., Tokutomi, S., Nagatani, A. & Chua, N-H. (2004) Photoreceptor ubiquitination by COP1 E3 ligase desensitizes phytochrome A signaling. *Genes & Development.* **18**: 617-622.

Shalitin, D., Yang, H., Mockler, T. C., Maymon, M., Guo, H., Whitelam, G. C. & Lin, C. (2002) Regulation of Arabidopsis cryptochrome 2 by blue-light-dependent phosphorylation. *Nature*. **417**: 763-767

Shimazaki, K-I., Doi, M., Assmann, S. & Kinoshita, T. (2007) Light regulation of stomatal movement. *Annu. Rev. Plant. Biol.* **58**: 219-247

Smalle, J. & Vierstra, R. D. (2004) The ubiquitin 26S proteasome proteolytic pathway. *Ann. Rev. Plant Biol.* **55**: 555-590

Somers, D. E., Kim, W-Y. & Geng, R. (2004) The F-box proteins, ZEITLUPE confers dosage-dependent control on the circadian clock, photomorphogenesis, and flowering time. *Plant Cell*. **16**: 769-782

Somers, D. E., Schultz, T. F., Milnamow, M. & Kay, S. A. (2000) ZEITLUPE encodes a novel clock-associated PAS protein from Arabidopsis. *Cell*. **101**: 319-329

Steinmann, T., Geldner, N., Grebe, M., Mangold, S., Jackson, C. L., Paris, S., Galweiler, L., Palme, K & Jurgens, G. (1999) Coordinated polar localization of auxin influx carrier PIN1 by GNOM ARF GEF. *Science*. **286**: 316-318

Stoelzle, S., Kagawa, T., Wada, M., Hedrich, R. & Dietrich, P. (2003) Blue light activates calcium-permeable channels in *Arabidopsis* mesophyll cells via the phototropin signaling pathway. *Proc. Nat. Acad. Sci. USA*. **100**(3): 1456-1461.

Stogios, P. J., Downs, G. S., Jauhal, J. J. Nandra, S. K. & Prive, G. G. (2005) Sequence and structural analysis of BTB domain proteins. *Genome Biology*. **6**: 1193-1198

Stowe-Evans, E. L., Harper, R. M., Motchoulski, A. V. & Liscum, E. (1998) NPH4, a conditional modulator of auxin-dependent differential growth responses in Arabidopsis. *Plant Physiology*. **139**: 151-162

Stowe-Evans, E. L., Luesse, D. R. & Liscum, E. (2001) The enhancement of phototropin-induced phototropic curvature in *Arabidopsis* occurs via a photoreversible phytochrome A-dependent modulation of auxin responsiveness. *Plant Physiology*. **126**: 826-834

Suesslin, C. & Frihnmeyer, H. (2003) An Arabidopsis mutant defective in UV-B light-mediated responses. *Plant Journal*. **33**: 591-601

Suetsugu, N & Wada, M. (2007) Phytochrome-dependent photomovement responses mediated by phototropin family proteins in cryptogram plants. *Photochem. Photobiol*. **83**: 87-93

Suetsugu, N., Kagawa, T. & Wada, M. (2005a) An auxilin-like J-domain protein, JAC1 regulates phototropin-mediated chloroplast movement in Arabidopsis. *Plant Physiology*. **139**: 151-162

Suetsugu, N., Mittmannn, F., Wagner, G., Hughes, J. & Wada, M. (2005b) A chimeric photoreceptor gene, NEOCHROME has arisen twice during plant evolution. *Proc. Natl. Acad. Sci. USA*. **102**: 13705-13709

Sullivan, S., Thomson, C.E., Lamont, D. J., Jones, M. A. & Christie, J. M. (2008) *In Vivo* Phosphorylation Site Mapping and Functional Characterization of Arabidopsis Phototropin 1. *Mol. Plant*, **1(1)**: 178-194.

Swartz, T. E., Corchnoy, S. B., Christie, J. M., Lewis, J. W., Szundi, I., Briggs, W. R. & Bogomolni, R. A. (2001) The photocycle of a flavin-binding domain of the blue light photoreceptor phototropin. *J. Biol. Chem.* **276**: 36493-36500

Swiedrych, A., Prescha, A., Matysiak-Kata, I., Biernat, J. & Szopa, J. (2002) Repression of the 14-3-3 gene affects the amino acid and mineral composition of potato tubers. *J. Agric. Food Chem.* **50**: 2173-2141

Szopja, J. (2002) Transgenic 14-3-3 isoforms in plants: the metabolite profiling of repressed 14-3-3 protein synthesis in transgenic potato plants. *Biochem. Soc. Trans.* **30**: 405-410

Takemiya, A., Inoue, S-I., Doi, M., Kinoshita, T. and Shimizaki, K-I. (2005) Phototropins promote plant growth in response to blue light in low light environments. *Plant Cell.* **17**: 1120-1127.

Talbott, L. D., Hammad, J. W., Harn, L. C., Nguyen, V. H., Patel, J. & Zeiger, E. (2006) Reversal by green light of blue light-stimulated stomatal opening in intact, attached leaves of Arabidopsis only occurs in the potassium-dependent, morning phase of movement. *Plant Cell Physiol.* **47**: 332-337

Tatematsu, K., Kumagi, S., Muto, H., Sato, A., Watahiki, M. K., Harper, R. M., Liscum, E. & Yamamoto, K. T. (2004) MASSUGU2 encodes Aux/IAA19, an auxin-regulated protein that functions together with the transcriptional activator NPH4/ARF7 to regulate differential growth responses of hypocotyl and formation of lateral roots in *Arabidopsis thaliana. Plant Cell.* **16**: 379-393

Taylor, B. L. & Zhulin, I. B. (1999) PAS domains: internal sensors of oxygen, redox potential, and light. *Microbiol. Mol. Biol. Rev.* **63**: 479-506

Tepperman, J. M., Zhu, T., Chang, H. S., Wang, X. & Quail, P. H. (2001) Multiple transcription-factor genes are early targets of phytochrome A signaling. *Proc. Natl. Acad. Sci. USA*. **98**: 9437-9442

Terry, M., J. (1997) Phytochrome chromophore-deficient mutants. *Plant Cell and Environment.* **20**: 740-745

Tsuboi, H., Suetsugu, N., Kawai-Toyooka, H. & Wada, M. (2007) Phototropins and Neochrome1 mediate nuclear movement in the fern *Adiantum capillus-veneris. Plant Cell Physiol.* **48**: 892-896

Ueno, K., Kinoshita, T., Inuoe, S., Emi, T. & Shimazaki, K. (2005) Biochemical characterization of plasma membrane H⁺-ATPase activation in guard cell protoplasts of Arabidopsis thaliana in response to blue light. *Plant Cell Physiol.* **46**: 955-963

von Arnim, A. G. & Deng, X-W. (1994) Light inactivation of *Arabidopsis* photomorphogenic repressor COP1 involves a cell-specific regulation of its nucleocytoplasmic partitioning. *Cell.* **79**: 1035-1045

Wada, M., Kagawa, T. & Sato, Y. (2003) Chloroplast movement. *Annu. Rev. Plant. Biol.* **54**: 455-468

Wade, H., Bibikova, T. N., Valentine, W. J. & Jenkins, G. I. (2001) Interactions within a network of phytochrome, cryptochrome and UV-B phototransduction pathways regulate chalcone synthase gene expression in *Arabidopsis* leaf tissue. *The Plant Journal* **25 (6)**: 675-685.

Wagner, D., Fairchild, C. D., Kuhn, R. M. & Quail, P. H. (1996) Chromophore-bearing NH2-terminal domains of phytochromes A and B determine their photosensory specificity and differential light liability. *Proc. Natl. Acad. Sci. USA.* **93**: 4011-4015

Wang, H., Ma, L-G., Li, J-M., Zhao, H-Y. & Deng, X-W. (2001) Direct interaction of Arabidopsis cryptochromes with COP1 in light control development. *Science.* **294**: 154-158

Watson, J. C. (2000) Light and Protein Kinases. *Advances in Botanical Research.* **32**: 149-184

Weston, E., Thorogood, K., Vinti, G. & Lopez-Juez, E. (2000) Light quality controls leaf-cell and chloroplast development in *Arabidopsis thaliana* wild type and blue-light-perception mutants. *Planta.* **211**: 807-815.

Whitelam, G. C. & Devlin, P. F. (1997) Roles of different phytochromes in *Arabidopsis* photomorphogenesis. *Plant Cell and Environment.* **20**: 752-758

Wilkins, M. B. (1997) Gravity and light-sensing guidance systems in primary roots and shoots. In: *Integration of activity in the higher plant.* (ed. D. H. Jennings) Society for Experimental Biology Symposium. Cambridge University Press, U.K.

Wilmoth, J. C., Wang, S., Tiwari, S. B., Joshi, A. D., Hagen, G., Guilfoyle, T. J., Alonso, J. M., Ecker, J. R. and Reed, J. W. (2005) NPH4/ARF7 and ARF19 promote leaf expansion and auxin-induced lateral root formation. *Plant Journal.* **43**:118-130.

Yan. J., He, C., Wang, J., Mao, Z., Holaday, S. A., Allen, R. D. & Zhang, H. (2004) Overexpression of the *Arabidopsis* 14-3-3 protein GF14λ in cotton leads to a "stay-green" phenotype and improves stress tolerance under moderate drought conditions. *Plant Cell Physiol.* **45**: 1107-1014

Yang, H-Q., Tang, R-H., & Cashmore, A. R. (2001) The signalling mechanism of *Arabidopsis* CRY1 involves direct interaction with COP1. *Plant Cell.* **13**: 2573-2587

Yang, H-Q., Wu, Y-J., Tang, R-H., Liu, D., Liu, Y. & Cashmore, A. R. (2000) The C termini of *Arabidopsis* cryptochromes mediate a constitutive light response. *Cell.* **103**: 815-827

Zegzouti, H., Anthony, R. G., Jahchan, N., Bogre, L. & Christensen, S. K. (2006) Phosphorylation and activation of PINOID by the phospholipid signaling kinase 3-phosphoinositide-dependent protein kinase 1 (PDK1) in *Arabidopsis. Proc. Natl. Acad. Sci. USA.* **103**: 6404-6409

Zeugner, A., Byrdin, M., Bouly, J-P., Bakrim, N., Giovani, B., Brettel, K. & Ahmad, M. (2005) Light-induced electron transfer in *Arabidopsis* cryotochrome-1 correlates with *in vivo* function. *J. Biol. Chem.* **280**: 19437-19440

Zhang, H., Wang, J., Hwang, I. & Goodman, H. M. (1995) Isolation and expression of an *Arabidopsis* 14-3-3-like protein gene. *Biochimica et Biophysica Acta.* **1266**: 113-116

Zhu, Y., Tepperman, J. M., Fairchild, C. D. & Quail, P. H. (2000) Phytochrome B binds with greater apparent affinity than phytochrome A to the basic helix-loop-helix factor PIF3 in a reaction requiring the PAS domain of PIF3. *Proc. Nat. Acad. Sci. USA*. **97**: 13419-13424

	Gene	Description	Bait	Comments
1	At1g02500.1	S-adenosylmethionine synthetase	N$_2$LOV2	Weak growth after re-streaking
2	At1g02850.2	gycosyl hydrolase family 1 protein	Phot1	Weak growth after re-streaking
3	At1g04140.1	transducin family protein WD-40 repeats	N$_2$LOV2	Weak growth after re-streaking
4	At1g05010.1	1-aminocyclopropanyl-carboxylate oxidase (ACC oxidase)	N$_2$LOV2	Weak growth after re-streaking
5	At1g05570.1	callose synthase	Phot1	Weak growth after re-streaking
6	At1g05810.1	acyl-[acyl carrier protein] thioesterase	Phot1	Weak growth after re-streaking
7	At1g06110.1	F-box family protein similar to FBX3 and SKIP2	Phot1	Did not grow after re-transformation
8	At1g06430.1	FtsH protease, putative	Phot1	Weak growth after re-streaking
9	At1g09070.1	C2 domain-containing protein/src2-like	Phot1	Weak growth after re-streaking
10	At1g11910.1	aspartyl protease family	Phot1	Weak growth after re-streaking
11	At1g12900.1	glyceraldehyde 3-phosphate dehydrogenase	N$_2$LOV2	Weak growth after re-streaking
12	At1g13260.1	DNA binding protein RAV1	N$_2$LOV2	Weak growth after re-streaking
13	At1g18450.1	expressed protein - similarity to actin-related protein	N$_2$LOV2	Weak growth after re-streaking
14	At1g20620.1	catalase 3	N$_2$LOV2	Weak growth after re-streaking
15	At1g20620.1	catalase 3	N$_2$LOV2	Weak growth after re-streaking
16	At1g20800.1	F-box family protein	Phot1	Weak growth after re-streaking
17	At1g20960.1	small nuclear ribonucleoprotein helicase	Phot1	Weak growth after re-streaking
18	At1g26630.1	eukaryotic translation initiation factor 5A	Phot1	Weak growth after re-streaking
19	At1g30440.1	photoresponsive NPH3 family protein	phot1	Investigated
20	At1g30440.1	photoresponsive NPH3 family protein	N$_2$LOV2	Investigated
21	At1g32640.1	bHLH protein	Phot1	Weak growth after re-streaking
22	At1g47128.1	cysteine proteinase (RD21A)/thiol proteinase	Phot1	Weak growth after re-streaking
23	At1g49570.1	peroxidase, putative	Phot1	Weak growth after re-streaking
24	At1g49570.1	peroxidase, putative	Phot1	Weak growth after re-streaking
25	At1g49570.1	peroxidase, putative	Phot1	Weak growth after re-streaking
26	At1g54830.3	CCAAT-box binding transcription factor. Hap5a	Phot1	Weak growth after re-streaking
27	At1g57770.1	amine oxidase family, flavin containing	N$_2$LOV2	Weak growth after re-streaking

28	At1g57770.1	amine oxidase family, flavin containing	N$_2$LOV2	Weak growth after re-streaking
29	At1g58080.1	ATP phosphoribosyl transferase	N$_2$LOV2	Weak growth after re-streaking
30	At1g58080.1	ATP phosphoribosyl transferase	N$_2$LOV2	Weak growth after re-streaking
31	At1g59359.1	40S ribosomal protein S2 (RPS2B)	Phot1	Weak growth after re-streaking
32	At1g62040.1	autophagy 8c (APG8c) microtublue-associated protein	Phot1	Weak growth after re-streaking
33	At1g63220.1	C2-domain containing protein similar to phloem protein RPP16 (rice)	Phot1	Auto-activates Y2H system
34	At1g64720.1	expressed protein with weak similarity to SPIP53809 phosphatidylcholine transfer protein	Phot1	Weak growth after re-streaking
35	At1g67280.1	putative lactoylglutathione lyase/ glycosylase 1	Phot1	Weak growth after re-streaking
36	At1g68560.1	alpha-xylosidase (XYL1)	Phot1	Weak growth after re-streaking
37	At1g71010.1	phosphatidylinositol-4-phosphate 5-kinase family protein	N$_2$LOV2	Weak growth after re-streaking
38	At1g72390.1	expressed protein	Phot1	Weak growth after re-streaking
39	At1g73820.1	Ssu72-like family protein	Phot1	Weak growth after re-streaking
40	At1g76160.1	multi-copper oxidase typeI family protein	Phot1	Weak growth after re-streaking
41	At1g78620.1	integral membrane family protein	N$_2$LOV2	Weak growth after re-streaking
42	At1g79040.1	photosystem2 10kDa polypeptide	N$_2$LOV2	Weak growth after re-streaking
43	At1g79270.1	integral membrane family protein	N$_2$LOV2	Weak growth after re-streaking
44	At1g79270.1	integral membrane family protein	N$_2$LOV2	Weak growth after re-streaking
45	At2g10710.1	DNAJ heat shock N-terminal domain containing protein similarity to AHM1	Phot1	Weak growth after re-streaking
46	At2g18280.1	tubby-like protein 2 (TULP2)	N$_2$LOV2	Did not grow after re-transformation
47	At2g27820.1	putative prephenate dehydratase	N$_2$LOV2	Weak growth after re-streaking
48	At2g30520.1	signal transducer of phototropic response RPT2	Phot1	Investigated
49	At2g40610.1	EXP8A	N$_2$LOV2	Weak growth after re-streaking
50	At2g40610.1	EXP8A	Phot1	Auto-activates system
51	At2g41100.1	touch responsive protein/calmodulin-related protein 3	Phot1	Sequence out of frame
52	At2g44130.1	kelch repeat-containing F-box	N$_2$LOV2	Sequence out of frame
53	At2g47170.1	ADP ribosylation factor 1 (ARF1)	N$_2$LOV2	Sequence out of frame
54	At3g01280.1	putative porin VDAC	N$_2$LOV2	Auto-activates Y2H

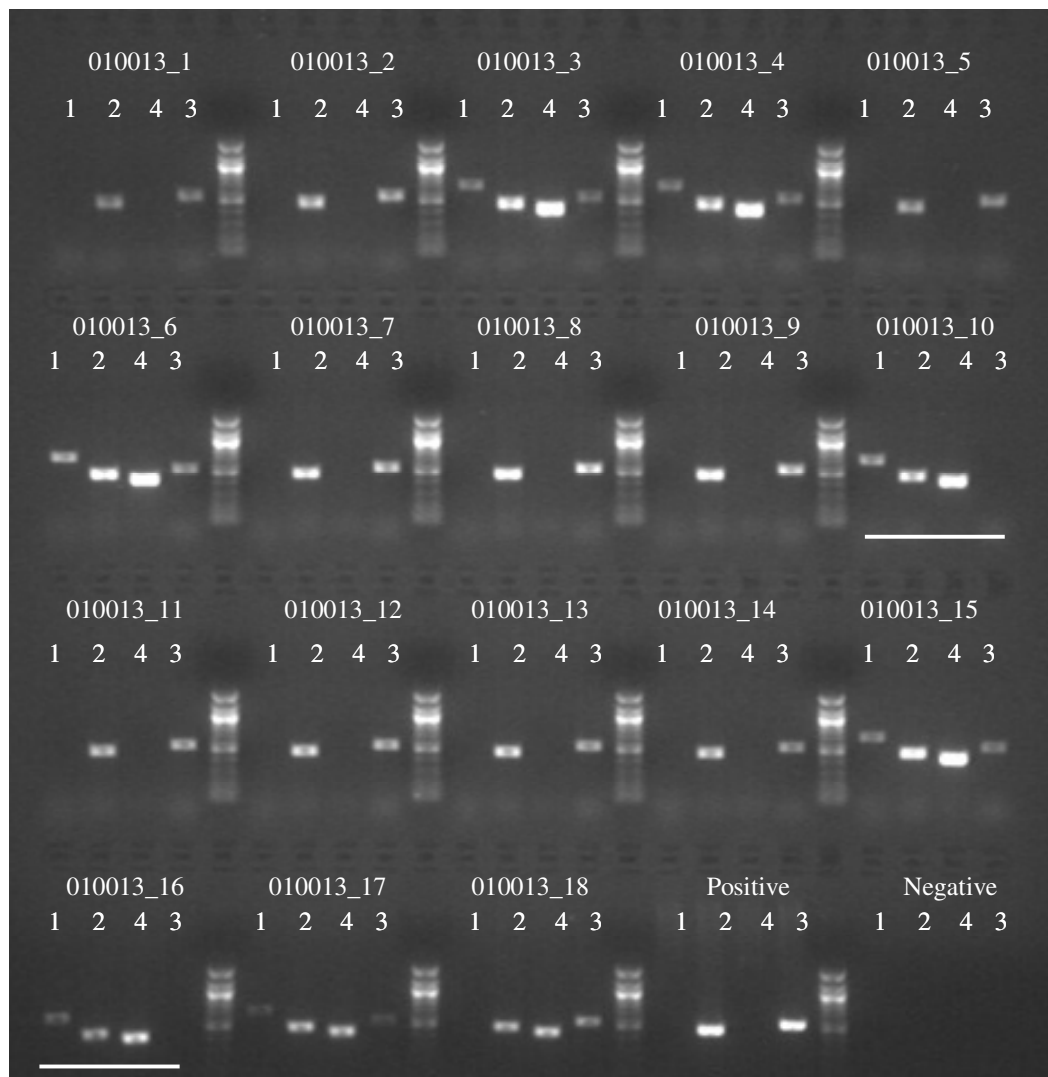|				
				system
55	At3g03380.1	Deg protease	N$_2$LOV2	Weak growth after re-streaking
56	At3g09260.1	glycosyl hydrolase family 1 protein	Phot1	Weak growth after re-streaking
57	At3g10630.1	glycosyl transferase family 1 protein	N$_2$LOV2	Weak growth after re-streaking
58	At3g11780.1	MD2-related lipid recognition domain	N$_2$LOV2	Weak growth after re-streaking
59	At3g16460.1	jacalin lectin family protein	Phot1	Weak growth after re-streaking
60	At3g19860.1	bHLH family protein	Phot1	Weak growth after re-streaking
61	At3g21720.1	putative isocitrate lyase	N$_2$LOV2	Weak growth after re-streaking
62	At3g21720.1	putative isocitrate lyase	N$_2$LOV2	Weak growth after re-streaking
63	At3g22120.1	protease inhibitor/ seed storage/ lipid transfer protein/	N$_2$LOV2	Weak growth after re-streaking
64	At3g22960.1	pyruvate kinase	N$_2$LOV2	Weak growth after re-streaking
65	At3g26650.1	glyceraldehyde 3-phosphate dehydrogenase A	Phot1	Weak growth after re-streaking
66	At3g26650.1	glyceraldehyde 3-phosphate dehydrogenase A	N$_2$LOV2	Weak growth after re-streaking
67	At3g26650.1	glyceraldehyde 3-phosphate dehydrogenase A	N$_2$LOV2	Weak growth after re-streaking
68	At3g28860.1	AtMDR1	phot1	Investigated
69	At3g28860.1	AtMDR1	phot1	Investigated
70	At3g29160.2	Snf1-related protein kinase (KIN11)	Phot1	Auto-activates Y2H system
71	At3g44310.2	nitrilase 1 (NIT1)	Phot1	Auto-activates Y2H system
72	At3g49120.1	putative peroxidase	Phot1	Weak growth after re-streaking
73	At3g51550.1	protein kinase family protein	N$_2$LOV2	Sequence out of frame
74	At3g51730.1	saposin B domain-containing protien	N$_2$LOV2	Weak growth after re-streaking
75	At3g62290.1	ADP ribosylation factor 2 (ARF2)	Phot1	Investigated
76	At3g62290.1	ADP ribosylation factor 2 (ARF2)	Phot1	Sequence out of frame
77	At3g62290.1	ADP ribosylation factor 2 (ARF2)	Phot1	Sequence out of frame
78	At4g01610.2	cathepsin B-like cysteine protease. Unusually short 5nt exon	Phot1	Weak growth after re-streaking
79	At4g03280.1	putative component of cytochrome B6-F complex	N$_2$LOV2	Weak growth after re-streaking
80	At4g04640.1	ATP synthase gamma chain 1 (chloroplast)	N$_2$LOV2	Weak growth after re-streaking
81	At4g05060.1	vesicle-associated membrane family protein	N$_2$LOV2	Weak growth after re-streaking
82	At4g05060.1	vesicle-associated membrane family protein	N$_2$LOV2	Weak growth after re-streaking

83	At4g08380.1	extensin-like protein	N$_2$LOV2	Weak growth after re-streaking
84	At4g08380.1	possible extensin-like protein	N$_2$LOV2	Weak growth after re-streaking
85	At4g08824.1	hypothetical protein	Phot1	Weak growth after re-streaking
86	At4g10510.1	subtilase family protein	Phot1	Weak growth after re-streaking
87	At4g13460.1	SET domain-containing protein (SUVH9),	N$_2$LOV2	Weak growth after re-streaking
88	At4g13460.1	SET domain-containing protein (SUVH9),	N$_2$LOV2	Weak growth after re-streaking
89	At4g14030.1	selenium binding protein	N$_2$LOV2	Weak growth after re-streaking
90	At4g14080.1	glycosyl hydrolase family	N$_2$LOV2	Weak growth after re-streaking
91	At4g14880.1	cytosolic O-acetylserine(thiol)lyase	N$_2$LOV2	Weak growth after re-streaking
92	At4g18670.1	leucine rich repeat family protein	Phot1	Weak growth after re-streaking
93	At4g21860.1	methionine sulphoxide reductase-domain containing protein	Phot1	Weak growth after re-streaking
94	At4g23710.1	vacuolar ATP synthase sub unit G2	N$_2$LOV2	Weak growth after re-streaking
95	At4g24280.1	heat shock protein 70	N$_2$LOV2	Weak growth after re-streaking
96	At4g25810.1	xyloglucan:xyloglucosyl transferase	Phot1	Weak growth after re-streaking
97	At4g30270.1	MERI-5protein. Endo-xyloglucan transferase	N$_2$LOV2	Auto-activates Y2H system
98	At4g30490.1	AFG1-like ATPase family protein	Phot1	Weak growth after re-streaking
99	At4g32070.1	octicosapeptide/Phox/Bem1p (PB1) domain-containing protein	N$_2$LOV2	Weak growth after re-streaking
100	At4g32070.1	octicosapeptide/Phox/Bem1p (PB1) domain-containing protein	N$_2$LOV2	Weak growth after re-streaking
101	At4g32070.1	octicosapeptide/Phox/Bem1p (PB1) domain-containing protein	N$_2$LOV2	Weak growth after re-streaking
102	At4g34260.1	hypothetical protien	N$_2$LOV2	Weak growth after re-streaking
103	At4g36360.2	putative B-galactosidase	N$_2$LOV2	Weak growth after re-streaking
104	At5g01210.1	anthranilate N-benzoyltransferase-like protein	N$_2$LOV2	Weak growth after re-streaking
105	At5g04140.1	ferredoxin-dependent glutamate synthase	N$_2$LOV2	Weak growth after re-streaking
106	At5g05360.1	putative protein	N$_2$LOV2	Weak growth after re-streaking
107	At5g05360.1	putative protein	N$_2$LOV2	Weak growth after re-streaking
108	At5g05600.1	leucoanthocyanidin dioxygenase-like protein	N$_2$LOV2	Weak growth after re-streaking
109	At5g10450.1	14-3-3 protein GF14 lambda (GRF6) (AFT1)	Phot1	Investigated

110	At5g15090.1	putative porin VDAC	Phot1	Auto-activates Y2H system
111	At5g15090.1	putative porin VDAC	N$_2$LOV2	Weak growth after re-streaking
112	At5g17060.1	ADP-ribosylation factor (ARF7)	Phot1	Investigated
113	At5g19440.1	cinnamyl-alcohol dehydrogenase-like protein	N$_2$LOV2	Weak growth after re-streaking
114	At5g20250.2	raffinose synthase family/seed inhibition protein	N$_2$LOV2	Weak growth after re-streaking
115	At5g20380.1	vesicular glutamate transporter 3	N$_2$LOV2	Weak growth after re-streaking
116	At5g20620.1	Polyubiquitin (UBQ4)	N$_2$LOV2	Weak growth after re-streaking
117	At5g22640.1	MORN (membrane occupation and recognition nexus) containing protein	Phot1	Weak growth after re-streaking
118	At5g26280.1	meprin + TRAF homology	N$_2$LOV2	Weak growth after re-streaking
119	At5g28050.1	putative cytidine deaminase	N$_2$LOV2	Weak growth after re-streaking
120	At5g35630.1	glutamine synthetase (GS2)	Phot1	Weak growth after re-streaking
121	At5g45775.2	60S ribosomal prtoein L11 (RPL11D)	Phot1	Weak growth after re-streaking
122	At5g46290.1	beta-ketoacyl-acp synthase I	N$_2$LOV2	Weak growth after re-streaking
123	At5g46700.1	senescence associated protein	Phot1	Weak growth after re-streaking
124	At5g48160.1	tropomyosin-related, coiled coil, actin binding	N$_2$LOV2	Weak growth after re-streaking
125	At5g50920.1	ATP dependant CLP protease	N$_2$LOV2	Weak growth after re-streaking
126	At5g54310.1	ARF GAP-like zinc-finger containing protein	Phot1	Sequence out of frame
127	At5g57150.1	bHLH protein	Phot1	Weak growth after re-streaking
128	At5g60360.1	cysteine proteinase AALP	N$_2$LOV2	Weak growth after re-streaking
129	At5g60360.1	cysteine proteinase AALP	N$_2$LOV2	Weak growth after re-streaking
130	At5g67360.1	putative subtilisin serine protease	N$_2$LOV2	Weak growth after re-streaking

Figure A2.1. Sequence of the NHP3-L gene

Genomic DNA sequence of the NH3-L gene. The location of the start and stop codons are highlighted in blue. Untranslated region are denoted in red lower case letters. Introns are denoted in purple lower case letters. Exons are denoted in yellow upper case letters. Primers used to screen potential knock out lines are highlighted in yellow and pink for the upper and lower primers, respectively. The location of the T-DNA insertion is shown by a purple triangle. Data from www.arabidopsis.org Sequence Viewer.
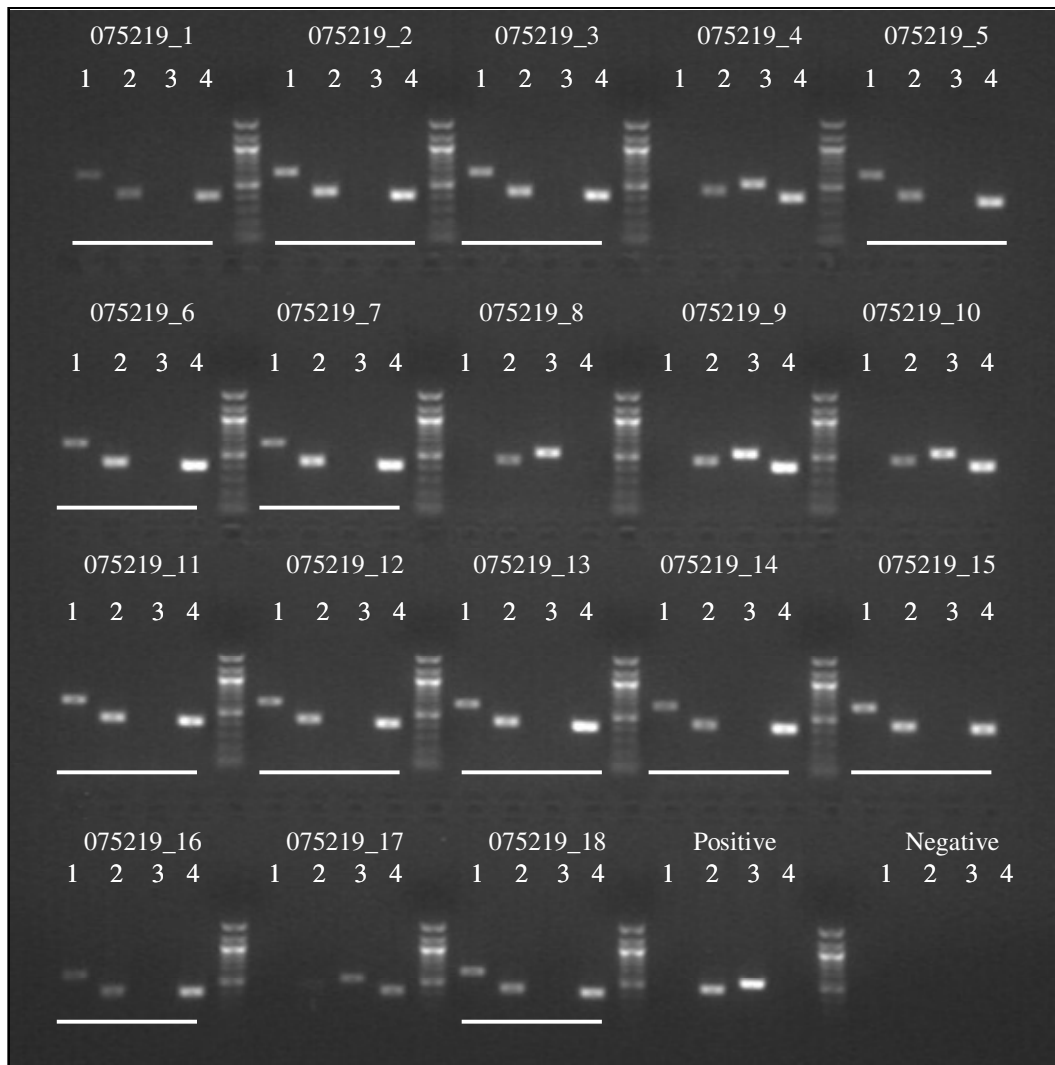
Figure A2.2 Genomic PCR of potential NPH3-L knockout lines

Genomic DNA extracted from a potential NPH3-L knockout line was screened for the T-DNA insertion as described in Sections 4.2.3 using primers designed against the T-DNA insertion element and against NPH3-L sequence (See Fig. A2.1). Primers sets (1, 2, 3 and 4) are described in Section 4.2.3 of the main text. Potentially homozygous knockout plants are identified by a white line underneath the PCR. Size markers are 1kb ladder.

Figure A3.1. Sequence of the 14-3-3λ gene

Genomic DNA sequence of the 14-3-3λ gene. The location of the start and stop codons are highlighted in blue. Untranslated region are denoted in red lower case letters. Introns are denoted in purple lower case letters. Exons are denoted in yellow upper case letters. Primers used to screen potential knock out lines are highlighted in yellow and pink for the upper and lower primers, respectively. The location of the T-DNA insertion is shown by a purple triangle. Data from www.arabidopsis.org Sequence Viewer.

Figure A3.2 Genomic PCR of potential 14-3-3λ knockout lines

Genomic DNA extracted from a potential 14-3-3λ knockout line was screened for the T-DNA insertion as described in Sections 4.2.3 and 5.2.8 using primers designed against the T-DNA insertion element and against 14-3-3λ sequence (See Fig. A2.1). Primers sets (1, 2, 3 and 4) are described in Section 4.2.3 of the main text. Potentially homozygous knockout plants are identified by a white line underneath the PCR. Size markers are 1kb ladder.